RNA and glia at the *Drosophila* neuromuscular junction: importance for synaptic plasticity

Dalia Sara Gala
Merton College
University of Oxford

A thesis submitted for the degree of Doctor of Philosophy
Trinity 2023

Dedication

Dla Natalii Michalskiej i Krystyny Michalskiej

Declaration

I hereby declare that this Thesis is my own work and the experiments described in the following pages were performed by myself, unless otherwise stated. The experiments were carried out in the Department of Biochemistry, University of Oxford. The Thesis has not been submitted for any other degree or professional qualifications.

Dalia Sara Gala

October 2023

The Impact of COVID-19 on my Work

My DPhil coincided with the lockdowns due to the COVID-19 pandemic, affecting my work. Even though a three-month extension was granted to my initial three-year funding, it could not fully mitigate the challenges I faced. Between March and June 2020, I suffered a devastating loss of around 40% of my fly stocks. Many of these were either sourced from collaborators or crossbred by me. This setback delayed my project by nearly seven months, as I waited for replacement stocks or attempted to recreate the desired crosses. During this time, I devoted myself to an in-depth study of my domain, which resulted in a now-published mini-review [1].

Once we could return to work, my access to microscopy, the most important technique of my project, was limited. Because of restrictions in place, if a room had more than one microscope, only one researcher was allowed at a time, significantly limiting my usage. From July 2020 to September 2021, I worked seven days a week for most weeks, resorting to doing imaging overnight to get access to microscopes.

Simultaneously, to contribute to the fight against the pandemic, I worked on a collaborative project with the labs of Alfredo Castello and Jane McKeating, studying viral infection dynamics, which was the only work permitted between March and July 2020. My involvement led to a publication in which I am the second author, but it also meant that I was juggling two projects simultaneously, even after the end of the most severe restrictions, until when it was published in January of 2022 [2]. While I have not showcased this work alongside my fly experiments due to the disparity in topics, its significance, and the demands it placed on my time, cannot be overlooked. Consequently, I had to narrow the scope of some of the fly experiments discussed here.

Abstract

Glial cells are essential components of both human and invertebrate nervous systems, including in the fruit fly, *Drosophila melanogaster*. Historically, research has focused more on neurons, with glia and their role in synaptic plasticity being somewhat overlooked. It is generally accepted that synaptic plasticity requires messenger ribonucleic acid (mRNA) and proteins localising at synapses, but the role of glia and mRNA localisation within glia in this process has been comparatively overlooked, despite the knowledge of their close association with synapses.

In recent research from the Davis laboratory, high-resolution microscopy was utilised to investigate mRNA and protein expression patterns in the larval nervous system. One common single molecule fluorescence in situ hybridisation (smFISH) probe was designed against the Yellow Fluorescent Protein (YFP) mRNA sequence of 200 *Drosophila* YFP fusion lines, allowing for the simultaneous detection of the reporter YFP protein and its mRNA within them. This study identified 19 mRNAs believed to be localised in the neuromuscular junction (NMJ) glia. This thesis aims to determine if these mRNAs and their corresponding proteins are indeed in the NMJ glial cells protrusions and if they play a role in regulating synaptic plasticity of the nearby motor neurons.

In Chapter 3, I verified that mRNAs of 18 of these transcripts are localised in the NMJ glial protrusions. Some were predominantly glia-specific, while others were also found in surrounding muscle. In Chapter 4, I evaluated the effects of knocking down these 18 mRNAs in glia using an RNA interference (RNAi) candidate screen. Some knockdowns led to NMJ defects, anatomical abnormalities, and, in a few cases,

lethality. A crawling impairment phenotype was observed only in the *Lachesin (Lac)*-RNAi larvae, making *Lac* a gene of significant interest.

In Chapter 5, I investigated the role of *Lac* in NMJ glia. *Lac* mRNA localises to specific and targeted NMJ glial structures, while in *Lac*-RNAi NMJs, the glial projections are disordered and aimless. I determined that the area occupied by Lac::YFP protein decreases after an assay which induces synaptic plasticity, similarly to glial area in control NMJs, and the axon terminal projection area stays constant. In *Lac*-RNAi larvae, the glial area does not decrease, and the neuronal area increases, suggesting a zero-sum game where the glial and neuronal projection areas at the NMJ exist in a conditional equilibrium. *Lac* mRNA preferentially associates with the glial and Blood-Brain Barrier (BBB) areas of the NMJ, and the knockdown of *Lac* in the subperineurial glia, which form the BBB in *Drosophila*, causes the most severe phenotype of all glial subtypes when comparing to the knockdown in all glia. *Lac* deficiency at the periphery of NMJ glial cells resulting in aberrant glial cell morphology could lead to altered synaptic plasticity in motor neurons and result in aberrant locomotor behaviour due to disruptions in glia-neuron communication, the BBB function and maintenance, altered neurotransmitter homeostasis, and changes in synaptic strength.

In summary, my thesis offers evidence suggesting that glial cell projections closely associated with synapses actively participate in the regulation of the synaptic plasticity happening at these synapses, and such control might be exerted through mRNA localisation of specific transcripts to the glial periphery. I anticipate that this thesis could serve as a valuable reference for subsequent studies on other proteins whose mRNAs might be localised to the glial periphery, possibly specifically ones related to BBB maintenance and formation.

Acknowledgements

I am extremely grateful to all the people who made my time at the University of Oxford during my DPhil special.

I never stopped being in awe of Josh Titlow's infectious passion when discussing fly neuroscience and was blown away by Rita Teodoro's hospitality when she hosted me in Lisbon and showed me the best places for polvo à lagareiro. Thank you both so much. I would like to thank Jeff Lee, Darragh Ennis, MK Thompson, Nicholas Hall, Richard Parton, Fran Robertson, Aino Järvelin, Maria Kiourlappou, David Ish-Horovicz, Julia Olivares-Abril, Jana Joha, Chloé Cassaro, Paris Jaggers and Tamar Torrance, from whom I never stopped learning, and who I always wanted to make laugh. I am grateful to my supervisors, Ilan Davis and Alfredo Castello, who allowed me the freedom to explore and always made it clear that the sky was the limit. I gratefully acknowledge the Department of Biochemistry, the Clarendon Fund and Merton College for funding my studies.

I wanted to thank my family: my parents, Aurelia and Sylwester Gala, who gave me my first toy microscope, my grandmother, Marta Margitta Gala, who motivated me to pursue higher education, Diana Forster and Peter Mothersole, my steadfast anchors and family away from home, and the rest of my family, who provided support throughout my endeavours. I am convinced nobody believes in me as much as they do. Thank you for everything.

Last, but certainly not least, my gratitude to Jo for unfailingly choosing to witness every shenanigan I pulled over the last 9 years.

Table of Contents

Table of Figures

Table of Tables

Abbreviations

α-HRP	α-Horseradish Peroxidase
A2RE	A2 Response Element
AG	Astrocyte-Like Glia
ALS	Amyotrophic Lateral Sclerosis
ATP	Adenosine Triphosphate
ATPase	Adenosine Triphosphatase
BBB	Blood-Brain Barrier
BDNF	Brain-Derived Neurotrophic Factor
BDSC	Bloomington *Drosophila* Stock Center
BSA	Bovine Serum Albumin
CG	Cortex Glia
CNS	Central Nervous System
CPTI	Cambridge Protein Trap Insertion
DAPI	4′,6-diamidino-2-phenylindole
DGRC	Department of *Drosophila* Genomics and Genetic Resources
DIOPT	*Drosophila* RNAi Screening Center Integrative Ortholog Prediction Tool
DIP	Dpr (Defective Proboscis Extension Response) Interacting Proteins
DLM	Dorsal Longitudinal Muscle
DNA	Deoxyribonucleic Acid
Dpr	Defective Proboscis Extension Response
dsRNA	Double-Stranded RNA
ECM	Extracellular Matrix
EG	Ensheathing Glia
FACS	Fluorescence-Activated Cell Sorting
FLARIM	Fluorescence Assay to Detect Ribosome Interactions With mRNA
$GABA_A$	Gamma-Aminobutyric Acid type A
GFAP	Glial Fibrillary Acidic Protein
GFP	Green Fluorescent Protein
GO	Gene Ontology

HL	Haemolymph-Like (Salines)
hnRNP A2	Heterogenous Ribonucleoprotein Particle A2
HS	Heat Shock
hSOD1s	human Superoxide Dismutase 1
IF	Immunofluorescence
Ig	Immunoglobulin
IgSF	Immunoglobulin Superfamily
IMP1	IGF2 mRNA-Binding Protein 1
ISH	In Situ Hybridisation
LAMP	Limbic System-Associated Membrane Protein
LTD	Long-Term Depression
LTP	Long-Term Potentiation
MBP	Myelin Basic Protein
MCP	MS2 Coat Protein
MOBP	Myelin Associated Oligodendrocyte Basic Protein
mRNA	Messenger RNA
MT	Microtubules
NEGR1	Neuronal Growth Regulator
NGF	Nerve Growth Factor
NIH	National Institutes of Health
NMJ	Neuromuscular Junction
Nrt	Neurotactin
Ntm	Neurotrimin
NVU	Neurovascular Unit
OBCAM	Opioid-Binding Cell Adhesion Molecule
OMgp	Oligodendrocyte-Myelin Glycoprotein
OPCs	Oligodendrocyte Precursor Cells
PAP	Peripheral Astrocyte Process
PBS	Phosphate-Buffered Saline
PG	Perineurial Glia

PNS	Peripheral Nervous System
PPG	Peripheral Perisynaptic Glia
PSCs	Perisynaptic Schwann Cells
RBP	RNA-Binding Protein
RFP	Red Fluorescent Protein
RNA	Ribonucleic Acid
RNAi	RNA interference
ROI	Region Of Interest
RT-PCR	Reverse Transcription - Polymerase Chain Reaction
SEM	Standard Error of the Mean
SJ	Septate Junction
smFISH	Single Molecule Fluorescence In Situ Hybridisation
SNP	Single Nucleotide Polymorphism
SPG	Subperineurial Glia
SSC	Saline Sodium Citrate
SunTag	SUperNova (Tag)
TJ	Tight Junction
UAS	Upstream Activating Sequence
UTR	Untranslated Region
UV	Ultraviolet
VDRC	Vienna *Drosophila* Resource Center
VNC	Ventral Nerve Cord
WG	Wrapping Glia
YFP	Yellow Fluorescent Protein
ZBP1	Zipcode Binding Protein 1

CHAPTER 1

1 Introduction

Throughout history, the anatomical residence of the human soul – the entity considered to contain all thoughts, emotions, and consciousness of a person – has been a subject of heated philosophical discussion. In ancient Egypt and traditional Chinese philosophy, it was thought to reside in various body organs like the heart or liver, while various Greek philosophers, like Herophilus, considered the soul to be contained to ventricles in the brain [3]. Descartes thought it was the pineal gland which hosted the soul [4].

What drove this human fascination with the location or essence of the soul? If the soul embodies what defines us as individuals, our pursuit might be fuelled by an urge to understand, preserve, or even recover this essence in instances of illness or trauma. Thanks to famous, and often tragic cases, like that one of Phineas Gage, scientists learned of the connection between the brain and all that “makes” a person: memories, personality, behaviour. Gage was a railroad worker who survived an accident where an iron rod was driven through his head, destroying large parts of his brain. He miraculously survived this accident, but his character and conduct were permanently altered. His story was among the pioneering instances highlighting the brain's pivotal role in shaping human identity, positing it as the seat of our consciousness and essence [5]. Not only that - the questions his story raises are far from antiquated, especially when faced with the devastating effects of neurodegenerative diseases, which strip away facets of our identity.

With the progress of research, both in the disciplines of neuroscience and cell biology, neurons emerged as the major group of cells which make up the brain [6]. The morphology and structure of those cells, as well as their interconnectivity, became

points of interest in the attempt to understand how the brain works. A focal point of this search was, and continues to be, the struggle to connect the basic biology of neurons and, therefore, the brain, to its emergent properties, like consciousness, movement, capacity to learn, memory formation, and the ability to experience emotions. In particular, the properties of synapses have always been of interest in this context [7].

Why specifically synapses? Key to neuron interconnectivity and circuit formation, synapses are the sites of communication between neurons. Neurotransmitters released from active zones relay varying messages across the synaptic cleft, leading to the excitation or silencing of the next neuron, which receives these signals through its own end of the synapse, the postsynaptic density [8]. Thus, synapses serve as intricate junctions with vast potential to influence subsequent neurons, which can be likened to crossroads, where a single synapse can give rise to a myriad of outcomes.

The formation of new synapses, and the alteration or removal of existing ones, are the processes thought to be underlying learning and memory formation, in the phenomenon called synaptic plasticity [9]. Processes like long-term potentiation (LTP) or long-term depression (LTD) lead to persistent increase or decrease, respectively, of signalling between neurons [10]. Both are underlain by countless changes requiring the prompt alteration of the neuronal molecular repertoire of the synapse, often involving rapid protein synthesis, enabled by messenger ribonucleic acid (mRNA) localisation [11]. The progress of research on synaptic plasticity currently allows us to better understand the formation of neural circuits and their subsequent function in memory formation or emotional processing, all of which brings us closer to understanding the molecular basis of personality [9].

Is a synapse merely a conversation between two neurons, then? Despite the fact that synapses have been known since the dawn of 19th century [12], a significant omission continued to be made in how neuroscientists thought about them. It was only about 20 years ago when the term “tripartite synapse” has been coined to describe a synapse formed not only by the active zones and the postsynaptic density, but also the synapse-associated glial cells [13]. The role of glia in nervous system function was not fully appreciated, and indeed was usually dismissed for many years. However, a series of papers in the last decade of the 20th century made significant discoveries regarding the synaptic roles of those glial cells – mainly astrocytes, in the Central Nervous System (CNS) and Perisynaptic Schwann Cells (PSCs) in the Peripheral Nervous System (PNS) [13]. Their discovered roles are extremely broad and well characterised on a molecular level, and many appear key in supporting neuronal synaptic plasticity. To name just a few, these include calcium-dependent neurotransmitter release, astrocyte to neuron signalling and modulation of synaptic transmission and synaptic networks, all of which have been extensively reviewed [13-19]. However, many of the molecular mechanisms for the roles of astrocytes and PSCs in synaptic function are still unclear and the roles of other glial subtypes in synaptic function remain poorly understood. Could glia, much like neurons, utilise mRNA localisation and local translation to influence synaptic plasticity of their neighbouring neurons?

1.1 What are the roles of different glial cells in synaptic plasticity?

Discovered in the late 19th century by Rudolf Virchow and considered to be the brain’s “support cells” for nearly a century, glial cells are now known to be anything but passive [20]. They contribute substantially to the maintenance of the neural circuitry

and homeostasis, thus enabling the formation and upkeep of the architecture which permits the brain to function [21].

How do glial cells exert such substantial influence? It happens largely due to their diverse specialised subtypes, each with distinct morphologies, strategically positioned within the nervous system. In mammals, there are multiple known glial subtypes, with variations between those in the CNS and the PNS. In the CNS, the most numerous cell type are astrocytes, so named because of their star-shaped morphology [22] (Figure 1-1). These cells are responsible for the formation of the Blood-Brain Barrier (BBB). This enables the maintenance of the neuronal homeostatic environment by the control of neurotransmitter reuptake and release, and the neuronal Ca^{2+} levels [13]. The two specialised subtypes of astrocytes, the Bergmann glia of the cerebellum and the Müller glia in the retina, are responsible for synaptic pruning in early cerebellar development and homeostatic maintenance of retinal cells, respectively [23, 24]. Oligodendrocyte lineage and precursor cells are responsible for the myelination of CNS axons, both in the context of development, but also nerve repair [25]. Microglia are the immune cells of the brain, responding to injury, infection, and inflammation [26]. Finally, ependymal cells produce the cerebrospinal fluid, and tanycytes and pituicytes are also thought to participate in the formation of the BBB, with roles in regulating neuroendocrine responses [27, 28].

In the PNS, Schwann cells are the equivalent of oligodendrocytes (Figure 1-2). Myelinating and non-myelinating (Remak) Schwann cells myelinate or wrap the PNS axons, respectively, and can become reactive and multiply to respond to injury [29].

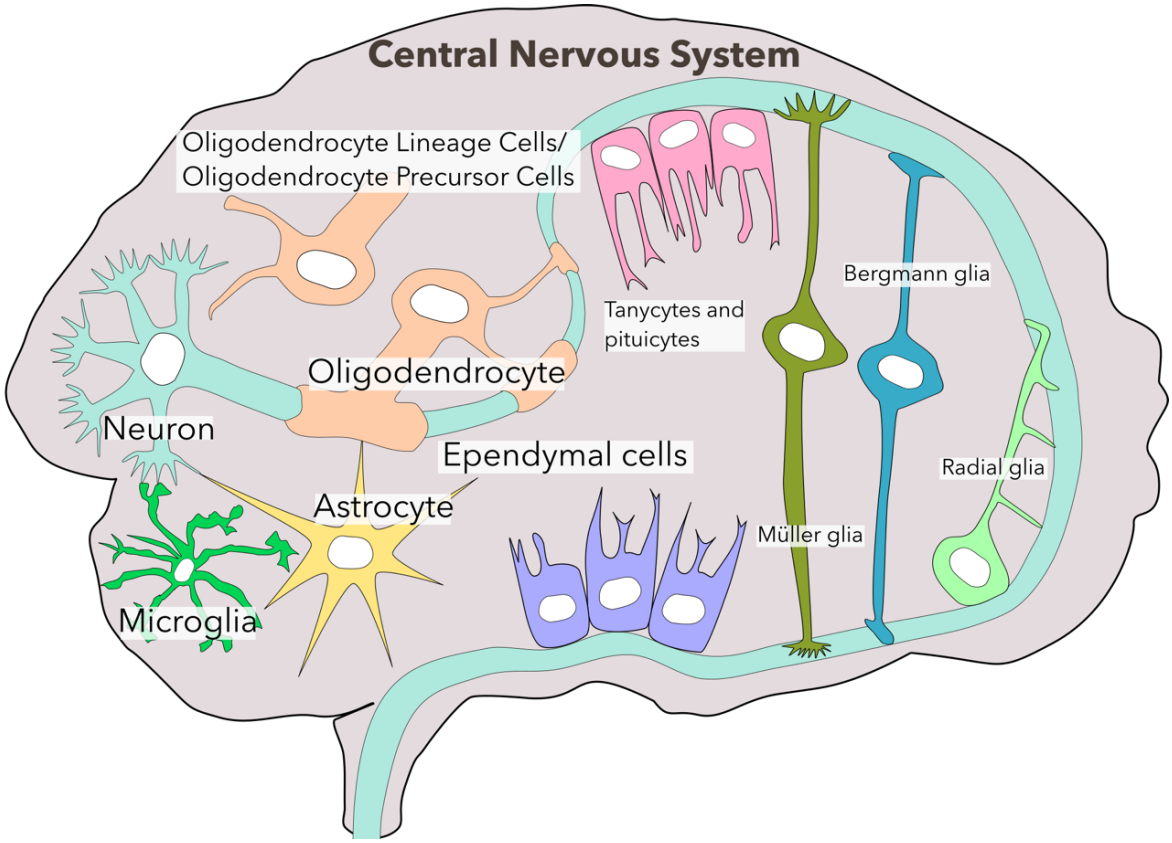

Figure 1-1 Illustration of mammalian glial cell types in the CNS

In the CNS, the major subtypes of glia are astrocytes, with specialised subtypes including Bergmann glia in the cerebellum and Müller glia in the retina, oligodendrocytes and their precursors, microglia, ependymal cells, tanycytes, and pituicytes. During development in the CNS, radial glia are present and differentiate into both neurons and certain glial subtypes.

Terminal Schwann cells, also called PSCs, are a subtype of Schwann cells which extends cytoplasmic protrusions to the neuromuscular junction (NMJ) synapse, actively participating in the control of its plasticity and function [30]. Satellite glia reside in sensory ganglia, where they aid with the neuronal signal transmission [31]. Lastly, enteric glia are a do-it-all cell type present in the digestive system ganglia, where they control the enteric nervous system homeostasis and intestinal reflexes, as well as monitor the neuroinflammation of the digestive system [32].

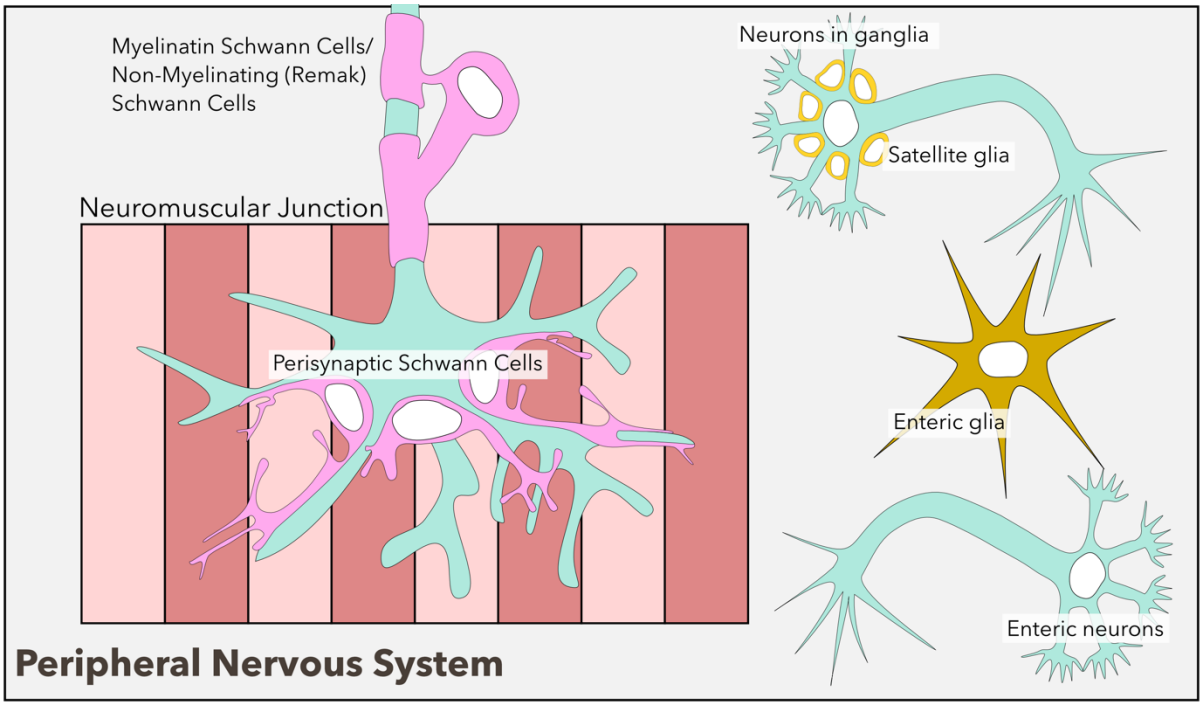

Figure 1-2 PNS glia

In the PNS, there are several subtypes of Schwann cells, such as myelinating and non-myelinating Schwann cells (also known as Remak Schwann cells) and perisynaptic/terminal Schwann cells. In addition, satellite glia surround the cell bodies of neurons in ganglia, and enteric glia (which may be considered a subtype of Schwann cells) can be found in the enteric nervous system.

What biochemical mechanisms underpin glial roles in synaptic plasticity? Though the general roles of the aforementioned glial cells are known, their specific molecular involvement with the regulation of synaptic plasticity is still poorly understood. Through insights such as the knowledge that mechanical stimulation of astrocytes results in increased neuronal Ca^{2+} levels, it is known that glia directly affect neuronal synaptic plasticity [33]. It is much harder to decipher how exactly these processes occur on a molecular level, and what are the consequences for synaptic plasticity if the correct function of the glia is disrupted, as in motor neuron or neurodegenerative diseases [34]. In the following sections, I will aim to briefly discuss what details are available regarding these functions of glial cells in neuronal synaptic plasticity. Where known, I

include details of studies concerned with the glial peripheral molecular repertoire, with the particular emphasis on mRNAs present locally close to synapses, and far away from the glial cell bodies.

1.1.1 Astrocytes - highly dynamic stars of synaptic plasticity

Astrocytes are among the most studied glial cell subtypes due to their known roles in synaptic plasticity and BBB formation. These cells, much like neurons, have long cytoplasmic projections, which are highly plastic and, depending on their environment, can undergo adaptive remodelling. Like neurons, the distal processes contact many distinct synapses and respond locally, independently, and at a long distance from the cell body [35, 36]. Astrocyte endings near synapses can produce phagocytic protrusions and physically interfere with the synaptic terminals [16, 17]. Astrocytes can also release neurotransmitters; both in cultured astrocytes, and in acutely isolated hippocampal slices, and Ca^{2+}-dependent glutamate release has been observed [13, 33]. Astrocytes also play metabolic and homeostatic roles important for plasticity. Mechanical, electrical and biochemical stimulation of astrocytes results in measurable changes in the functioning of the neighbouring neurons [13]. These observations give a clear indication that astrocytes sense and respond, with such responses having direct consequences on neuronal function. The roles of astrocytes in the modulation of synaptic plasticity are possibly best studied and have been extensively reviewed [35-41].

Many of the functions performed by astrocytes, like Ca^{2+}-mediated cellular excitability and release of gliotransmitters and vesicles, have parallels in neurons. Such glial processes often start in a protrusion and spread through the whole cell, and could be explained, at least in part, by local protein synthesis at peripheral compartments

[42-44]. Recent studies of mRNA localisation in astrocytes support these hypotheses, showing that transcriptomes and translatomes of astrocyte peripheral processes change upon fear conditioning in mice, and demonstrating numerous localised transcripts and local translation at the astrocyte periphery [1, 45-50].

1.1.2 Myelin produced by oligodendrocytes can modulate synaptic plasticity

Like astrocytes, oligodendrocytes are also active players in synaptic plasticity and their level of secretion of myelin shapes brain function and plasticity [51]. Furthermore, there is emerging evidence that activity-dependent myelination contributes to memory consolidation and recall [52]. In mice, fear-learning induces precursor cells to become oligodendrocytes that produce myelin in the prefrontal cortex [53]. Loss of oligodendrocytes is a major mechanism of neurodegenerative diseases, which is thought to be partly abrogated by activity-dependent remyelination via new and surviving oligodendrocytes [54]. Oligodendrocytes have also been found to modulate neurotransmission and properties of the pre-synapse through secretion of brain-derived neurotrophic factor (BDNF) and to express post-synaptic proteins, like PSD95, which can modulate myelin sheath formation [55, 56]. Two proteins secreted by myelin – oligodendrocyte-myelin glycoprotein (OMgp) and the reticulon RTN4 (Nogo) – suppress LTP [57]. It was also shown that some Oligodendrocyte Precursor Cells (OPCs) express voltage-gated sodium and potassium channels, which can receive signals from axons as well as produce action potentials upon depolarisation [58]. Interestingly, oligodendrocytes were also found to increase the conduction velocity of action potentials in the brain [59]. The rates of action potentials in neurons were shortened upon direct depolarisation of oligodendrocytes. In summary, considerable evidence from a variety of different studies all point to the fact that oligodendrocytes

have active and important roles in how information is processed in the brain, thus potentially contributing to plasticity underlying learning and memory.

Myelination and myelin remodelling themselves could also be directly modulating plasticity. Neural activity can influence myelination; playing a computer game [60] or learning to juggle [61] are known to affect the structure of white matter in humans, and learning motor skills was found to cause changes in myelination in rodents [62], all of which suggests a direct interplay between myelin levels and animal behaviour.

mRNA localisation in oligodendrocytes has been studied most extensively of all glial cell types and forms the basis for the mRNA localisation model in all elongated cells. It is discussed in detail in section 1.4.2.

1.1.3 Microglial motility and phagocytic functions contribute to synaptic plasticity

Microglia have been known to be involved in the modulation of synaptic plasticity for some time. Three roles for microglia in plasticity have been suggested: modification of the perisynaptic environment by extracellular matrix (ECM) proteolysis, dendritic spine remodelling and engulfment of dendritic spines and axon terminals [63]. Microglia-dependent pruning of synapses during the development of the visual critical period is another early example of microglial plasticity [64]. Microglia are also known to respond to light intensity by changing the position of their processes and motility [65] and have been found to be indispensable for plasticity and pruning of synapses in the mouse visual cortex [66]. Many of the microglial roles in synapse formation and elimination both in health and in disease could be compared to the roles of tripartite synapse glia, reviewed elsewhere [26, 67-70].

Interestingly, microglia were found to engulf presynaptic terminals in response to neural activity [64], and it has been suggested that the synapses that are destined to be engulfed express C3b-opsonisation, which is recognised by microglia, the only known CNS cells to express the C3 receptor [71, 72]. Therefore, microglia have a key role during triaging for synaptic pruning or maintenance of synapses, which could suggest that they might need rapid production of cytoskeletal proteins at their periphery, pointing to the need for mRNA localisation and local translation. New studies are starting to emerge which explore these ideas in microglia [73-77].

1.1.4 Radial glia control early developmental plasticity

Radial glia are stem cells of the developing nervous system with unique elongated morphology supporting their roles in guiding the radial migration of new-born neurons. They are also known to differentiate into various types of CNS cells, such as neurons, astrocytes and oligodendrocytes [78]. Radial glia are known to utilise polarised mRNA transport within their specialised radial morphology adapted to support neuronal migration [79]. It is also possible that radial glia locally regulate various facets of neuronal development, including synapse formation [73]. N-Cadherin accumulates at the site of interaction of radial glia with cortical neurons, and axons project at the opposite side of the neuron from the contact site [80]. It seems reasonable to hypothesise that these polarisation events involve mRNA transport and localised translation in both the glia and the neuron for the purpose of synaptic plasticity regulation.

1.1.5 Müller glia participate in retinal synaptic plasticity

A subtype of radial glia, called Müller glia, are the most common glia in the vertebrate retina which persist into adulthood [81]. In contrast to radial glia, Müller glia are born

much later in the retina, only after the first types of neurons are already present [82]. Müller glia can also dedifferentiate to become actively dividing neuronal progenitors [83]. Interestingly, Müller glia have a wide range of functions equivalent to those of oligodendrocytes and astrocytes in other contexts. These roles include: control of free radicals, gliotransmitter release, uptake and recycling of neurotransmitters and potassium homeostasis, all of which could suggest their involvement in synaptic plasticity in the retina [24].

Müller glia have extensive cytoplasmic projections that interact closely with microglial and neuronal projections. Several proteins have been shown to localise specifically to the apical ends of Müller glial projections, including GLUT2, a facilitated-diffusion glucose transporter isoform [84]. Pals1, a protein associated with Lin seven 1 (also known as Mpp5, MAGUK p55 subfamily member 5), was shown to be necessary for the correct localisation of Crumbs gene family group members to the sub-apical region of Müller glia [85]. Two studies also addressed mRNA localisation in Müller glia, and they both identified glial fibrillary acidic protein (GFAP) transcripts in Müller glia processes [86, 87].

1.1.6 Bergmann glia modify plasticity in the cerebellum

Bergmann glia are another subtype of radial glia. These glia can also be considered to be a specialised type of astrocytes, given their extensive arborisation [81]. These cells, also known Golgi epithelial cells or radial astrocytes, are in direct contact with Purkinje cells in the cerebellum. Purkinje cells play important roles in regulating motor movement and have some of the most extensive cytoplasmic neurite branching of any neuronal cell.

Interestingly, both Bergmann and Müller glial cells were shown to express multiple glutamate and other receptors, which are known to have synaptic localisation[88, 89]. Furthermore, activating these receptors with glutamate treatment in cell culture leads to changes in receptor gene expression levels [90]. Bergmann glia have processes containing Gamma-Aminobutyric Acid type A ($GABA_A$) receptors and wrap around inhibitory synapses, suggesting that Bergmann glia sense GABAergic synaptic function [91]. Selective animal behaviours were also shown to modify Bergmann glial networks [92]. All of this presents both Bergmann and Müller glial cells as potential active players in the modulation of synaptic efficacy and plasticity, in which local protein synthesis could play a role [93].

1.1.7 PSCs respond to and modulate neuromuscular plasticity

PSCs have been known to be present near NMJ synapses since the 1960's [94]. PSCs are thought to be required for synaptic stability and plasticity, but the details of the molecular mechanisms by which they achieve such functions remain poorly understood. During development, PSCs guide the growing nerve and are likely to be responsible for the long-term maintenance of NMJ synapses. Furthermore, PSCs allow the NMJ to adapt to muscle activity, and to participate in nerve regeneration after injury. Interestingly, PSCs can become phagocytic when nerves are injured to clear debris, and form "bridges" along which the neuron endings can grow to reinnervate the muscle. They also influence synaptic transmission through purinergic and cholinergic activity and can phagocytose competing nerve terminals to "favour" one synaptic connection over another. More specific roles of PSCs have been previously reviewed [30, 95-98].

PSCs are capable of inserting cytoplasmic finger-like processes into the synaptic cleft, causing a blockage that weakens the nerve-muscle interaction [99]. These processes could be using an already existing and readily available pool of protein. Alternatively, the glial cytoplasmic projections could be dynamic and plastic, in response to mRNA transport and localised translation of mRNAs encoding key proteins. While, to date, no localised transcriptomic studies have been conducted on PSCs, bulk mRNA sequencing of fluorescence-activated cell sorting (FACS)-sorted PSCs has revealed that many of the transcripts present in those cells encode proteins involved in the modulation of synaptic activity and myelination [100].

1.2 Studying neuron-glia interactions: the challenges

Many studies referenced in prior sections predominantly use mammals or cell cultures as their primary research models. This presents challenges; cell cultures may not always reflect physiological conditions, and mammalian models, due to their cellular complexity, can be challenging to dissect, particularly when differentiating between densely packed similar cell types.

How to best examine the roles of not only individual glial cells, but maybe even individual molecules in those cells, in regulating plasticity? The introduction of single-cell transcriptomics and spatial transcriptomics marked significant progress in distinguishing various glial subtypes and emphasizing the differences between them [101-103]. Researchers can gain valuable insights into the distinct molecular signatures of glial cell types and the variations in their transcriptional programs through such methods. However, these studies have their limitations: notably, they do not capture data on transcripts in glial processes, which are lost during the tissue disaggregation needed for individual cell body separation [104]. Existing techniques

also fall short in terms of sensitivity, coverage, resolution, and the ability to simultaneously detect mRNA, its protein, and other structures of interest in individual cells, particularly across complex tissues. Current sequencing-based spatial transcriptomics techniques also can not differentiate between the individual glial cell processes in intact nervous systems. Since most of the glial cytoplasm resides in projections, high-resolution imaging methods, such as single molecule fluorescence *in situ* hybridisation (smFISH), are crucial to determine the mRNA profiles present in glial cell projections.

Drosophila, with its fewer cells, provides a distinct advantage. It proved to be an excellent model system for the study of glial biology due to the relatively low (~10,000) cell number in the larval nervous system, which allows for easy and reliable identification and labelling of individual cells, as well as the similarity and high conservation of the glial cell types and functions in *Drosophila* when compared to vertebrates [105, 106]. Overall, this organism can be an excellent model for studying neuron-glia interactions, especially at the molecular level.

1.3 *Drosophila* as a model to study neuron-glia interactions

The fruit fly *Drosophila melanogaster* is a well-known and widely used model, famed for its experimental tractability, genetic accessibility, and neuroscientific malleability [107]. Established as a model in the early 20th century by Thomas Morgan at Columbia University, it led to several Nobel-prize worthy discoveries, including, just to name some, in the areas of embryonic development and fine, RNA-level regulation thereof, understanding of chromosome biology, olfactory systems, circadian rhythm and the immune system [107]. The ease of maintenance and high number of offspring continue to make this organism the model of choice in multiple areas of modern research.

Particularly, the *Drosophila* 3rd instar larvae offer an exciting system for neuroscientific observation due to the ease of accessibility of not only the developing brain, but also the NMJ, which can be easily imaged using confocal microscopy [108]. A suite of well-established and reliable antibodies allows researchers to image the whole intact nervous system, thus providing an opportunity to build a big-picture, high-level understanding of its molecular governance [109].

1.3.1 Neuron-glia interactions in *Drosophila*

Glial cells constitute 10-20% of the cells in the *Drosophila* nervous system [110]. The most widely accepted classification names six kinds of glial cells in *Drosophila*, depicted in Figure 1-3: surface glia present both in the CNS and the PNS, which encompass the 1) perineurial (PG) and 2) subperineurial glia (SPG); CNS-specific 3) cortex (CG), 4) astrocyte-like (AG) and 5) ensheathing glia (EG); and PNS-specific 6) wrapping glia (WG) [111].

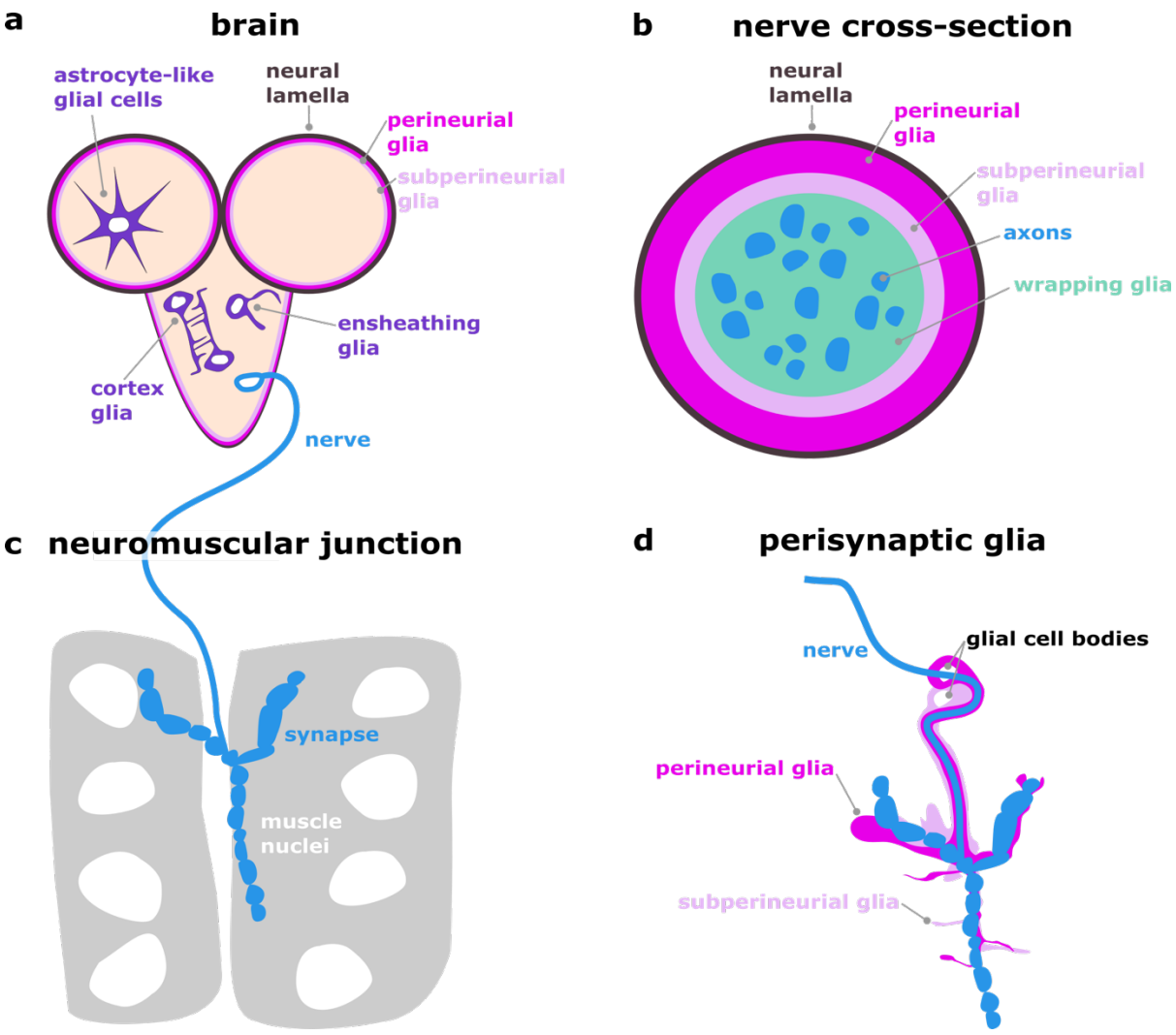

Figure 1-3 Known glial cell types in *Drosophila*, depicted in the larval nervous system

a) In the brain, five of the six glial subtypes can be found. Surface glia, the collective name for SPG and PG, form the BBB and are similar to mammalian astrocytes. CG connect SPG and neurons. AG regulate neurotransmitter levels and participate in plasticity events. EG compartmentalise the brain and can act as phagocytes. b) Three glial subtypes, including surface glia, can be found in the nerves. WG wrap neurons but do not myelinate PNS nerves unlike their mammalian equivalents, Schwann cells. c) All three subtypes of glia found in the nerves make projections reaching the NMJ. d) PG and SPG extend from nerve bundles towards NMJ synapses, and actively interact with them.

To briefly summarise these subtypes, surface glia are responsible for the formation of the BBB in *Drosophila*, thus being somewhat equivalent to mammalian astrocytes [112]. CG provide the connection between the SPG and the neurons [113]. AG also bear many functional similarities to their vertebrate namesakes, astrocytes, and

participate in the neurotransmitter level regulation and homeostasis maintenance of the fly brain [114]. Interestingly, AG are thought to be key in early plasticity events in *Drosophila*. In a recent study, AG were found to invade the neuropil in the early *Drosophila* larval motor circuit to close the critical period, a developmental interval during which heightened synaptic plasticity occurs due to neuronal activity [115]. AG can regulate olfactory processing by directly affecting the strength of the synaptic connections formed between olfactory receptor neurons and projection neurons [116]. EG localise to the surface of the neuropil which results in brain compartmentalisation and can act as phagocytes in the adult *Drosophila* brain [117]. WG wrap the neurons present in the sensory and motor nerves and could therefore be compared to oligodendrocytes or Schwann cells, which can affect the axon diameter and conductance velocity in the *Drosophila* PNS [118]. However, WG do not myelinate PNS nerves, unlike their vertebrate counterparts. Nevertheless, they do enwrap individual or small bundles of axons, a process which is regulated by RalA GTPase and the exocyst complex, and by the Neuregulin homologue, Vein [119, 120]. It is the PG and SPG which extend from the nerve bundles towards the NMJ synapses in flies, and a parallel could be drawn between them and the vertebrate PSCs [121]. Whether or not WG extend their projections to the NMJ is a point of discussion, with some sources suggesting that they do, while others disagree [111, 114, 118, 119].

1.3.2 Characterisation of *Drosophila* peripheral glia

Drosophila peripheral glia were first studied in the 1980s and 1990s, when their roles during embryonic development, and axon guidance were actively explored; the migration of glia into the PNS and their interactions with neurons during development have been described in detail [122-125]. During larval development, peripheral glia

extend processes that become progressively more elaborate and reach the NMJ [126]. After the initial motor neurons extend beyond the glia into the periphery, the glial migration starts along a pre-established axonal growth cone pathway. Glial cell bodies move outwards, and their cytoplasmic extensions grow ahead of them, never extending past the foremost part of a pioneering growth cone. Since in vertebrates, Schwann cells are seen following, not leading, these pioneer growth cones, it seems *Drosophila* PNS glia also likely need axons as a foundation for their migration into the PNS [127]. Further research explored various roles of *Drosophila* PNS glia in synaptic pruning at the mature synapses [128].

What are the roles of the *Drosophila* peripheral glia? To date, few studies dealt with the detailed morphology, molecular repertoire, and function of these cells. Interestingly, the *Drosophila* high-affinity glutamate reuptake transporter, dEAAT1, was found to be present in the glial cells in the NMJ of the adult flies, but not in the embryonic or larval peripheral glia, which could suggest that glial-mediated glutamate reuptake is necessary for regular NMJ activity in adults, but not in other fly developmental stages, contradicting the previous notion suggesting that glia are not present at the adult NMJ synapse [129, 130]. Another study identified a *Drosophila* cystine/glutamate transporters (xCTs) homolog, named *genderblind*, which was found to be expressed in CNS and PNS glia. It was confirmed that *genderblind* codes for a transporter that regulates extracellular glutamate, which has the capacity to desensitise receptors and hence inhibits glutamate receptor clustering at synapses [131]. Later, *wingless* was found to be a target of Repo, a well-known glial transcription factor in *Drosophila* larvae and Repo was observed to regulate *wingless* expression in the NMJ glia which in turn affected the glutamate receptor clustering and synaptic physiology [132].

Are terminal *Drosophila melanogaster* NMJ glia akin to PSCs, then? NMJ glia are known to affect muscle-to-motor neuron retrograde signalling and glutamate receptor clustering *in vivo* [132, 133] and even to rapidly migrate to the NMJ and engulf immature synaptic boutons [134]. Larval NMJ glia were found to be involved in the clearance of the presynaptic debris resulting from synaptic destabilisation and pruning [134], but were not found to be involved in the dismantling of the NMJ during the process of metamorphosis [135]. Interestingly, the growth of the larval glial NMJ processes was found to be coordinated with that of the synapse itself, and glia were found to create intricate and varying morphologies at the NMJ, suggesting a breadth of possible functions (Figure 1-4) [121]. Despite the relative scarcity of *Drosophila* glial NMJ focused literature, the picture painted is clear and hints strongly at the heavy involvement of glial cells in all the important processes occurring at this synapse, just like in the tripartite synapse model.

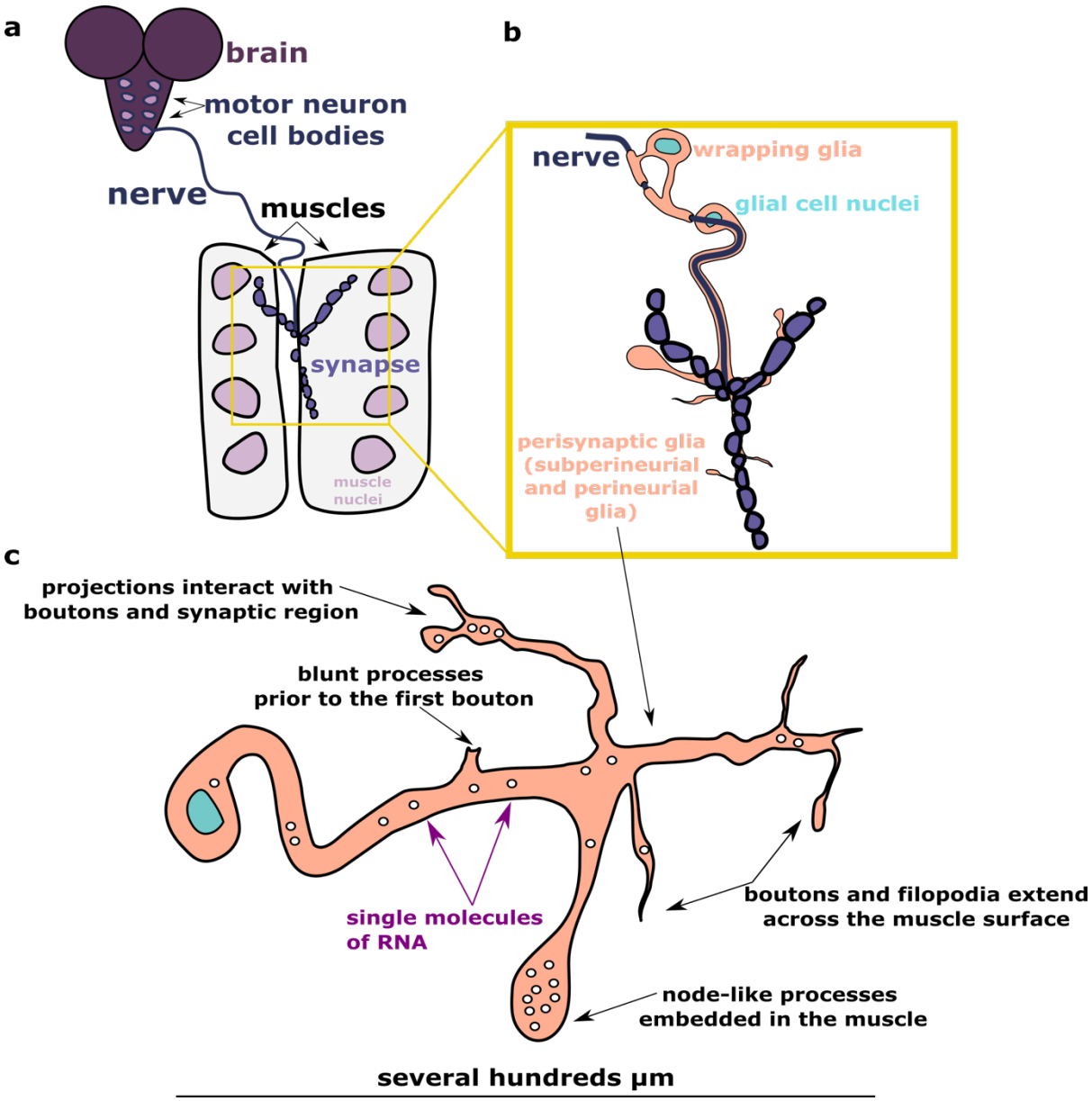

Figure 1-4 Various glial cell morphologies of *Drosophila* NMJ

a) The location of the NMJ synapse with respect to the *Drosophila* CNS. b) The glial cell types present in the *Drosophila* PNS. WG wrap in between the axon bundles. Both the surface glia and the WG are described to make projections to the *Drosophila* NMJ in the literature, but the WG projections are reported to be very small and stop before the synapse area. These observations were made at the larval synapse by the Auld lab [121]. c) A visual representation of the types of processes formed by perisynaptic glia observed by the Auld lab at the NMJ [121]. Some of these resemble bouton structures made by the axon terminal. These glia can extend over several hundreds of µm. Localisation of mRNA is shown at significant distances from the cell body. Local translation could play roles in the functions of those glia at the NMJ.

1.3.3 *Drosophila* and the tripartite synapse

The tripartite model of the synapse (pre-synaptic, post-synaptic and associated glia) found in mammals is also conserved in *Drosophila*. A tripartite synapse model has been first proposed in adult *Drosophila* and it was shown to exhibit similar morphological and functional properties to the ones described previously for the mammalian tripartite synapses [136]. This model was established for the adult Dorsal Longitudinal Muscle (DLM) neuromuscular synapse, and the presence of the features previously observed for the mammalian tripartite synapse, like the regulation of extracellular glutamate and glial calcium transients evoked by synaptic activity, was confirmed [136]. Furthermore, an equivalent glial cell type to the PCSs, named PPG – Peripheral Perisynaptic Glia – has been identified and described in adult *Drosophila*, and it has been noted that the morphology and functions of these cells are different in larvae and in adults [137]. Glia were labelled using Glutamine Synthetase 2 (Gs2), an enzyme in *Drosophila* which is homologous to Glutamine Synthetases in mammals [138]. The tripartite nature of the synapses was presented in different adult NMJs, and glial labelling closely followed the neuronal labelling, as is expected for a tripartite synapse. The larval NMJs, however, showed different morphologies, and the glia were not as closely associated with the neurons as in the adults, but more embedded in the muscle, and surrounding the NMJ synapse [121, 137].

Various functions of glia at the *Drosophila* tripartite synapse were also examined. Exosomes released by SPG, containing miR-274, were found to be incorporated into the motor neurons. This resulted in stimulation of bouton formation by downregulation of expression of the receptor tyrosine kinase pathway inhibitor, *Sprouty*, in turn enhancing signalling via MAPK and promoting cell growth [139]. This process is important in the NMJ response to hypoxia, making the miR-274 somewhat of a

“gliotransmitter”, which enables communication between the glia and the tracheal cells. It was additionally found that under hypoxic conditions, the fine processes of the NMJ glia enter the NMJ boutons [140]. Sima, the hypoxia-induced factor, activates *wingless* in glia, similarly to what was described before [132]. This activation leads to the reorganisation of the NMJ boutons as a response to hypoxia [140]. The effects of heat shock (HS) were also studied on the tripartite synapse at the DLM. Flies treated with HS lost the ability to fly, and displayed neuronal, glial and muscle degeneration. When HSP23, a small HS protein, was overexpressed in the muscle, protection against HS was provided in a cell-autonomous manner for the muscle, and in a nonautonomous manner for neurons and glia [141].

1.3.4 *Drosophila* glia: summary

Could *Drosophila* offer a window into the molecular roles of glia in synaptic plasticity? Undeniably, the extensive molecular characterisation already present in the literature, and the experimental tractability of *Drosophila* NMJ are both tempting alternatives to the complexity and comparative inaccessibility of the vertebrate NMJ synapses when it comes to their molecular manipulation, particularly the lack of cell-specific molecular markers which could allow for the isolation or morphological characterisation of these cells [100]. The roles of glia at the NMJ are highly conserved, and the fly system can yet again be exploited for its experimental tractability and high evolutionary conservation of basic functions. Despite their varied morphologies, *Drosophila* glia at found at synapses seem to exhibit many functions reminiscent of those observed in mammalian tripartite synapse studies. This suggests that *Drosophila* could serve as a promising parallel model to study glial impairment in motor neuron and neurodegenerative diseases to an unprecedented molecular level. The capacity of

Drosophila as a model system to enable the study of the tripartite synapse and the synapse-associated glia has not been exhausted, with both *Drosophila* larvae and adults constituting great model systems for investigating mRNA localisation.

1.4 mRNA localisation in the nervous system

1.4.1 mRNA localisation in neurons

The importance of RNA processing in the regulation of gene expression in health and disease has been underestimated for a long time. Significant focus has traditionally been placed on the regulation of transcription and the very process of translation, with the regulation of mRNA behaviour being eclipsed by those two. The importance of RNA localisation has been noted as early as 1929, when it has been described to have a key role in developmental biology and organising the anterior-posterior polarity of insect eggs and embryos [142]. RNA localisation, however, only gained more interest in the 1980's when a series of studies were conducted which concluded that mRNA localisation and localised expression regulate *Drosophila* embryogenesis and result in the formation of intricate expression patterns, responsible for the establishment of the future body plan of the animal [143-147].

With time, it became clear that embryogenesis is not the only process in which RNA localisation plays an instructive role. Particularly, a hypothesis has been formed that mRNA localisation might play an important role in the development and functioning of the nervous system. Why was this suspected? Neuronal morphology distinguishes them from other cell types. Particularly, the existence of a long axon, which can extend up to one meter in the human sciatic nerve, and highly branched neurites, which also reach far from the cell body, point to the possibility of local translation [148]. The

studies of synaptic plasticity solidified this hypothesis. It has been hypothesised that the often-rapid changes occurring at the synapses would require the local presence of mRNAs, ready to be translated to respond to stimulation; the synapse would be much less adaptable and plastic were it to wait for the mRNA to be produced in the soma and transported all the way along the axons. Several high-profile reviews summarised these hypotheses [11, 149-154].

1.4.2 mRNA localisation in glia

RNA localisation studies in the nervous system have been largely focused on neurons and mostly omitted the other key player: glia, with the notable exception of oligodendrocytes. Glia are a cell type that constitutes between 10–20% of the *Drosophila* nervous system and 50%, or possibly more, of human brain cells [110]. Even in *Drosophila*, where glia constitute a smaller percentage of the nervous system cells, mutations in *repo*, the pan-glial transcription factor responsible for gliogenesis, are embryonic lethal [155]. How come that for such an abundant and vital cell type, glia have remained so underappreciated in the nervous system, often overshadowed by neurons in past studies? Perhaps research initially gravitates towards more immediately noticeable or accessible players, like neurons. Yet, when these focal points fail to provide comprehensive answers, the scope broadens, which is precisely the trend recently observed with increased attention to glia and glial mRNA localisation [1, 21, 34, 73, 74, 156].

As previously discussed, glial cells can display a range of morphologies, ranging from immune-cell like microglial cells to elongated and myelinating oligodendrocytes and Schwann cells, but not all of their detailed roles in nervous system function and development are established [157]. In particular, a parallel could be drawn between

neurons and the elongated glia which accompany them to their synapses, as their somas might also be a significant distance away from their furthermost processes. This could suggest that local mRNA translation might also play a significant role in the largely unknown glial functions at synapses. For the purpose of this section, the term “glia” will be used to describe glial cells associated with synapses and displaying morphologies similar to neurons.

Most early mRNA localisation studies were focused on mRNA localisation in neurons, and glia were often considered a “contaminant”, which can clearly be seen when reading reviews describing those studies [158]. Despite this, localised mRNAs have been observed in glial cells very early into the development of in situ hybridisation (ISH) techniques [159], sometimes being the main focus of the study, and sometimes in concert with observations made in neurons. Early studies examined Schwann cells and oligodendrocytes because of their unique myelinating properties.

The earliest of these studies demonstrated that, although most protein synthesis occurred in the perinuclear regions, localised RNAs and protein synthesis were also observed in the Schwann cell and oligodendrocyte processes [160, 161]. ISH has shown that in initial stages of myelination in Schwann cells and oligodendrocytes, the MBP, myelin basic protein, was indeed accumulated in the perinuclear region, but as myelination proceeded, the MBP mRNA was found localised away from the nucleus [162, 163]. Similar localisation has been shown for astrocytes and radial glia in the embryonic brain for GFAP [86, 163]. Moreover, a specific 3' UTR (untranslated region) of the MBP mRNA has been identified to be necessary for its transport and localisation, later named A2 response element (A2RE) because of its binding to the heterogenous ribonucleoprotein particle A2 (hnRNP A2) which mediates its transport

along the microtubule cytoskeleton towards the myelin-producing compartments in the oligodendrocyte processes [164-166]. Subsequently, the mRNA for another myelin-localised protein, myelin associated oligodendrocyte basic protein (MOBP), was also found to contain a similar RNA sequence to that of A2RE [167].

Subsequent research on these matters resulted in identification of several mechanisms by which mRNAs could be transported towards the myelinating glial cell periphery, particularly in oligodendrocytes. One of the first observations was that the movement of MBP mRNA in oligodendrocytes is microtubule, but not microfilament dependent, and kinesin is necessary for that process [168]. These observations together with further studies led to the development of a robust model, reviewed by Carson and colleagues, which is presented in Figure 1-5 [169].

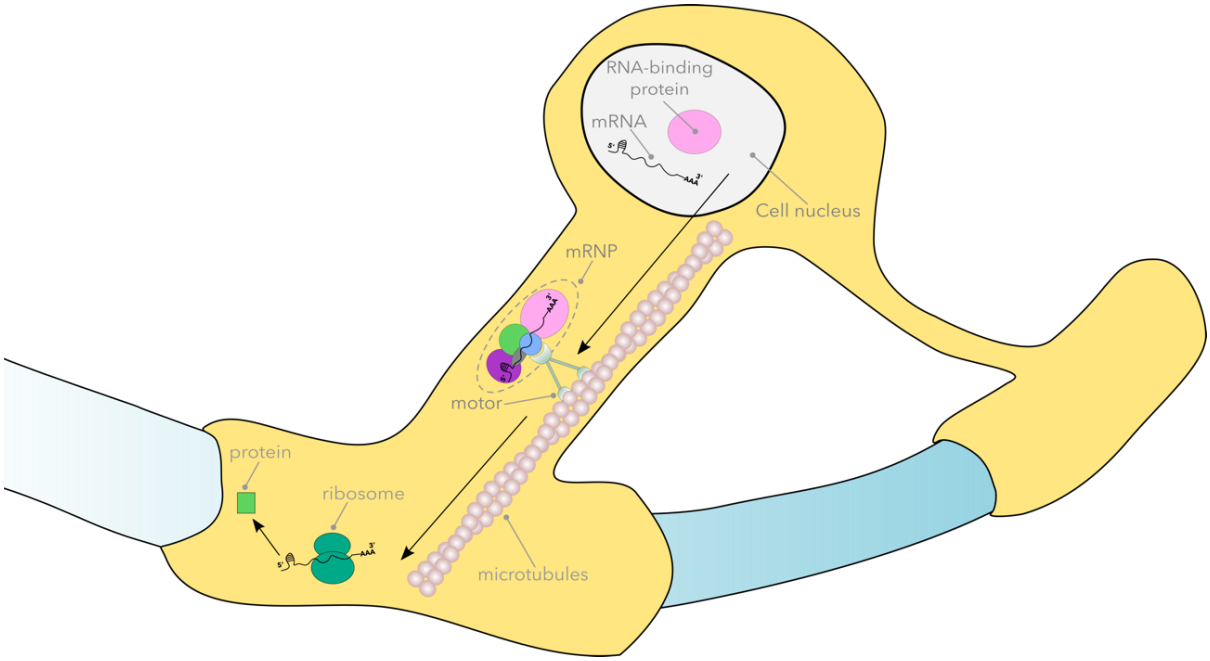

Figure 1-5 mRNA trafficking in glia – a generalised overview

A nascent mRNA is bound in the nucleus by an RNA-binding protein (RBP), such as hnRNP A2 in oligodendrocytes, via a 3′UTR response element. Other well-known RBPs have been identified in dendrites and neuronal growth cones, such as zipcode binding protein 1 (ZBP1) or IMP1 (IGF2 mRNA-binding *protein* 1). Yet, their roles in trafficking mRNAs other than MBP in glia are uncertain, though plausible. The transport of the mRNA-RBP complex out of the nucleus is followed by the assembly into messenger ribonucleoprotein (mRNP) granules in the cytoplasm. Motor proteins, such as kinesin, transport these granules along microtubules (MTs) towards the site of translation, away from the cell body. There, localised translation machinery is used to produce the necessary protein.

In this model, the MBP mRNAs interact with hnRNP A2 by their A2RE, which causes the shuttling of hnRNP A2 out of the nucleus. In the cytoplasm, the hnRNP A2 with its bound mRNA is assembled into granules which get transported to the myelin compartment by a dual kinesin-dynein motor mechanism, kinesin acting as the anterograde motor transporting the granules away from the cell body, and dynein acting as the retrograde motor, mediating the transport towards the cell body. Finally, it has been shown that translation machinery is present in the oligodendrocyte processes and hence it has been hypothesised that the trafficked mRNA is

translationally repressed during transport, and unrepressed once it reaches its destination [170]. Further studies have been conducted to identify additional components of this system, and the question of the regulation of mRNA localisation in oligodendrocyte myelination continues to be explored nowadays [171-173].

1.4.3 *Drosophila* as a model to study mRNA localisation in glia in disease

One of the main difficulties in the study of compartment-specific mRNA localisation and translation, especially in cells like PSCs, is that they are physically connected to neurons and cannot be easily isolated [100]. Therefore, the possibility of contamination in those datasets is high, even when FACS sorting is used. However, it is likely that elongated and polarised cells like neurons, astrocytes, radial glia and others transport and transcribe a similar set of transcripts at their periphery [47]. Therefore, the *Drosophila* larval NMJ is likely to be a good model to study common aspects of mRNA localisation in several different types of synaptic glia, like astrocytes or PCSs, to understand the basic mechanisms of the fundamental molecular crosstalk between the neuron and any type of a glial cell at the synapse.

Drosophila is already an excellent experimental model that offers great possibilities for studying mRNA localisation in the context of disease, including Amyotrophic Lateral Sclerosis (ALS) [174, 175]. Glial expression of mutant and wild type hSOD1s (human Superoxide Dismutase 1) whose mutations are heavily linked to ALS, impaired the performance of flies in a climbing assay and reduced their motor ability [176]. Interestingly, in mice, SOD1 interaction with G3BP1 (Ras GTPase-activating protein-binding protein) was found to alter stress granule dynamics, producing pathological cytoplasmic inclusions in motor neurons [177]. In one study, SOD1 was found to be localised to RNA-rich stress granules in mice spinal cord tissue and in HeLa cells, but

SOD1 itself did not bind any mRNA molecules. This could suggests that SOD1 impacts stress granules, including, RNA dynamics and splicing, without binding RNA directly [178]. It would be interesting to see if hSOD1s mRNA localises to synapses and is locally translated by glia in *Drosophila*, and if hSOD1 is present in stress granules in *Drosophila* glia.

Similar observations were made regarding Tar DNA-binding protein (DNA – deoxyribonucleic acid) an RBP linked to ALS. It was shown that overexpressing *Drosophila* TDP-43, the fly homologue of this protein, in glial cells resulted in accelerated fly death and age related disfunction. Both knockdown and overexpression of *Drosophila* TDP-43 influence the mRNA levels of the glutamate transporters EAAT1 and EAAT2 [179]. These results were further expanded when it was found that expressing mutated TDP-43 resulted in different responses in motor neurons versus glia, both of which, however, can result in similar phenotypic defects related to locomotor impairment [180]. The molecular basis of the glial versus neuronal impairment has been hypothesised to be due to TDP-43 regulating different mRNA targets. This idea is supported by the fact that TDP-43 is localised to the nucleus in motor neurons but in glial cells it localises to cytoplasmic puncta.

1.5 Identification of 19 potential glial-protrusion localised mRNAs

In a recent study performed in the Davis laboratory, various transcripts were identified by smFISH to be found to be localised to the area near the neuron at the NMJ [181]. In this screen, selected lines from the Cambridge Protein Trap Insertion (CPTI) collection were used [182]. 3rd instar *Drosophila* larvae from 200 of these lines were imaged to generate a database of expression patterns of different proteins fused to Yellow Fluorescent Protein (YFP) in the larval nervous system. Additionally, smFISH

probes were designed against the mRNA sequence of YFP fused to those proteins, simultaneously enabling the visualisation of their respective mRNAs.

The work of Joshua Titlow and Ana Palanca Cuñado focused on the PNS and the NMJ. As discussed previously, this is a well-known and an easily accessible synapse in the 3rd instar *Drosophila* larvae [183, 184]. Many proteins and their mRNAs were found to be expressed at the NMJ, including nineteen mRNAs which appeared to be present nearby the NMJ, but not specifically in the axon terminal or the postsynaptic density (Figure 1-6). These were: *nervana 2* (*nrv2*), *Gliotactin* (*Gli*), *Flotillin 2* (*Flo2*), *Cdc42-interacting protein 4* (*Cip4*), *CG1648* (*CG1648*), *lost* (*lost*), *CG42342* (*CG42342*), *Vacuolar H+-ATPase 55kD subunit* (*Vha55*; ATPase - adenosine triphosphatase, ATP - adenosine triphosphate), *Na pump α subunit* (*Atpα*), *Neuroglian* (*Nrg*), *Lachesin* (*Lac*), *α Catenin* (*α-Cat*), *Protein disulfide isomerase* (*Pdi*), *sidekick* (*sdk*), *karst* (*kst*), *coiled* (*cold*), *short stop* (*shot*), *Gs2* and *Orosomucoid 1-like* (*ORMDL*). It has been hypothesised that these proteins might be present in the NMJ glia, particularly since some of them are well known glial markers, like Gs2 and nrv2 [118, 137]. Table 1-1 showcases these results.

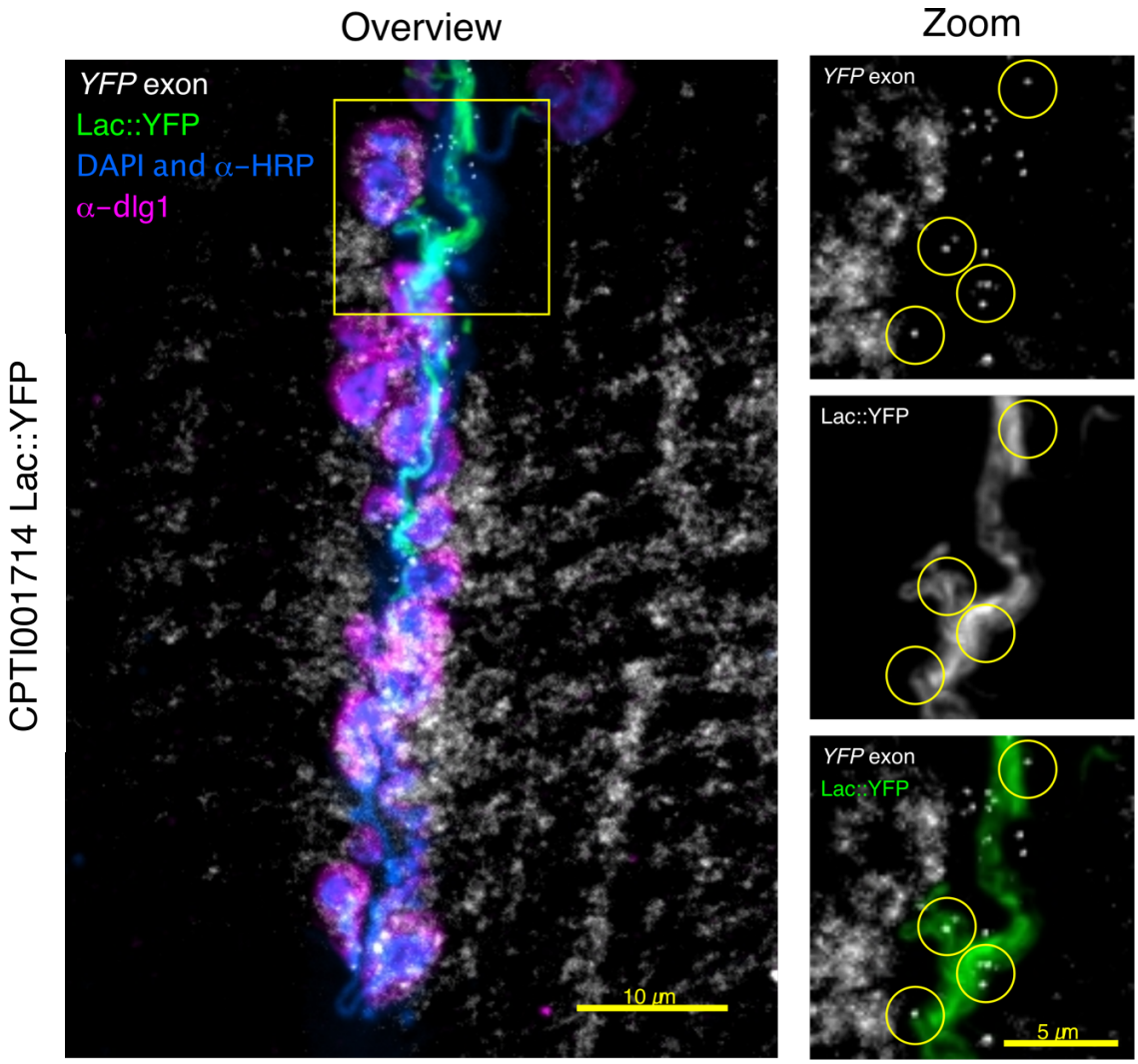

Figure 1-6 Sample image of the larval NMJ from the CPTI screen

Confocal images of a *Drosophila* 3rd instar larval NMJ from the Lac protein trap line, Lac::YFP line. In the "Overview" image (left, scale bar - 10 μm), the yellow square region of interest (ROI) corresponds to the areas enlarged in the remaining panels (right, labelled "Zoom", scale bar 5 μm, see label in the top left for details of what is presented). The NMJ has been stained with 4′,6-diamidino-2-phenylindole (DAPI) and α-Horseradish Peroxidase (α-HRP) antibody conjugated to Alexa 405 fluor (blue) to visualise nuclei and neurons, respectively, and α-dlg1 detected with a secondary Ab labelled with Alexa 568 (magenta) to visualise the postsynaptic density. α-*YFP* exon probe was used to see the mRNA for the proteins fused to YFP (Atto 633, white). In "Zoom" panels, yellow circular ROIs highlight areas rich in molecules of mRNA which seem to overlap with the protein signal. Lac protein seen through the YFP signal from the CPTI collection (Lac::YFP, green) makes an unusual pattern which does not directly match α-HRP or α-dlg1. Such pattern has been noted for nineteen genes, including this one. It was suggested that these could be glial proteins which also have their mRNAs localised to fine glial projections at the NMJ. Data generated by Dr Ana Palanca Cuñado.

Table 1-1 Summary of relevant NMJ scoring from the CPTI screen

Gene symbol	Gene name	CPTI Line ID	Protein in glia?	RNA in glia?	GO molecular function/Biological Process
nrv2	*nervana 2*	CPTI001455	yes	yes	cation transmembrane transporter activity, ATPase activator activity, sodium:potassium-exchanging ATPase activity
Gli	*Gliotactin*	CPTI002805	yes	yes	carboxylic ester hydrolase activity, neurexin family protein binding, signalling receptor activity
Flo2	*Flotillin 2*	CPTI001427	yes	yes	structural molecule activity
Cip4	*Cdc42-interacting protein 4*	CPTI003231	yes	yes	protein binding, phospholipid binding, GTPase activating protein binding, lipid binding
CG1648	*CG1648*	CPTI100012	yes	yes	-
lost	*lost*	CPTI002437	yes	yes	pole cell development, pole plasm mRNA localisation, pole plasm oskar mRNA localisation
CG42342	*CG42342*	CPTI000033	yes	yes	ECM structural constituent
Vha55	*Vacuolar H^+-ATPase 55kD subunit*	CPTI002645	yes	yes	rotational mechanism, ATP binding, proton-transporting ATPase activity
Atpα	*Na pump α subunit*	CPTI002636	yes	yes	cation transmembrane transporter activity, ATP binding, sodium:potassium-exchanging ATPase activity
Nrg	*Neuroglian*	CPTI002761	yes	yes	calcium ion binding, cell adhesion molecule binding
Lac	*Lachesin*	CPTI001714	yes	yes	protein homodimerisation activity
α-Cat	*α Catenin*	CPTI002408	yes	yes	actin filament binding, cytoskeletal protein binding, actin binding, protein binding, cadherin binding, structural molecule activity
Pdi	*Protein disulfide isomerase*	CPTI002342	yes	yes	peptide disulphide oxidoreductase activity, protein disulphide isomerase activity
sdk	*sidekick*	CPTI000688	yes	yes	compound eye cone cell differentiation, homophilic cell adhesion via plasma membrane adhesion molecules, negative regulation of photoreceptor cell differentiation, pigment cell differentiation
kst	*karst*	CPTI001728	yes	no	cytoskeletal protein binding, protein binding, microtubule binding, phospholipid binding, actin binding
cold	*coiled*	CPTI001277	yes	no	establishment of BBB, maintenance of BBB, septate junction (SJ) assembly
shot	*short stop*	CPTI001962	yes	yes	calcium ion binding, cytoskeletal protein binding, actin binding, protein binding, structural molecule activity, microtubule binding
Gs2	*Glutamine synthetase 2*	CPTI001918	yes	yes	glutamate-ammonia ligase activity
ORMDL	*Orosomucoid 1-like*	CPTI002636	no	yes	cellular sphingolipid homeostasis, ceramide metabolic process, negative regulation of ceramide biosynthetic process

Summary of the scoring results from the Davis lab screen for all the CPTI lines of genes which had either the protein-YFP or the *YFP* mRNA localised to the NMJ in a pattern suggesting their presence in the glia. Nineteen lines corresponding to nineteen different proteins have been hypothesised to contain either protein or RNA in the NMJ glia. Where available, gene ontology (GO) molecular function from FlyBase (http://flybase.org/) has been specified, and where that was unavailable, the biological process information has been specified (underlined). The space has been left empty where neither was available. Data generated by Dr Joshua Titlow and Dr Ana Palanca Cuñado.

1.6 Thesis objectives

The paucity of information regarding glia and mRNA in *Drosophila* in general, and the preliminary data collected in the Davis laboratory, provide an obvious starting point for my thesis project, the goal of which is to explore mRNA localisation in larval PPG of the NMJ, using techniques like smFISH [185]. The accessibility and the ease of genetic manipulations of the *Drosophila* larval NMJ makes it an ideal model to label these glia, observe their morphology and look for mRNAs which are expressed at the synapse. Membrane targeted fluorescent proteins under the pan-glial promoter, Repo transcription factor, clearly label synaptic glia at the *Drosophila* NMJ; they display polarity, extending processes and forming boutons [121]. One can then try to understand how mRNA localisation is linked to structural synaptic plasticity using other well-established *Drosophila* neuroscientific techniques to further explore the roles of mRNA localisation and glial cells at the *Drosophila* NMJ. Thus, the overarching goal of my thesis is to investigate how *Drosophila* larval NMJ glia modulate structural synaptic plasticity, and whether mRNA localisation could impact this process.

Below I list specific questions which I would like to explore in my thesis.

Question 1: Which of the candidate transcripts are indeed localised to *Drosophila* NMJ glial periphery?

Motivation: This question allows me to understand the localisation of the candidate mRNAs of interest with respect to glial membrane labelling, which was not present when the original observations were made in the lab. Thus, I could confirm or refute the hypothesis that these mRNAs are localised to the NMJ glial periphery.

Question 2: Which of these genes are functionally required in glia for the correct development of the larvae and the NMJ?

Motivation: Localised mRNAs could have different roles depending on the developmental timeline during which they are translated. Showing that some of these localised mRNAs affect the morphology of the developing synapse, or the overall viability or anatomy of the larvae, could shed light on the regulation of these developmental process.

Question 3: Are any of these genes functionally required in glia for structural synaptic plasticity?

Motivation: This question is one of the most fundamental ones to answer because of how little is known about perisynaptic glia in the PNS and the role of the localised RNAs in plasticity of the motor neuron, especially in the context of debilitating illnesses like motor neuron diseases, particularly ALS [34]. It would be an exciting discovery to show that localised mRNAs in glia could participate in modulation of motor neuron synapse behaviour.

Question 4: Are any of these genes necessary for the regulation of the larval movement?

Motivation: High level observations such as impairment of movement are a common manifestation of underlying molecular changes. If the genes of interest are needed in glia for larval crawling, a direct connection can be made between the NMJ glia and movement, thus rendering them necessary for correct structural synaptic plasticity.

Question 5: Which glial cells extend their projections to the NMJ, and what is the relationship between the candidate transcripts and these cells?

Motivation: Despite numerous reports, which specific subtypes of glial cells make their projections to the *Drosophila* NMJ is a point of contention [111]. It would be interesting to confirm it, which would allow for visual inspection of the localisation of mRNAs of interest with respect to these cells, and potential further functional examinations.

CHAPTER 2

2 Materials and Methods

2.1 Fly stocks

Drosophila melanogaster flies utilised in my research were reared on standard cornmeal-agar food and raised in 18°C or 25°C incubators with 12-hour day-night cycle. All stocks were purchased from Drosophila Genomics and Genetic Resources (https://www.dgrc.kit.ac.jp/, DGRC), Vienna Drosophila Resource Center (https://shop.vbc.ac.at/vdrc_store/, VDRC) and Bloomington Drosophila Stock Center (https://bdsc.indiana.edu/index.html, BDSC). Desired stocks were then crossbred from these stocks, or, where indicated, provided by collaborators. Please refer to Table 2-1 for a comprehensive list of all lines employed in this study.

To label glial cells in as described in Chapter 3 experiments, a crossbreeding strategy was employed to obtain the following stock: UAS-mCD8-mCherry/CyoGFP; Repo>GAL4/Tm6B, Tb (UAS – Upstream Activating Sequence, GFP – Green Fluorescent Protein). This line is henceforth referred to as the Repo>mCherry line. This stock was then crossed with each of the CPTI lines and the offspring were selected based on the presence of YFP and mCherry fluorescence.

To label glia for experiments with RNA interference (RNAi) targeting transcripts of interest in glial cells as described in Chapter 4, a stock was constructed as follows: UAS-mCD8-GFP/UAS-mCD8-GFP; Repo>GAL4/Tm6B, Tb. This line is henceforth referred to as Repo>GFP line. For each RNAi experiment, a homozygous line with a hairpin targeting the coding sequence of the gene of interest and the least number of off-targets was selected. These lines were crossed with the UAS-mCD8-GFP/UAS-mCD8-GFP; Repo-GAL4/Tm6B, Tb line, and the offspring were selected based on

GFP fluorescence and the absence of the Tm6B, Tb phenotype. These lines are henceforth denoted as Repo>GFP, *Transcript*-RNAi lines, where "*Transcript*" is replaced by the ENSEMBL v99 symbol (see Section 2.2) of the candidate transcript of interest [186]. The control for each experiment in this thesis which used any RNAi of any gene of interest in glial cells as marked by Repo-GAL4 was UAS-mCD8-GFP/+; Repo-GAL4/UAS-*mCherry*-RNAi. The control for experiments with knockdown in motor neuron was OK6-GAL4, UAS-mCD8 mCherry/+; UAS-*Luciferase*-RNAi/+. This control is referred to as "OK6>mCherry, *Luciferase*-RNAi" or "OK6>Control".

For experiments described in Chapter 5, 46F-GAL4 and Mdr65-GAL4 were crossed to UAS-mCD8-GFP and made homozygous. All fluorescent driver lines were then crossed to *Lac*-RNAi (VDRC GD 35524). The knockdown experiments for all glial drivers also had their respective controls, all of which were also the given driver line crossed to *mCherry*-RNAi.

Table 2-1 List of *Drosophila melanogaster* stocks used in this project

Line name	Line ID	Line source	Line description
nrv2::YFP	CPTI001455	DGRC	*nervana 2* gene YFP protein trap line (Lowe *et al.*, 2014)
Gli::YFP	CPTI002805	DGRC	*Gliotactin* gene YFP protein trap line
Flo2::YFP	CPTI001427	DGRC	*Flotillin 2* gene YFP protein trap line
Cip4::YFP	CPTI003231	DGRC	*Cdc42-interacting protein 4* gene YFP protein trap line
CG1648::YFP	CPTI100012	DGRC	*CG1648* gene YFP protein trap line
lost::YFP	CPTI002437	DGRC	*lost* gene YFP protein trap line
CG42342::YFP	CPTI000033	DGRC	*CG42342* gene YFP protein trap line
Vha55::YFP	CPTI002645	DGRC	*Vacuolar H+-ATPase 55kD subunit* gene YFP protein trap line
Atpα::YFP	CPTI002636	DGRC	*Na pump α subunit* gene YFP protein trap line
Nrg::YFP	CPTI002761	DGRC	*Neuroglian* gene YFP protein trap line
Lac::YFP	CPTI001714	DGRC	*Lachesin* gene YFP protein trap line
α-Cat::YFP	CPTI002408	DGRC	*α Catenin* gene YFP protein trap line
Pdi::YFP	CPTI002342	DGRC	*Protein disulfide isomerase* gene YFP protein trap line
sdk::YFP	CPTI000688	DGRC	*sidekick* gene YFP protein trap line
kst::YFP	CPTI001728	DGRC	*karst* gene YFP protein trap line
cold::YFP	CPTI001277	DGRC	*coiled* gene YFP protein trap line
shot::YFP	CPTI001962	DGRC	*short stop* gene YPF protein trap line
Gs2::YFP	CPTI001918	DGRC	*Glutamine synthetase 2* gene YFP protein trap line
ORMDL::YFP	CPTI002636	DGRC	*ORMDL* gene YFP protein trap line.
Repo-GAL4	7415	BDSC	Expresses GAL4 in glia [155]
UAS-mCD8-mCherry/cyo-GFP	27391	BDSC	Expresses Cherry red fluorescent protein (RFP) fused to the mouse CD8 extracellular and transmembrane domains for membrane targeting under UAS control.
UAS-mCD8-GFP/cyo-GFP	63045	BDSC	Expresses GFP fused to the mouse CD8 extracellular and transmembrane domains for membrane targeting under UAS control.
cyo-GFP/Gla; tm6, tb/pri	Crossed from BDSC stocks	BDSC	A double balanced stock carrying CyoGFP over Gla on the 2nd chromosome and tm6, tb over prickle on the 3rd chromosome.
nrv2-RNAi	GD960	VDRC	Expresses double-stranded RNA (dsRNA) for RNAi of *nrv2* under UAS control in the pUAST vector pMF3.
Gli-RNAi	GD1735	VDRC	Expresses dsRNA for RNAi of *Gli* under UAS control in the pUAST vector pMF3.
Flo2-RNAi	VSH 330316	VDRC	Expresses dsRNA for RNAi of *Flo2* under UAS control in the WALIUM20 vector.
Cip4-RNAi	GD8513	VDRC	Expresses dsRNA for RNAi of *Cip4* under UAS control in the WALIUM20 vector.
CG1648-RNAi	GD9177	VDRC	Expresses dsRNA for RNAi of *CG1648* under UAS control in the WALIUM20 vector.
lost-RNAi	GD8391	VDRC	Expresses dsRNA for RNAi of *lost* under UAS control in the WALIUM20 vector.
CG42342-RNAi	KK111891	VDRC	Expresses dsRNA for RNAi of *CG42342* under UAS control in the pUAST vector pMF3.
Vha55-RNAi	GD9363	VDRC	Expresses dsRNA for RNAi of *Vha55* under UAS control in the pUAST vector pMF3.
Atpα-RNAi	32913	BDSC	Expresses dsRNA for RNAi of *Atpα* under UAS control in the VALIUM20 vector.
Atpα-RNAi	GD3093	VDRC	Expresses dsRNA for RNAi of *Atpα* under UAS control in the pUAST vector pMF3.

Line name	Line ID	Line source	Line description
Nrg-RNAi	28724	BDSC	Expresses dsRNA for RNAi of *Nrg* under UAS control in the VALIUM10 vector.
Lac-RNAi	GD 35524	VDRC	Expresses dsRNA for RNAi of *Lac* under UAS control in the pUAST vector pMF3.
Lac-RNAi	KK 107450	VDRC	Expresses dsRNA for RNAi of *Lac* under UAS control in the pUAST vector pMF3.
α-Cat-RNAi	KK107298	VDRC	Expresses dsRNA for RNAi of *α-Cat* under UAS control in the pUAST vector pMF3.
Pdi-RNAi	GD13418	VDRC	Expresses dsRNA for RNAi of *Pdi* under UAS control in the pUAST vector pMF3.
sdk-RNAi	GD2553	VDRC	Expresses dsRNA for RNAi of *sdk* under UAS control in the pUAST vector pMF3.
kst-RNAi	33933	BDSC	Expresses dsRNA for RNAi of *kst* under UAS control in the VALIUM20 vector.
cold-RNAi	GD789	VDRC	Expresses dsRNA for RNAi of *cold* under UAS control in the pUAST vector pMF3.
shot-RNAi	28336	BDSC	Expresses dsRNA for RNAi of *shot* under UAS control in the VALIUM10 vector.
Gs2-RNAi	GD 9378	VDRC	Expresses dsRNA for RNAi of *Gs2* under UAS control in the pUAST vector pMF3.
mCherry-RNAi	35785	BDSC	Expresses dsRNA for RNAi of *mCherry* under UAS control in the VALIUM20 vector.
Nrv2-GAL4; UAS-mCD8-GFP/CyoGFP	-	-	Recombined stock which expresses GAL4 in WG and drives expression of membrane targeted GFP, kindly gifted by Prof Rita Teodoro. Based on BDSC stocks 6800 and 63045.
46F-GAL4	-	-	Expresses GAL4 in PG[187]. Gift from Prof Stefanie Schirmeier.
Mdr65-GAL4	50472	BDSC	Expresses GAL4 in SPG.
OK6-GAL4 > UAS-mCD8 mCherry	-	Constructed in the Davis lab	GAL4 expressed in motor neurons, recombined with membrane targeted mCherry.
Imp-RNAi	34977	BDSC	Expresses dsRNA for RNAi of *Imp* under UAS control in the VALIUM20 vector.
Nrx-IV::GFP	CA06597	-	Carnegie collection protein trap for *neurexin IV*, labelled with GFP, kindly gifted by Prof Rita Teodoro[188].
brp::GFP	-	-	Protein trap for *bruchpilot* (brp), labelled with GFP, kindly gifted by Prof Hugo Bellen.
Luciferase-RNAi	35788	BDSC	Expresses firefly Luciferase under the control of UAS in the VALIUM10 vector.

2.2 Fly gene nomenclature

The nomenclature for the fly genes, mRNAs and proteins mentioned in this thesis follows that of ENSEMBL v99, which is also the same convention reflected on FlyBase [186, 189]. Capitalisation of gene and protein full names and symbols is therefore consistent with those resources. Gene full names and symbols are italicised. mRNA transcript symbols are italicised. Protein symbols are not italicised. The nomenclature used for candidate glial-protrusion localised transcripts of interest is summarised in Table 2-2.

Table 2-2 Selected fly gene, mRNA and protein nomenclature used in this project

Full gene name	Gene symbol	mRNA symbol	Protein symbol
nervana 2	*nrv2*	*nrv2* (mRNA)	nrv2
Gliotactin	*Gli*	*Gli* (mRNA)	Gli
Flotillin 2	*Flo2*	*Flo2* (mRNA)	Flo2
Cdc42-interacting protein 4	*Cip4*	*Cip4* (mRNA)	Cip4
CG1648	*CG1648*	*CG1648* (mRNA)	CG1648
lost	*lost*	*lost* (mRNA)	lost
CG42342	*CG42342*	*CG42342* (mRNA)	CG42342
Vacuolar H^+-ATPase 55kD subunit	*Vha55*	*Vha55* (mRNA)	Vha55
Na pump α subunit	*Atpα*	*Atpα* (mRNA)	Atpα
Neuroglian	*Nrg*	*Nrg* (mRNA)	Nrg
Lachesin	*Lac*	*Lac* (mRNA)	Lac
α Catenin	*α-Cat*	*α-Cat* (mRNA)	α-Cat
Protein disulfide isomerase	*Pdi*	*Pdi* (mRNA)	Pdi
sidekick	*sdk*	*sdk* (mRNA)	sdk
karst	*kst*	*kst* (mRNA)	kst
coiled	*cold*	*cold* (mRNA)	cold
short stop	*shot*	*shot* (mRNA)	shot
Glutamine synthetase 2	*Gs2*	*Gs2* (mRNA)	Gs2
Orosomucoid 1-like	*ORMDL*	*ORMDL* (mRNA)	ORMDL

This convention was not followed for the GAL4 driver lines, and all driver line genes are capitalised and not italicised.

2.3 Solutions and reagents

The solutions employed in this study were either prepared and autoclaved by the Department of Biochemistry media kitchen or prepared by me using the solutions provided by the media kitchen. The Haemolymph-Like (HL) salines were prepared following the previously described methods [190, 191]. A list of the solutions used in this thesis can be found in Table 2-3.

Table 2-3 List of solutions used in this project

Solution	Composition
HL3 0.3 mM Ca^{2+}+	NaCl 70 mM, KCl 5 mM, $MgCl_2$ 20 mM, $NaHCO_3$ 10 mM, trehalose 5 mM, HEPES 5 mM, sucrose 115 mM, Ca^{2+} 0.3 mM, pH 7.2
HL3 1 mM Ca^{2+}	NaCl 70 mM, KCl 5 mM, $MgCl_2$ 20 mM, $NaHCO_3$ 10 mM, trehalose 5 mM, HEPES 5 mM, sucrose 115 mM, Ca^{2+} 1 mM, pH 7.2
HL3 high K^+	NaCl 40 mM, KCl 90 mM, Ca^{2+} 1.5 mM, $MgCl_2$ 20 mM, $NaHCO_3$ 10 mM, trehalose 5 mM, HEPES 5 mM, sucrose 5 mM, pH 7.2
10x PBS (phosphate-buffered saline)	1.37 M NaCl, 27mM KCl, 100mM Na_2HPO_4, 20mM KH_2PO_4, pH 7.4
PBSTx	PBS 1x, 0.3% Triton X (v/v)
20xSSC (saline sodium citrate)	20g NaCl, 100.5g Tri-Sodium Citrate, pH 7.0 in 1L
TE	10 mM Tris-HCL, 1mM EDTA, pH 8.0
10X TAE Buffer	0.4 M Tris, 10 mM EDTA (pH 7.5), 1.2% (v/v) glacial acetic acid

2.4 Biochemical techniques

For all probes and antibodies described in this section, the symbol α means “anti” and denotes that that probe or antibody target whatever follows the symbol.

2.4.1 Reverse Transcription - Polymerase Chain Reaction (RT-PCR)

To investigate the CPTI insertion in the ORMDL::YFP line, an RT-PCR experiment was carried out. RNA extraction from 3rd instar wandering larvae was performed using the Cytiva Life Sciences™ (formerly GE Healthcare Life Science) illustra™ RNAspin Mini Isolation Kit. RNA concentration was measured using the NanoDrop spectrophotometer, and the reverse transcription reaction was performed using the RevertAid First Strand cDNA Synthesis Kit (Thermo Scientific). 10% of the reverse

transcription product was used in the PCR reaction with the Taq PCR Kit (NEB) using the primer sequences specified in Appendix Table A-1. The products were run on a 2% agarose gel and visualised using ethidium bromide (Section 2.4.2).

2.4.2 DNA gel electrophoresis

2% agarose concentration was achieved by dissolving agarose powder in 1x TAE buffer and heating, and ethidium bromide was added before the gel set (3 µl per 50 ml of gel). The RT-PCR product was mixed 1:1 with water. 5 µl of 5x gel loading dye (NEB) was added to the mixture which was loaded onto the gel which was run at 100 V in 1x TAE buffer. Ultraviolet (UV) transilluminator was used to visualise the DNA and the product sizes were compared to 1 kb Plus DNA Ladder from NEB loaded in the 1st well.

2.4.3 smFISH probes design

Probes for the smFISH protocol were designed using a protocol described before [192]. A set of oligonucleotides (24 for *ORMDL*, 48 for *Lac* exon, 48 for *Lac* intron, 28 for *YFP*) against the target sequence was composed using LGC Biosearch Technologies' Stellaris® RNA FISH Probe Designer. The oligonucleotides were pooled and elongated overnight at 37ºC with a ddUTP conjugated to a desired dye (Atto 633 for α-*YFP* and α-*Lac* exon probes, and Alexa 568 for α-*Lac* intron, α-*Lac* exon and α-*ORMDL* probes) using terminal deoxynucleotidyl transferase enzyme from Life Technologies (Thermo Fisher Scientific). The fluorescently labelled oligonucleotides were then purified by Zymo Research® Ethanol DNA Purification kit and eluted in TE buffer, after which their concentration and degree of labelling were measured using a NanoDrop spectrophotometer. The probes were diluted with TE

buffer to 25μM concentration. All probe sequences can be found in Appendix Table B-1.

2.5 Microscopy techniques

2.5.1 smFISH on the *Drosophila* larval fillet

The mRNA smFISH technique was performed following established protocols [185]. In brief, wandering 3rd instar larvae were dissected in HL3 solution containing 0.3 mM Ca^{2+} as previously described to obtain a larval fillet exposing the NMJs [109, 183]. The samples were fixed at room temperature for 30 minutes using 4% paraformaldehyde in phosphate-buffered saline (PBS) supplemented with 0.1% Triton-X (PBSTx). Subsequently, the samples were subjected to two rounds of permeabilisation for 20 minutes each in PBSTx at room temperature.

Pre-hybridisation was performed by incubating the samples in wash buffer (2x SSC (saline sodium citrate), 10% formamide obtained from Sigma-Aldrich, F9037) at 37ºC for 20 minutes. The hybridisation step followed, where the samples were incubated overnight at 37ºC in a hybridisation buffer composed of 10% formamide, 10% dextran sulphate (Alfa Aesar, J62787.18), 250 nM of the smFISH probe(s), and α-Horseradish Peroxidase (α-HRP) (refer to Table 2-4 and section 2.5.2) in 2x SSC. Subsequently, the samples were rinsed in wash buffer and counterstained with 4′,6-diamidino-2-phenylindole (DAPI) at a dilution of 1:1000 from a stock concentration of 0.5 mg/mL in wash buffer. The counterstaining step lasted for 45 minutes at room temperature.

After counterstaining, the samples underwent a 45-minute wash in wash buffer at room temperature. Following the wash, the samples were incubated in Vectashield anti-fade mounting medium (Vector Laboratories) adjusted to match the objective's refractive

index for 30 minutes. Finally, the samples were mounted on slides using the mounting medium.

2.5.2 Immunofluorescence (IF) on the *Drosophila* larval fillet

The 3rd instar larvae were dissected and prepared according to the smFISH protocol. Following dissection, the larvae were blocked in blocking buffer (PBSTx, 1.0% Bovine Serum Albumin (BSA)) at 4ºC for 1 hour. Subsequently, the samples were incubated overnight at 4ºC with the primary antibody (refer to Table 2-4) in the blocking buffer. On the following day, the samples were washed for approximately 1 hour and then incubated with the secondary antibody solution (conjugated to Alexa Fluor 488, 568, or 647) at a 1:500 dilution from Life Technologies. The secondary antibody solution was prepared in PBSTx and contained DAPI (1:1000 from a 0.5mg/mL stock), and this incubation lasted for an 1 hour. Afterward, the samples were washed for 45 minutes in PBSTx at room temperature and incubated in Vectashield. Finally, the samples were mounted following the steps outlined in the smFISH protocol (2.5.1).

Table 2-4 List of primary antibodies used in this project

Antibody	Target	Source	Species	Dilution
α-dlg1	Disks large, a post-synaptic scaffolding protein	Developmental Studies Hybridoma Bank, https://dshb.biology.uiowa.edu/	Mouse	1:200
α-HRP conjugated to Alexa 405, 488, 568 or 647	Neurons [193]	Jackson Immuno Research Europe Ltd	Goat	1:100

2.6 Image acquisition and processing

2.6.1 Microscopy protocol

In the smFISH experiments described in Chapter 3, the larvae were subjected to dissection, fixation, and staining with DAPI, α-HRP antibody labelled with DyLight 405 dye, and α-*YFP* exon probe labelled with Atto 633 dye, following the smFISH protocol.

A minimum of 3 larvae and 15 NMJs were evaluated for these experiments. For the unstimulated and stimulated NMJ experiments in Chapter 4, a minimum of 5 control larvae and 5 RNAi larvae were used for each experiment. The samples were fixed, stained with DAPI, α-HRP antibody labelled with Alexa 647 dye, and α-dlg1 antibody as described in the IF protocol (see section 2.5.2). The glial membrane was labelled with Repo>GFP. For Chapter 5, please refer to specific figure captions, as channels imaged vary. All prepared specimens were imaged using either an inverted Olympus FV3000 laser scanning confocal microscope or Olympus CSU-W1 SoRa laser spinning disk confocal microscope. The imaging was performed using specific objectives (60x 1.4NA Oil UPlanSApo objective for FV3000 and 100x 1.51NA Oil UPlanSApo objective, 100x 1.4NA Oil UPlanSApo objective, or 60x 1.51NA Oil UPlanSApo objective for SoRa) and laser units (solid state 405, 488, 568, and 640 lasers for both microscopes).

2.6.2 Image processing

The acquired images were processed using ImageJ software (https://imagej.nih.gov/ij/) [194]. The glial processes at the NMJ, being mostly flat, were analysed by measuring the two-dimensional areas of the GFP-labelled glial membranes, which included sections of non-synaptic motor axon branches from full Z-stack 2D projections and glial membranes near the synaptic lamella [121]. The neurite areas were measured similarly but using α-HRP labelling. The measurements were conducted using the linear auto-contrast, auto-threshold, and area measurement functions of NIH (National Institutes of Health) ImageJ [195].

2.7 Image features quantification

2.7.1 NMJ morphometrics feature quantification

For statistical analysis, R Studio was utilised. Each two-dimensional area measured from each NMJ constituted an independent replicate (denoted as "n"). The specific n values for each genotype and experiment are provided in the corresponding figure legends or Appendix. In the spaced potassium stimulation experiment (see Section 2.8.1) and unstimulated NMJ “ghost bouton” quantification experiments, the average log2 fold change of bouton counts after compared to RNAi controls was quantified and reported. Regarding the areas' quantification, the fold change in glial protrusion area, neurite area, and their ratio upon knockdown of glial protrusion-localised transcripts was calculated. The ratio of the areas was calculated using the following equation:

$$ratio = \frac{\text{glial projection area in } \mu m^2}{\text{motor neuron axon terminal projection in } \mu m^2}$$

For the spaced potassium stimulation experiment (see Section 2.8.1), these calculations were performed in two sets: before and after the potassium activation assay. The average fold change for each gene was determined in each set. Student's t-tests were employed to evaluate significant differences in the data. In the spaced potassium stimulation experiment, the “ghost boutons” were manually quantified. The Wilcoxon rank sum test was performed for statistical analysis of “ghost bouton” numbers. Details of statistical analysis can be found in Section 2.9 The summary statistics can be found in Appendix Table C-1 (unstimulated NMJs areas), Appendix Appendix Table C-2 (stimulated NMJs areas) and Table C-3 (stimulated NMJs “ghost boutons”).

2.7.2 smFISH foci quantification

To count *Lac::YFP* or *Lac* exon smFISH spots in the images, I employed a modified version of Big-FISH analysis [196]. The images were pre-processed to subtract the background, and Laplacian of Gaussian filtering was utilised to further reduce background noise. The threshold intensity for real signal was obtained by manually examining multiple representative spots from three images from the dataset and obtaining a line profile through the centre of each spot. The threshold was then set to half of the intensity of that spot, which resulted in the elimination of most of the noise from the images. The detection of correct smFISH foci was verified visually.

After detecting the RNA smFISH spots in each image using the approach, I correlated their coordinates with their respective "mask" images representing the region of interest (ROI) in that image. The mask images were obtained using the linear auto-contrast, auto-threshold and saving a binary image in ImageJ. This allowed me to calculate the total number of single mRNA molecules in the ROI.

2.7.3 Protein intensity signal quantification

In Chapter 5, Lac::YFP channel images were background subtracted using rolling ball subtraction method (radius = 50px) in ImageJ. Background intensity was obtained by creating five background ROI and quantifying their raw pixel integrated density (RawIntDen) values as well as area in ImageJ, then using these in the following equation:

$$background\ intensity = \frac{RawIntDen}{Area}$$

Mean background intensity was then calculated from individual images' background intensities. For each image, the fluorescence signal intensity of Lac::YFP signal was quantified from maximum pixel values across the Lac::YFP area ROI and then normalised to the mean signal density of background using the following equation:

$$signal\ intensity = \frac{YFP\ RawIntDen - (mean\ background\ intensity * YFP\ area)}{YFP\ Area}$$

2.8 Larval neuroscientific techniques

2.8.1 Spaced High K^+ depolarisation paradigm

The spaced potassium assay (also referred to as "spaced potassium stimulation assay/experiment/protocol" or simply the "stimulation" experiment throughout this thesis) was conducted following established protocols [190, 191, 197]. In summary, the larvae were dissected in 0.3 mM Ca^{2+} HL3 solution and subsequently transferred to 1 mM Ca^{2+} HL3 solution. For each experiment reported in Chapter 4, the larvae in a relaxed state were then subjected to a series of 2 minutes, 2 minutes, 2 minutes, 4 minutes, and 6 minutes washes with high K^+ HL3 solution, with 15 minutes intervals of 1 mM Ca^{2+} HL3 in between [191]. For each experiment reported in Chapter 5, the larvae in a relaxed state were then subjected to a series of three 2-minute washes with high K^+ HL3 solution with 10 minutes intervals of 1 mM Ca^{2+} HL3 in between [197]. Each experiment included a minimum of 5 control larvae and 5 RNAi larvae. Additionally, for Chapter 4 experiments, an internal control stimulation experiment was conducted simultaneously, where Repo>GFP larvae were crossed with UAS-RNAi line targeting the mCherry protein, which is absent in these larvae. In Chapter 5, the controls for each experiment consisted of larvae which were dissected in 0.3 mM Ca^{2+} HL3 solution and immediately fixed ("unstimulated" larvae). The results of each

experiment were compared only to its corresponding internal control. Following the spaced potassium pulses, the larvae were re-stretched, allowed to rest for 30 minutes, and then fixed and labelled according to the IF protocol (2.5.2). Imaging of muscle segments 6/7 in the A2-A5 region was performed for all experiments.

2.8.2 Larval locomotion assay

2.8.2.1 Manual tracking assay

The manual tracking has been performed as described previously [198]. Briefly, larvae were acclimatised to room temperature for 1h before the assay commencement. 5cm apple juice plates were removed from the fridge and left to achieve room temperature. 3rd instar wandering larvae were then isolated and cleaned by washing in ddH_2O with the use of a paintbrush. A mobile phone camera was placed in an elevated position, parallel to the apple juice plate surface. The apple juice plate was placed below the camera and on top of a 'dartboard' paper with concentric rings to facilitate the tracking. A ruler was added next to the plate to obtain scale for further analysis (Figure 2-1 A). 10 larvae per genotype were placed consecutively in the centre of the plate and recorded using the mobile phone camera at 1080p with a frame rate of 30 frames per second for 30 seconds or until they reached the plate edge. The plate was changed after each animal. The obtained videos were then analysed in ImageJ. The videos were converted from video format to image sequences (jpegs). Using the ruler in the videos, the scale was set in ImageJ using Select: Analyse>Set Scale and set to Global to analyse all videos. The larvae were tracked using: Select: Plugins > Tracking > Manual Tracking and clicking on the larvae mouth parts until they reached the plate edge. The tracks were then analysed in RStudio.

2.8.2.2 Automated tracking assay

I analysed larval locomotion behaviours using automated tracking following a modified version of an established approach [199]. 3rd instar wandering larvae were allowed to acclimate to room temperature for 1 hour before being placed in the centre of a 9-cm petri dish containing 1% agarose, with a maximum of five larvae introduced at a time. After an additional 1-minute acclimation period on the stage, the larvae were moved back to the centre of the plate and were recorded crawling freely at 1080p with a frame rate of 30 frames per second. To enhance contrast, white light was illuminated from beneath the dish (Figure 2-1 B). The larvae's movement was tracked using standard tracking mode in BIOImageOperation software (available at https://joostdefolter.info/bio-research) (Figure 2-1 C). Background subtraction with threshold of 0.05-0.1 was used and adapted to achieve visual matching of the tracks detected when compared to the video obtained. Upon the larva reaching the outer perimeter of the dish or colliding with another larva, the tracking was concluded. 5 larvae per genotype were used and 3 replicates were performed per day. The plates were rinsed after each repeat. Each experiment was repeated on 3 separate days.

2.8.3 Crawling assay results quantification and analysis

The output from BIOImageOperation was processed using the suite of 'tidyverse' R packages to calculate locomotion parameters. Tracking results were plotted and again compared with the videos post filtering, and artefactual tracks were removed.

I quantified crawling speed (expressed in centimetres/second, or cm/s), using the following equation:

$$crawling\ speed = \frac{total\ distance\ crawled}{distance\ betweem\ the\ origin\ and\ end\ coordinates}$$

and path straightness, using the following equation:

$$path\ straightness = \frac{\text{total distance crawled (cm)}}{\text{origin coordinate to end coordinate distance (cm)}}$$

The R package 'trajr' was employed to calculate measures of movement linearity and irregularity, which were the measures of frequency of directional change, and the standard deviation of directional change [200].

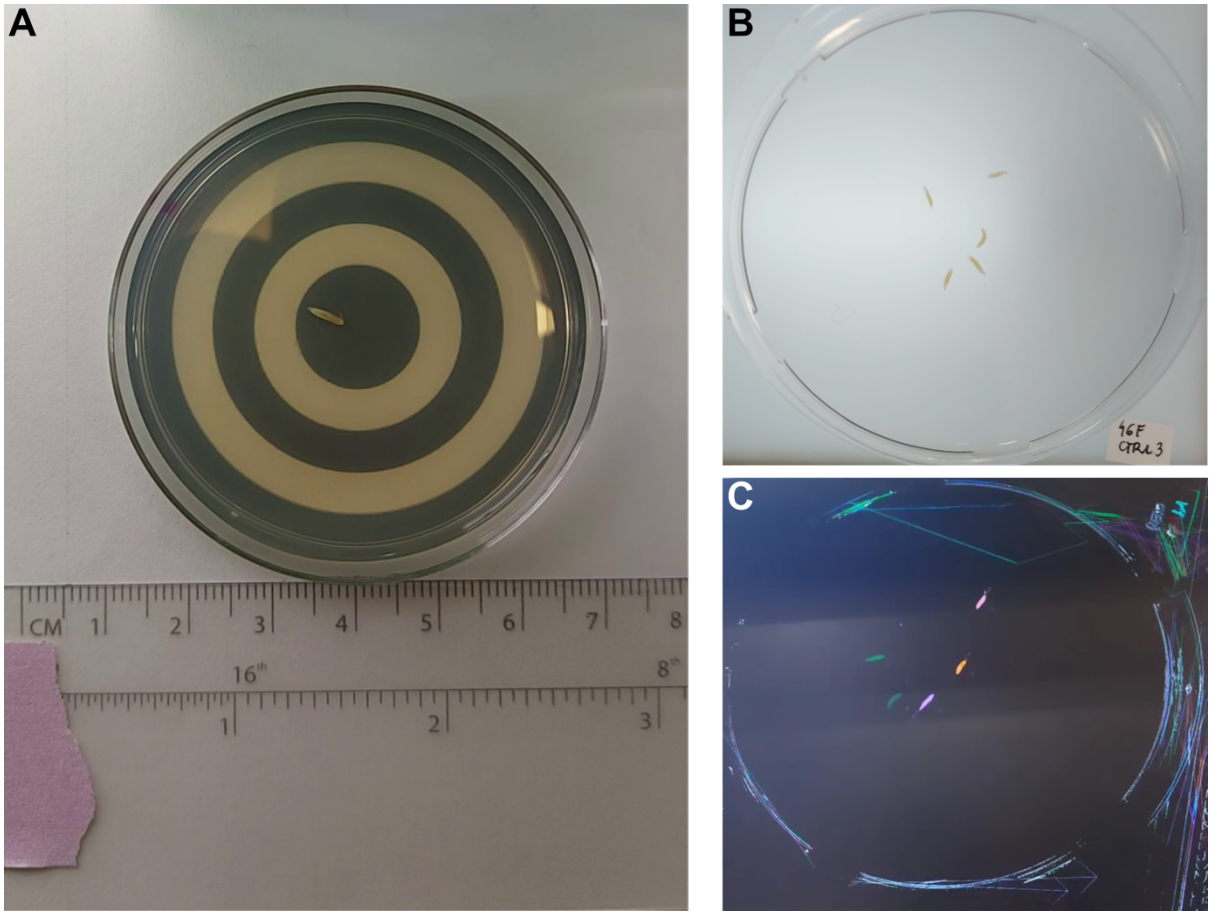

Figure 2-1 Crawling assay setup

A) Manual larval tracking assay stage setup with the “dartboard” paper under the apple juice plate. B) Automated larval crawling assay stage set up with white light illumination below the plate. C) The screen view of the BIOImageOperation software tracking the larvae.

2.9 Statistical analysis

Statistical evaluations were conducted using the R package 'rstatix'. I determined data normality through the Shapiro-Wilk test. I utilised parametric tests such as the t-test or non-parametric tests like Wilcoxon signed-rank test and Dunnett's test, depending on the data. When multiple comparisons were made, p-values were adjusted with the Bonferroni or Bonferroni–Holm techniques (see figure legend). All data was explored using the 'tidyverse suite' in the RStudio framework and plotted using other RStudio packages including 'ggplot2', 'ggforce', 'ggbeeswarm', 'colorspace' and 'patchwork'. Subsequent plot modifications were executed in Serif Affinity Designer.

CHAPTER 3

3 Confirmation of Localisation of Eighteen Candidate Transcripts to the Glial Periphery at the Larval NMJ

3.1 Introduction

The functions of cells with complex and long extensions, such as neurons and glia, are tightly regulated by the distinct molecular events confined to specialised compartments. As discussed in the Introduction (Section 1.1), such cells require intricate spatiotemporal control at their peripheries, at their sites of interaction with neighbouring cells. mRNA localisation and local translation are attractive mechanisms for executing such control (Section 1.4), where the presence of specific mRNAs and their associated proteins can be adjusted in alignment with cellular requirements.

mRNA localisation and localised translation mechanisms have been widely studied in neurons in a diversity of experimental systems. However, in recent years, there has also been significant progress in the glial field [1, 34, 74]. Specifically, the importance of the regulation of neuronal functions through glial mRNA localisation and local translation at the tripartite synapses is only now gaining traction. Research on mRNA localisation and local translation in both neurons and glia can therefore shed light on some of the fundamental processes underlying memory and learning, including the roles which glial cells play in these. Essentially, localised translation in both neurons (near their synapses) and in perisynaptic glial cells (which come in contact with neuronal synapses) is a very attractive mechanisms for explaining how different synapses in the same neurons can be regulated independently and rapidly at a distance from the cell nucleus.

Some of the elementary functions of neurons and glia are highly tractable in model organisms, including *Drosophila melanogaster.* Flies have successfully been used in many basic neuroscientific studies, including a recent one from our laboratory [181]. Based on these results, there was strong indication that some transcripts identified to be present at the *Drosophila* 3rd instar NMJ were, in fact, predominantly glial transcripts [181]. As described previously (Section 1.5), the aim of this research was to analyse the localisation of mRNA and protein of 200 genes using their YFP protein traps [182]. Because each of the 200 different genes had the same insertion of DNA encoding the YFP protein within their sequence, the same set of smFISH probes against the *YFP* sequence could be used to detect all 200 mRNAs. Furthermore, the pattern of the YFP protein fluorescence allowed for the simultaneous examination of the protein expression and its comparison between the different YFP trap lines (Figure 3-1).

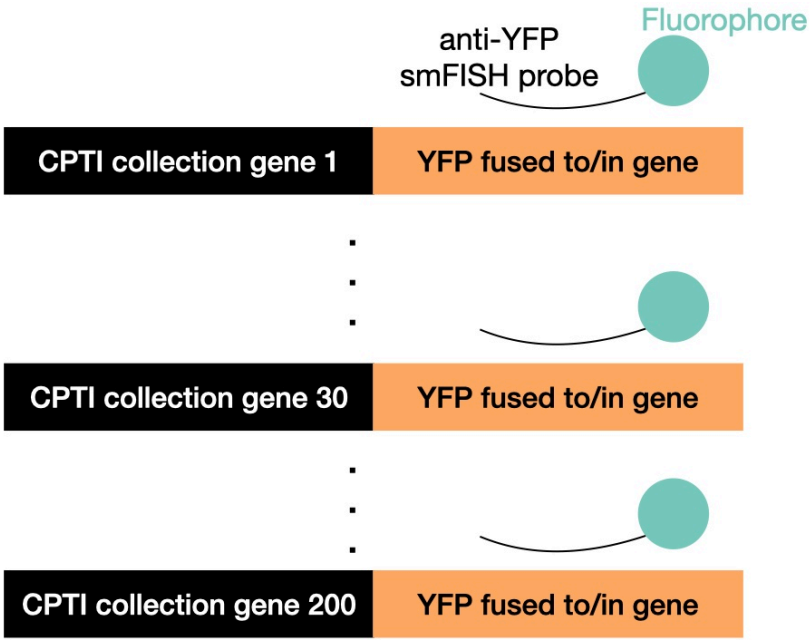

Figure 3-1 Davis laboratory CPTI collection screen principle

A simplified schematic of the experimental principle behind the study from the Davis laboratory which identified suspected nineteen transcripts present in the *Drosophila* 3rd instar NMJ glia[181]. Because all CPTI collection genes had *YFP* sequence inserted in them, using α-*YFP* probe allowed to detect the mRNA of any of those genes without having to design multiple probes. This principle was exploited to analyse the pattern of mRNA and protein localisation in the whole *Drosophila* 3rd instar nervous system. Nineteen of the analysed lines appeared to have mRNA and/or protein present at the NMJ in a pattern which matched neither the pre-synaptic nor the post-synaptic labelling.

The pattern of protein and mRNA observed at the *Drosophila* 3rd instar NMJ of nineteen CPTI lines was unusual (Table 1-1). The YFP protein and some fluorescent spots representing single mRNA molecules observed at the NMJ were found neither directly in the axon terminal, nor in the postsynaptic density, but somewhere around and between the two, and often also in the NMJ muscle cells (Figure 1-6). Moreover, at least one of the proteins identified was a previously known glial marker (nrv2), and several of them were septate junction (SJ) proteins known to reside at the BBB created by the NMJ glia (Nrg, Atpα, Gli, Lac, cold and nrv2) [118, 201-208]. The pattern which these known glial-associated proteins made at the NMJ was comparable to that of the

remaining proteins on the “candidate glial protrusion-localised” list (Table 1-1), thus further indicating that all nineteen transcripts and proteins could be present in glial projections near the NMJ synapses. However, even though they all showed similar patterns of expression at the NMJ, the intensity of the YFP protein signal and the area occupied by it differed greatly, as did the numbers and distributions of the smFISH foci of the mRNAs encoding the proteins, labelled by probes against the *YFP* sequence [181].

While the glial localisation observed for the nineteen candidates in the preliminary results from our laboratory was striking, it remained a strong suggestion that was not conclusive in the absence of co-labelling with glial markers during the CPTI screen project. For that reason, it was necessary to use more definitive glial markers to confirm the location of putative glial transcripts and proteins at the NMJ with greater certainty. Repo-GAL4 driving the expression of membrane-targeted fluorescent proteins under UAS control is known to label the projections of glial cells whose distal compartments reach the *Drosophila* 3rd instar NMJ [121].

In this chapter, I used such glial projection labelling at the NMJ to assess the relationship between the glial projection boundaries and the pattern made by the mRNAs and protein of interest from CPTI lines of candidate projection-localised transcripts previously identified in our laboratory [181]. Confirmation of the presence of proteins of interest and their mRNAs in the glial periphery at the *Drosophila* 3rd instar NMJ could be indicative of their importance in the functioning of the NMJ synapse through glial control. Further research could then be done on the confirmed transcripts to understand their importance in the NMJ peripheral glia.

3.2 Specific aims of this chapter

1. To test if any of the candidate transcripts with terminal mRNA and protein localisation at the *Drosophila* 3rd instar NMJ are localised to glial NMJ projections.
2. To characterise the types of genes with mRNAs present in NMJ glia.
3. To understand what patterns of mRNA localisation and protein expression these transcripts produce and assess their potential significance.

3.3 Publication

Parts of the research presented in this chapter have now been published in the Journal of Cell Biology, a paper in which I am one of the authors.

Joshua S Titlow, Maria Kiourlappou, Ana Palanca, Jeffrey Y Lee, Dalia S Gala et al., 2023. “Systematic analysis of YFP traps reveals common mRNA/protein discordance in neural tissues.” Journal of Cell Biology, https://doi.org/10.1083/jcb.202205129.

The research presented in this chapter has also been published as a pre-print, where I am a co-first author, now under revision in the Journal of Cell Biology.

Dalia S. Gala, Jeffrey Y. Lee, Maria Kiourlappou, Joshua S. Titlow, Rita O. Teodoro, Ilan Davis, “Mammalian glial protrusion transcriptomes predict localisation of *Drosophila* glial transcripts required for synaptic plasticity”, bioRxiv, https://doi.org/10.1101/2022.11.30.518536.

Multiple co-authors contributed to both publications. I solely present the results which I have produced.

3.4 Materials and methods

3.4.1 Fly stocks

To test whether the nineteen NMJ localised mRNAs and proteins identified in the previous study from our laboratory are localised to *Drosophila* 3rd instar NMJ glia, I built a fly line to express UAS-mCD8-mCherry under the control of a pan-glial promoter in *Drosophila,* Repo (Repo>mCherry line), as described previously (2.12.1). I then crossed this line to all nineteen CPTI collection lines to test for the glial expression, and only larvae showing both mCherry and YFP expression were selected for assessment. The goal was to determine if the mCherry signal overlaps with the α-*YFP* probe signal or the YFP protein signal at the NMJ. Table 3-1 lists all the stocks used in this chapter.

3.4.2 Microscopy techniques

I used the smFISH technique (Section 2.5.1) as well as confocal microscopy (Section 2.6.1) to examine the patterns made by the individual molecules of mRNA at the NMJ. Minimum 3 larvae and 15 NMJs were imaged and assessed, and images representative of this assessment are displayed in the Results section of this chapter (3.5). α-*YFP* probe sequences can be found in Table B-2 in the Appendix. The descriptions of the antibodies used can be found in Table 2-4.

Table 3-1 List of *Drosophila melanogaster* stocks used in Chapter 3

Line name	Line ID	Line source	Line description
Oregon-R	5	BDSC	Wild-type control
nrv2::YFP	CPTI001455	DGRC	*nervana 2* gene YFP protein trap line (Lowe *et al.*, 2014)
Gli::YFP	CPTI002805	DGRC	*Gliotactin* gene YFP protein trap line
Flo2::YFP	CPTI001427	DGRC	*Flotillin 2* gene YFP protein trap line
Cip4::YFP	CPTI003231	DGRC	*Cdc42-interacting protein 4* gene YFP protein trap line
CG1648::YFP	CPTI100012	DGRC	*CG1648* gene YFP protein trap line
lost::YFP	CPTI002437	DGRC	*lost* gene YFP protein trap line
CG42342::YFP	CPTI000033	DGRC	*CG42342* gene YFP protein trap line
Vha55::YFP	CPTI002645	DGRC	*Vacuolar H+-ATPase 55kD subunit* gene YFP protein trap line
Atpα::YFP	CPTI002636	DGRC	*Na pump α subunit* gene YFP protein trap line
Nrg::YFP	CPTI002761	DGRC	*Neuroglian* gene YFP protein trap line
Lac::YFP	CPTI001714	DGRC	*Lachesin* gene YFP protein trap line
α-Cat::YFP	CPTI002408	DGRC	*α Catenin* gene YFP protein trap line
Pdi::YFP	CPTI002342	DGRC	*Protein disulfide isomerase* gene YFP protein trap line
sdk::YFP	CPTI000688	DGRC	*sidekick* gene YFP protein trap line
kst::YFP	CPTI001728	DGRC	*karst* gene YFP protein trap line
cold::YFP	CPTI001277	DGRC	*coiled* gene YFP protein trap line
shot::YFP	CPTI001962	DGRC	*short stop* gene YPF protein trap line
Gs2::YFP	CPTI001918	DGRC	*Glutamine synthetase 2* gene YFP protein trap line
ORMDL::YFP	CPTI002636	DGRC	*ORMDL* gene YFP protein trap line.
Repo-GAL4	7415	BDSC	Expresses GAL4 in glia [155]
UAS-mCD8-mCherry/cyo-GFP	27391	BDSC	Expresses Cherry RFP fused to the mouse CD8 extracellular and transmembrane domains for membrane targeting under UAS control.
cyo-GFP/Gla; tm6, tb/pri	Crossed from BDSC stocks	BDSC	A double balanced stock carrying Cyo-GFP over Gla on the 2nd chromosome and tm6, tb over prickle on the 3rd chromosome.

3.4.3 Biochemical techniques

I used RT-PCR to confirm the site of insertion of the *YFP* exon for one of the candidate genes (Section 2.4.1). The detailed design of this experiment has been illustrated in Figure 3-26. The primers used for this experiment are listed in Table A-1 in the Appendix.

3.5 Results

3.5.1 Control experiments

The α-*YFP* probe was used in all experiments. I therefore I carried out two control experiments. Firstly, the α-*YFP* probe was applied to wild-type Oregon-R (OrR) NMJs to confirm there was no unspecific binding of this probe at the NMJ in the wild type NMJ. No signal was observed in the terminal axon projections at the NMJ (Figure 3-2).

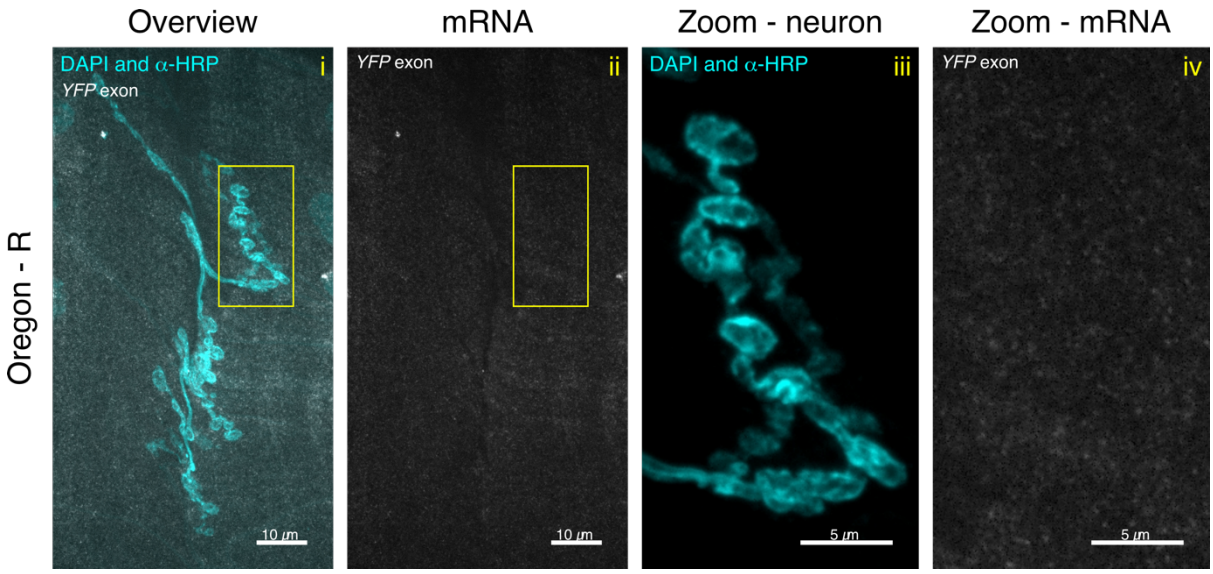

Figure 3-2 Control experiment for α-*YFP* probe signal in Oregon-R wild type

Representative confocal microscopy image of the *Drosophila* 3rd instar NMJ in the control experiment with the use of wild-type Oregon-R line and α-*YFP* probe. DAPI and α-HRP antibody conjugated to Alexa 405 fluorophore are depicted in cyan, and the α-*YFP* probe, labelled with Atto 633, is depicted in white. The yellow ROI in the Overview (i) and mRNA (ii) panels (see top left corner for label details) is what is magnified in the Zoom-neuron (iii, α-HRP antibody only) and Zoom-mRNA (iv, α-*YFP* probe only) panels. Virtually no labelling is observed in the smFISH channel. Compare with signal observed in Figure 3-4 - Figure 3-24. Scale bar – i) and ii): 10 μm, iii) and iv) - 5 μm.

Secondly, the α-*YFP* probe was used on the Repo>mCherry line to confirm that there was no non-specific binding within the glial region of the NMJ. No signal was observed in the terminal axon or glial projections at the NMJ (Figure 3-3). Overall, through these

controls I confirmed the lack of unspecific binding of the α-*YFP* probe in the NMJ region, as expected.

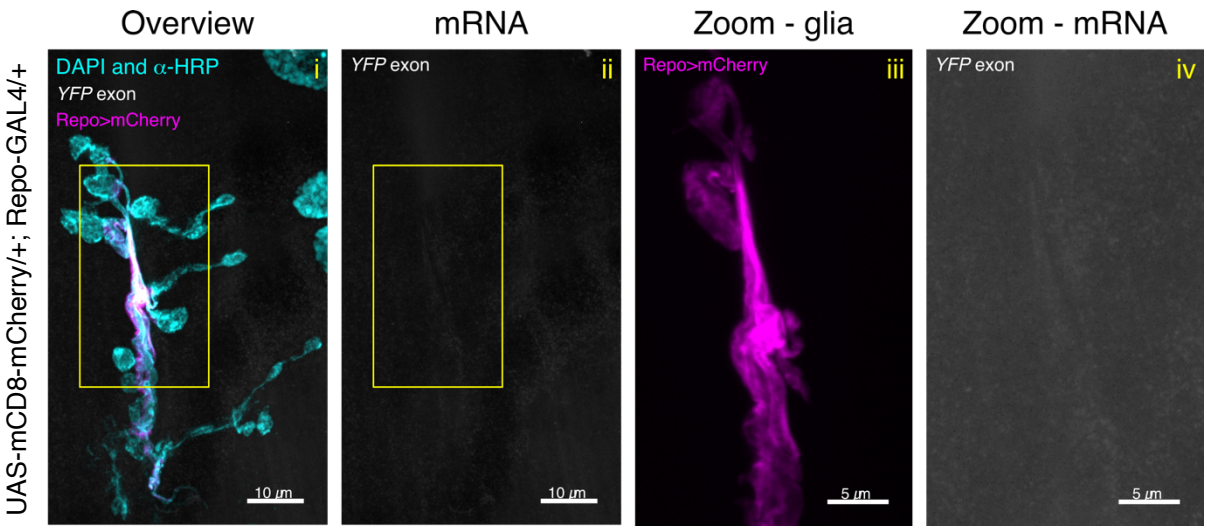

Figure 3-3 Control experiment for α-*YFP* probe signal in Repo>mCherry line

Representative confocal microscopy image of the *Drosophila* 3rd instar NMJ in the control experiment with the use of the line which was constructed to label the glial cells (magenta, Repo>mCherry, genotype UAS-mCD8-mCherry/+; Repo-GAL4/+) and α-*YFP* probe (white, α-*YFP* probe conjugated to Atto 633) at the *Drosophila* 3rd instar NMJ. DAPI and α-HRP antibody conjugated to Alexa 405 fluorophore are depicted in cyan. The yellow ROI in the Overview (i) and mRNA (ii) panels (see top left corner for label details) is what is magnified in the Zoom-glia (iii, Repo>mCherry only) and Zoom-mRNA (iv, α-*YFP* probe only) panels. Virtually no labelling is observed in the smFISH channel. Compare with signal observed in Figure 3-4 - Figure 3-24. Scale bar – i) and ii): 10 μm, iii) and iv) - 5 μm.

3.5.2 Exploration of the mRNA and protein localisation of the candidates to the NMJ glial projections

After the crossing of the CPTI lines to the Repo>mCherry line, I examined the patterns made by the transcripts and observed where the mRNA spots were in comparison with the glial cell projection labelling (Repo>mCherry). These results are summarised in Table 3-2.

The α-*YFP* probe smFISH signal indicating the mRNA distribution fell into three classes:

1. mRNAs preferentially seen in the NMJ glial projections: *nrv2* (Figure 3-4), *Gli* (Figure 3-5), *Flo2* (Figure 3-6), *Atpα* (Figure 3-7), *Lac* (Figure 3-21), *cold* (Figure 3-18), *CG42342* (Figure 3-9), *sdk* (Figure 3-14), *ORMDL* (Figure 3-13). This is marked as “Preferentially” in Table 3-2.
2. mRNAs seen both in the NMJ glial projections and in the surrounding muscle or other tissue: *CG1648* (Figure 3-8), *Vha55* (Figure 3-11), *Pdi* (Figure 3-19), *lost* (Figure 3-10), *α-Cat* (Figure 3-12), *kst* (Figure 3-15), *Cip4* (Figure 3-17), *shot* (Figure 3-16), *Nrg* (Figure 3-20). This is marked as “Not preferentially” in Table 3-2.
3. mRNAs seen in the NMJ glial projections in some NMJs, but both in the NMJ glial projections and in the surrounding muscle in others: *Gs2* (Figure 3-22, Figure 3-23, Figure 3-24). This is a mix of “Preferentially” and “Not preferentially” and is indicated as “Varying” in Table 3-2.

The proteins were distributed in a manner that fell into 3 classes:

1. Protein preferentially present within the NMJ glial projections labelling: nrv2, Gli, Flo2, Lac, cold, Gs2, Nrg, CG42342, CG1648, Pdi, Vha55, Cip4. This is marked as “Preferentially” in Table 3-2.
2. Protein present both within the NMJ glial projections labelling and in other areas: kst, shot, Atpα. This is marked as “Not preferentially” in Table 3-2.
3. Protein not present within the NMJ glial projections labelling: sdk, ORMDL, lost, α-Cat. This is marked as “No” in Table 3-2.

Table 3-2 Comparison of CPTI lines mRNA and protein localisation with glial cell labelling

Transcript knocked down	Is mRNA in glia?	Is protein in glia?
nrv2	Preferentially	Preferentially
Gli	Preferentially	Preferentially
Flo2	Preferentially	Preferentially
Cip4	Not preferentially	Preferentially
CG1648	Not preferentially	Preferentially
lost	Not preferentially	No
CG42342	Preferentially	Preferentially
Vha55	Not preferentially	Preferentially
Atpα	Preferentially	Not preferentially
Nrg	Not preferentially	Preferentially
Lac	Preferentially	Preferentially
α-Cat	Not preferentially	No
Pdi	Not preferentially	Preferentially
sdk	Preferentially	No
kst	Not preferentially	Not preferentially
cold	Preferentially	Preferentially
ORMDL	Preferentially	No
Gs2	Varying	Preferentially
shot	Not preferentially	Not preferentially

I classify the presence of mRNA in the glia as either present “Preferentially”, where many of the mRNA spots overlap with the glial labelling, and there aren’t many more mRNA spots outside of the glial area, “Not preferentially”, where the mRNA spots are everywhere in the imaged area, and “Varying”, which is a combination of “Preferentially” and “Not preferentially. For protein, “Preferentially” means that the protein signal overlaps with the glial labelling, “Not preferentially” means that the protein is making a different, not necessarily glial-projection-resembling pattern (which does not exclude the protein presence from glia, rather indicates that it can also be present in different areas), and “No”, which means the protein is not seen in the NMJ glial projections.

Below, I proceed to discuss individual candidate protrusion-localised transcripts of the nineteen genes previously identified in the Davis laboratory and their mRNA and protein distribution with respect to the NMJ glial projection labelling.

3.5.2.1 nrv2 is a known marker of WG and an enzyme subunit

nrv2 protein is a known marker of WG [118]. The *nrv2* gene encodes two isoforms of nrv2 protein, nrv2.1 and nrv2.2, which are β subunits of the Na^+/K^+ ATPase enzyme which is part of SJ complexes. The enzyme is an α/β multimer, and the α subunits are

encoded by *Atp*α, also involved in my research, which I discuss later. Through the transport of three sodium cations out of and two potassium cations into the cell per single ATP molecule hydrolysis, the Na^+/K^+ ATPase is responsible for producing an electrochemical gradient across the neuronal plasma membrane [209]. The members of this enzyme complex, including nrv2 and Atpα, are necessary for the control of the size of the epithelial tubes in the *Drosophila* tracheal system and correct SJ function [203].

SJs, which nrv2 is a part of, are functional equivalents of the mammalian Tight Junctions (TJs) [207]. At the *Drosophila* 3rd instar NMJ, they participate in the formation of the BBB, where SPG form SJs to prevent paracellular diffusion [210].

The pattern which I observed for the nrv2::YFP expression is consistent with the known nrv2 function in SPG, but since I used a pan-glial driver, Repo, I cannot distinguish the glial subtypes with this experiment. Both protein and mRNA were observed within the NMJ glial projection labelling (Figure 3-4).

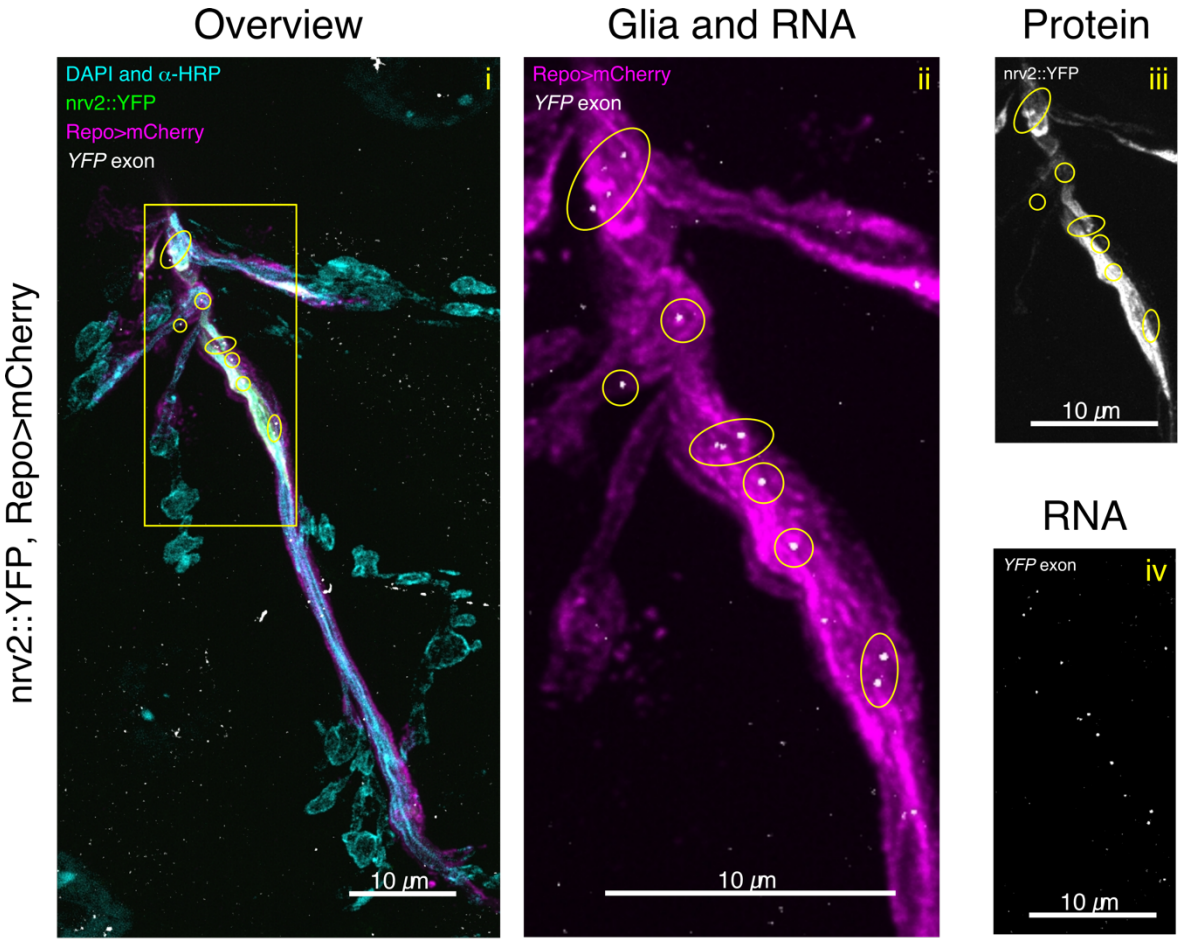

Figure 3-4 *nrv2::YFP* protein and multiple mRNA molecules are present in terminal glial projections

i) Representative confocal microscopy image of the nrv2::YFP protein (green) and mRNA (white, α-*YFP* probe labelled with Atto 633) expression patterns in the *Drosophila* 3rd instar NMJ glial projections (Repo>mCherry, magenta). DAPI and α-HRP antibody conjugated to Alexa 405 fluorophore are depicted in cyan. Several mRNA foci overlap with the glial membrane signal (yellow oval and circular ROIs), and so does the protein signal. ii-iv) Zoomed-in view of the yellow rectangular ROI from i) (see labels for details). Scale bar - 10 μm.

3.5.2.2 Gli is a SJ protein

Gli is also a SJ protein necessary for the correct function of the BBB [201]. The amount of mRNA expressed at the NMJ was low, and so was the amount of protein. The area occupied by the protein signal seemed lower than in the case of nrv2 (Figure 3-5).

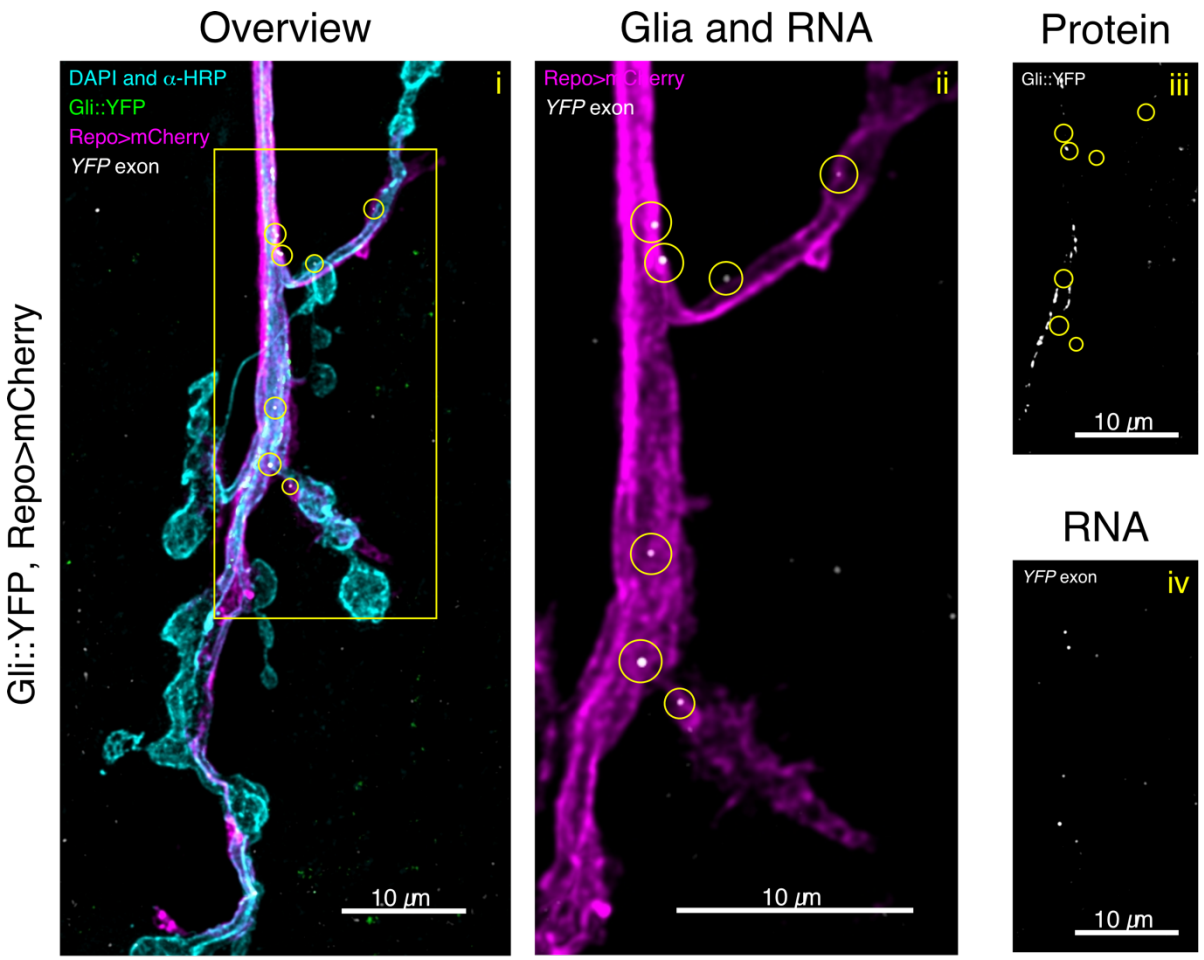

Figure 3-5 Several *Gli::YFP* mRNA molecules and little yet specifically concentrated protein signal are present in terminal glial projections

i) Representative confocal microscopy image of the Gli::YFP protein (green) and mRNA (white, α-*YFP* probe labelled with Atto 633) expression patterns in the *Drosophila* 3rd instar NMJ glial projections (Repo>mCherry, magenta). DAPI and α-HRP antibody conjugated to Alexa 405 fluorophore are depicted in cyan. Numerous individual mRNA foci overlap with the glial membrane signal (yellow circular ROIs). There is very little protein signal. ii-iv) Zoomed-in view of the yellow rectangular ROI from i) (see labels for details). Scale bar - 10 μm.

3.5.2.3 Flo2 is a lipid raft protein

Flo2 is a protein belonging to the flotillin family. The members of this family are highly conserved among different species and reside in caveolae-enriched lipid rafts in the plasma membrane [211]. Flotillins also interact closely with SJs [212]. Flo2 is known to be highly expressed in the *Drosophila* nervous system and present at specific synaptic sites [213].

When comparing the expression of *Flo2::YFP* mRNA and protein to the glial membrane labelling pattern at the NMJ, I observed that several mRNA molecules were found within the glial labelling area, but some were found in the muscle area, and the protein pattern matched the pattern of the glial projection labelling very closely (Figure 3-6).

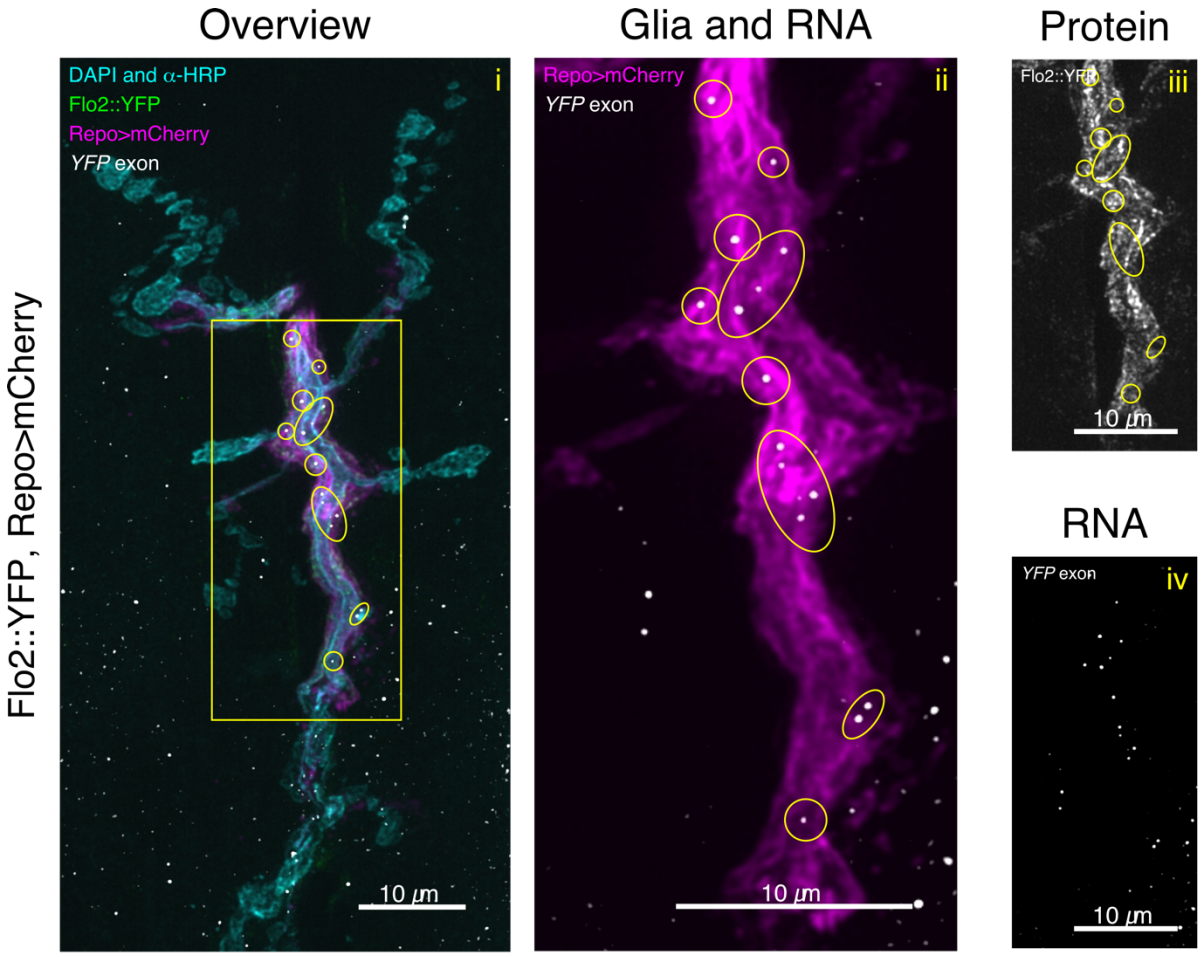

Figure 3-6 *Flo2::YFP* protein fills glial projections, while numerous mRNA molecules are present both inside the terminal glial projections and elsewhere

i) Representative confocal microscopy image of the Flo2::YFP protein (green) and mRNA (white, α-*YFP* probe labelled with Atto 633) expression patterns in the *Drosophila* 3rd instar NMJ glial projections (Repo>mCherry, magenta). DAPI and α-HRP antibody conjugated to Alexa 405 fluorophore are depicted in cyan. Several mRNA molecules overlap with the glial membrane signal (yellow oval and circular ROIs). The protein signal overlaps closely with the glial membrane. ii-iv) Zoomed-in view of the yellow rectangular ROI from i) (see labels for details). Scale bar - 10 μm.

3.5.2.4 Atpα is a catalytic enzyme subunit

Much like nrv2, Atpα, is part of the same Na+/K+ ATPase enzyme complex at SJs. It is also necessary for the correct function of SJs and epithelial tube size in the *Drosophila* tracheal system [203]. *Atpα* encodes the catalytic subunit of the Na^+/K^+ ATPase, and mutations in *Atpα* lead to numerous aberrations, including behavioural irregularities and the hyperexcitability of the neurons [214].

Through my results, I observed that Atpα::YFP protein pattern at the NMJ appeared to follow the pattern of the neuronal staining (Alexa 405 conjugated α-HRP antibody) as well as the glial membrane labelling. mRNA molecules appeared to be present in the region of overlap between the neuronal and glial membrane labelling, as well as in the muscle cells (Figure 3-7).

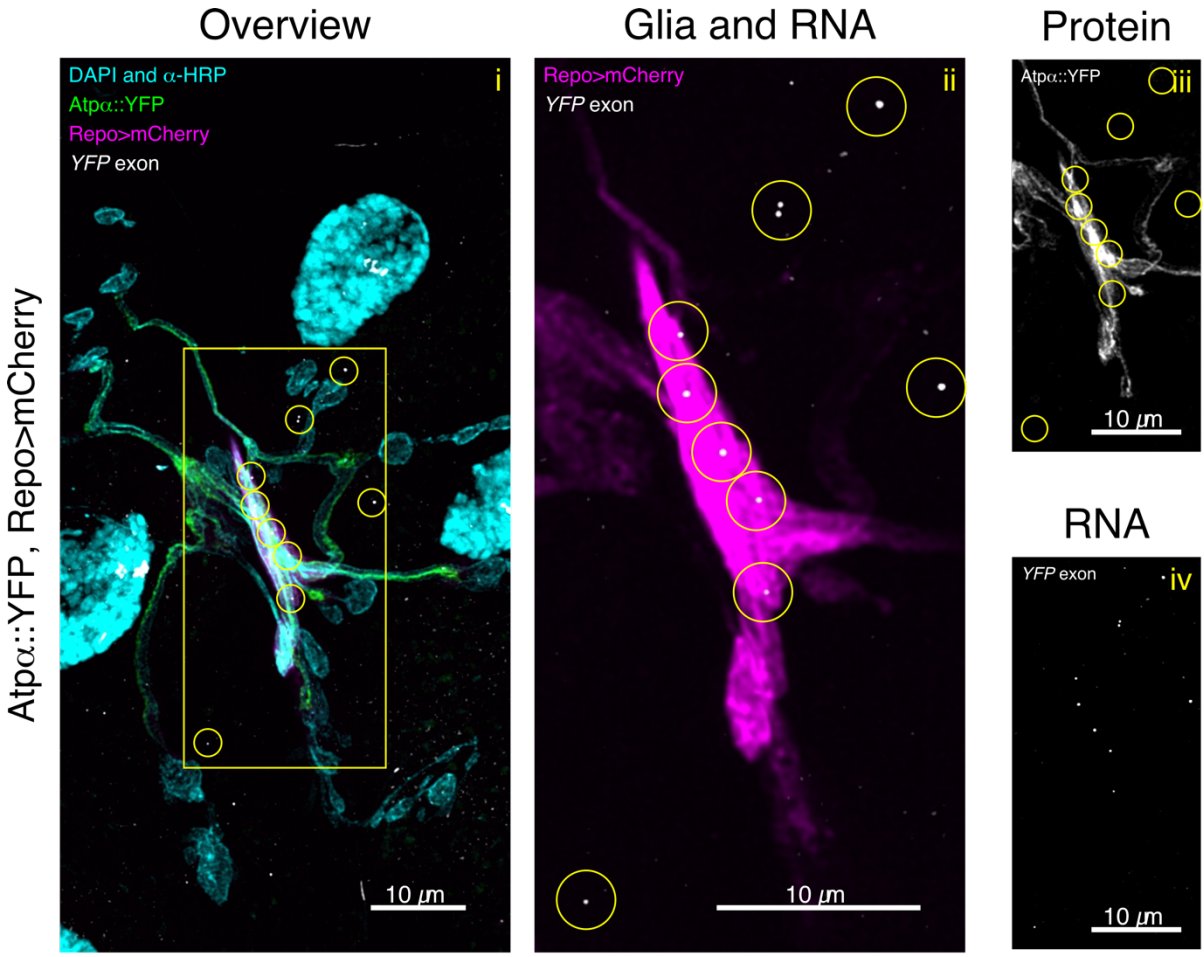

Figure 3-7 Few *Atpα::YFP* mRNA molecules are present in terminal glial projections and the protein is abundant in both glial and axon projections

i) Representative confocal microscopy image of the Atpα::YFP protein (green) and mRNA (white, α-*YFP* probe labelled with Atto 633) expression patterns in the *Drosophila* 3rd instar NMJ glial projections (Repo>mCherry, magenta). DAPI and α-HRP antibody conjugated to Alexa 405 fluorophore are depicted in cyan. Atpα::YFP protein pattern resembles that of the neuronal membrane labelling closely. The mRNA molecules are distributed both where the neuronal and glial labelling overlaps, but also in the muscle area (yellow circular ROIs). ii-iv) Zoomed-in view of the yellow rectangular ROI from i) (see labels for details). Scale bar - 10 μm.

3.5.2.5 *CG1648* is not a well characterised gene in *Drosophila*

CG1648 does not have well characterised roles in *Drosophila*. One paper reports that its expression is known to decrease in mated females relative to virgin females [215]. Using *Drosophila* RNAi Screening Center Integrative Ortholog Prediction Tool (DIOPT; http://www.flyrnai.org/diopt), *CG1648* predicted human orthologue is PLIN4, which is a protein that coats nascent lipid droplets, indicating that CG1648 protein could perform a similar function [216, 217]. However, the rank of this prediction is low, and, ultimately, not much is known about the function of this protein in *Drosophila.*

I have observed that the expression of the YFP tagged CG1648 overlaps with the neuronal and glial labelling, and its mRNA is present densely throughout the NMJ (Figure 3-8).

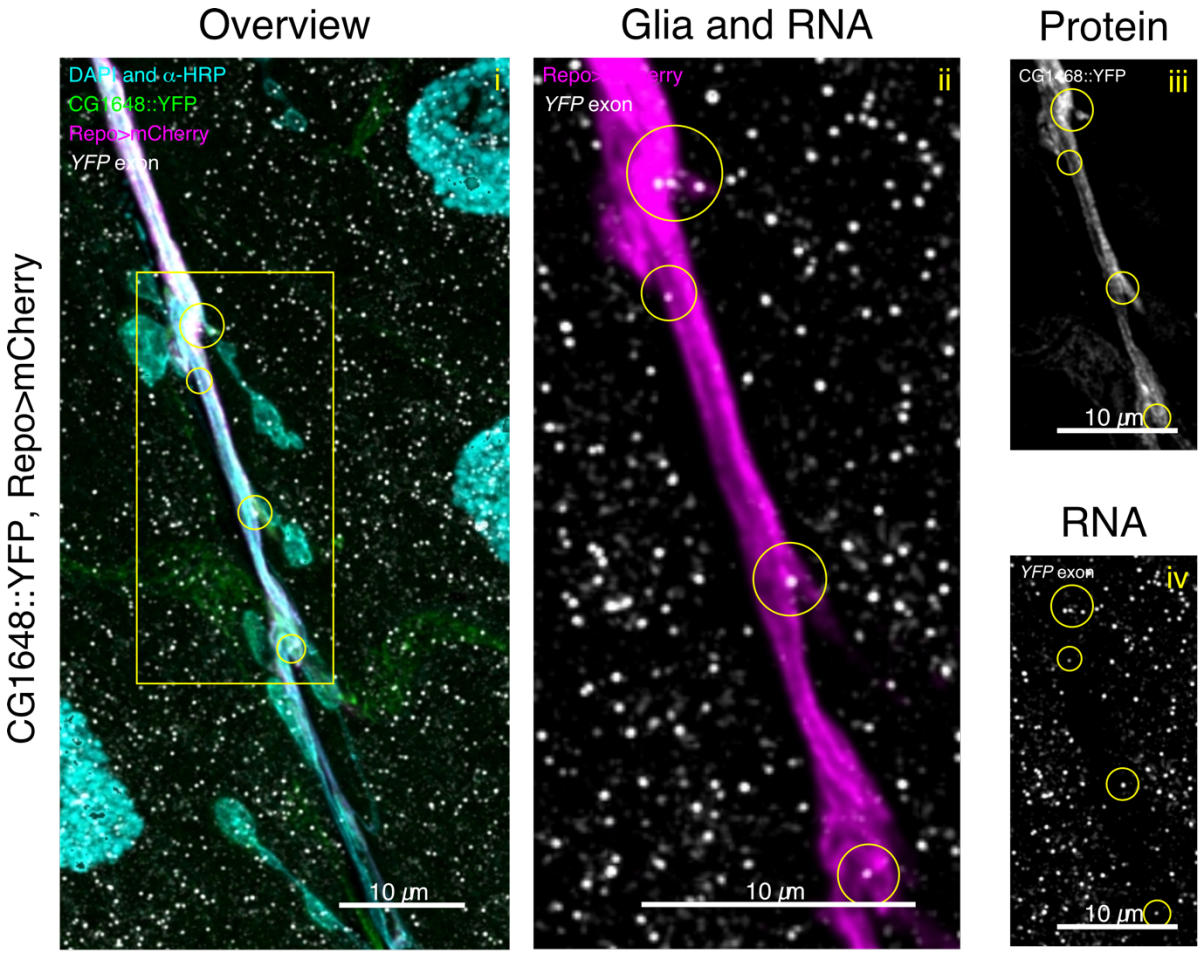

Figure 3-8 *CG1648::YFP* mRNA is plentiful at the NMJ and the protein is present in terminal glial and axon projections

i) Representative confocal microscopy image of the CG1648::YFP protein (green) and mRNA (white, α-*YFP* probe labelled with Atto 633) expression patterns in the *Drosophila* 3rd instar NMJ glial projections (Repo>mCherry, magenta). DAPI and α-HRP antibody conjugated to Alexa 405 fluorophore are depicted in cyan. CG1648::YFP protein pattern resembles that of the glial membrane labelling closely, but simultaneously the protein appears to also be in the neuronal boutons. *CG1648::YFP* mRNA is distributed ubiquitously and densely in the NMJ. Some mRNA molecules overlap with the glial membrane signal (yellow circular ROIs). ii-iv) Zoomed-in view of the yellow rectangular ROI from i) (see labels for details). Scale bar - 10 µm.

3.5.2.6 *CG42342* is a predicted *Drosophila* collagen gene

This gene is also not well characterised in *Drosophila*. It is orthologous to human COL13A1 (collagen type XIII alpha 1 chain), and thus predicted to be a component of the ECM [217]. It has previously been shown that collagen XIII is necessary for the integrity of the neuromuscular synapse, both pre- and post-synaptically [218].

Upon the examination of the pattern made by this protein tagged with YFP and its mRNA, it appeared that CG42342::YFP was mostly localised to the *Drosophila* NMJ glia, while the mRNA molecules were both in glia and in the surrounding muscle, though sparsely distributed (Figure 3-9).

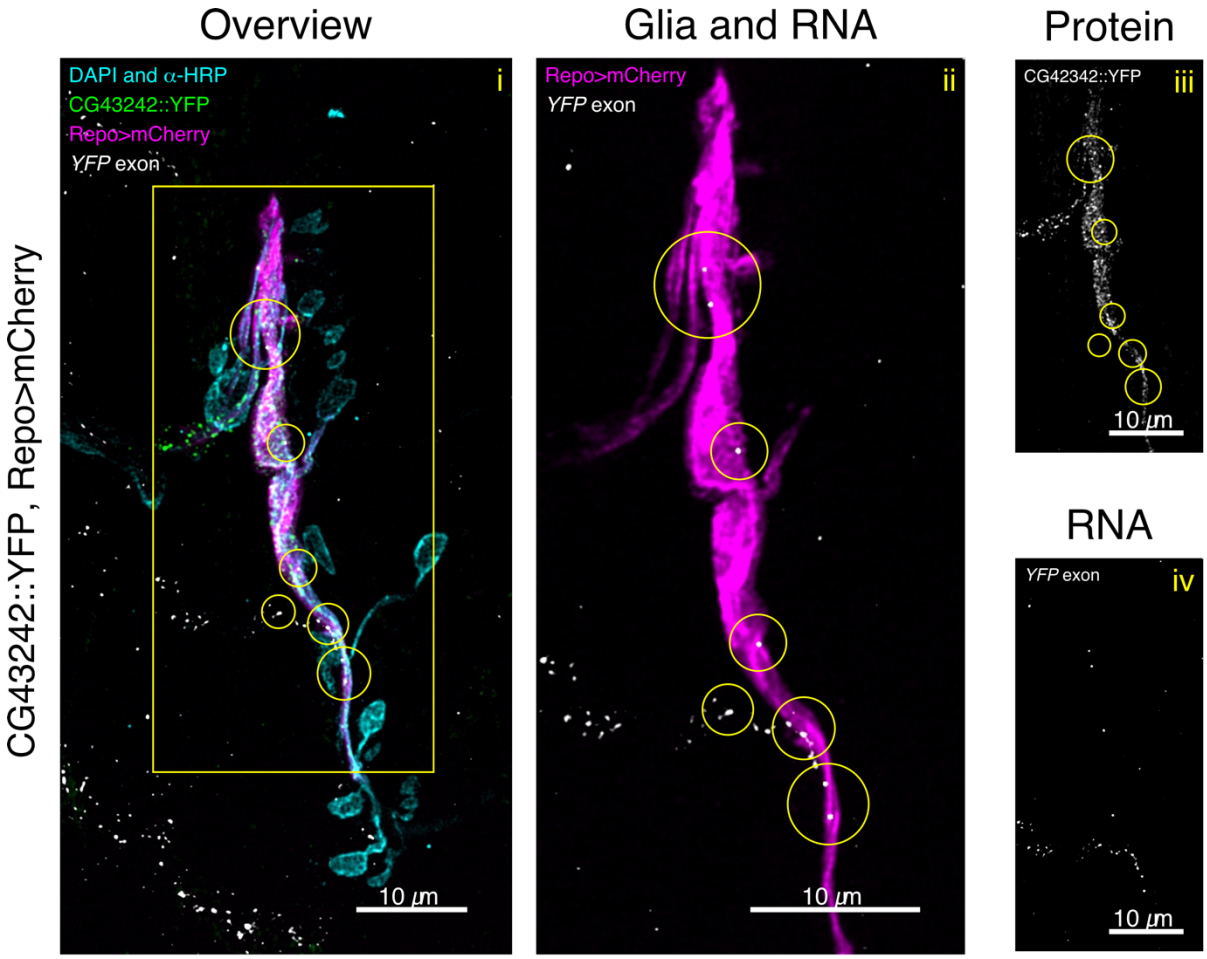

Figure 3-9 Few *CG42342::YFP* mRNA molecules are present in terminal glial projections and elsewhere at the NMJ but the protein is more exclusive to the terminal glial projections

i) Representative confocal microscopy image of the CG42342::YFP protein (green) and mRNA (white, α-*YFP* probe labelled with Atto 633) expression patterns in the *Drosophila* 3rd instar NMJ glial projections (Repo>mCherry, magenta). DAPI and α-HRP antibody conjugated to Alexa 405 fluorophore are depicted in cyan. *CG42342::YFP* mRNA is sparse and mostly within the glial labelling (yellow circular ROIs). CG42342::YFP protein expression pattern is overlapping closely and accurately with that of the glial labelling. ii-iv) Zoomed-in view of the yellow rectangular ROI from i) (see labels for details). Scale bar - 10 μm.

3.5.2.7 lost is a protein of known importance in mRNA localisation

The gene *lost* encodes a protein which is known to be involved in correct mRNA localisation during *Drosophila* embryogenesis through interaction with RBPs [219]. Thus, its presence in my dataset was promising, as it could indicate the need to localise or locally regulate the mRNA repertoire of the NMJ synapse and its glia.

Both the lost::YFP protein and mRNA seemed to be diffusely localised throughout the entire NMJ. The protein appeared like it could be present in the strata of the muscle cells of the NMJ, as well as within the NMJ glial projections labelling (Figure 3-10).

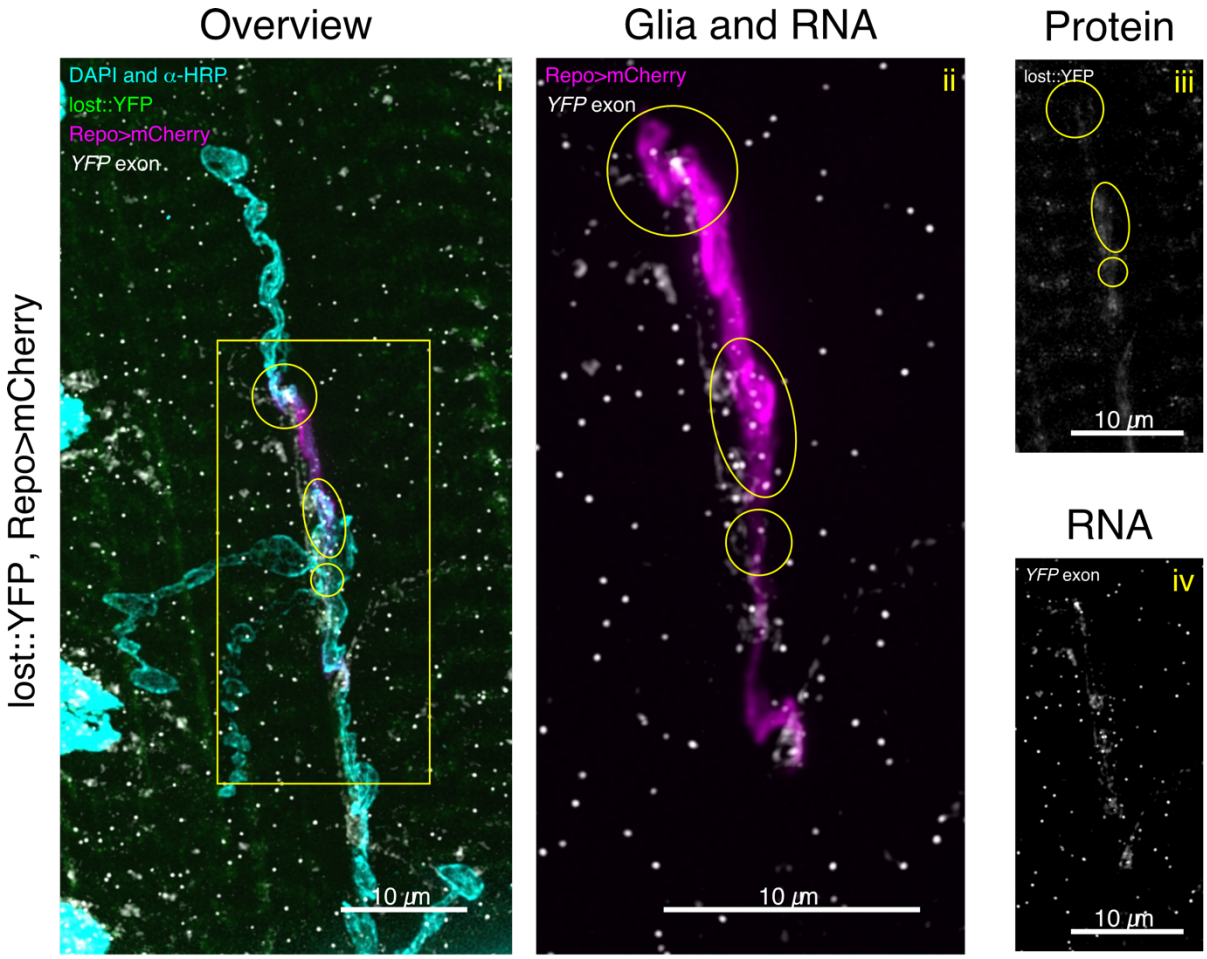

Figure 3-10 Many *lost::YFP* mRNA molecules are present at the NMJ, including in terminal glial projections, while the protein signal is weak and diffuse

i) Representative confocal microscopy image of the lost::YFP protein (green) and mRNA (white, α-*YFP* probe labelled with Atto 633) expression patterns in the *Drosophila* 3rd instar NMJ glial projections (Repo>mCherry, magenta). DAPI and α-HRP antibody conjugated to Alexa 405 fluorophore are depicted in cyan. lost::YFP mRNA is present ubiquitously within the glial projection labelling (yellow oval and circular ROIs) and the surrounding area. lost::YFP protein is present within the NMJ glial projections labelling, but the signal is weak, and is also present in the surrounding muscle cells. ii-iv) Zoomed-in view of the yellow rectangular ROI from i) (see labels for details). Scale bar - 10 μm.

3.5.2.8 Vha55 is a subunit of a proton pump enzyme

Vha55 gene encodes the non-catalytic subunit of the vacuolar (H^+)-ATPase (V-ATPase) responsible for the acidification of selected intra and extracellular compartments [220]. This protein is required for planar cell polarity, and it has been shown on numerous occasions that mutations in its gene are lethal [220, 221]. It was interesting that this protein was identified in our laboratory to be potentially present in the NMJ glia, because it was previously observed that the pattern of expression of Vha55 in the nervous system resembled that of cell junctions characteristic of the PG, as well as that of Moody antibody staining, characteristic of contacts between SPG and the underlying CG [111, 112, 222, 223].

From my observations, it appeared that the protein was indeed mostly concentrated in the same area as the NMJ glial projection labelling, but it was also present in the muscle. Moreover, the mRNA was evenly distributed in the entire NMJ area, with several molecules localising to the same area as glial projection labelling (Figure 3-11).

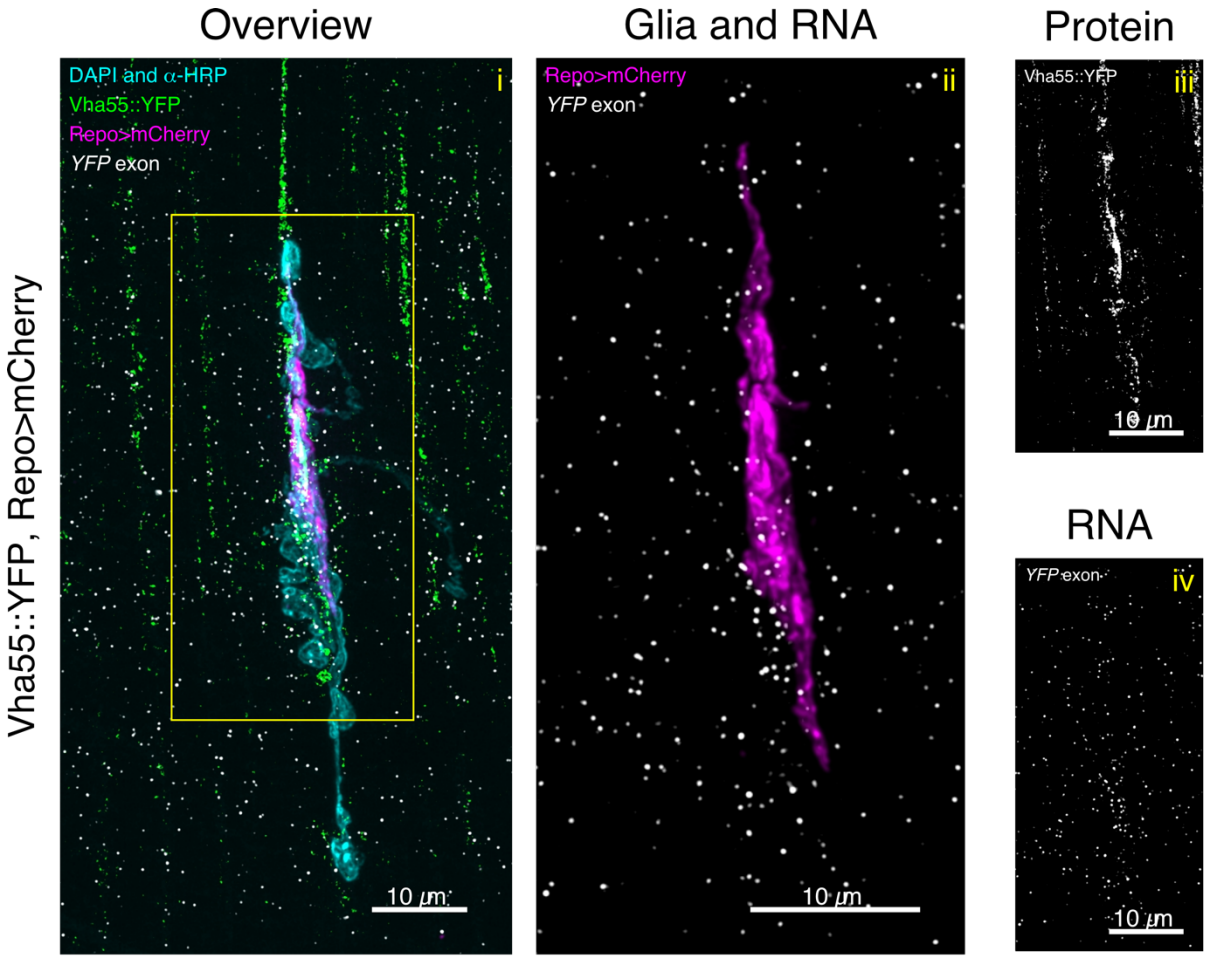

Figure 3-11 Numerous *Vha55::YFP* mRNAs are present at the NMJ, with some in terminal glial projections, where the protein is concentrated

i) Representative confocal microscopy image of the Vha55::YFP protein (green) and mRNA (white, α-*YFP* probe labelled with Atto 633) expression patterns in the *Drosophila* 3rd instar NMJ glial projections (Repo>mCherry, magenta). DAPI and α-HRP antibody conjugated to Alexa 405 fluorophore are depicted in cyan. The mRNA is uniformly distributed throughout the entire NMJ area, and several mRNA molecules overlap with the glial membrane labelling. The protein signal seems to be present mostly within the glial labelling, but also partially in the muscle area. ii-iv) Zoomed-in view of the yellow rectangular ROI from i) (see labels for details). Scale bar - 10 μm.

3.5.2.9 α-Cat is an adherens junction protein

This protein interacts with multiple representatives of the cadherin family, through which a link is made to the actin filament network [224]. Thus, α-Cat can modulate cell-adhesion properties of cadherins and is instrumental in adherens junctions stability [225, 226].

From my observation, α-Cat::YFP protein is not present in the glial labelling area of the NMJ; the mRNA is distributed sparsely throughout the whole area, and some mRNA spots overlap with the glial labelling (Figure 3-12).

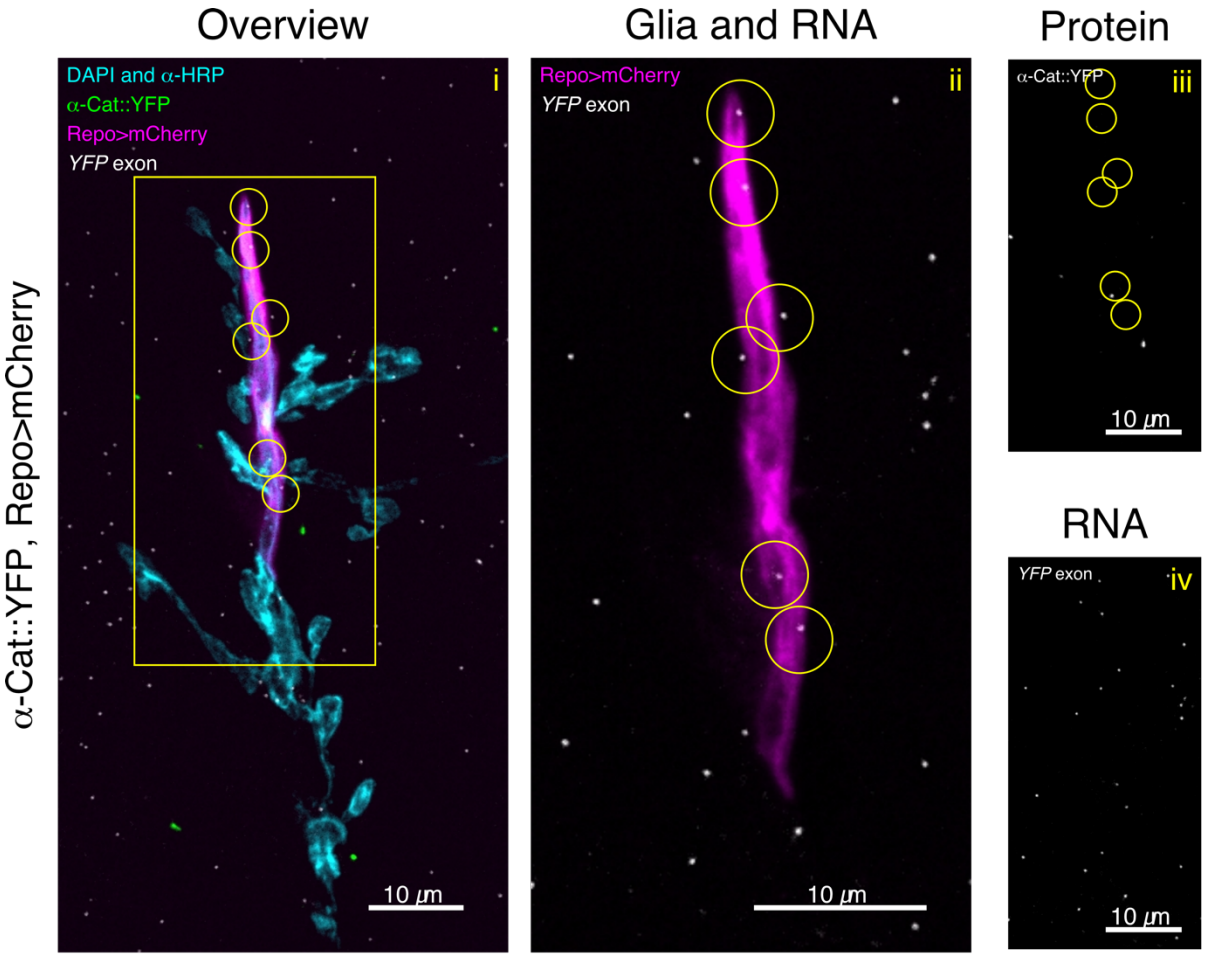

Figure 3-12 *α-Cat::YFP* mRNAs are sparsely distributed throughout the NMJ, including few in terminal glial projections

i) Representative confocal microscopy image of the α-Cat::YFP protein (green) and mRNA (white, α-*YFP* probe labelled with Atto 633) expression patterns in the *Drosophila* 3rd instar NMJ glial projections (Repo>mCherry, magenta). DAPI and α-HRP antibody conjugated to Alexa 405 fluorophore are depicted in cyan. The mRNA is sparsely distributed throughout the entire NMJ area, and several mRNA molecules overlap with the glial membrane labelling (yellow oval and circular ROIs), but there is no obvious protein pattern made by this protein at the NMJ. ii-iv) Zoomed-in view of the yellow rectangular ROI from i) (see labels for details). Scale bar - 10 μm.

3.5.2.10 ORMDL is a sphingolipid synthesis regulator

The ORMDL family of proteins are endoplasmic reticulum transmembrane proteins known to regulate sphingolipid synthesis [227]. They are studied extensively in asthma and other respiratory conditions, including in the fly, where it was found that deregulation of ORMDL, the only *Drosophila* member of this family, modulates repair pathways in *Drosophila* airways and causes increased stress responses [228].

Intriguingly, my examination of the pattern which ORMDL::YFP and its mRNA made at the *Drosophila* NMJ revealed very high mRNA levels overlapping nearly perfectly with the glial labelling (Figure 3-13). In contrast to this observation, the presence of mRNA was not accompanied by high level of protein expression, as there was no protein signal observed at the NMJ. Thus, I was unsure if this YFP trap was indeed representative of ORMDL protein.

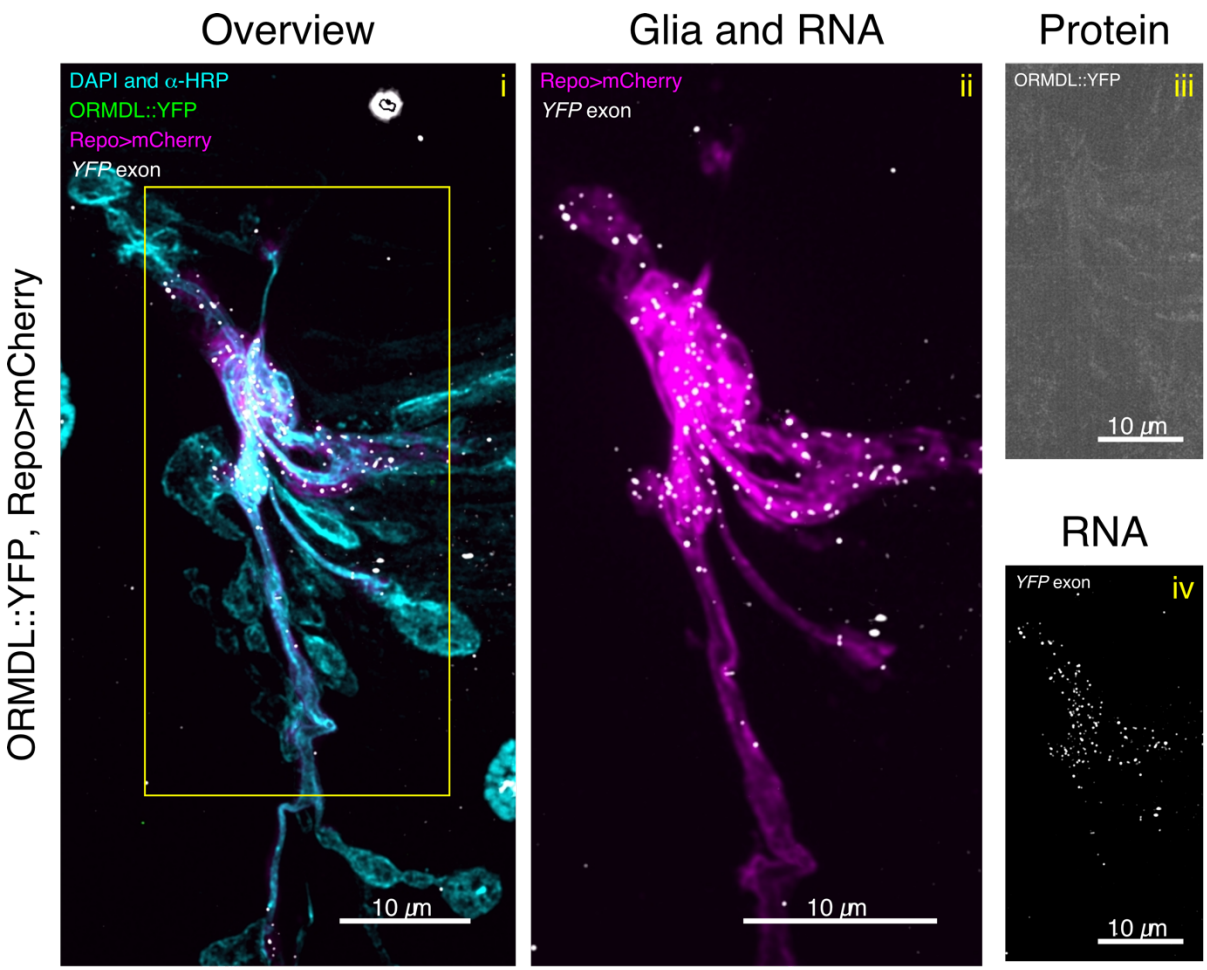

Figure 3-13 *ORMDL::YFP* mRNA is concentrated in terminal glial projections but no protein is present at the NMJ

i) Representative confocal microscopy image of the ORMDL::YFP protein (green) and mRNA (white, α-*YFP* probe labelled with Atto 633) expression patterns in the *Drosophila* 3rd instar NMJ glial projections (Repo>mCherry, magenta). DAPI and α-HRP antibody conjugated to Alexa 405 fluorophore are depicted in cyan. *ORMDL::YFP* mRNA appears to be present exactly where the glial signal is seen, while ORMDL::YFP protein does not appear to be present at all at the NMJ. ii-iv) Zoomed-in view of the yellow rectangular ROI from i) (see labels for details). Scale bar - 10 μm.

3.5.2.11 sdk is a member of tricellular adherens junctions

sdk is also a protein which modulates the actin cytoskeleton through participation in E-cadherin dynamics at tricellular adherens junctions and synapses [229, 230]. It is a member of the immunoglobulin (Ig) superfamily (IgSF); it promotes actin branching and lengthening of cell-cell contacts, necessary for pattern formation in the *Drosophila* eye [231, 232].

Similar to ORMDL::YFP, during my investigation of the sdk::YFP protein and mRNA patterns at the *Drosophila* NMJ, I discovered a significant overlap between the mRNA levels and the glial labelling. However, in contrast to this finding, the presence of mRNA did not correspond to a high level of protein expression. Notably, no protein signal was observed at the NMJ (Figure 3-14).

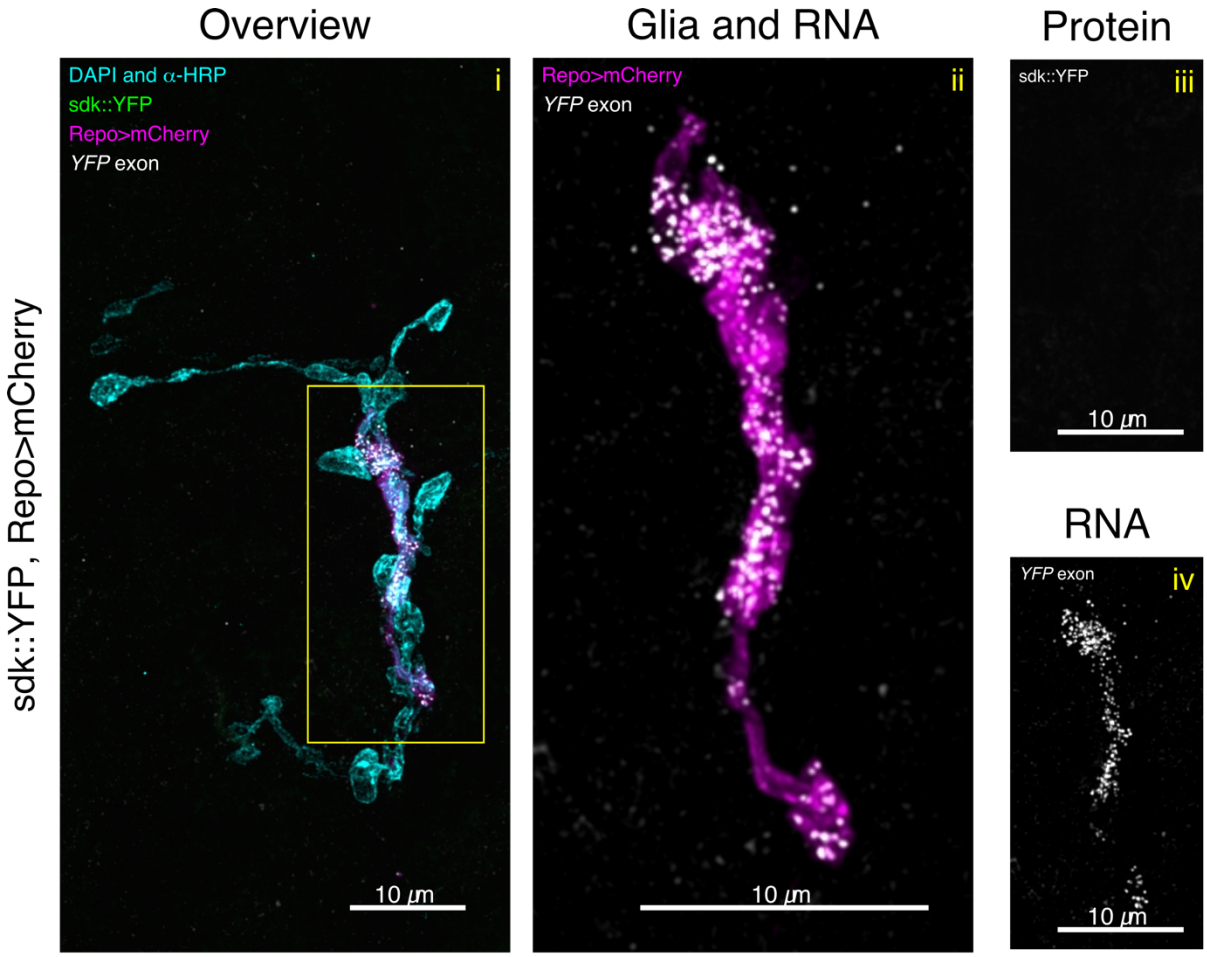

Figure 3-14 *sdk::YFP* mRNA is densely concentrated in terminal glial projections, but no protein signal is present at the NMJ

i) Representative confocal microscopy image of the sdk::YFP protein (green) and mRNA (white, α-*YFP* probe labelled with Atto 633) expression patterns in the *Drosophila* 3rd instar NMJ glial projections (Repo>mCherry, magenta). DAPI and α-HRP antibody conjugated to Alexa 405 fluorophore are depicted in cyan. sdk::YFP protein does not appear to be present at all at the NMJ, while *sdk::YFP* mRNA appears to be present exactly where the glial signal is seen, much like in the ORMDL::YFP line (Figure 3-13). ii-iv) Zoomed-in view of the yellow rectangular ROI from i) (see labels for details). Scale bar - 10 μm.

3.5.2.12 kst is a spectrin required for actin dynamics

kst protein is a member of the spectrin family and is also known as the *Drosophila* ßHeavy-Spectrin. α-Spectrin and ßHeavy-Spectrin form a heterotetramer which performs a scaffold function by crosslinking F-actin [233]. kst together with nrv2 were previously found to be important in correct polarisation of EG; mutations in *kst* resulted in abnormal locomotion comparable to that observed in complete ablation of EG [234].

I observed both kst::YFP protein and mRNA at the *Drosophila* NMJ. The protein was partially present in the glia, particularly in one of the glial protrusions on the muscle surface, while only a few spots of mRNA overlapped with the glial labelling (Figure 3-15).

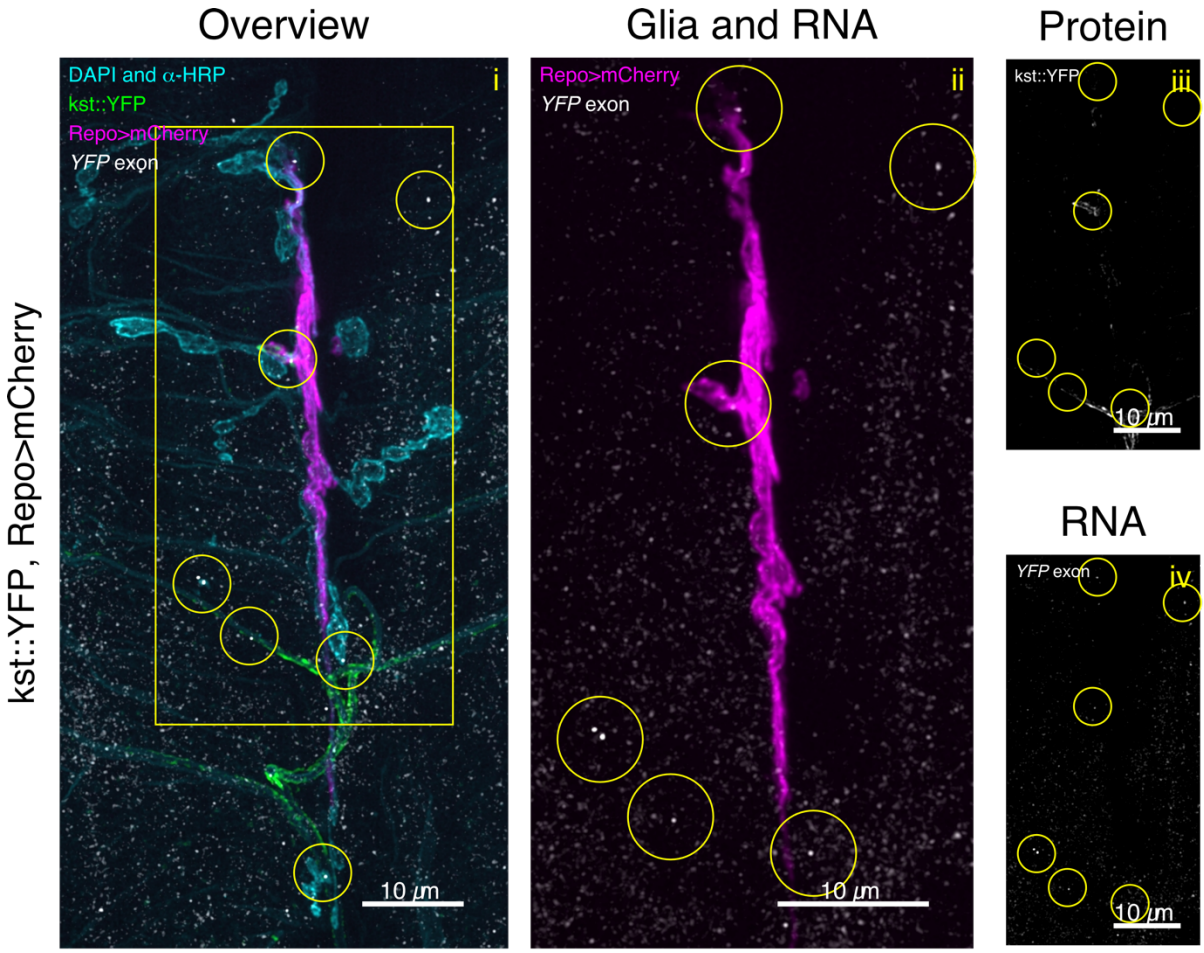

Figure 3-15 Very few *kst::YFP* mRNA molecules are present at the NMJ, while the protein is localised to the trachea

i) Representative confocal microscopy image of the kst::YFP protein (green) and mRNA (white, α-*YFP* probe labelled with Atto 633) expression patterns in the *Drosophila* 3rd instar NMJ glial projections (Repo>mCherry, magenta). DAPI and α-HRP antibody conjugated to Alexa 405 fluorophore are depicted in cyan. kst::YFP protein is present in the NMJ glia, but also in the trachea (auto-fluorescent in the 405 channel), while *kst::YFP* mRNA appears to be present in the surrounding muscle and the trachea, with two molecules co-localising with the glial signal (yellow circular ROIs). ii-iv) Zoomed-in view of the yellow rectangular ROI from i) (see labels for details). Scale bar - 10 μm.

3.5.2.13 shot is a cytoskeletal linker protein

shot is a spectraplakin family member. These proteins are cytoskeletal linker molecules which connect both actin and microtubules (MTs), and other scaffold proteins [235]. shot also participates in muscle-tendon junction formation and filopodia formation during neuronal growth by controlling microtubule assembly [236, 237].

My experiments revealed shot::YFP signal at the NMJ overlapping with glia, but also, partially, the neuronal staining (Figure 3-16). There were very few mRNA spots of *shot::YFP* mRNA at the NMJ, and some of them overlapped with the glial labelling, too.

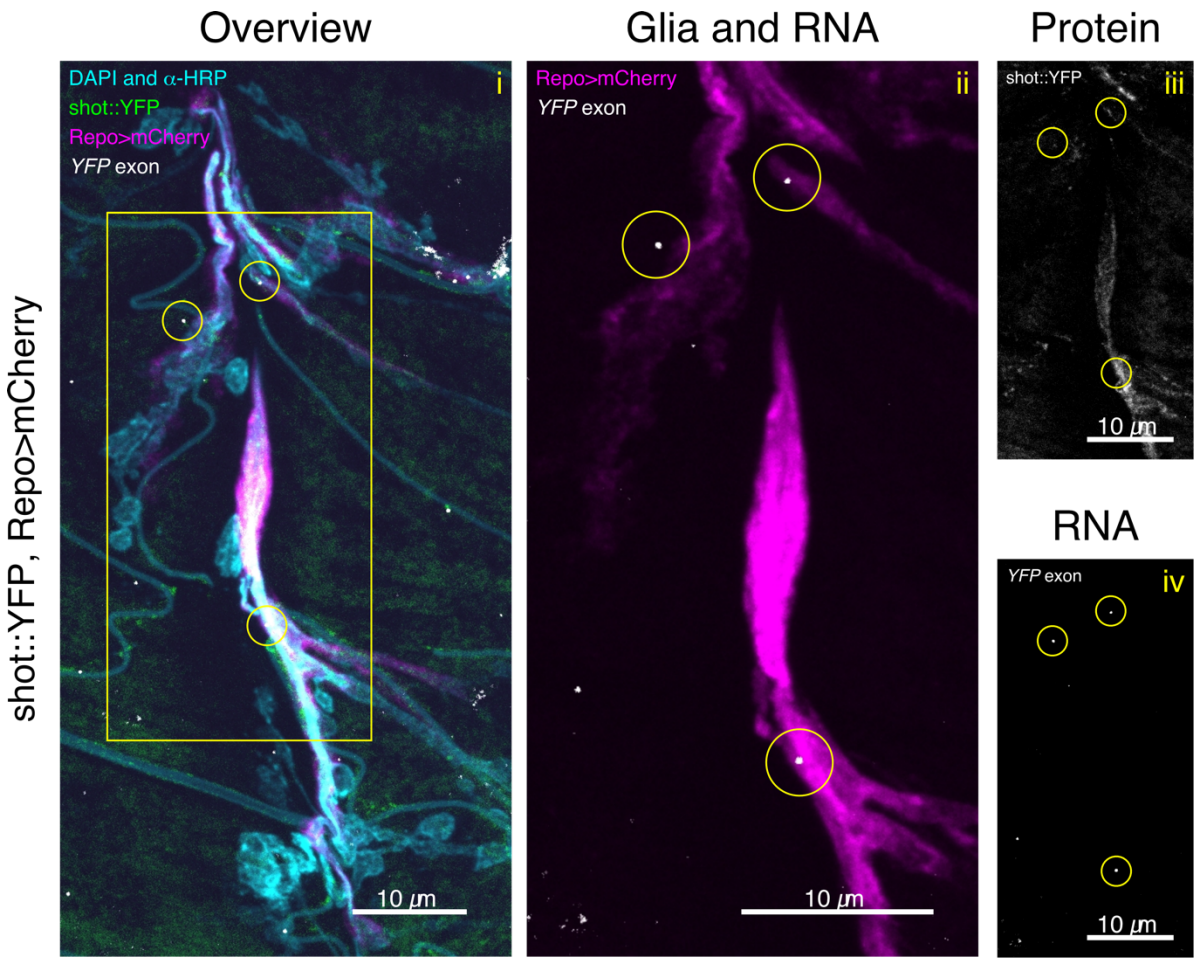

Figure 3-16 Minimal *shot::YFP* mRNAs are present at the NMJ, with few in terminal glial projections, where protein signal can be observed

i) Representative confocal microscopy image of the shot::YFP protein (green) and mRNA (white, α-*YFP* probe labelled with Atto 633) expression patterns in the *Drosophila* 3rd instar NMJ glial projections (Repo>mCherry, magenta). DAPI and α-HRP antibody conjugated to Alexa 405 fluorophore are depicted in cyan. There are only a few mRNA spots of *shot::YFP* mRNA, and most of them overlap with the glial membrane labelling signal (yellow circular ROIs). The protein expression of *shot::YFP* is quite weak; it overlaps with glial signal, but also appears diffuse throughout the muscle. ii-iv) Zoomed-in view of the yellow rectangular ROI from i) (see labels for details). Scale bar - 10 µm.

3.5.2.14 Cip4 is a membrane curvature regulator

Cip4 is a membrane dynamics regulator possessing an F-BAR domain [238, 239]. At the *Drosophila* NMJ, Cip4 was found to inhibit synaptic growth by acting post-synaptically and reducing the secretion of retrograde NMJ growth signals [240].

I have observed mRNA of Cip4::YFP throughout the *Drosophila* NMJ and not confined to the area of the glial labelling. I have however observed a faint pattern of Cip4::YFP protein overlapping with the glial labelling, and largely within its confines (Figure 3-17).

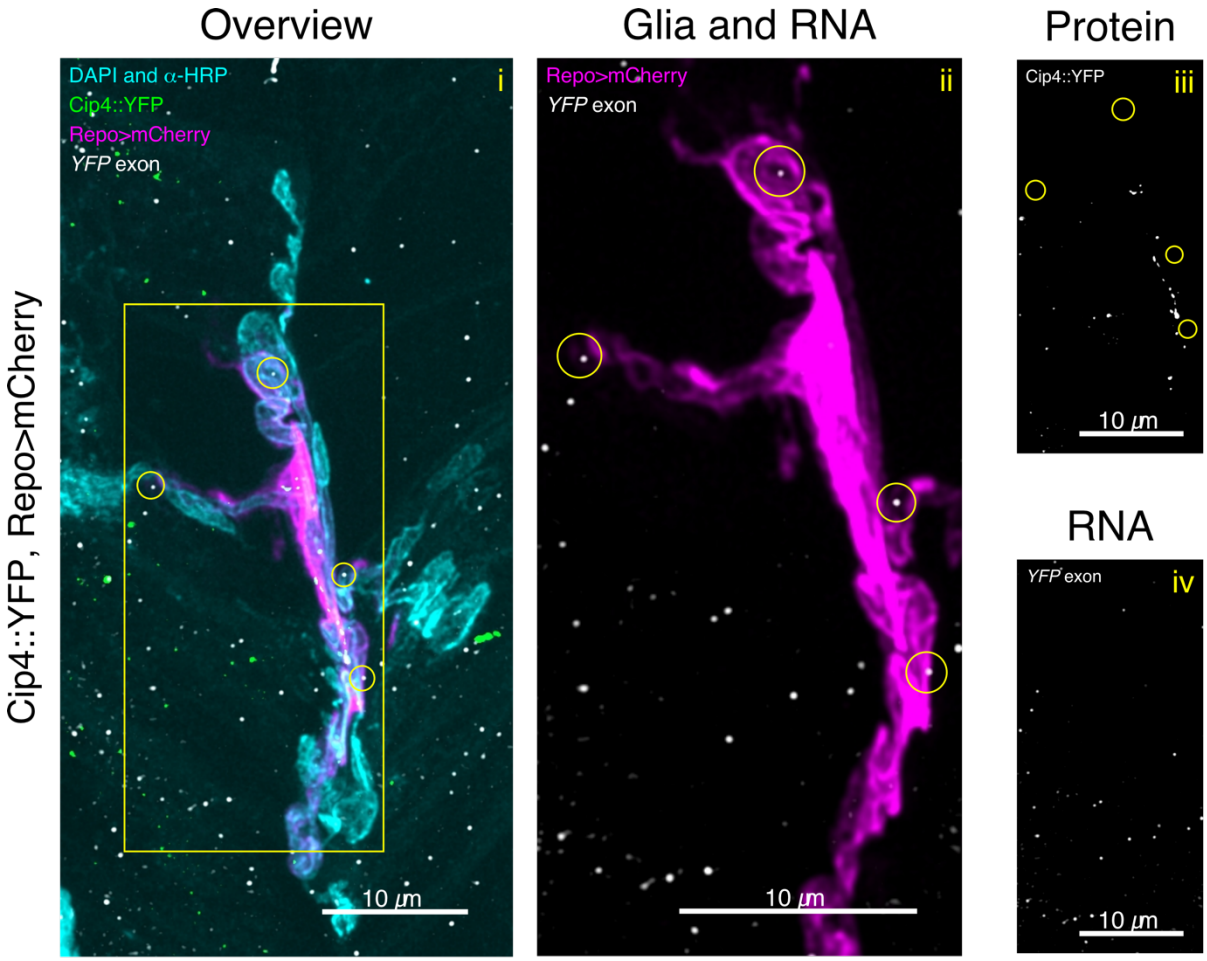

Figure 3-17 Some *Cip4::YFP* mRNA molecules are present at the NMJ, including a few in terminal glial projections, where the *Cip4::YFP* protein signal is almost exclusively found

i) Representative confocal microscopy image of the Cip4::YFP protein (green) and mRNA (white, α-*YFP* probe labelled with Atto 633) expression pattern in the *Drosophila* 3rd instar NMJ glial projections (Repo>mCherry, magenta). DAPI and α-HRP antibody conjugated to Alexa 405 fluorophore are depicted in cyan. The mRNA expression is sparse everywhere in the NMJ, and a few individual foci overlap with the glial signal (yellow circular ROIs). The protein signal is low, but the visible almost exclusively in the glia. ii-iv) Zoomed-in view of the yellow rectangular ROI from i) (see labels for details). Scale bar - 10 μm.

3.5.2.15 cold is a SJ protein

cold encodes a protein which is necessary for SJ formation which belongs to Ly6 family of membrane glycoproteins [208]. It has been studied in the context of BBB formation in *Drosophila,* where it was found to be necessary for the correct placement of SJs between the SPG, and the maintained barrier integrity [206, 241].

cold::YFP protein expression pattern overlapped very closely with the glial labelling pattern. *cold::YFP* mRNA was sparse at the NMJ, but mostly present within the glial labelling area (Figure 3-18).

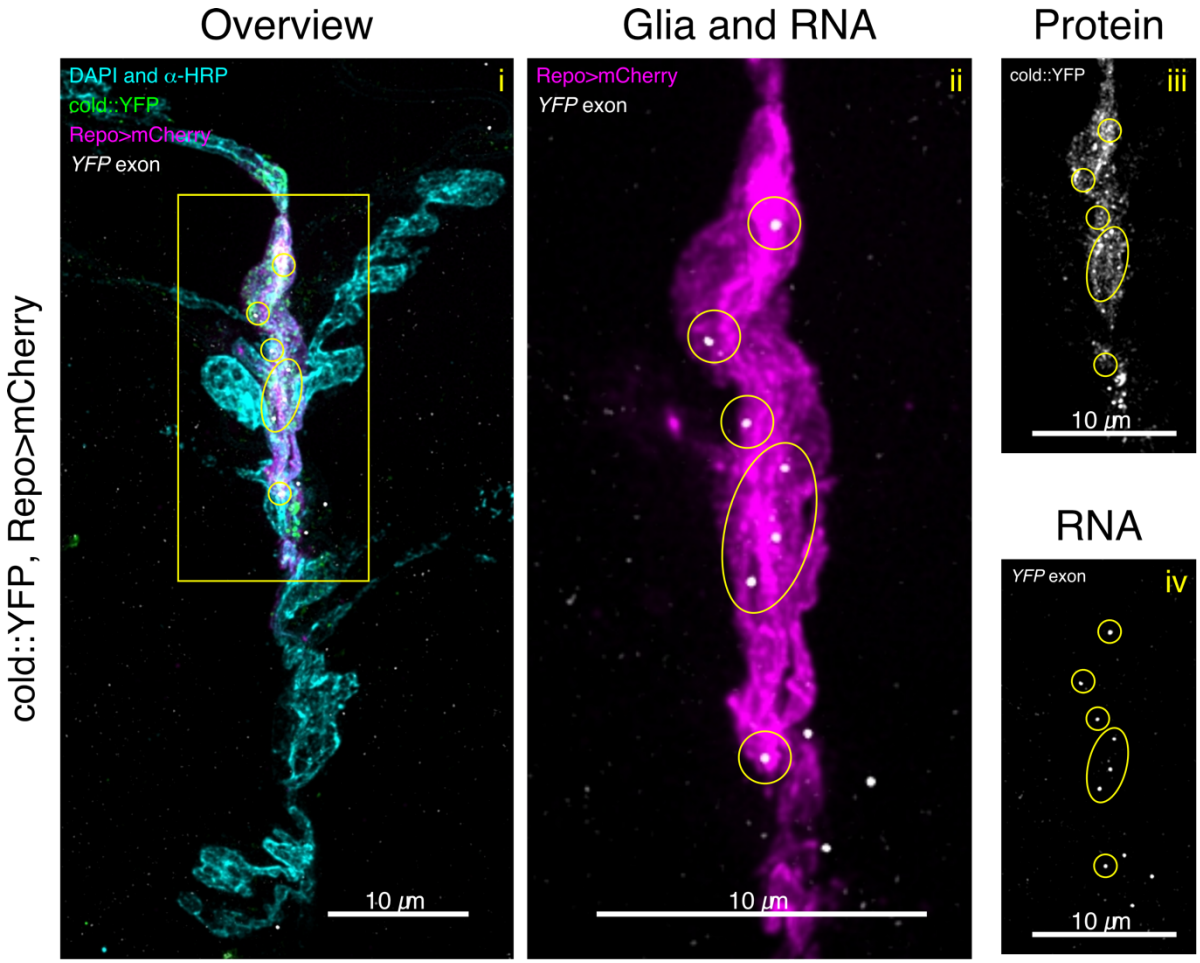

Figure 3-18 *cold::YFP* protein is concentrated in terminal glial projections accompanied by few mRNAs

i) Representative confocal microscopy image of the cold::YFP protein (green) and mRNA (white, α-*YFP* probe labelled with Atto 633) expression pattern in the *Drosophila* 3rd instar NMJ glial projections (Repo>mCherry, magenta). DAPI and α-HRP antibody conjugated to Alexa 405 fluorophore are depicted in cyan. The mRNA expression and protein expression overlap nearly perfectly with the glial labelling (yellow circular ROIs). The protein signal is low, but visible almost exclusively in the glia. ii-iv) Zoomed-in view of the yellow rectangular ROI from i) (see labels for details). Scale bar - 10 μm.

3.5.2.16 Pdi is a protein disulfide-isomerase

Pdi is a protein disulfide-isomerase necessary for the folding of proteins containing disulfide bonds [242, 243]. It was interesting to learn that it was suspected to be present in the NMJ glia as these cells have long projections which reach far away from the cell nucleus. One could expect that protein folding might take place closer to the soma rather than in the protrusions.

Pdi::YFP protein pattern overlapped nearly perfectly with the glial labelling. Its mRNA was distributed sparsely and evenly throughout the NMJ area, with several spots also overlapping with the glial labelling (Figure 3-19).

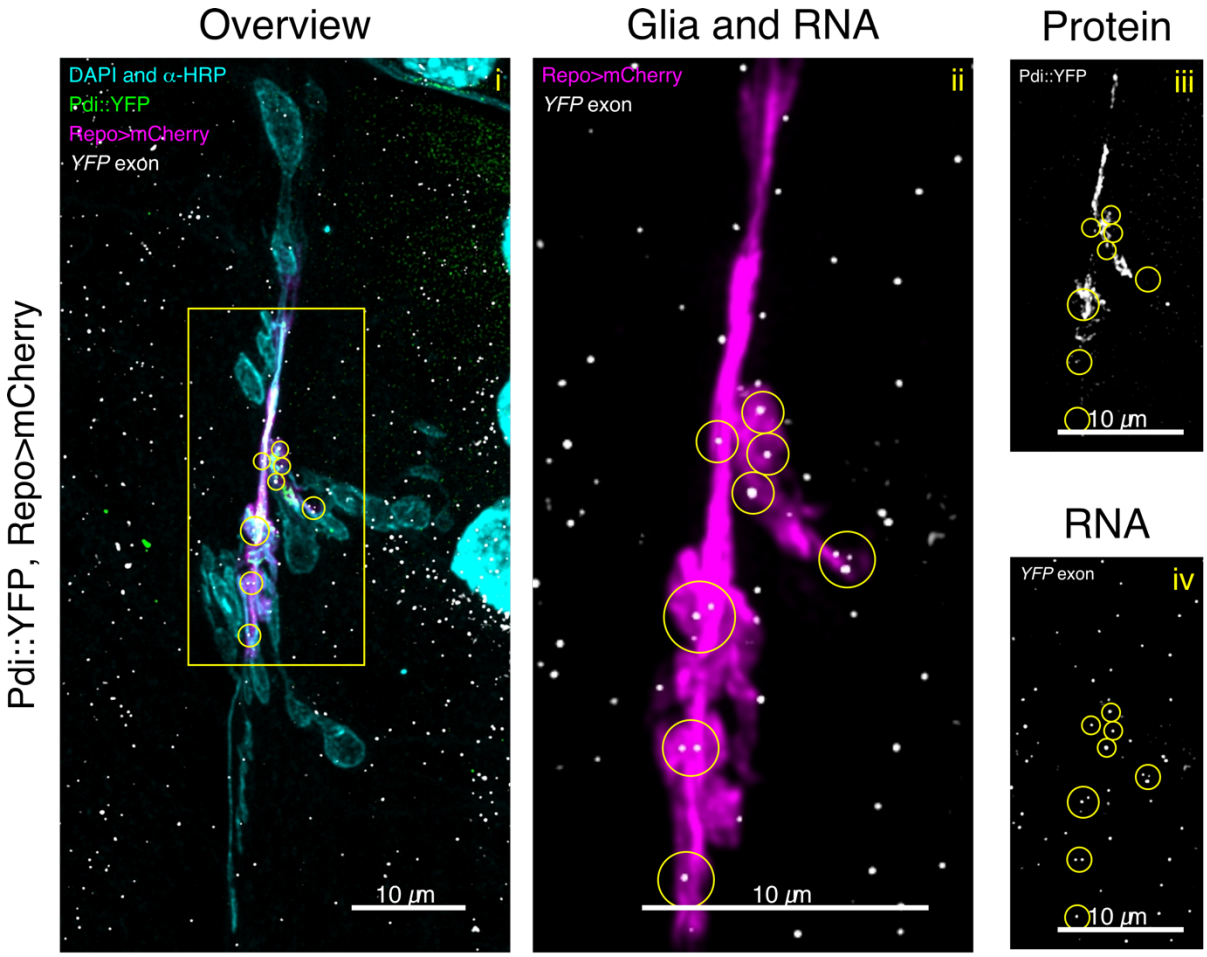

Figure 3-19 *Pdi::YFP* mRNA is abundant at the NMJ and protein is concentrated to the terminal glial projections, where several mRNA molecules can be found

i) Representative confocal microscopy image of the Pdi::YFP protein (green) and mRNA (white, α-*YFP* probe labelled with Atto 633) expression pattern in the *Drosophila* 3rd instar NMJ glial projections (Repo>mCherry, magenta). DAPI and α-HRP antibody conjugated to Alexa 405 fluorophore are depicted in cyan. *Pdi::YFP* mRNA is distributed uniformly in the whole NMJ, and several mRNA molecules are found in glia (yellow circular ROIs). Pdi::YFP protein is found exclusively in glia. ii-iv) Zoomed-in view of the yellow rectangular ROI from i) (see labels for details). Scale bar - 10 μm.

3.5.2.17 Nrg is a cell adhesion protein important in neurite outgrowth

Nrg protein participates in cell-cell adhesion, particularly processes such as SJ formation and axon guidance, as well as neurite outgrowth during developmental neuritogenesis and axonogenesis [202, 244, 245]. It is also known to take part in synapse formation, where it organises MTs in the synaptic terminal, leading to correct formation of active zones [246].

I observed that Nrg::YFP protein expression overlaps closely with the glial labelling, but also appears to be present in the muscle cells. *Nrg::YFP* mRNA seems to be distributed evenly throughout the NMJ area, and many mRNA spots overlap with the glial labelling (Figure 3-20).

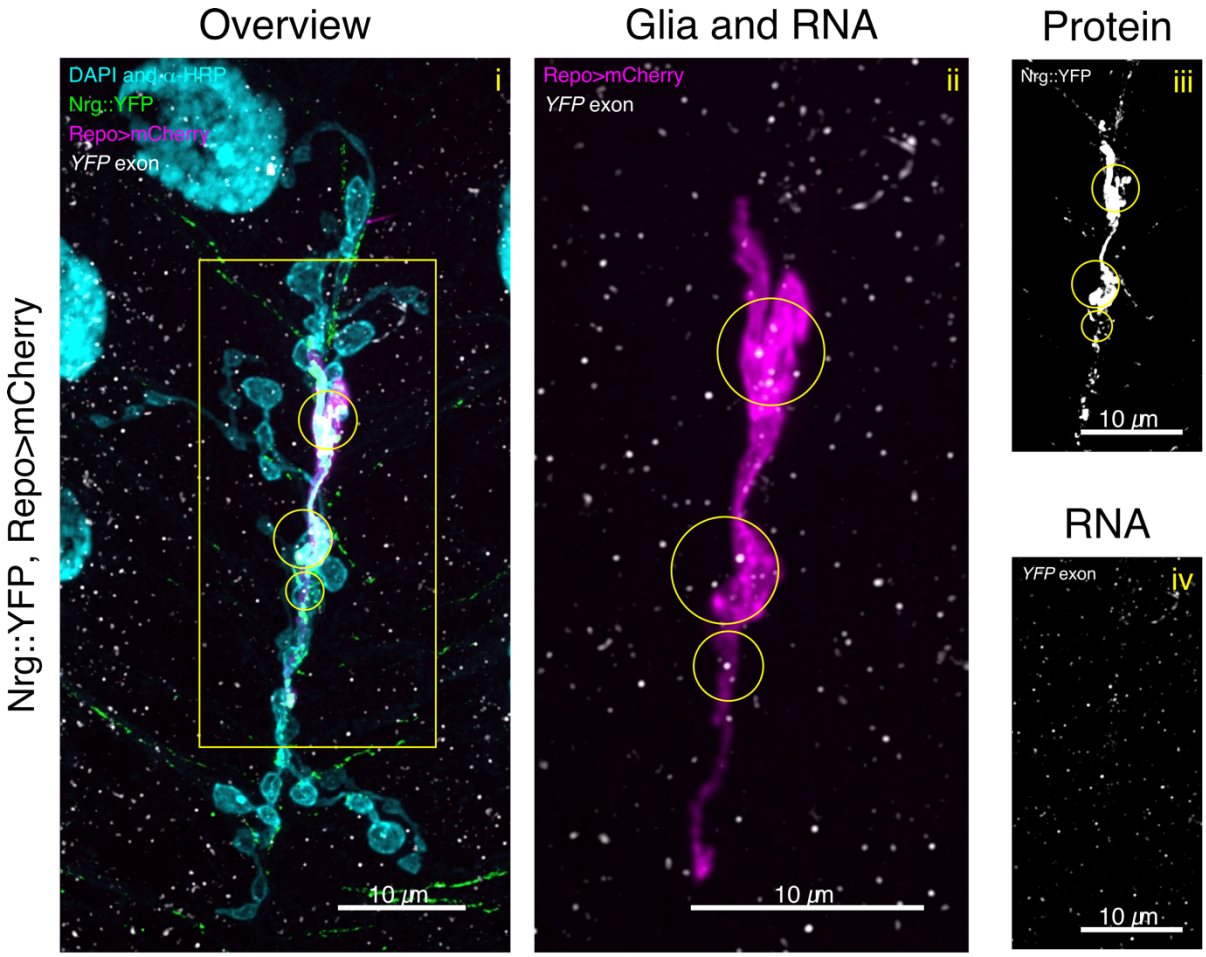

Figure 3-20 Numerous *Nrg::YFP* mRNAs are distributed in the NMJ while the protein is more specific to the terminal glial projections

i) Representative confocal microscopy image of the Nrg::YFP protein (green) and mRNA (white, α-*YFP* probe labelled with Atto 633) expression pattern in the *Drosophila* 3rd instar NMJ glial projections (Repo>mCherry, magenta). DAPI and α-HRP antibody conjugated to Alexa 405 fluorophore are depicted in cyan. *Nrg::YFP* mRNA is distributed evenly in the NMJ area, and several mRNA molecules are found in glia (yellow circular ROIs). Nrg::YFP protein expression overlaps with the glial labelling, but is also found in the muscle strata. ii-iv) Zoomed-in view of the yellow rectangular ROI from i) (see labels for details). Scale bar - 10 μm.

3.5.2.18 Lac is a SJ protein

Lac is yet another protein which participates in cell adhesion. It belongs to the IgSF and is expressed on the cell surface [205]. Like many other candidate glial-projection localised genes observed in the CPTI screen in our laboratory, this protein is also a member of SJ complexes and it participates in correct formation of the tracheal system in *Drosophila* [204].

In my experiments, I observed that Lac::YFP protein expression overlapped nearly perfectly with the glial membrane labelling at the NMJ. *Lac::YFP* mRNA spots appeared to be mostly overlapping with the glial labelling, but some mRNA spots were also present in the muscle area (Figure 3-21).

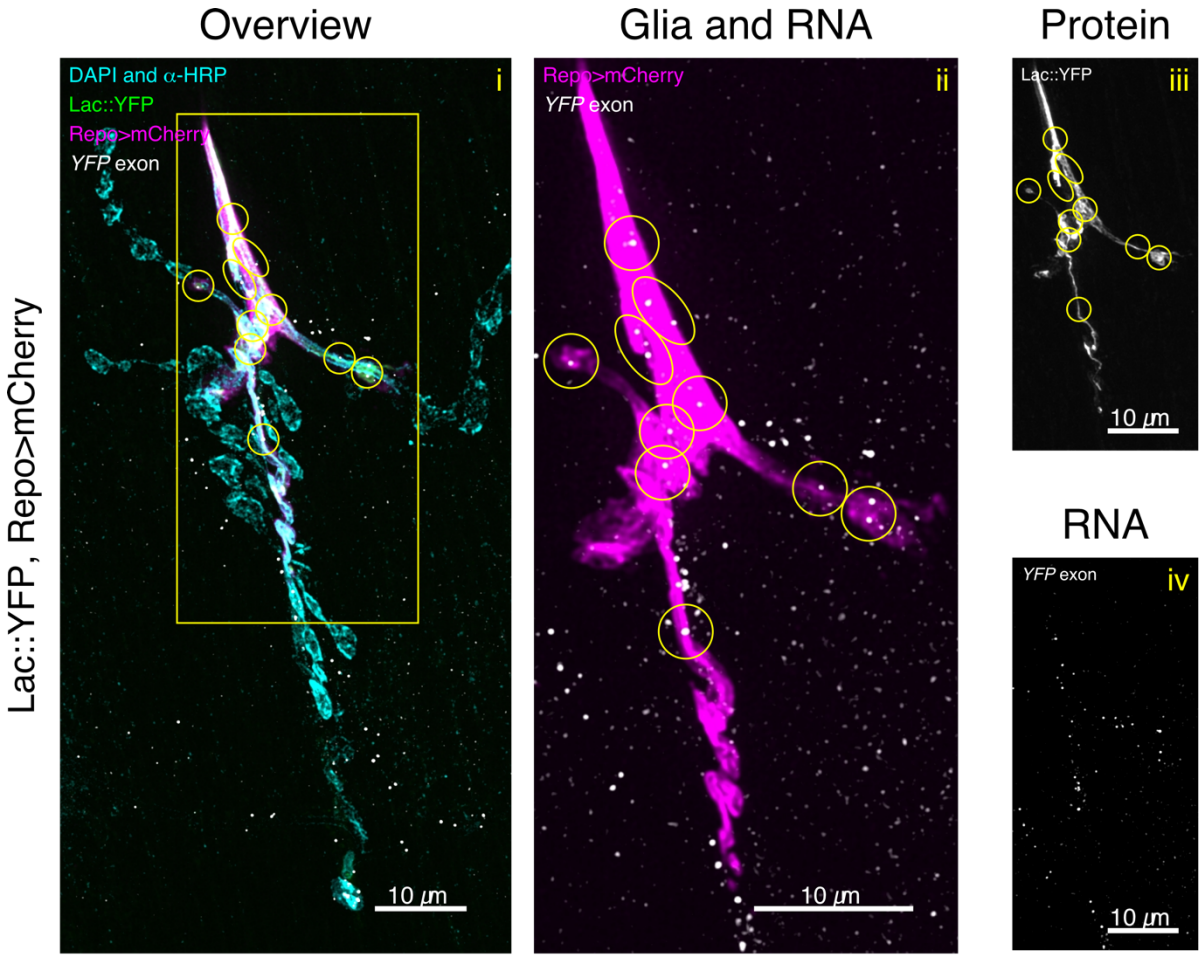

Figure 3-21 Several *Lac::YFP* mRNAs are present in the NMJ in terminal glial projections with bright and concentrated *Lac::YFP* protein signal

i) Representative confocal microscopy image of the Lac::YFP protein (green) and mRNA (white, α-*YFP* probe labelled with Atto 633) expression pattern in the *Drosophila* 3rd instar NMJ glial projections (Repo>mCherry, magenta). DAPI and α-HRP antibody conjugated to Alexa 405 fluorophore are depicted in cyan. Lac::YFP protein expression overlaps very closely with the glial labelling. *Lac::YFP* mRNA is mostly found in the glia (yellow circular ROIs), but some spots are also found in the muscle area. ii-iv) Zoomed-in view of the yellow rectangular ROI from i) (see labels for details). Scale bar - 10 μm.

3.5.3 *Gs2::YFP* protein and mRNA localise to “glial boutons”

One of the most interesting candidate protrusion-localised transcripts was *Gs2*, which is an enzyme responsible for converting glutamate to glutamine [247]. Gs2::YFP protein and mRNA were found in different compartments in different NMJs. In some cases, both the mRNA and protein expression overlapped nearly perfectly with the glial labelling (Figure 3-22). In others, however, the mRNA expression seemed to be present everywhere in the muscle, while the protein expression was still confined to the glial labelling area (Figure 3-23). This was an interesting observation, because it suggested that mRNA of *Gs2* could be selectively expressed in varying tissues, pointing to some type of temporal or spatial control.

In some NMJs, Gs2::YFP protein was observed to be localised to areas with the glial labelling which were independent of and separate from the axon terminal boutons, which I refer to as “glial boutons”. Moreover, these “glial boutons” contained several molecules of *Gs2::YFP* mRNA each (Figure 3-24). Hence, it is possible to speculate that Gs2 protein performs a key function in these boutons, and local translation might be necessary for that function.

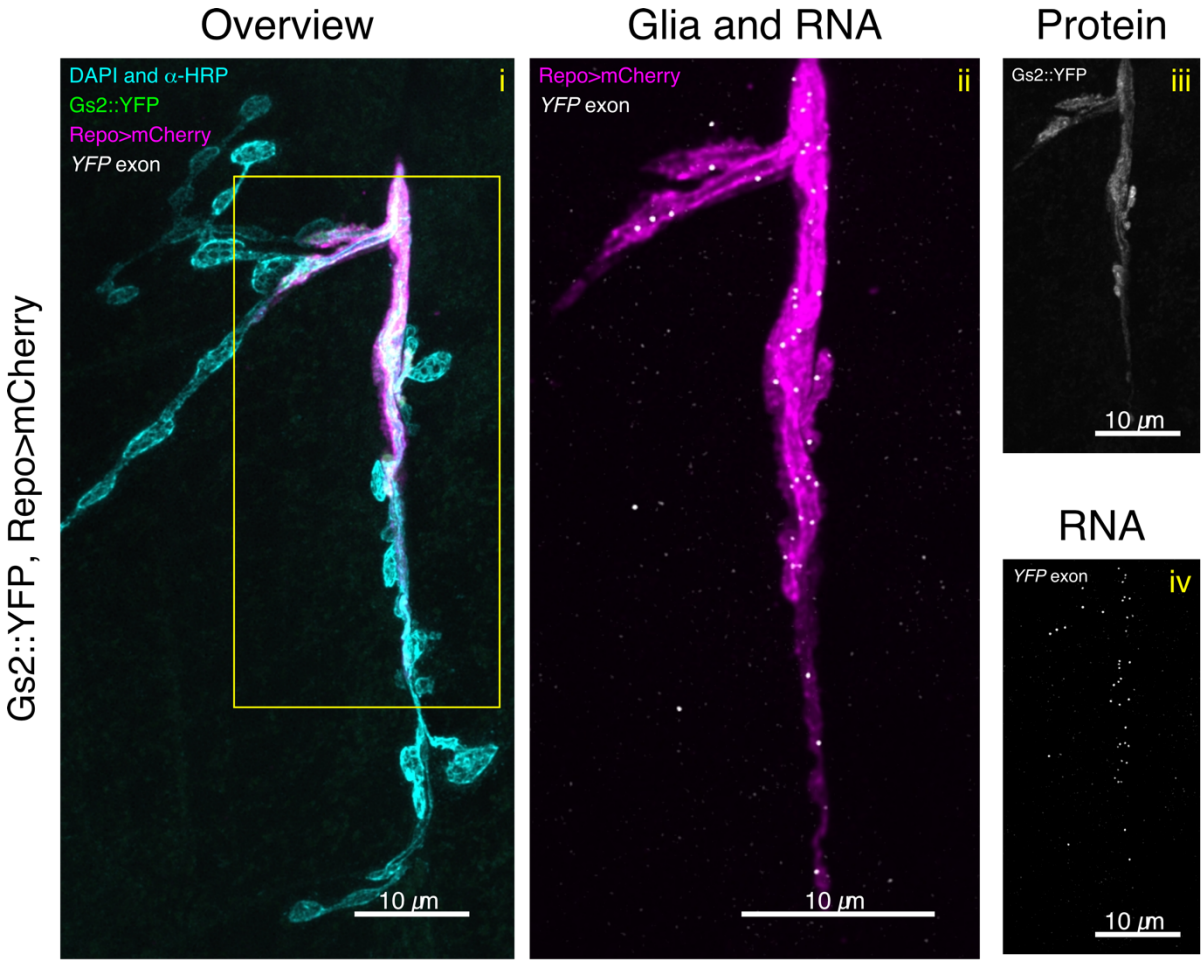

Figure 3-22 *Gs2::YFP* mRNA and protein are specifically concentrated in terminal glial projections

i) Representative confocal microscopy image of the Gs2::YFP protein (green) and mRNA (white, α-*YFP* probe labelled with Atto 633) expression pattern in the *Drosophila* 3rd instar NMJ glial projections (Repo>mCherry, magenta). DAPI and α-HRP antibody conjugated to Alexa 405 fluorophore are depicted in cyan. Gs2::YFP protein closely overlaps with the Repo>mCherry expression. *Gs2::YFP* mRNA is present nearly exclusively in the glia in this NMJ. ii-iv) Zoomed-in view of the yellow rectangular ROI from i) (see labels for details). Scale bar - 10 μm.

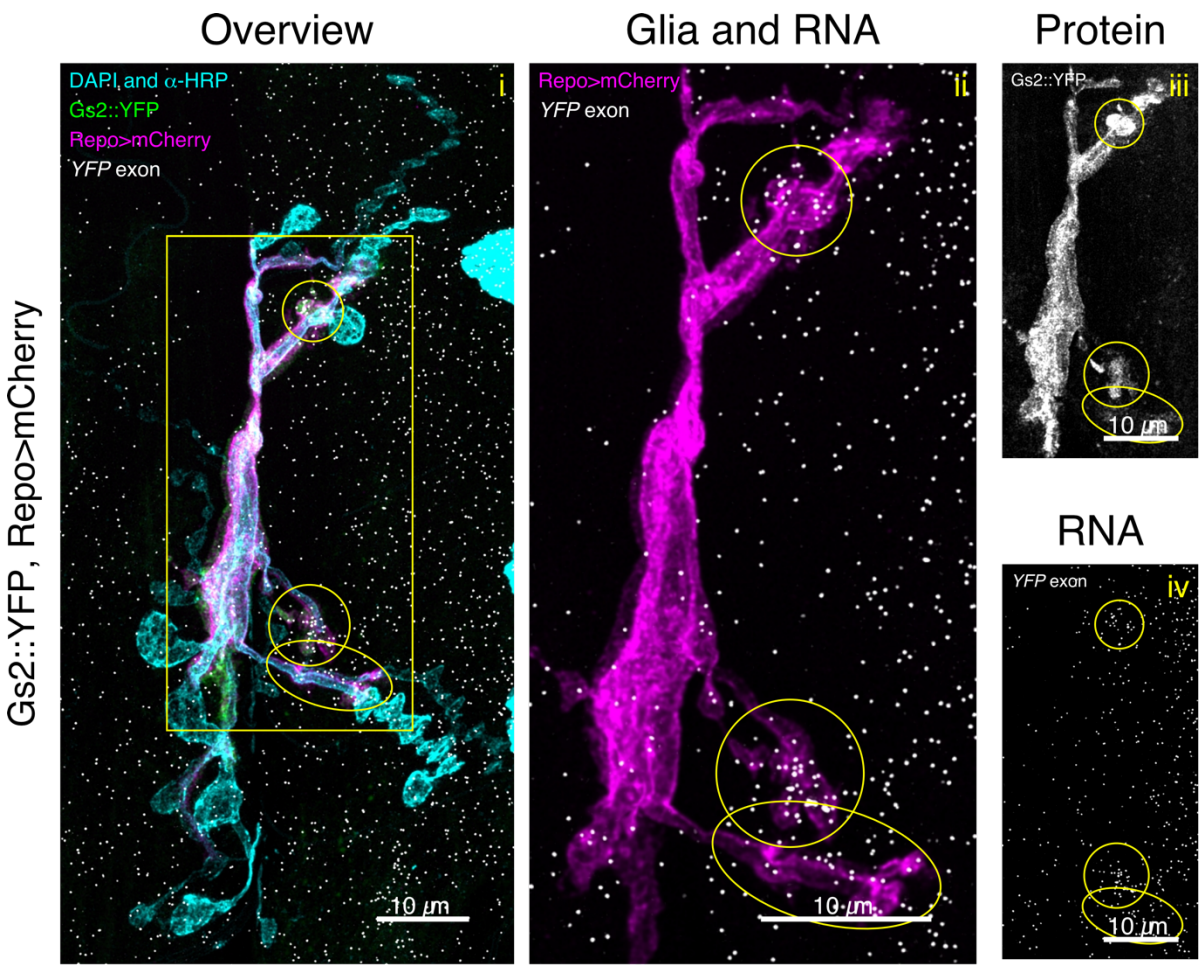

Figure 3-23 Abundant *Gs2::YFP* mRNAs are present everywhere in the NMJ while the protein signal is still concentrated and exclusive to terminal glial projections

i) Representative confocal microscopy image of the Gs2::YFP protein (green) and mRNA (white, α-*YFP* probe labelled with Atto 633) expression pattern in the *Drosophila* 3rd instar NMJ glial projections (Repo>mCherry, magenta). DAPI and α-HRP antibody conjugated to Alexa 405 fluorophore are depicted in cyan. Gs2::YFP protein closely overlaps with the Repo>mCherry expression. *Gs2::YFP* mRNA is present both in the glia, including in some regions with particularly high concentration of molecules of *Gs2::YFP* mRNA glia (yellow circular ROIs), but also everywhere in the surrounding muscle, thus showing a different mRNA expression pattern when compared to Figure 3-22. ii-iv) Zoomed-in view of the yellow rectangular ROI from i) (see labels for details). Scale bar - 10 μm.

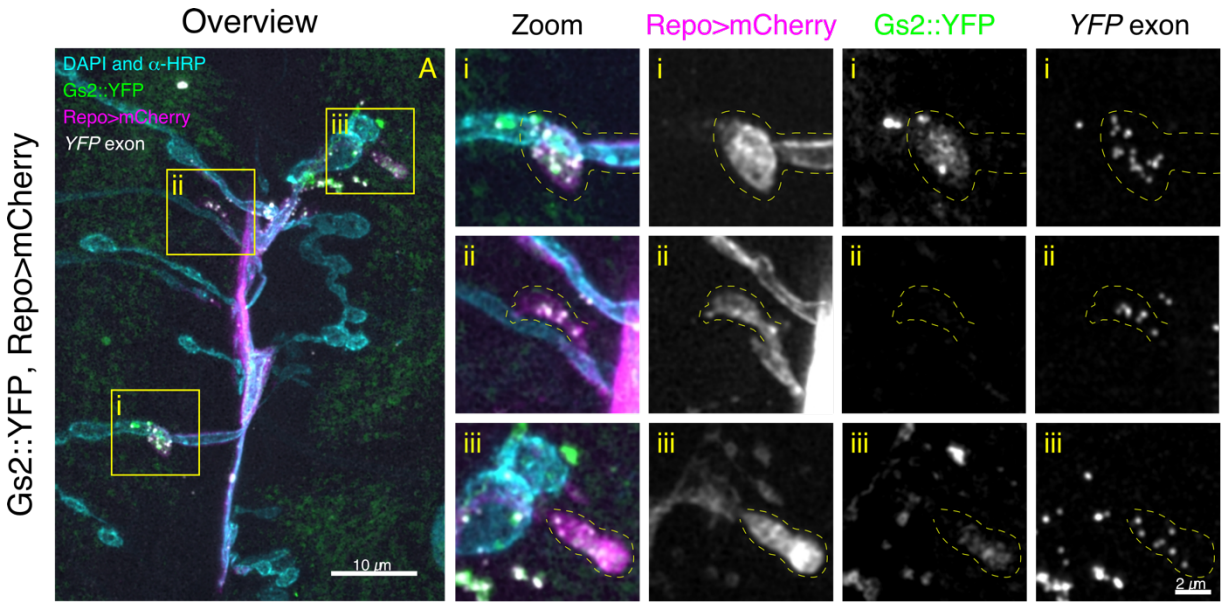

Figure 3-24 *Gs2::YFP* mRNA and protein are present in glial structures separate from the axon terminal boutons

A. Confocal microscopy image presenting the Gs2::YFP protein (green) and mRNA (white, α-*YFP* probe labelled with Atto 633) expression pattern in the *Drosophila* 3rd instar NMJ glial projections (Repo>mCherry, magenta). DAPI and α-HRP antibody conjugated to Alexa 405 fluorophore are depicted in cyan. Gs2::YFP protein and mRNA localise to glial boutons which do not overlap with synaptic boutons. Red panels in the overview (i-iii) are enlarged on the right (Zoom) and individual channels (see label above) present three individual glial boutons with Gs2::YFP protein and mRNA in them. The yellow dotted line ROIs in each panel (i-iii) correspond to the glial bouton outline in each case. For all three boutons, the glial bouton does not overlap with the axon terminal and is a separate, independent structure in which local translation might be happening, based on the abundance of mRNA and, sometimes, protein (i and iii), in those boutons. Scale bars - 10 μm (Overview), 2 μm (Zoom).

3.5.4 Two perplexing genes: high RNA levels, but no protein

ORMDL::YFP and *sdk::YFP* were the two genes which stood out in my experiments because they had the highest levels of mRNA in glial processes. Remarkably, neither line contained protein within the NMJ glial labelling. This discordance in the level of mRNA and protein could be explained by strong translational repression of the mRNA, or by a technical artefact. To rule out the latter, I designed a gene-specific smFISH probe against the coding sequence of *ORMDL* (labelled with Alexa 568) and compared it to the signal from the *YFP* smFISH probe in the same sample. The endogenous *ORMDL* mRNA pattern looked nothing like the α-*YFP* probe pattern, indicating that the α-*YFP* exon smFISH signal does not arise from an *ORMDL* reporter (Figure 3-25). The absence of protein signal suggests that the reporter is not inserted into an open reading frame and is therefore not being properly translated.

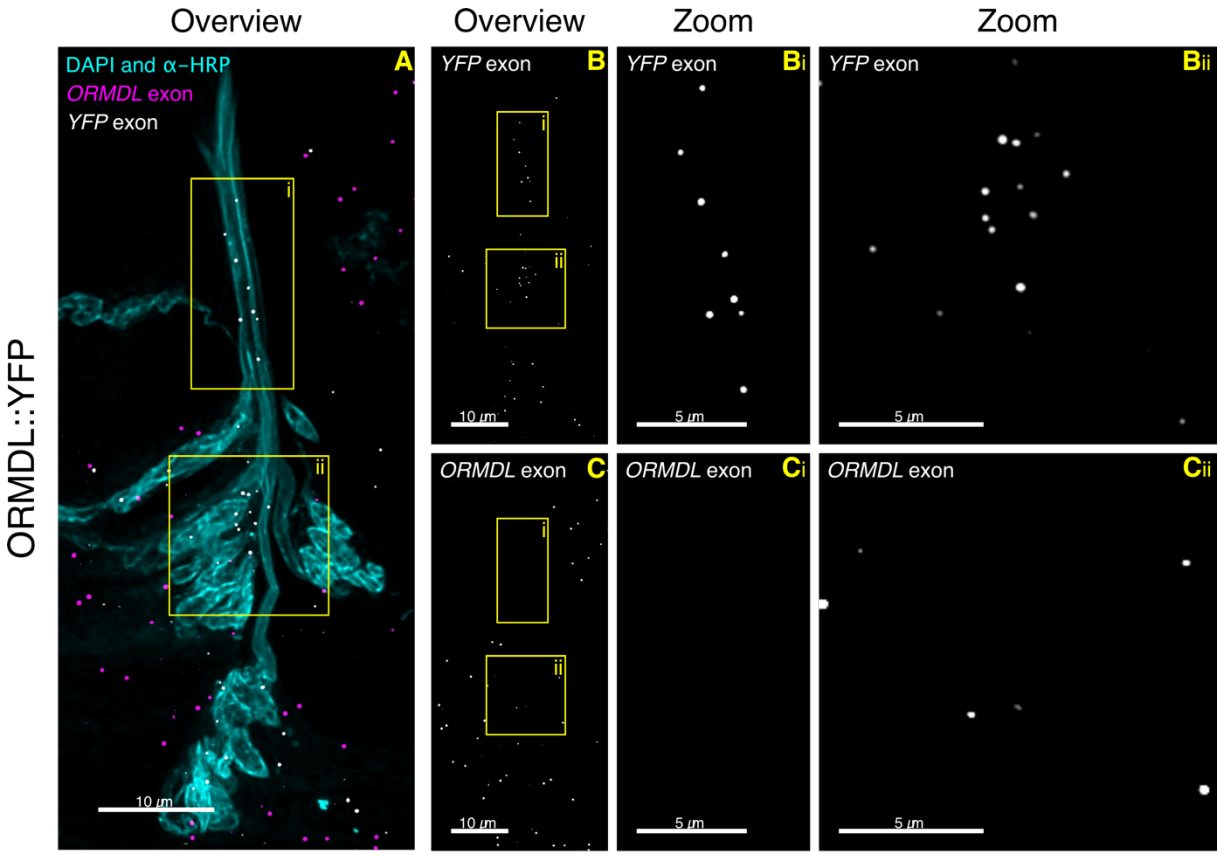

Figure 3-25 α-*YFP* probe in ORMDL::YFP line does not co-localise with α-*ORMDL* exon probe

A. Representative confocal microscopy image of a *Drosophila* 3rd instar larval NMJ from the ORMDL::YFP line, labelled with both the α-*YFP* exon (Atto 633) and α-*ORMDL* exon (Alexa 568) smFISH probes. DAPI and α-HRP antibody conjugated to Alexa 405 fluorophore are depicted in cyan. B-C. A zoomed in view showing only the smFISH channel with α-*YFP* probe (B) and α-*ORMDL* exon probe (C). B-C. i-ii) depict the respective zoomed in ROIs of individual smFISH channels which show that *ORMDL::YFP* mRNA signal does not co-localise with the endogenous *ORMDL* exon mRNA signal. Scale bars – 10 μm (A-C), 5 μm (B-C i-ii)).

The ORMDL::YFP line had the following warning in the original publication which described the lines: *Possible insertion in 5' UTR of ORMDL. RACE data indicate insertion in Hsp70B. Nuclear GP localisation not consistent with either. Use with caution* [182]. Intrigued by the unusually strong mRNA expression pattern and the lack of clarity regarding the insertion site, I performed genetic analysis of the insertion to better understand what caused the artefact. RT-PCR was carried out with primers especially designed to amplify the *YFP* sequence and the insert sequences from both sides and understand whether possibly *YFP* was inserted in the wrong orientation in the ORMDL::YFP line (Figure 3-26). While the *YFP* sequence was amplified, no sequences were amplified when “neighbouring” *ORMDL* probes were used (Figure 3-27).

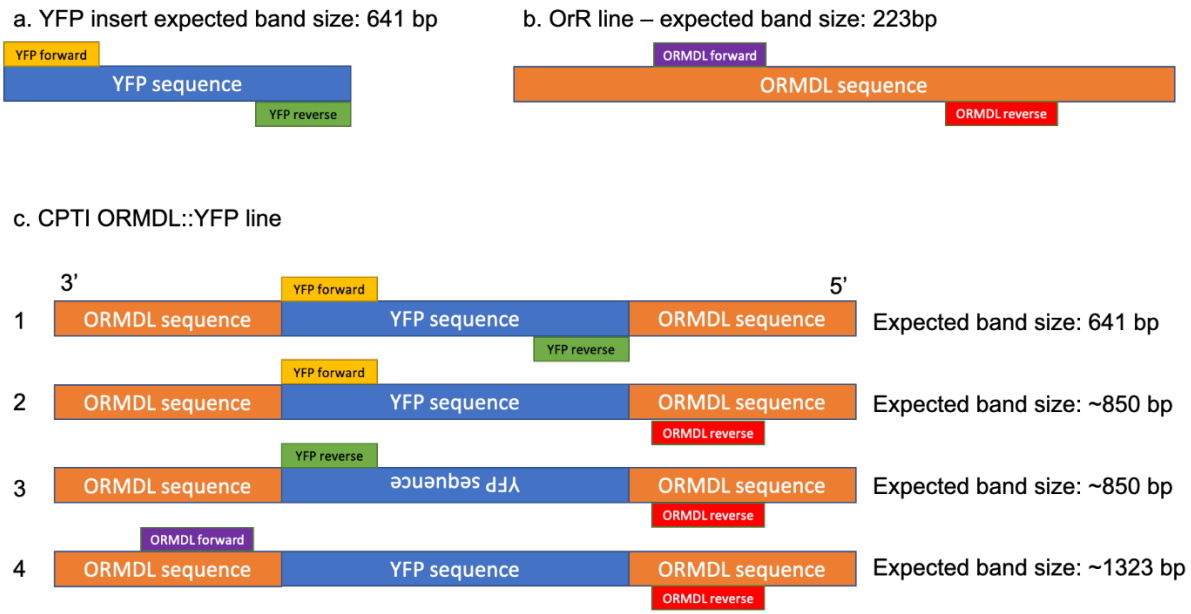

Figure 3-26 RT-PCR experimental design

Forward and reverse primers were designed against both the *YFP* sequence (a) and against a middle fragment of the *ORMDL* sequence (b). c) Four experimental sets (1-4) were designed and used in three different experiments: with ORMDL::YFP line, negative control where water was used instead of DNA, and OrR line. It was expected that in experiment 1, only ORMDL::YFP line would have a fragment amplified, because it is the only one which should have the *YFP* sequence, and similarly either experiment 2 or 3 would show a band for ORMDL::YFP line, depending on the *YFP* orientation in the insert. Experiment 4 was expected to have a band for both the OrR and ORMDL::YFP line (since the CPTI lines can be heterozygous and have one wild type chromosome and one chromosome with the *YFP* insertion). Hence, 12 experiments were run: 4 for the ORMDL::YFP line, 4 for the empty PCR control and 4 for the OrR line.

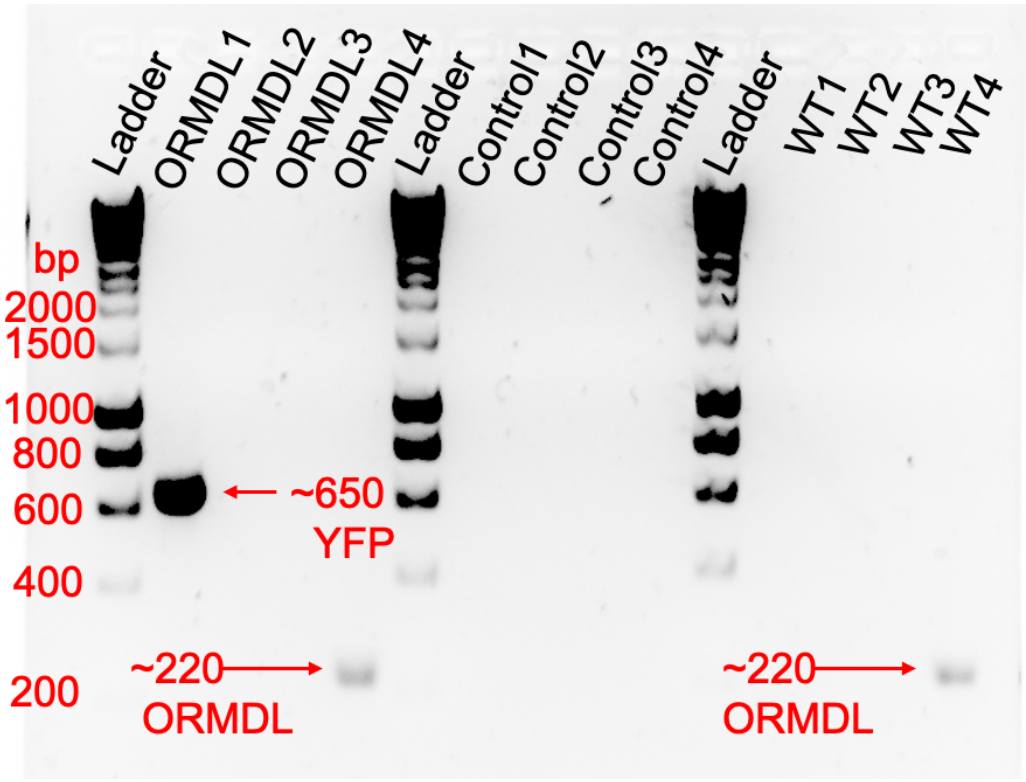

Figure 3-27 Result of the RT-PCR experiment with the ORMDL::YFP line

ORMDL::YFP line (ORMDL1-4), the empty control (Control1-4) and the OrR positive control (WT1-4). As expected, the *YFP* sequence is amplified for experiment 1 in the ORMDL::YFP line, and for experiment 4, *ORMDL* sequence without the insert is amplified both for the OrR (WT4) control and for the ORMDL::YFP (ORMDL4) line. The negative control worked, as nothing is amplified, and WT1-4 show no *YFP* mRNA expression, as expected. However, in the ORMDL::YFP line experiments, ORMDL2 and ORMDL3 have no bands, indicating that the insert is not in the *ORMDL* gene. Considering that no protein expression was observed in the smFISH experiments (Figure 3-13), it is reasonable to assume that the *YFP* is inserted in some different region which is not translated but is transcribed in glial cells. Since ORMDL4 band is similarly pronounced to the WT4 band, it is not certain whether the *YFP* is inserted anywhere near the *ORMDL* gene at all in the ORMDL::YFP line simply based on the CPTI lines being heterozygous.

Based on the results of the RT-PCR experiment, a conclusion could be reached that the *YFP* insert is probably not in the *ORMDL* gene. *sdk::YFP* mRNA shows a similar expression pattern with no protein expression. It was therefore possible the insert is mapped incorrectly for this gene, too. Upon the examination of the larval ventral nerve cords (VNCs), however, I noticed sdk::YFP protein signal. However, in the ORMDL::YFP larvae, there was still no YFP protein signal and a lot of mRNA signal (Figure 3-28).

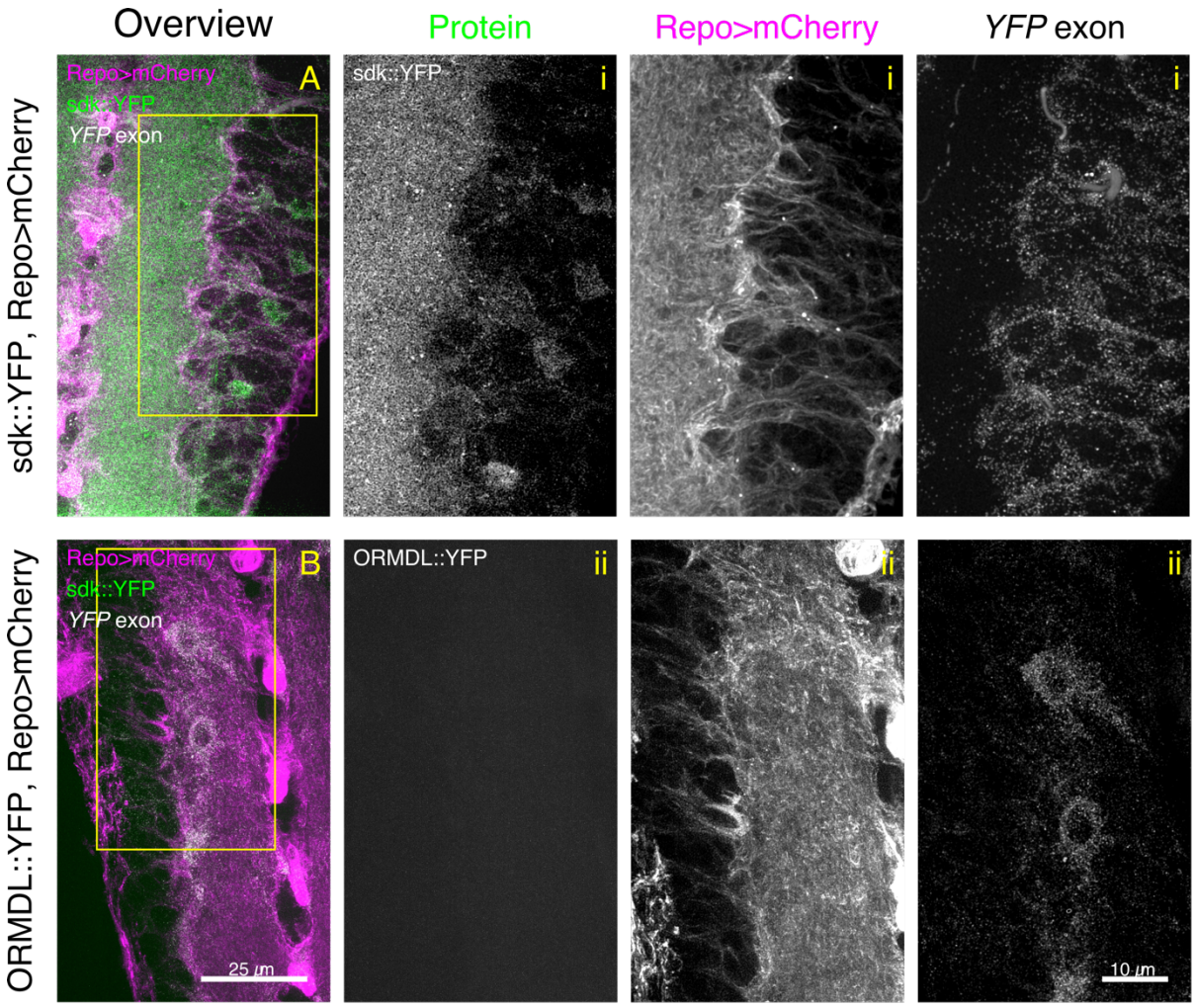

Figure 3-28 Comparison of the larval brains from the sdk::YFP and ORMDL::YFP lines

A. Representative confocal microscopy image of the sdk::YFP protein (green) signal clearly visible in the VNC of the *Drosophila* 3rd instar larvae. mRNA is shown in white (α-*YFP* probe labelled with Atto 633) and glial cells membrane in magenta (Repo>mCherry). Panels labelled i) present a zoomed-in single-channel view of the yellow rectangular ROI from A. (see labels for details). Scale bar - 25 µm (see B, Overview), 10 µm (see B i). B. Representative confocal microscopy image showing the lack of ORMDL::YFP protein (green) signal in VNC of the *Drosophila* 3rd instar larvae. mRNA is shown in white (α-*YFP* probe labelled with Atto 633) and glial cells membrane in magenta (Repo>mCherry). Panels labelled ii) present a zoomed-in single-channel view of the yellow ROI from B (see labels above row A for details). Scale bar - 25 µm (Overview), 10 µm (ii).

3.6 Discussion

The results show conclusively that for all the candidate genes, at least some mRNA spots detected with α-*YFP* probe in their CPTI lines were observed to overlap with the glial projection membrane labelling at the *Drosophila* NMJ. These mRNAs are therefore located very near the sites of synaptic activity at the *Drosophila* NMJ. Additionally, the analysis of previous literature confirms that many of these candidates have been found localised to glial projections in various studies and in different organisms, even in different glial cell types, or produced a defect when knocked down by RNAi in glial cells of *Drosophila* [248, 249].

3.6.1 Protrusion-localised transcripts tie to cell adhesion and cytoskeleton

As previously discussed in the introduction to this chapter, many of the identified genes whose transcripts are localised to the terminal glial NMJ projections are known to be involved in cell-cell adhesion and SJs formation. SPG of the NMJ form the BBB, and they maintain its integrity and selective permeability through SJs [210]. Six of the identified genes (*Nrg*, *Atpα*, *Gli*, *Lac*, *cold* and *nrv2*) directly participate in SJ formation [207]. It is plausible to imagine that with plasticity, new SJs which are necessary for the maintenance of BBB could be formed from localised mRNAs. Ultrastructural analysis coupled with direct and simultaneous labelling of multiple SJ components with the use of structural synaptic plasticity experiments would have to be done to explore this hypothesis.

Other examined genes could be broadly classified into those related to cytoskeleton, cell adhesion, remodelling and other physical properties of glial cells (*Flo2*, *α-Cat*, *sdk*, *kst*, *shot*, *Cip4*). There were also many genes related to metabolism and cell homeostasis (*nrv2*, *Gs2*, *Vha55*, *ATPα*, *Pdi*). Particularly, the presence of three genes

related to ATP synthesis (*nrv2*, *Vha55*, *ATPα*) points to the possibility that the glial cells in *Drosophila* are secreting ATP into the extracellular space, as described before for PSCs [250]. Both cell adhesion and metabolism regulation have been previously described as important for PSCs [30]. This could indicate that the presence of localised mRNA might facilitate local translation of the proteins required to control these important glial functions in a rapid and compartmentalised manner.

3.6.2 α-*YFP* probe and α-*ORMDL* exon probe show no overlap in the ORMDL::YFP line

I explored *ORMDL* in depth because of the interesting pattern its transcript made at the NMJ. *Ormdl3*, the mouse homologue of this gene, has been previously identified to be necessary for sphingolipid synthesis and proper neurological function [251]. Considering this and its presence in glial periphery in other studies [45], it could be expected to have a significant role in glia. Indeed, it seemed like *ORMDL::YFP* mRNA was abundant in the NMJ glia (Figure 3-13). Yet, my investigation into the ORMDL::YFP line has shed doubt on that hypothesis (Figure 3-25, Figure 3-27). Interestingly, for both *sdk::YFP* and *ORMDL::YFP* which both showed highest and most concentrated mRNA expression in the NMJ glia, the *YFP* insert appears to be placed in the opposite direction compared to the directionality of the genes (Figure 3-29, Figure 3-30). Hence, it is possible that directionality is related to the apparent abundance of the *YFP* mRNA at the NMJ in glial projections. Considering my observations, I decided not to include *ORMDL* in my future experiments, because I have confirmed by smFISH that the α-*YFP* exon probe and endogenous α-*ORMDL* exon probe do not overlap (Figure 3-25).

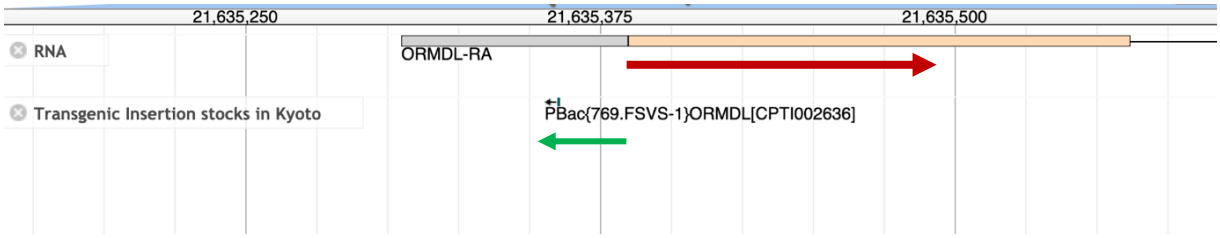

Figure 3-29 CPTI site of insertion for the ORMDL::YFP line as reported by FlyBase

An image from FlyBase JBrowse (http://flybase.org/jbrowse/) indicating the site of the CPTI insertion for the ORMDL::YFP line. The red arrow indicates the directionality of the gene, and the green arrow indicates the direction of the insert. The insert seems to be placed inside the 3'UTR of the gene (gray), which could explain the lack of the protein. However, the RT-PCR experiment performed on the ORMDL::YFP line (Figure 3-27) did not allow for the amplification of the mRNA sequence with the insert, hence it is unlikely that the insert is actually where FlyBase maps it.

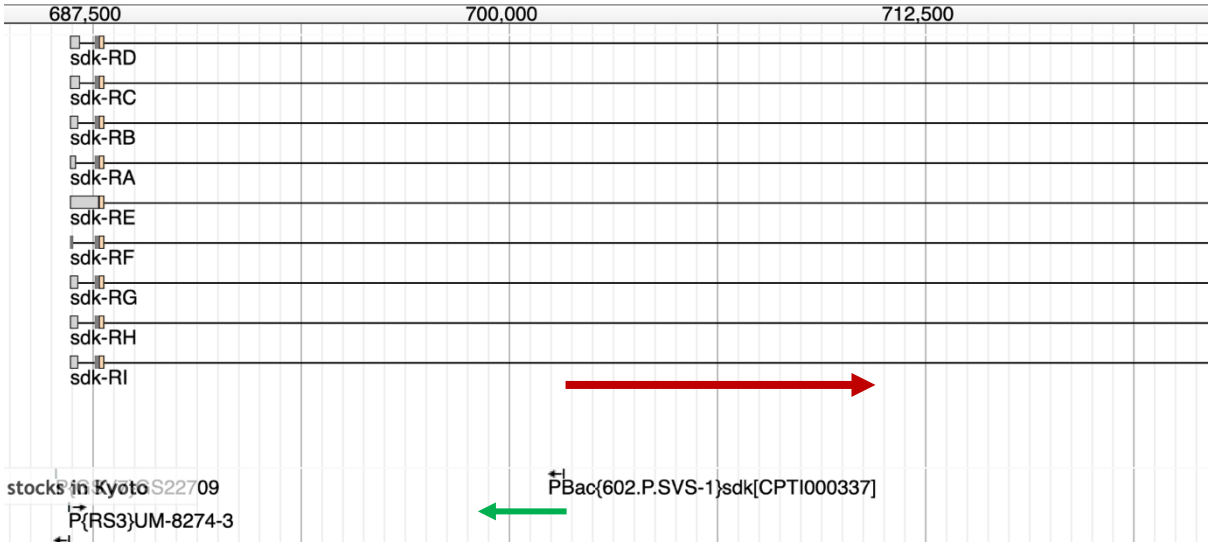

Figure 3-30 CPTI site of insertion for the sdk::YFP line as reported by FlyBase

An image from FlyBase JBrowse (http://flybase.org/jbrowse/) indicating the site of the CPTI insertion for the sdk::YFP line. The red arrow indicates the directionality of the gene, and the green arrow indicates the direction of the insert. The insert is placed inside an intron (black horizontal line), so theoretically *YFP* should be present. No protein was observed at the NMJ, but it was observed in the brain. The mRNA expression pattern at the NMJ is very similar to that of ORMDL::YFP line, which suggested these two lines might have something in common.

3.6.3 Chapter limitations

One of the limitations of this chapter is the fact that some YFP traps from the CPTI collection are heterozygous, implying that potentially only half of the mRNA molecules might be visible. However, the main emphasis in this chapter was the confirmation of the mRNA presence in glia as opposed to quantifying it, and for all genes their mRNA was found within glial projection labelling. Quantitative analysis would have to be carried out in homozygous CPTI lines only, and, where impossible, endogenous probe against the mRNA of interest would have to be used. Moreover, the evaluation of the mRNA presence in projections was done qualitatively and was limited to the visible area of the glial membrane labelling at the NMJ. This does not in fact guarantee the presence of this mRNA inside the glial projection, rather implies it, especially for mRNAs where only limited molecules were observed. Super-resolution microscopy coupled with 3D analysis could offer clarification and confirmation.

Another limitation is that the mRNA of the genes of interest was identified using the α-*YFP* probe, rather than a probe against the target gene's exon sequence. This constitutes the strength of the CPTI screen previously conducted in our laboratory (Figure 3-1). Identifying the *YFP* sequence integrated into the gene sequence eliminates the need for designing 200 individual probes against 200 genes and instead allows for their imaging with the same α-*YFP* probe [181]. Simultaneously, this approach could present challenges. A notable example is the *ORMDL* gene, in which the *YFP* probe did not detect the expected mRNA of the *ORMDL* gene, seemingly because the *YFP* insert is not where it is reported to be (Figure 3-25, Figure 3-27, Figure 3-29).

The accuracy of insertions in most of the other genes was supported by their known functions and corroborated by images from antibody stains and other protein traps in prior literature. However, the other CPTI lines used in this chapter could be akin to ORMDL::YFP and their *YFP* insert might be in another gene. To fully verify this, I would need to design probes targeting the endogenous mRNA sequence of each gene. Given the significant cost and time associated with designing and testing 18 more probes, I chose to cautiously proceed with my experiments under the assumption that all lines, apart from ORMDL::YFP, had the *YFP* insert in the reported gene, and therefore it is that reported gene whose protrusion-localised mRNAs I observed. I however decided to validate any priority candidate genes using an endogenous probe at a later stage.

3.6.4 Future considerations

There are interesting questions to consider related with the expression patterns of some of the projection-localised transcripts explored in this chapter. Why do some mRNAs localise specifically to glia in some NMJs, but are present everywhere in the muscle in others, like for *Gs2*? Does the pattern of expression of the glial-specific mRNAs change upon structural synaptic plasticity? Are they important not only in structural synaptic plasticity, but also for synapse development?

Inevitably, answers to some of these questions could confirm many of the previously examined roles of local translation in perisynaptic glia, like astrocytes and PSCs. When it comes to PSCs, the glia whose projections reach the mammalian NMJ, there is a gap in the understanding of this local translation despite their morphological similarity to both astrocytes and neurons [47]. Few studies have explored mRNA localisation and local translation in PSCs [100]. One of them found that Annexin A2

transcript and protein accumulate at the tips of the PSC processes in response to hydrogen peroxide treatment in the murine NMJ [252]. Additionally, the PSCs processes were shown to undergo extensive remodelling of the cytoskeleton upon hydrogen peroxide treatment; therefore, local translation in PSCs could enable them to move towards and respond to damage [252].

The glial projections at the *Drosophila* NMJ which I studied and labelled in this chapter are most likely equivalent to PSCs, and their roles could overlap with those of PSCs. However, mRNA localisation studies similar to experiments performed in this chapter cannot be performed easily in the same manner for mammalian PSCs. *Drosophila* NMJ is easy to expose and label thanks to established antibodies and permissive larval anatomy [109, 184]. The mammalian PSCs are not very abundant and physically connected to neurons, which makes them harder to culture, isolate or observe individually [100]. This makes *Drosophila* particularly suited for studies pertaining to the potential roles of mRNA localisation and local translation in the NMJ-associated glial cells, particularly in the context of potential PSCs involvement in motor neuron disease [30, 95, 97, 98, 253].

As previously mentioned, the mRNA localisation and local translation have been explored much more extensively in astrocytes, the other type of glial cells known to be present at tripartite synapses, just like PSCs. Exploring mRNA localisation in astrocytes was more common potentially due to the possibility to culture them and their abundance in the brain. mRNA and ribosomes have been shown to be present in peripheral astrocyte processes (PAPs) *in vivo*. Hundreds of transcripts enriched in the PAPs were identified [45, 46, 49]. Those transcripts have been found to have longer 3′UTRs and their proteins participate in various cellular processes like

glutamate and GABA transport and metabolism (similarly to Gs2), but also biosynthesis of unsaturated fatty acids [49]. Motors and cytoskeletal proteins, such as GFAP, also had PAP-localised transcripts [254]. Some of the most abundant PAP transcripts could also be coding for ribosomal proteins [45].

Based on these astrocytic studies, it is possible to speculate that glial cells have to keep a pool of glutamate metabolism related mRNAs ready to translate near the synaptic sites in case glutamate management and uptake becomes necessary as a consequence of synaptic activity. Considering that *Gs2* is one of the most interesting transcripts in my study and it codes for an enzyme that catalyses the synthesis of glutamine from glutamate [132], this hypothesis could extend to invertebrates, making the mRNA-localisation-controlled management of glutamate metabolism a conserved featured of all synapse-associated glia.

3.6.5 Chapter 3: conclusions

To summarise, I concluded that there was sufficient evidence to confirm that mRNA of eighteen of the nineteen candidates was present in the *Drosophila* NMJ glia. Much is still unknown about the role of perisynaptic glia of the PNS, and, considering the available literature and what is known about astrocytes and PSCs, it seems like much can still be uncovered. The candidate genes whose presence in the NMJ glia I confirmed are likely to play active roles in some of the most fundamental processes for which the glial cells are necessary, based on the previous findings described throughout the results section. The strength of *Drosophila* as a model system is its simplicity, ease of genetic manipulation, and the relative lack of redundancy of the genes. It therefore is a perfect system in which one can explore the ways in which

those glial-localised transcripts contribute to development and structural synaptic plasticity, something which I go on to examine in the next chapters.

CHAPTER 4

4 RNAi Knockdown Screen of Glial Protrusion-Localised Transcripts Reveals Morphology and Structural Synaptic Plasticity Defects

4.1 Introduction

Drosophila melanogaster is a well-known model organism whose utility was first established in the early 20th century by Thomas Hunt Morgan and his contemporaries. A rapid generational time, high progeny number, and readily discernible phenotypic variants were attractive to those early investigators, who used them to study the basis of inheritance and heredity through their work. This body of work ultimately earned Morgan the Nobel Prize in Physiology or Medicine in 1933 [255].

Subsequent to its central role in the discipline of genetics, *Drosophila* became instrumental for the elucidation of principles of developmental biology, with studies focusing on the Notch signalling pathways and making first observations about “neurogenic” phenotypes related to loss of *Notch* [256]. Following that, scientists utilised mutagenesis in *D. melanogaster* to identify conserved Hox genes, responsible for controlling the organism's body plan, leading to the award of the Nobel Prize in Physiology or Medicine in 1995 to Edward B. Lewis, Christiane Nüsslein-Volhard, and Eric Wieschaus [257-259]. Though not directly designed to study genes affecting neuronal function, these experiments nonetheless identified 139 genes that affect the larval development, many being novel players later shown to be important in axon guidance, neurogenesis, neural cell differentiation and neuronal migration [260-263].

Thus, *Drosophila* emerged as possibly the strongest model to study nervous system development and, more recently, for the study of the genetic basis of circuits and behaviour. The simplicity of the *Drosophila* nervous system, containing approximately 100,000 neurons in the adult brain, coupled with the robust genetic tools previously developed, allowed researchers to look deeper into the genetic and molecular underpinnings of numerous neurological processes, such as behaviour, circadian rhythms, as well as learning and memory [255].

To study behaviour and circadian rhythms, various assays have been in continuous use for both adult flies and larvae alike [198, 264-266]. *Drosophila* 3rd instar NMJ, meanwhile, has become a powerful system lending itself to experimental manipulation permitting the study of structural synaptic plasticity, the process underlying learning and memory formation [108].

The *Drosophila* NMJ has proven to be exceptionally valuable, primarily due to its functional similarities with mammalian CNS synapses [267]. The *Drosophila* NMJ, a glutamatergic synapse similar to most excitatory synapses in the mammalian brain, displays activity-dependent changes in synaptic strength and structure, akin to LTP and LTD observed in mammalian systems [268-272]. The ease of genetic manipulation, dissection and access for image acquisition provide additional benefits, rendering it an ideal model to study the fundamental molecular and cellular processes underlying structural synaptic plasticity [109, 183]. Moreover, the *Drosophila* NMJ possesses large, individually resolvable synaptic boutons that facilitate detailed morphological and electrophysiological studies of axonal terminals [273].

The spaced high K^+ depolarisation paradigm in *Drosophila* has emerged as a particularly valuable protocol in studying structural synaptic plasticity. It uses

intermittent pulses of potassium-rich solution and low-potassium solution, both containing Ca^{2+} ions, applied to the *Drosophila* larval fillet [191, 197, 274]. The high potassium phases result in the induction of depolarisation in the motor neurons and contraction of the larval body muscles (Figure 4-1). Subsequently, increased structural synaptic plasticity of the larval NMJs causes the formation of new, immature synaptic boutons, characterised by the presence of the pre-synaptic compartment, which is labelled by the α-HRP antibody, and lacking the post-synaptic compartment, labelled by the α-dlg1 antibody [191]. These boutons are called “ghost boutons”, and their numbers can be quantified using microscopy.

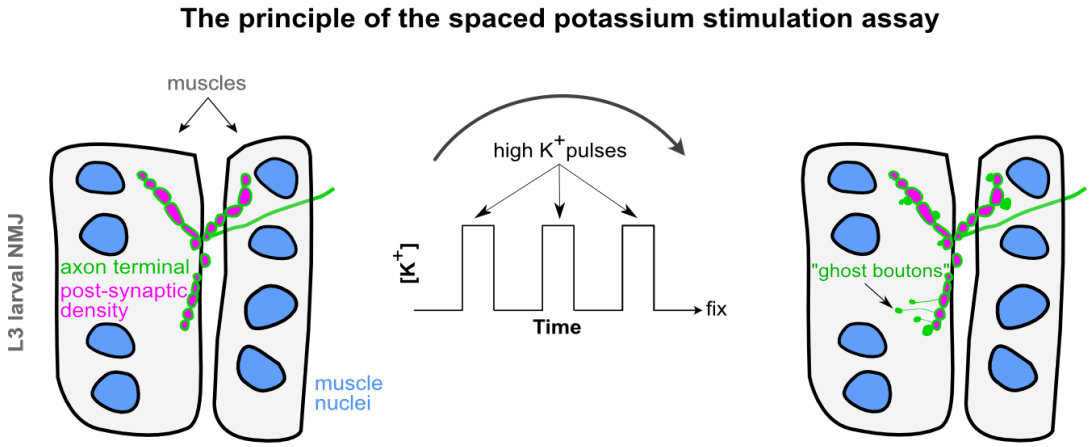

Figure 4-1 Schematic of the principle behind the spaced potassium stimulation assay

A 3rd instar *Drosophila* larva is dissected to expose the NMJs and flooded with pulses of potassium-rich solution in the presence of Ca^{2+} ions, interspersed with rest periods in low-potassium solution. Following fixation and imaging, “ghost” synaptic boutons can be observed. Mature synaptic boutons comprise the axon terminal, stained with the α-HRP antibody (labelled in green) and the postsynaptic density, stained with the α-dlg antibody (labelled in magenta). “Ghost boutons” have the axon terminal part, but not the postsynaptic density marker.

Several other techniques exist which can elicit bouton formation in response to rapid electrophysiological pulses, optogenetics or heat [190, 191, 197, 273, 275]. Though

these techniques differ with respect to invasiveness, physiological interference, and reproducibility, they remain the gold standard for studying the basis of NMJ structural synaptic plasticity.

However, it is crucial to note that “ghost boutons” formed through experiments described above may not necessarily mature into fully functional new synapses, despite serving as indicators of increased neuronal activity. Consequently, while “ghost boutons” emergence signifies neuronal activity, it may not accurately reflect the occurrence of synaptogenesis. It is essential to emphasise this distinction when studying any functional implications of potential mRNA localisation and local translation on synaptic plasticity. RNAi-mediated knockdown of a candidate gene might influence the structural synaptic plasticity, as quantified by the emergence of “ghost boutons” but might not have direct effect on further “ghost bouton” maturation and thus the complete process of synaptogenesis. Further synapse maturation experiments would have to be conducted to provide a more nuanced interpretation of any potential results.

Furthermore, *Drosophila* NMJ offers a unique opportunity to study the fine molecular interactions between glial and neuronal projections at the synapse [126]. During and after development, glial processes play a vital role in establishing and maintaining the connectivity between neurons and muscles and contribute to synaptic pruning and maturation of synapses [121, 128].

Broadly, the true value of *Drosophila* as a model system in neuroscientific studies stems from its versatility, rather than its specialisation in any one particular area. Mammalian model organisms, while suitable for studying aspects like complex behaviours, often lack the capacity for concurrent detailed histological or molecular

examination of the nervous system. In contrast, cell cultures provide insights at the molecular and cellular levels but cannot capture the nuances of a complete nervous system's physiology. *Drosophila* bridges these gaps by offering a comprehensive study model. It facilitates molecular and cellular biology research due to well-established techniques, ease of dissection, and an extensive range of antibodies and labels. Furthermore, *Drosophila* provides simultaneous insights into the intact nervous system's physiology, anatomy, and associated behaviours.

In this chapter, I fully capitalised on the advantages of using *Drosophila* as an exemplary model system for neuroscientific studies by embarking on an RNAi knockdown candidate screen of previously identified glial protrusion-localised transcripts (Figure 4-2). The presence of specific transcripts in the peripheral protrusions of glial cells at the NMJ, as confirmed in Chapter 3, is not synonymous with them being functionally required. I wanted to investigate their functional importance, or lack thereof, in glial cells. The fundamental question which I wanted to ask was: what would the ramifications be – cellularly, physiologically, or behaviourally – of the absence of these transcripts from the glial cells? Specifically, I wanted to understand the roles of protrusion-localised transcripts in glia in the overall *Drosophila* development and viability, as well as NMJ morphology. Employing the spaced high K^+ depolarisation paradigm (Section 2.8.1), I could then try to identify any potential defects in structural synaptic plasticity. To complement and extend these findings, I planned to use the larval locomotion behaviour assay (Section 2.8.2). My goal was to correlate potential developmental, morphological, or structural synaptic plasticity defects with tangible macroscopic results, such as impaired crawling. This comprehensive experimental approach, spanning from microscopic to macroscopic perspectives, was made possible by the exceptional attributes of *Drosophila* as a

neuroscientific model: its remarkable experimental adaptability and ease of manipulation.

4.2 Specific aims of this chapter

1. To explore the effects of glial RNAi-mediated knockdown of the glial protrusion-localised transcripts on the development and viability of *Drosophila* larvae.
2. To establish whether the glial RNAi-mediated knockdown of the glial protrusion-localised transcripts influences the NMJ structural synaptic plasticity and morphology of *Drosophila* 3rd instar larvae.
3. To establish any potential correlations between altered NMJ morphology and larval locomotion behaviour.

4.3 Publication

The research presented in this chapter has been published as a pre-print, where I am a co-first author, now under revision in the Journal of Cell Biology.

Dalia S. Gala, Jeffrey Y. Lee, Maria Kiourlappou, Joshua S. Titlow, Rita O. Teodoro, Ilan Davis, “Mammalian glial protrusion transcriptomes predict localisation of *Drosophila* glial transcripts required for synaptic plasticity”, bioRxiv, https://doi.org/10.1101/2022.11.30.518536.

Multiple co-authors contributed to this pre-print. I solely present the results which I have produced.

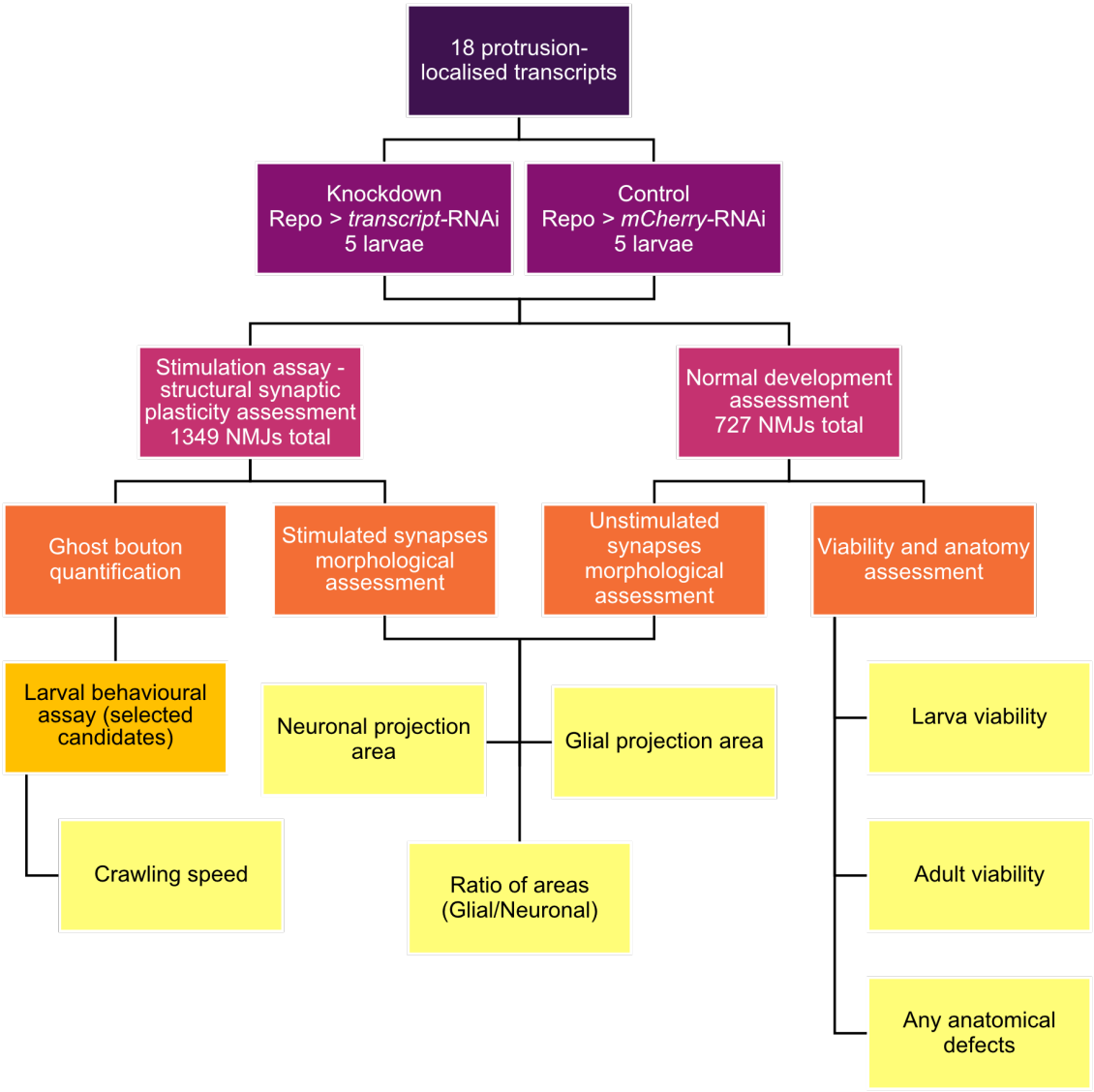

Figure 4-2 Detailed breakdown of the candidate screen plan

For each of the eighteen protrusion-localised transcripts, each knockdown experiment had its own internal control experiment conducted simultaneously, including a minimum of 5 control larvae and 5 RNAi-mediated knockdown larvae, no less than 20 NMJs each. Two assays were run in parallel: structural synaptic plasticity assessment and normal development assessment, for which 727 and 1,349 synapses were analysed, respectively, totalling 2,076 synapses analysed in the whole candidate screen. Quantification of NMJ morphometrics was done for both. For normal development assessment, larval and adult viability, as well as any anatomical defects, were noted. For stimulated synapses, “ghost boutons” were also quantified. Transcripts whose knockdown resulted in “ghost bouton” phenotypes were also assessed using the larval locomotion behaviour assay.

4.4 Materials and methods

4.4.1.1 Fly stocks

To carry out the candidate screen and test the effects of mRNA knockdown of glial protrusion-localised transcripts in the *Drosophila* larvae, I constructed a fly line to express UAS-mCD8-GFP under the control of a pan-glial promoter in *Drosophila,* Repo-GAL4 (henceforth referred to as Repo>GFP line), equivalent to the Repo>mCherry line which I used in Chapter 3. I crossed this line to 20 RNAi lines against 18 glial protrusion-localised transcripts, since 2 of the used lines resulted in lethality (further discussed in Results (Section 4.5)). These lines are henceforth referred to as Repo>*Transcript*-RNAi. One line per gene was used with the goal of identifying any lines which showed any developmental, structural synaptic plasticity or locomotion abnormalities. All selected lines targeted all isoforms of the mRNA of interest, and all lines had less than 3 off target effects as verified by VDRC website if the line was from the VDRC library (www.vdrc.at), and UP-TORR [276].

The control for each of the knockdown experiments was UAS-mCD8-GFP/+; Repo-GAL4/UAS-*mCherry*-RNAi (henceforth referred to as Repo>*mCherry*-RNAi or control). All experimental results pertaining to NMJ morphology or “ghost bouton” numbers are quantified as fold change with respect to that control. Table 4-1 presents detailed information about the RNAi lines used in the experiments described in this chapter.

Table 4-1 List of *Drosophila melanogaster* RNAi stocks used in Chapter 4

RNAi target	Source	Library	Chromosome	Off targets?	Isoforms targeted?	ID?
Gs2	VDRC	shRNA	2	0	6 of 6	330302
cold	VDRC	GD	3	0	2 of 2	44197
α-Cat	VDRC	GD	3	0	2 of 2	8808
Gli	VDRC	GD	2	2	5 of 5	37115
lost	VDRC	GD	3	0	1 of 1	23918
Lac – line 1	VDRC	GD	3	0	1 of 1	35524
Lac – line 2	VDRC	KK	2	0	1 of 1	107450
CG42342	VDRC	KK	2	3	12 of 12	102525
CG1648	VDRC	GD	2	2	3 of 3	32686
nrv2	VDRC	GD	2	0	6 of 6	2660
Cip4	VDRC	GD	2	0	11 of 11	18492
Pdi	VDRC	GD	3	2	2 of 2	23359
Vha55	VDRC	GD	1	1	3 of 3	46554
Atpα – line 1	VDRC	GD	2	0	11 of 11	12330
Atpα – line 2	Bloomington	TRiP	3	0	11 of 11	32913
sdk	VDRC	GD	2	0	9 of 9	9437
kst	Bloomington	TRiP	3	0	7 of 7	33933
Flo2	VDRC	shRNA	2	0	12 of 12	330316
Nrg	Bloomington	TRiP	3	0	9 of 9	28724
shot	Bloomington	TRiP	3	0	22 of 22	28336
mCherry	Bloomington	TRiP	2	-	-	35785

4.4.1.2 Spaced high K^+ depolarisation paradigm

The spaced high K^+ depolarisation paradigm (also referred to as spaced potassium paradigm/assay) was carried out as previously described (Section 2.8.1) [191]. For all RNAi crosses, the larvae underwent washes of 2 minutes, 2 minutes, 2 minutes, 4 minutes, and 6 minutes of potassium-rich solution, respectively, with 15-minute intervals of low potassium solution in between each wash [191]. No less than 5 control larvae and 5 RNAi larvae and no less than 20 NMJs per condition were used.

4.4.1.3 Larval locomotion behaviour assay

The locomotion behaviour was observed using the manual tracking assay as previously described in Section 2.8.2.1 [198]. Briefly, larvae were acclimatised for 1h at room temperature. Apple juice plates (5cm) were warmed to room temperature. 3rd

instar *D. melanogaster* larvae were cleaned in ddH_2O using a paintbrush. Videos were recorded using an overhead mobile phone camera set above the plate on a 'dartboard' paper (Figure 2-1A). 10 larvae of each genotype were filmed at 1080p and 30fps for 30 seconds or until reaching the plate's edge. Videos were analysed in ImageJ, converted to jpeg sequences, scaled using the ruler, and larvae were manually tracked. Data was then processed in RStudio.

4.4.1.4 Image acquisition and processing

Drosophila 3rd instar NMJ morphology was assessed using confocal microscopy, following previously outlined techniques (Section 2.5.2). Antibody details are available in Table 2-4. For the spaced potassium stimulation assay experiments, I quantified “ghost boutons” manually using descriptions from previous literature [191, 275]. For both pre- and post-stimulation NMJ morphology quantification, I measured glial cell projections in abdominal segments 2-5, labelled by Repo-GAL4 driving UAS-mCD8-GFP, referred to as "glial projection area". Additionally, I quantified axon terminal projections in the same segments, also referred to as “axon terminal”, “neurite” or “α-HRP” areas. These measurements were done in 2D using ImageJ and analysed in R Studio, including “glial to neuron” ratios [194]. Methodology specifics are available in Section 2.7.1.

4.5 Results

4.5.1 Impact of RNAi knockdown of glial protrusion-localised transcripts on overall development

I initially set out to explore the overall viability and appearance of the animals following the RNAi-mediated knockdown of candidate glial protrusion-localised transcripts.

Table 4-2 summarises these results.

Table 4-2 Viability assessment after glial knockdown of glial protrusion-localised transcripts

RNAi Target	ID	Larva	Adult
Gs2	330302	Viable	Viable
cold	44197	Abnormality	Viable
α-Cat	8808	Viable	Viable
Gli	37115	Viable	Viable
lost	23918	Viable	Viable
Lac – line 1	35524	Abnormality	Lethal
Lac – line 2	107450	Lethal	Lethal
CG42342	102525	Viable	Viable
CG1648	32686	Viable	Viable
nrv2	2660	Viable	Lethal
Cip4	18492	Lethal	Lethal
Pdi	23359	Viable	Viable
Vha55	46554	Abnormality	Lethal
Atpα – line 1	12330	Lethal	Lethal
Atpα – line 2	32913	Viable	Viable
sdk	9437	Viable	Viable
kst	33933	Viable	Viable
Flo2	330316	Viable	Viable
Nrg	28724	Viable	Viable
shot	28336	Viable	Viable

The RNAi targets are specified in the “RNAi Target” column, and the ID of the RNAi stock is added in the “ID” column, which can also be found in Table 4-1, where more details about the RNAi stocks are provided. The “Larva” and “Adult” columns specify the larval and adult viability, respectively. To be specific, “Viable” means that 3rd instar larvae or adults of the correct phenotypes were observed in the cross progeny. “Abnormality” means that larvae of correct phenotypes were observed, but they differed in some manner when compared to control. This is discussed in detail in the sections below. ”Lethal” means that no larvae or no adults of correct phenotypes were observed in the cross progeny.

Glial RNAi-mediated knockdown of 12 out of the 18 glial protrusion-localised transcripts (*Gs2, α-Cat, Gli, lost, CG42342, CG1648, Pdi, sdk, kst, Flo2, Nrg, shot*) had no obvious impact on the viability or development of either larvae or adults.

Glial RNAi-mediated knockdown of 3 candidates resulted in no viable progeny (*Lac* (line ID 107450), *ATPα* (line ID 12330), *Cip4* (line ID 18492)). I utilised two different, non-lethal lines to replace these for further experiments (*Lac* line ID 35524, *ATPα* line ID 32913). I did not have a different line for *Cip4* and did not continue experiments on this gene, thereby decreasing the glial protrusion-localised transcripts pool to seventeen genes. Glial RNAi-mediated knockdown of 3 transcripts resulted in adult, but not larval lethality (*Lac* (line ID 35524), *nrv2*, *Vha55*).

I observed developmental abnormalities upon RNAi-mediated knockdown of 3 of the candidate glial protrusion-localised transcripts. All abnormalities were related to the larval brain morphology. The VNCs of *cold*-RNAi (Figure 4-3) and *Lac*-RNAi (line ID 35524) (Figure 4-4) larvae were significantly elongated (Figure 4-6). This phenotype is similar to ones described before, where it was shown that interactions between glial cells and the ECM are required for the shaping of the developing *Drosophila* nervous system [277-279]. This could suggest that cold and Lac could impact nervous system development. Additionally, *Lac*-RNAi larvae appeared smaller than control 3rd instar *Drosophila* larvae.

The final of the glial protrusion-localised transcripts whose knockdown resulted in a developmental brain abnormality was *Vha55*. *Vha55*-RNAi larval brains were much smaller compared to control larval brains, and the hemispheres appeared to be reduced in size, while the VNCs were significantly shorter (Figure 4-5, Figure 4-6).

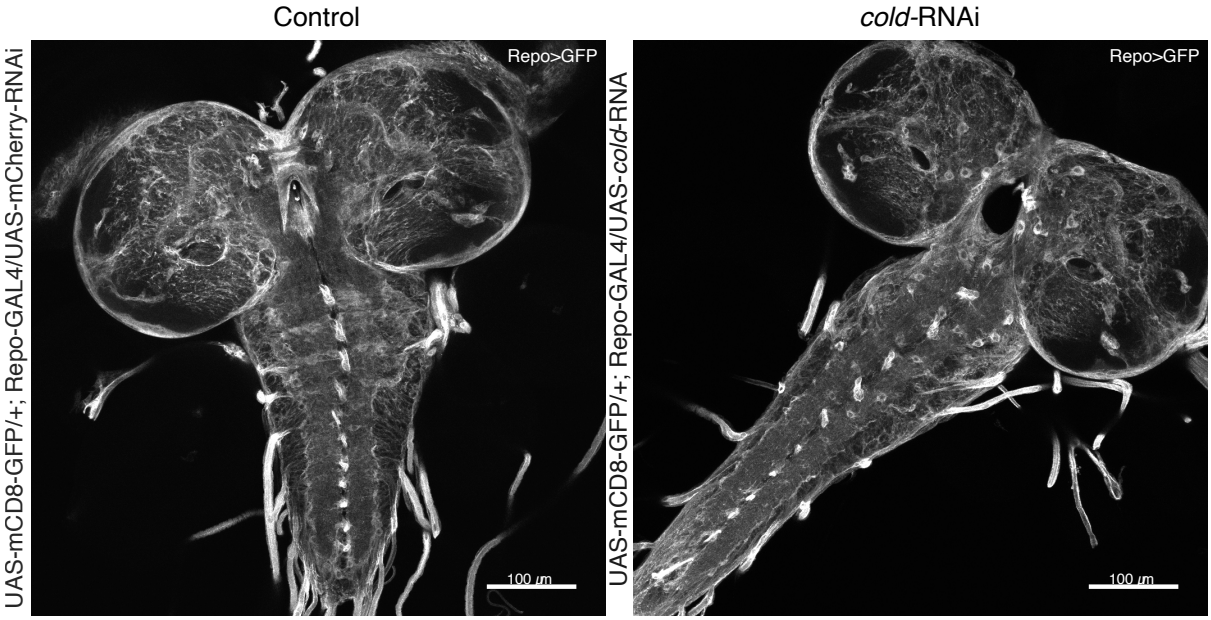

Figure 4-3 *cold*-RNAi in glia causes elongated VNC phenotype

Representative confocal images of control (left) and *cold*-RNAi (right) brains labelled with Repo>GFP (white, the only channel presented). The VNCs of *cold*-RNAi brains are elongated (representative of 5 brains for each condition). Scale bar – 100 μm.

Figure 4-4 *Lac*-RNAi in glia causes elongated VNC phenotype

Representative confocal images of control (left) and *Lac*-RNAi (right) brains labelled with Repo>GFP (white, the only channel presented). The VNCs of *Lac*-RNAi brains are elongated, much like for *cold*-RNAi (Figure 4-3) (representative of 5 brains for each condition). Scale bar – 100 μm.

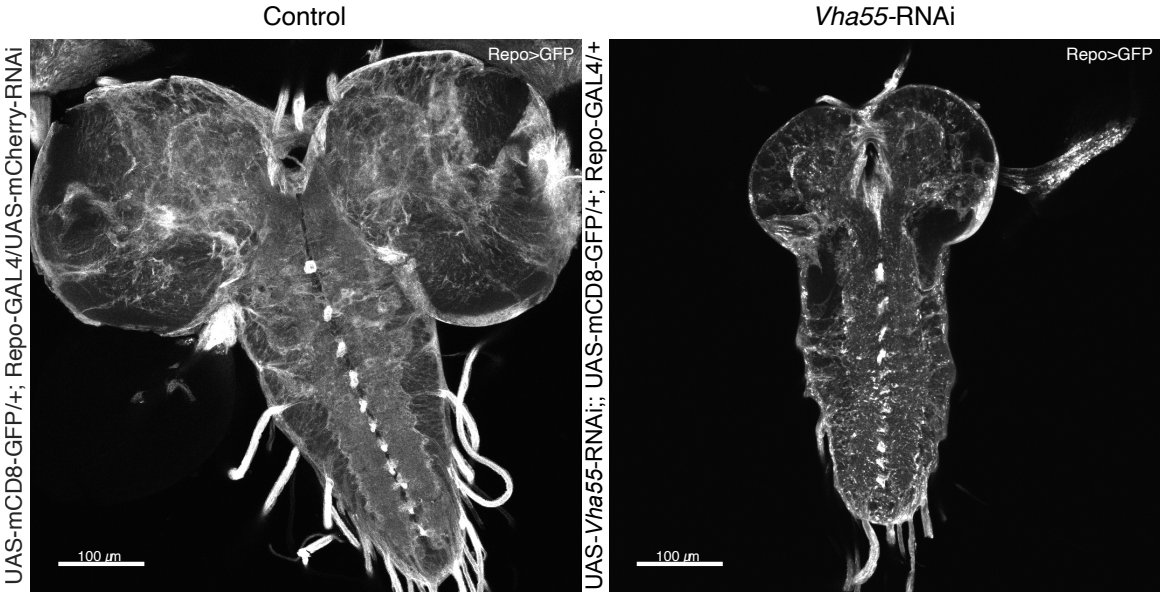

Figure 4-5 *Vha55*-RNAi in glia causes small brain hemisphere phenotype

Representative confocal images of control (left) and *Vha55*-RNAi (right) brains labelled with Repo>GFP (white, the only channel presented). *Vha55*-RNAi brains are much smaller for 3rd instar larvae when compared to brains of the control larvae of very similar sizes (representative of 5 brains for each condition). Scale bar – 100 μm.

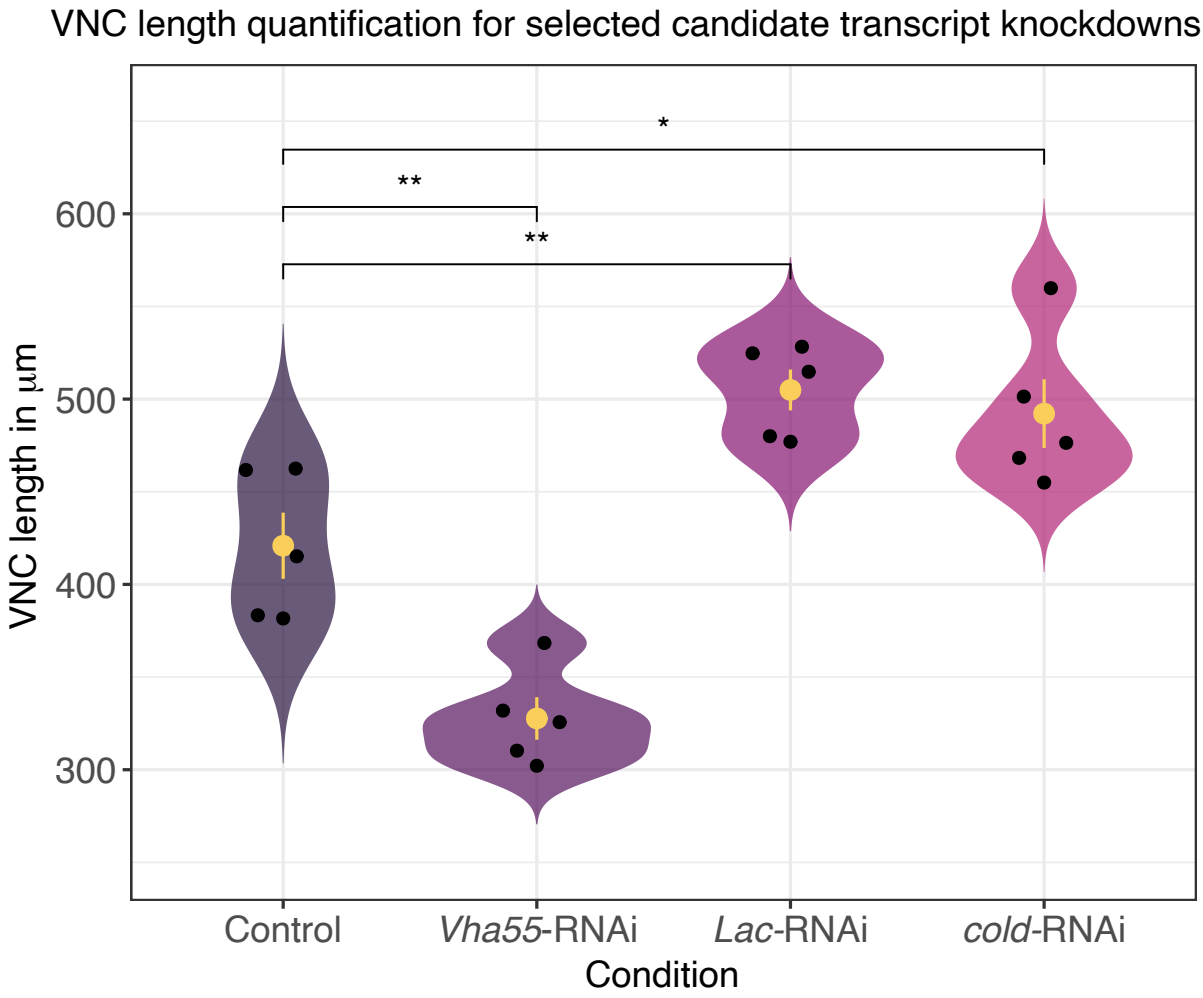

LEGEND	
LABEL	**GENOTYPE**
Control	UAS-mCD8-GFP/+; Repo-GAL4/UAS-*mCherry*-RNAi
Vha55-RNAi	UAS-*Vha55*-RNAi;; UAS-mCD8-GFP/+; Repo-GAL4/+
Lac-RNAi	UAS-mCD8-GFP/+; Repo-GAL4/UAS-*Lac*-RNAi
cold-RNAi	UAS-mCD8-GFP/+; Repo-GAL4/UAS-*cold*-RNAi

Figure 4-6 VNC length quantification for Control, *Vha55*-RNAi, *Lac*-RNAi and *cold*-RNAi

Violin plots accompanied by raw data presenting the quantification of the VNC lengths in larvae with the knockdowns of those transcripts which resulted in developmental brain abnormalities. VNC lengths are expressed in µm. Wilcoxon rank sum test p-values are reported. Quantification of n=5 brains of each genotype has been performed. See legend for genotype details.

4.5.2 Impact of glial RNAi knockdown of protrusion-localised transcripts on NMJ morphology

I then investigated the effects of glial protrusion-localised transcripts knockdown in glial cells on glial projection morphology and wild-type axon terminal projection morphology at the NMJ, summarised in Figure 4-7 (raw data and detailed genotypes are reported in Figures C-1 and C-2 in the Appendix). Analysing 3rd instar NMJ glia with RNAi expression and wild-type motor neuron axon terminal projections, I found that many gene knockdowns caused increase or reduction in glial projection areas, as well as a change in the ratio of glial to neuron surface areas when compared to control, even without stimulation. I also saw varying defects in the sizes of both glial and neuronal projections after spaced potassium stimulation (Figure 4-8, raw data and detailed genotypes are reported in Figures D-1 and D-2 in the Appendix).

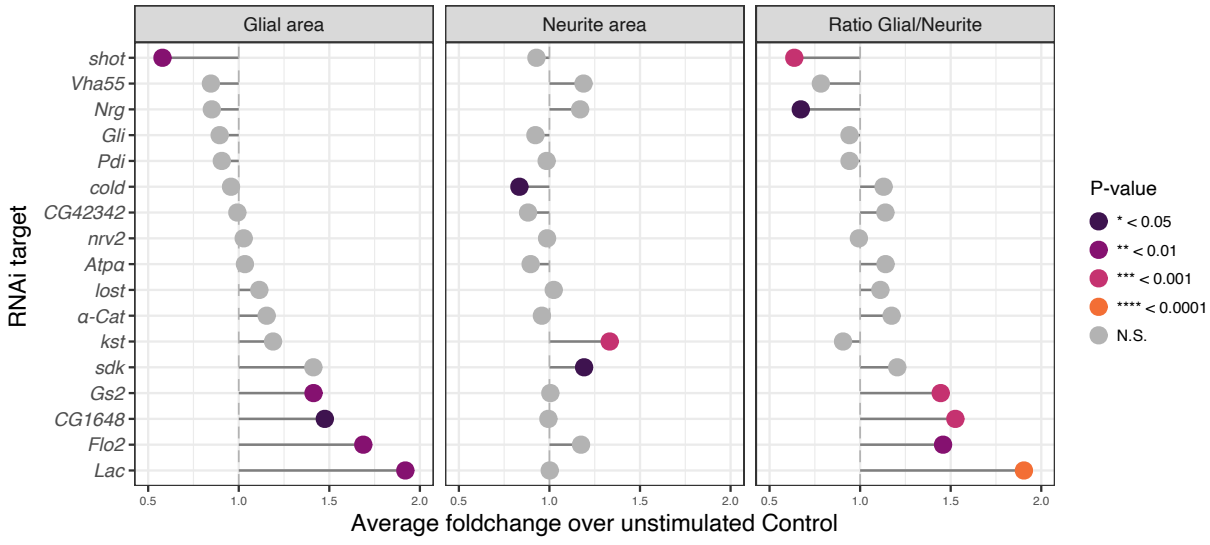

Figure 4-7 Summary of change in glial protrusion area, neurite area and their ratio

Foldchange in the NMJ glial protrusion area, neurite area and their ratio upon knockdown of glial protrusion-localised transcripts when compared to unstimulated control. Data represents average foldchange for each gene. Student's t-test; p-values were normalised with internal day-to-day controls. Statistics and n numbers are reported in Table C-1 in the Appendix. Raw data and detailed genotypes are reported in Figures C-1 and C-2 in the Appendix.

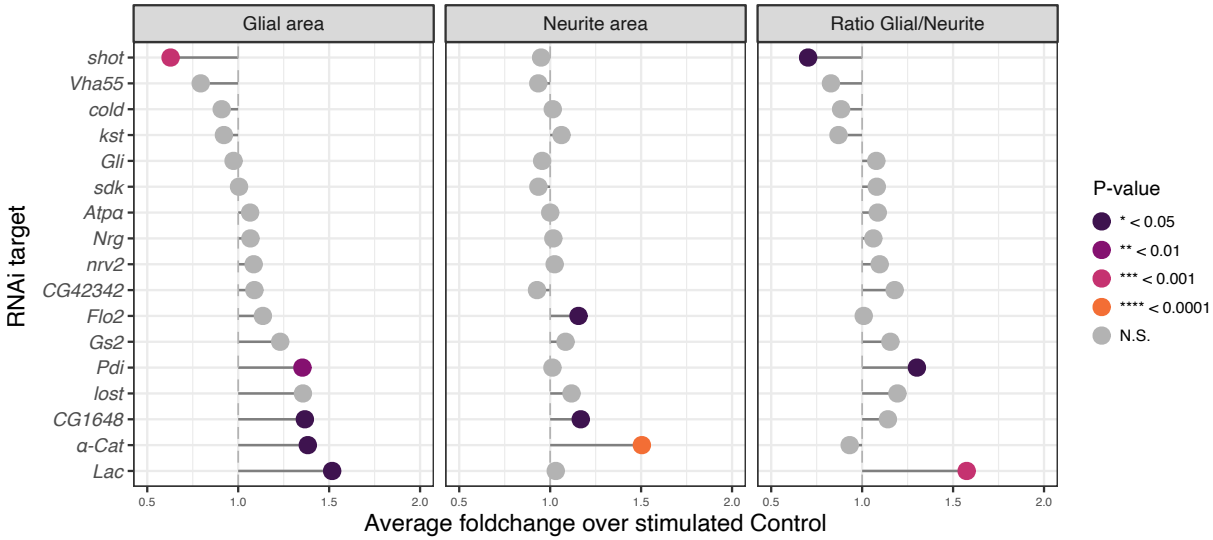

Figure 4-8 Summary of change in glial protrusion area, neurite area and their ratio after stimulation

Foldchange in glial protrusion area, neurite area and their ratio upon knockdown of glial protrusion-localised transcripts after the spaced potassium activation assay when compared to stimulated control. Data represents average foldchange for each gene. Student's t-test. Statistics and n numbers are reported in Table C-2 in the Appendix. Raw data and detailed genotypes are reported in Figures D-1 and D-2 in the Appendix.

As an example, *shot*-RNAi in glia nearly eradicated glial NMJ projections. *shot*-RNAi glial projections ($p<0.01$) and the ratio of glial to neurite area ($p<0.001$) were significantly decreased. In control larvae, glial projections spread on muscle cell surfaces, but in *shot*-RNAi larvae, while motor axon branches are glial-membrane-covered, there is a distinct lack of glial projections on the muscle surface (Figure 4-9).

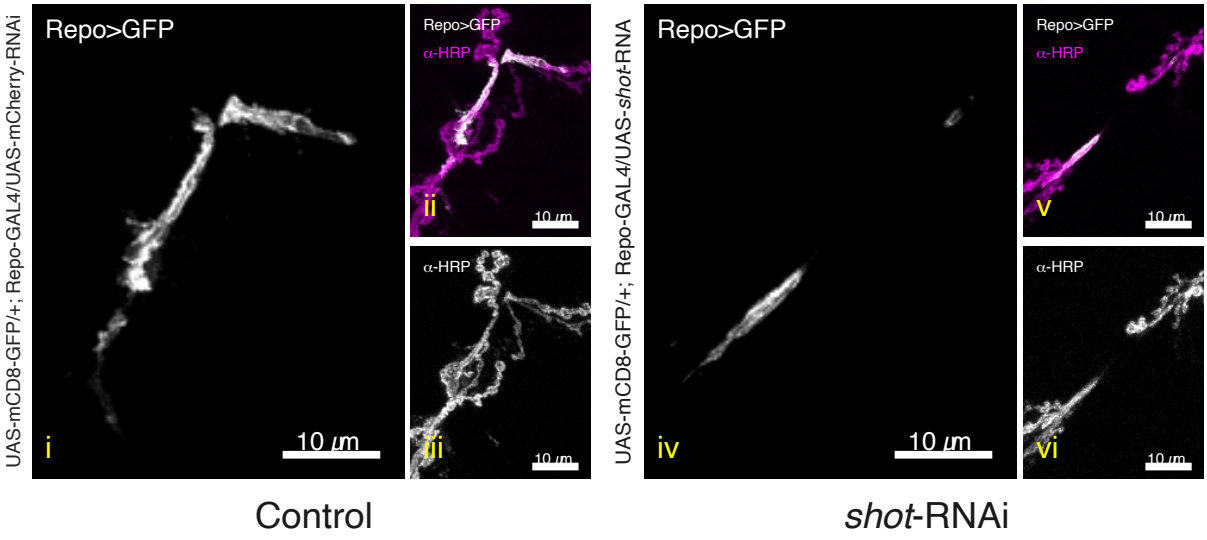

Figure 4-9 *shot*-RNAi glial projections are hypomorphic

Confocal images of the glial and axon terminal projection (α-HRP) channels from control (i-iii, Repo>*mCherry*-RNAi) and *shot* knockdown (iv-vi, Repo>*shot*-RNAi) 3rd instar *Drosophila* NMJs. Glial projections, labelled with Repo>GFP, are shown in white; α-HRP conjugated to Alexa 568 labelling the axon terminal is shown in magenta. Images i) and iv) present glial channel only in white; images ii) and v) present the glial channel in white in conjunction with the neuronal channel in magenta, and images iii) and vi) present the neuronal channel only in white. All NMJs presented are segment A3. Control glial projections make extensions on the muscle surface (i), while *shot*-RNAi glial projections make virtually no extensions (iv). Scale bar – 10 μm.

An opposite example was *Lac*-RNAi, where glial projections ($p<0.01$) and their ratios to the neurite area ($p<0.0001$) were increased when compared to unstimulated control NMJs, creating elongated, thin cytoplasmic extensions (Figure 4-10).

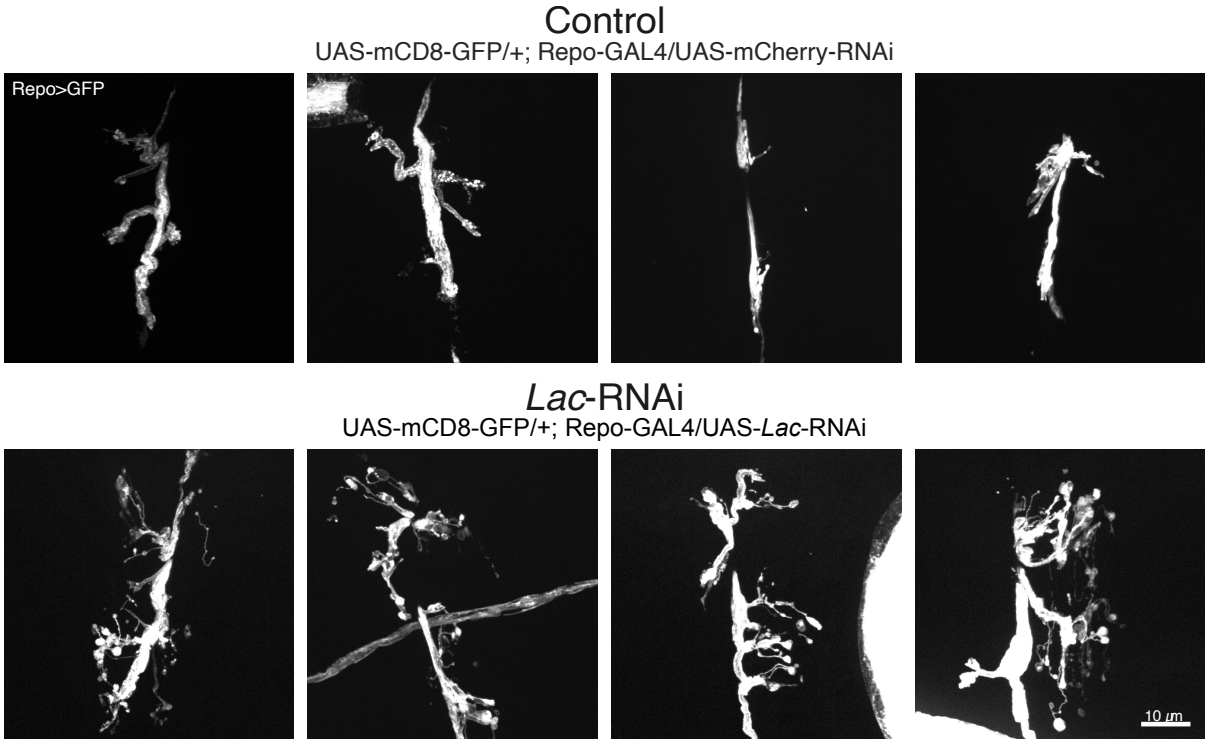

Figure 4-10 *Lac*-RNAi glial projections are hypermorphic

Confocal images of the glial channels from control (top row, Repo>*mCherry*-RNAi) and *Lac* knockdown (bottom row, Repo>*Lac*-RNAi) 3rd instar *Drosophila* NMJs labelled with Repo>GFP (white, the only channel presented). All NMJs presented are segment A2. *Lac*-RNAi glial projections make hypermorphic extensions and appear much more expansive and complex when compared to control NMJs. Scale bar – 10 μm.

4.5.3 4 of 17 RNAi-mediated knockdown experiments resulted in altered “ghost bouton” numbers after potassium stimulation

I next implemented the spaced potassium stimulation paradigm to test the effect of glial-specific RNAi on the motor neuron structural synaptic plasticity by quantitating the emergence of "ghost boutons” at the NMJ (Figure 4-1) [191]. RNAi-mediated knockdown of 4 transcripts in glia displayed discernible effects on structural synaptic plasticity of the wild-type motor neuron axon terminal at the NMJ (Figure 4-11; raw data and detailed genotypes are reported in Figure D-3 in the Appendix.). Among those 4 transcripts, knockdown of 2 of them (*Pdi, CG1648*) led to a significant increase

in “ghost bouton” numbers following potassium pulses ($p<0.0001$ and $p<0.01$ respectively). The knockdown of the remaining 2 (*Lac, CG42342*) resulted in a significant decrease in “ghost bouton” numbers ($p<0.05$ and $p<0.0001$ respectively). From this, I concluded that Pdi, CG1648, Lac and CG42342 could play an essential role in glia to maintain the proper plasticity of motor neuron synapses and selected them for the follow-up experiments.

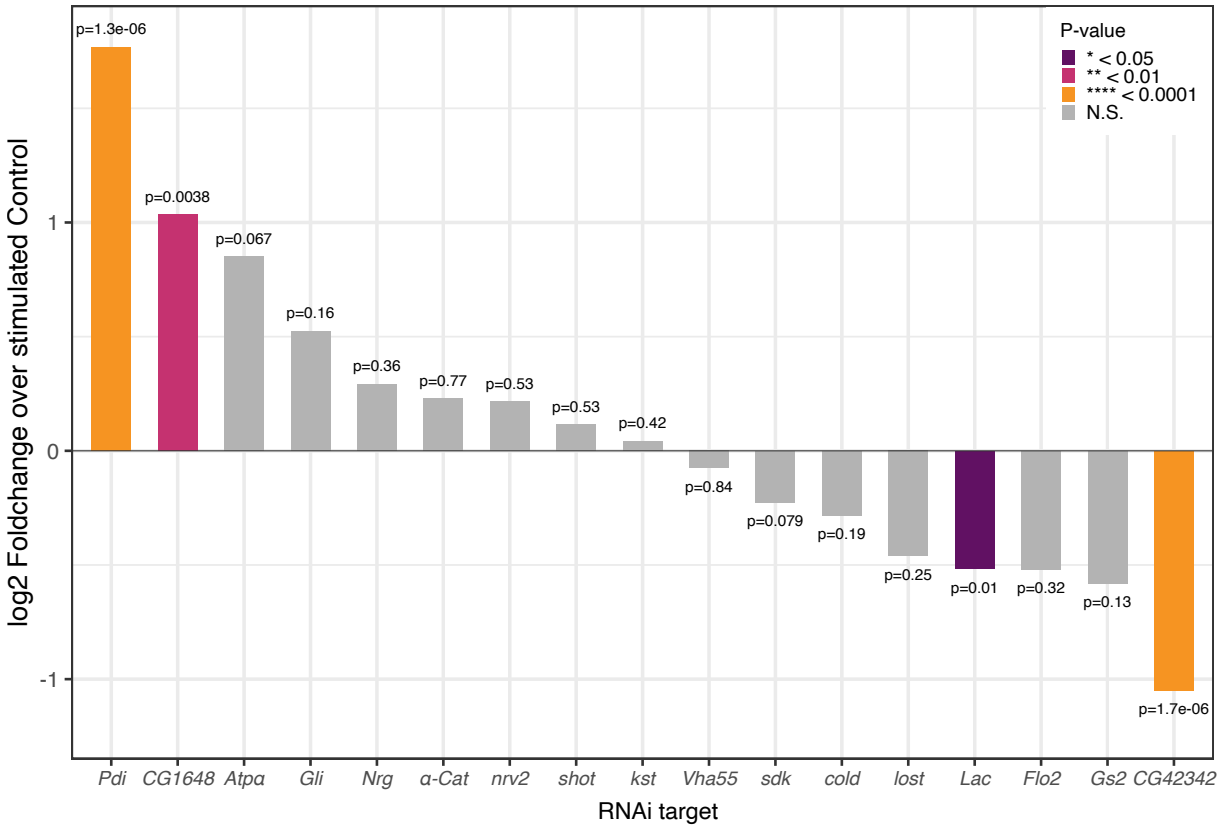

Figure 4-11 Candidate transcripts knockdown in glia affects wild-type motor neuron plasticity

The bar graph displays the average log2 FoldChange in “ghost bouton” counts after potassium stimulation relative to RNAi controls. Changes with statistical significance are marked in as described in the legend (top right corner). Wilcoxon rank sum test p-values are reported. Statistics and n numbers are reported in Table C-3 in the Appendix. Raw data and detailed genotypes are reported in Figure D-3 in the Appendix.

4.5.4 Larval crawling is impaired in *Lac*-RNAi larvae

Overall, my results so far demonstrated that many of the glial-protrusion localised transcripts are required for the correct morphology of *Drosophila* NMJ, and 4 are specifically necessary in glia for the correct structural synaptic plasticity of their neighbouring neuron. I next wanted to use an orthogonal method to observe the movement patterns of the knockdown larvae with the knockdown of those 4 candidate glial protrusion-localised transcripts (*Pdi, CG1648, CG42342, Lac*), as described previously [198]. The results of the larval locomotion assay indicated that *Lac*-RNAi larvae had impaired crawling capacity, while the other knockdown larvae were not significantly affected (Figure 4-12). The crawling velocity of *Lac*-RNAi larvae when compared to control larvae was significantly ($p < 0.01$) reduced (Figure 4-13).

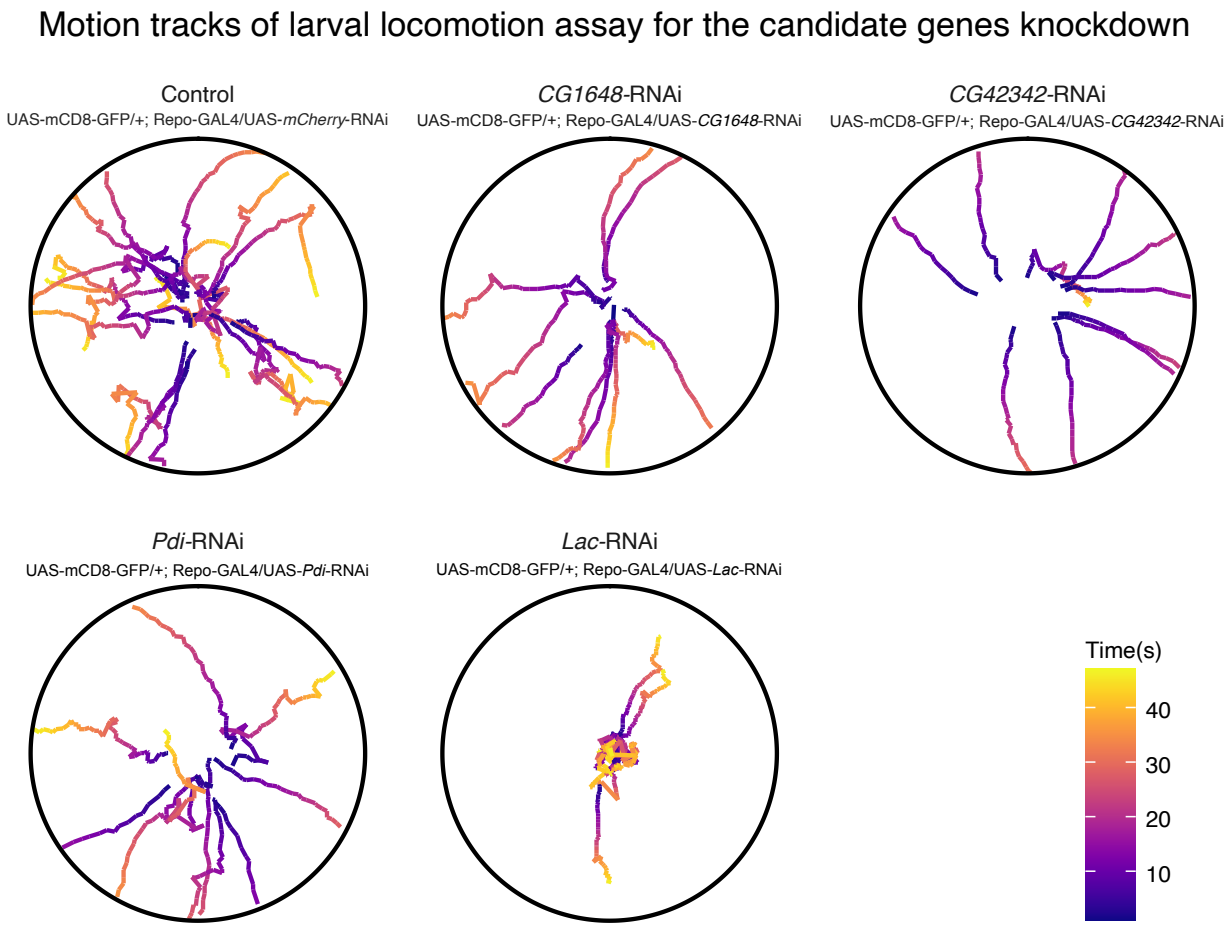

Figure 4-12 *Lac*-RNAi in glia affects larval crawling

Representative locomotion tracks of free-crawling 3rd instar larvae with post-stimulation-selected candidate glial protrusion-localised transcript knockdowns in glia. See label above for detailed genotypes. Tracks are colour-coded by time. *Lac*-RNAi larvae display a visibly different pattern of crawling when compared to control condition or the other knockdown conditions.

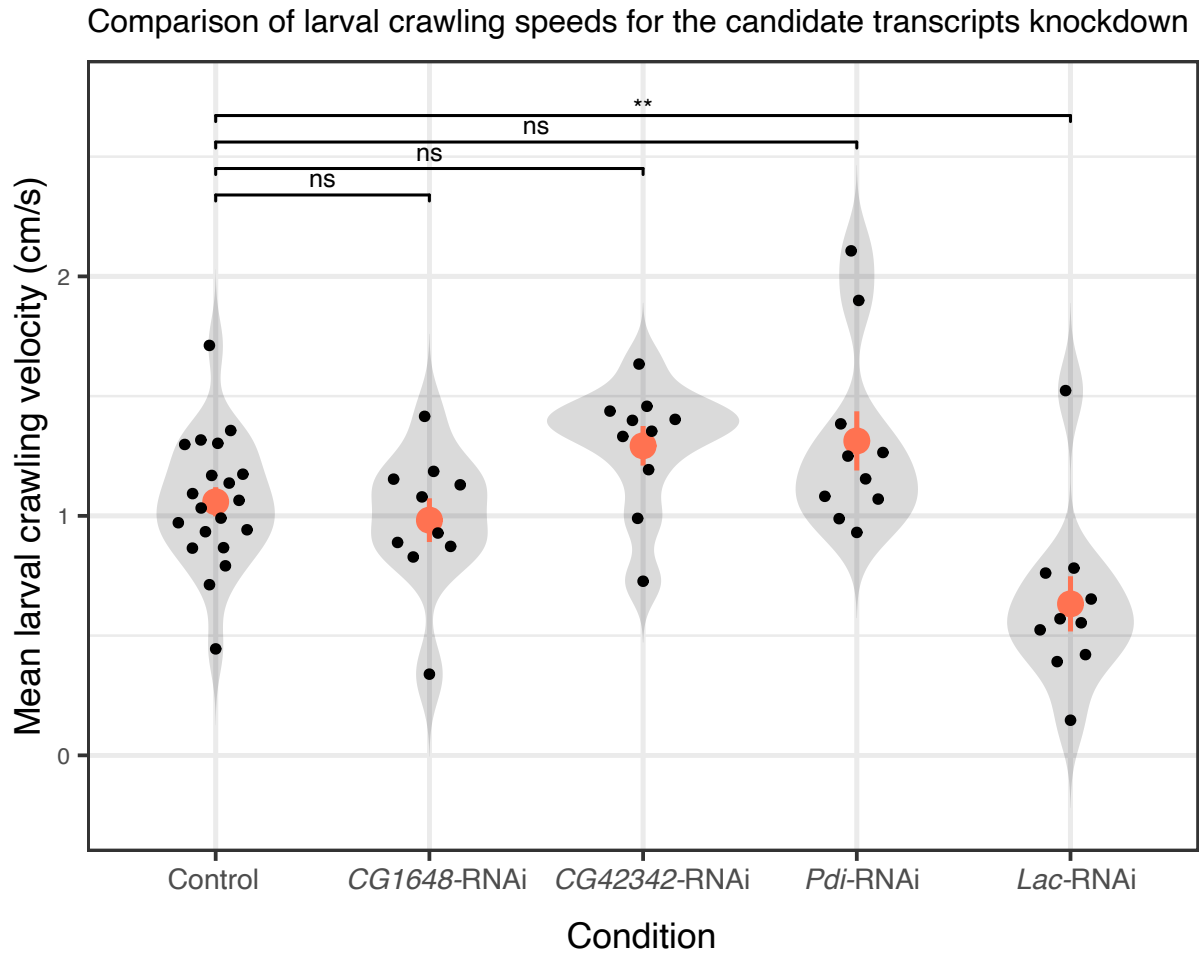

LEGEND	
LABEL	**GENOTYPE**
Control	UAS-mCD8-GFP/+; Repo-GAL4/UAS-*mCherry*-RNAi
CG1648-RNAi	UAS-mCD8-GFP/+; Repo-GAL4/UAS-*CG1648*-RNAi
CG1648-RNAi	UAS-mCD8-GFP/+; Repo-GAL4/UAS-*CG42342*-RNAi
Pdi-RNAi	UAS-mCD8-GFP/+; Repo-GAL4/UAS-*Pdi*-RNAi
Lac-RNAi	UAS-mCD8-GFP/+; Repo-GAL4/UAS-*Lac*-RNAi

Figure 4-13 *Lac*-RNAi in glia causes lower larval crawling velocity

Violin plots presenting mean crawling velocities of larvae of different RNAi-mediated knockdowns. See legend below for detailed genotypes. Wilcoxon signed-rank test Bonferroni adjusted p-values are reported. Means±SEM (Standard Error of the Mean) are displayed in orange. *Lac*-RNAi larvae crawl significantly slower than control larvae.

4.6 Discussion

4.6.1 Recap of the experimental rationale and results summary

In this chapter, I explored the roles of glial protrusion-localised transcripts within glial cells of *Drosophila* larvae by performing their RNAi-mediated knockdown. My rationale was to determine the impact of RNAi-mediated knockdown on *Drosophila* development, NMJ morphology and function, as well as their potential collective contribution to behaviour, assessed by the larval crawling assay. This exploration was motivated by the possible importance of mRNA localisation to the glial protrusions in development and structural synaptic plasticity, as suggested by previous research [46, 47, 49, 79, 181, 248, 280].

In the research presented here, I prioritised a candidate screen over a detailed investigation of each of the candidate glial protrusion-localised transcripts knockdown effects in glial cells. I aimed to identify any transcripts whose RNAi-mediated knockdown in glia produced any phenotypes. I next wanted to select the transcripts the knockdown of which had the most significant effects for subsequent research stages. Consequently, genes without observable impacts were deprioritised, while others were advanced to further analysis.

To answer my questions, I quantified numerous metrics. I started by observing the overall viability and development of larvae with glial RNAi-mediated knockdown of glial protrusion-localised transcripts (Table 4-2). I also measured NMJ neurite and glial projection areas and their ratio pre- and post- spaced potassium stimulation (Figure 4-7 and Figure 4-8). I further quantified “ghost bouton” numbers after potassium stimulation (Figure 4-11). Finally, I assessed larval crawling velocities of selected transcripts (Figure 4-13). These measurements were essential to gauge the overall

level of importance of a given glial protrusion-localised transcript in glial cells with respect to nervous system development and function and to try to pinpoint when and if its absence manifests itself.

I started with eighteen glial protrusion-localised transcripts, as confirmed in Chapter 3. Six of these transcripts belong to SJ genes (*Nrg, Atpα, Gli, Lac, cold, nrv2*) [207], several relate to cytoskeleton and cell adhesion (*Flo2, α-Cat, sdk, kst, shot, Cip4, CG42342*) or metabolism and cell homeostasis (*nrv2, Gs2, Vha55, ATPα, Pdi*). Some are important in mRNA localisation (*lost*), others have unknown roles (*CG1648*).

I identified various glial protrusion-localised transcripts that influenced NMJ morphology both pre- and post-stimulation. Knockdowns of four of these transcripts produced changes in “ghost bouton” numbers after the potassium stimulation assay. Notably, *Lac*-RNAi presented phenotypes in the brain, NMJ morphology, and “ghost bouton” counts. Finally, based on its compelling phenotype in the larval locomotion assay, *Lac* was prioritised for further exploration.

4.6.2 Experimental considerations

It is important to highlight that the primary aim of the work presented in this chapter was to undertake a candidate screen, the goal of which was identifying the most impactful knockdown phenotypes, rather than a comprehensive analysis for each gene. As a result, there are inherent limitations to the depth and breadth of the work presented here.

Firstly, a single RNAi knockdown line was utilised for each candidate transcript, posing the risk of secondary effects influencing observed phenotypes or the phenotype not being manifested due to a weak RNAi line.

Secondly, Repo-GAL4 pan-glial driver was used in the experiments described in this chapter. Because it determines the glial fate, Repo-GAL4 drives expression across all *Drosophila* glial cells [155]. The universal impact of Repo-GAL4 on all glial cells means that effects seen in the brain and cell soma cannot be differentiated from those at the glial cell periphery at the larval NMJ. It is also challenging to pinpoint when and why defects occur or identify the specific glial cell subtype causing observed effects.

Furthermore, upon analysing the larval brain anatomy and measuring the areas of glial and neurite protrusions and their ratios in both stimulated and unstimulated NMJs, I identified several significant phenotypes, but I did not have time to characterise these phenotypes in detail. Ultimately, given the already complex and time-consuming analysis of an extensive number of transcripts and metrics examined (Figure 4-2), it was not deemed feasible to apply further validation or detailed analysis to every candidate transcript at this stage, as such work would exceed the scope of my thesis.

Despite these constraints, the results of this chapter serve as a starting point for deeper, more detailed analyses. Specifically, in Chapter 5, I go on to explore the role of *Lac* in NMJ glia in more detail, addressing some of the outlined limitations. Moreover, the phenotypes which I uncovered offer attractive avenues for future research, and my colleagues in our laboratory are already working on more detailed analysis for some of them.

4.6.3 Candidate glial protrusion-localised transcripts knockdown in glia impacts normal larval development

Knocking down the candidate glial protrusion-localised transcripts in all glial cells in *Drosophila* 3rd instar wandering larvae using the GAL4/UAS system, I have observed instances of larval and adult lethality, as well as brain and NMJ morphology alterations.

4.6.3.1 *Lac*-RNAi and *cold*-RNAi brain abnormalities

The identified *Lac*-RNAi and *cold*-RNAi brain abnormalities suggest systemic anatomical developmental challenges arising from the knockdown of these candidate transcripts. The effects similar to those observed for *cold* and *Lac* knockdowns have been described before. Previous research has demonstrated the essential role of interactions between glial cells and the ECM in the formation of the developing *Drosophila* nervous system, the disruption of which resulted in VNC elongation (Figure 4-6) [277-279].

Both cold and Lac are members of SJs which are cell-cell adhesion foci with essential roles in determining the cell size and boundaries during early development through nerve ensheathment and insulation [204, 205, 207, 208]. Thus, it could be hypothesised that the observed phenotypes are indicative of cold and Lac having key roles in the size specification of the VNC. Furthermore, the VNC is an interesting region of the brain because rather than undergoing uniform growth, it undergoes elongation, then condensation to the correct size [281]. The observation of the elongated VNC is suggestive of impaired condensation, which could be interpreted as cold and Lac potentially contributing to this process. Interestingly, larvae with *cold*-RNAi knockdown mature to adulthood and seem largely unaffected. In contrast, *Lac*-RNAi larvae do not reach adulthood. While I observed these larvae transitioning to pupation, I did not see any emerge as viable adults. This leads me to hypothesise that they likely die during the pupation stage, although this has not been quantified.

Such observations suggest that while both genes are likely to play a role in condensation, *Lac* might be more important for subsequent developmental stages that culminate in a mature adult nervous system. On the other hand, *cold* may primarily

influence embryonic and larval phases. Additionally, it is possible that the effects of *cold* knockdown could be compensated for by another gene with a similar function.

4.6.3.2 *Vha55*-RNAi brain abnormality

The knockdown of *Vha55* led to a noticeable reduction in the size of the larval brain. This finding was initially unexpected, especially since the overall sizes of these larvae appeared comparable to the control group. Vha55 has been previously studied in the context of the CNS BBB, where it was predicted as a target possibly causing SPG to have increased permeability [282]. It has also been shown that Vha55 and other subunits of the V-ATPase capacitate the hyperplastic glial growth in a *Drosophila* model of gliomagenesis [283]. Thus, it suggests that the removal of *Vha55* mRNA might be causing insufficient growth of CNS glial cells, which then manifests in the reduced VNC length (Figure 4-6). To my knowledge, this is the first time this phenotype is reported in literature [248].

4.6.3.3 *shot*-RNAi NMJ morphology phenotype

In the NMJs with glial *shot*-RNAi, glial projections were either absent or nearly absent from the muscle surface (Figure 4-9). Notably, despite these changes, these larvae matured into viable adults without any discernible abnormalities, contrasting with the larvae expressing *Lac*-RNAi in glia, suggesting that hypomorphic *shot*-RNAi glial projections might be less deleterious than the hypermorphic projections seen in *Lac*-RNAi larvae.

Since shot is a spectraplakin, it interacts not only with F-actin, but also MTs and intermediate filaments, as is unique for spectraplakins. Moreover, as adaptor proteins, they interact with other adaptor and membrane proteins, having been dubbed cytoskeleton master regulators [284-286]. It is reasonable to hypothesise that

dysregulation of the glial cytoskeleton is the likely cause of the lack of glial projections at the NMJ in *shot*-RNAi larvae. shot is also responsible for attaching MTs to MT organizing centres (MTOC) [287]. This suggests that perhaps shot is required for attaching MTs to either a centrosomal or non-centrosomal MTOC and that correct MT attachment can be required for glial growth.

4.6.3.4 *Lac*-RNAi NMJ morphology phenotype

Glial *Lac*-RNAi NMJs had hypermorphic glial projections which appeared more complex than those of control NMJs and extended visibly further along the muscle surface (Figure 4-10). *Lac*-RNAi animals were not adult viable, and even larvae were significantly affected, appearing smaller, stunted and less mobile.

Lac encodes an IgLON family member protein which resides on the cell surface and participates in SJ formation [204, 205]. This family of proteins are known to have diverse roles in nervous system development. In mammals, *neuronal growth regulator 1* (*NEGR1*), which is a high-fidelity homologue of *Lac*, is known to play a role in psychiatric disorders. *Negr1*$^{-/-}$ mice show behavioural deficits and altered brain anatomy including decrease in the overall brain volume [288]. Interestingly, little is known about the function of this protein in glia, as even its mammalian name indicates neuronal focus.

The unusual morphology of the glial projections of the *Lac*-RNAi NMJs could suggest that Lac plays important roles in regulating not only neuronal, but also glial growth. As Lac is an adhesion molecule, it could be speculated that that in its absence within glia, disruption of signalling pathways responsible for proper adhesion and glia-glia or neuron-glia communication might occur. Such perturbations could prompt an over-

extension of the glial cell boundary, potentially driven by an attempt to “locate” and “adhere” to other glia or neurons.

4.6.4 Summary: candidate glial protrusion-localised transcripts knockdown in glia impacts normal larval development

Upon knockdown of a collection of candidate glial protrusion-localised transcripts, I observed numerous effects spanning lethality, anatomical abnormalities and NMJ morphology phenotypes. Particularly interesting were the brain phenotypes of *Lac*-, *cold*- and *Vha55*-RNAi, as well as the NMJ phenotypes observed for *Lac*- and *shot*-RNAi.

Overall, my findings reinforce the notion that glial protrusion-localised transcripts for which phenotypes were noted have distinct, yet crucial roles in proper glial cell development. Differentiating the direct influence of those glial protrusion-localised transcripts on structural synaptic plasticity is challenging due to potential developmental impacts and the intertwined nature of synapse development and function, but the role of localised mRNA in glial projections at the synapse remains worthy of investigation in both the developmental and plasticity contexts.

4.6.5 Glial protrusion-localised transcripts knockdown causes structural synaptic plasticity defects after spaced potassium stimulation

Post-stimulation “ghost bouton” counts revealed an increase for two transcripts (*Pdi*, *CG1648*) and a decrease for two others (*CG42342*, *Lac*). It is key to underscore that while the glial protrusion-localised transcript is knocked down in glial cells, the manifested effects which I described here are based on the number of “ghost boutons” produced by the axon terminal. My investigation thus highlights the intercellular

contribution of glial cells to motor neuron structural synaptic plasticity, reinforcing the essential and indispensable role of glia in neuronal function. As mentioned in the introduction to this chapter, however, “ghost boutons” do not always become fully functional new synapses. Therefore, the conclusions can be drawn solely for the first part of synaptogenesis process, namely, the formation of the active zones.

4.6.6 Glial protrusion-localised transcripts knockdown has effects on larval locomotion

I further demonstrated that *Lac*-RNAi knockdown in glial cells affected larval locomotion. While other larvae with knockdowns of glial protrusion-localised transcripts which previously displayed “ghost bouton” phenotypes exhibited normal crawling relative to the control, *Lac* knockdown larvae were notably mostly stationary (Figure 4-12), since *Lac*-RNAi larvae crawling velocity was considerably decreased (Figure 4-13). Consequently, *Lac* emerged as a particularly compelling gene of interest within this chapter. Its multi-faceted phenotypic expression spans abnormalities in the brain and NMJ morphology, “ghost bouton” numbers, impaired locomotion, and adult lethality.

However, the locomotion of the larvae with RNAi knockdowns of the other transcripts with previous “ghost-bouton” phenotypes was not affected. It could indicate that their role in the NMJ glia affects pathways unrelated to locomotion, which is also possible for the knockdown of *Lac*, since correlation of altered NMJ morphology and impaired crawling does not imply causation. Moreover, as mentioned in the introduction to this chapter, “ghost boutons” are immature synapses which do not necessarily become fully functional new synapses. Consequently, though serving as markers of neuronal activity, they are not indispensably indicative of synaptogenesis. This could also

explain why the mobility of the larvae remained unaffected despite the RNAi knockdowns targeting the remaining three transcripts associated with prior “ghost-bouton” phenotypes. In this scenario, the formation of the active zones, as quantified by the emergence of “ghost boutons”, could be affected by the RNAi knockdown of the candidate transcript, as measured by the spaced potassium stimulation protocol. The synapse maturation, however, and the overall synapse number might not be affected, considering no locomotion impairments. For that reason, it would be worthwhile to further explore the “ghost bouton” phenotypes observed for *Pdi*-, *CG1648*- and *CG42342*-RNAi mediated knockdown mechanistically, and better understand their role in glia in motor neuron “ghost bouton” formation.

4.6.7 Conclusions

In this chapter, I embarked on a candidate screen, the goal of which was a comprehensive investigation of the consequences of knocking down glial protrusion-localised transcripts in *Drosophila* larval glia. This was approached both in the context of typical development, but also structural synaptic plasticity, utilising the established spaced potassium stimulation protocol [191]. The former was carried out to assess whether developmental effects caused by RNAi knockdowns themselves affects the parameters also measured for the latter. The goal was to understand which transcripts, if any, produced discernible effects when knocked down, thereby setting the stage for further focused inquiries. Consequently, genes that did not exhibit pronounced effects were deprioritised, while those displaying distinct phenotypes were brought to the forefront of consideration.

I found that glial RNAi-mediated knockdown of several candidate transcripts had a substantial influence on correct larval development, as well as NMJ morphology in

both pre- and post-stimulation scenarios. It was especially noteworthy that the knockdown of four of these candidates in glial cells introduced changes in “ghost bouton” numbers after the potassium stimulation assay. This emphasises the role of perisynaptic glial cells in influencing motor neuron structural synaptic plasticity.

While the observed developmental irregularities present experimental challenges, as discerning the direct impact of the candidate glial protrusion-localised transcripts on structural synaptic plasticity becomes complex, they simultaneously underscore the potential importance of mRNA localisation to the glial periphery. This emphasises the possible significance of mRNA localisation not just in development, but also in the realm of structural synaptic plasticity — reinforcing the notion that structural synaptic plasticity is intricately intertwined with developmental processes.

Among all candidates, *Lac*-RNAi was particularly salient, not only for its range of phenotypes observed in the larval brain and NMJ morphology, but also as the sole transcript whose knockdown resulted in a larval locomotion phenotype. This unique impact on larval movement further underscored the significance and need for *Lac* in glial cells for the correct motor neuron function, marking *Lac* as a principal candidate for rigorous examination in the subsequent phases of my research.

CHAPTER 5

5 *Lac* is the Most Promising Protrusion-Localised Transcript Required in Glia for Neuronal Structural Synaptic Plasticity and Locomotion

5.1 Introduction

Intercellular communication between neurons and glia underlies the complex processes involved in the establishment of the nervous system connectivity. While countless cells in tissues like the liver or fat might perform their functions in a relatively uniform fashion, in the vast tapestry of the nervous system, every single cell is an individual player, with unique connections and intercellular interactions.

There are countless contacts and exchanges, both between the individual cells of the nervous system, but also in interactions with the target cells of other systems, like muscular, endocrine, digestive or vascular system. Some of these contacts include cell-cell signalling via canonical signalling pathways involving tyrosine kinase receptors (Trks) and the neurotrophins which bind them, like nerve growth factor (NGF) and BDNF [289]. Other cell-cell communication happens through the release and uptake of neurotransmitters like glutamate, oxytocin, dopamine, adrenaline or serotonin, or secretion of exosomes and ectosomes, which has been linked to numerous fundamental functions such as neurogenesis, myelin formation, synaptic plasticity and neuroinflammation [290].

Despite all these mechanisms, one of the most basic and simple modes of cell-cell communication in the nervous systems is through cell-cell adhesion. Adhesion molecules play essential roles in neural network development, including

synaptogenesis and axon guidance, as well as neuron-glia interactions. Though the basic adhesion machinery is shared between nervous system and epithelial cell junctions, unique classes of specialised adhesion molecules specific to the nervous system have been extensively studied, including, but not limited to, neurexins, neuroligins, nervous-system-specific cadherins and protocadherins, and neural cell adhesion molecules (NCAMs) [291-298].

A prominent group of cell adhesion molecules significant in the nervous system is the IgSF, unified by a shared Ig domain. High conservation between vertebrates and invertebrates characterises the IgSF molecules key for the processes involving the cells of the nervous system, in contrast to the immune system IgSF proteins [299, 300]. In 1995, three members of the IgSF — limbic system-associated membrane protein (LAMP), opioid-binding cell adhesion molecule (OBCAM), and Neurotrimin (Ntm) — were categorised into a new subclass based on their high homology [301]. Named IgLON in homage to the initial three members, this subclass is prominently expressed on nervous system cell surfaces and can interact across or on the same side of synaptic clefts to achieve their functions either through homophilic or heterophilic binding [302]. The IgLON family now includes five members, IgLON1-5 [303]. IgLON4, also known as NEGR1, stands out as the most researched since its identification in 1999 [304]. Notably, *NEGR1* is the best match mammalian homologue to *Lac*, the gene highlighted in Chapter 4, sharing 45% similarity and 30% identity upon protein sequence alignment using DIOPT (http://www.flyrnai.org/diopt) [217] (Figure 5-1).

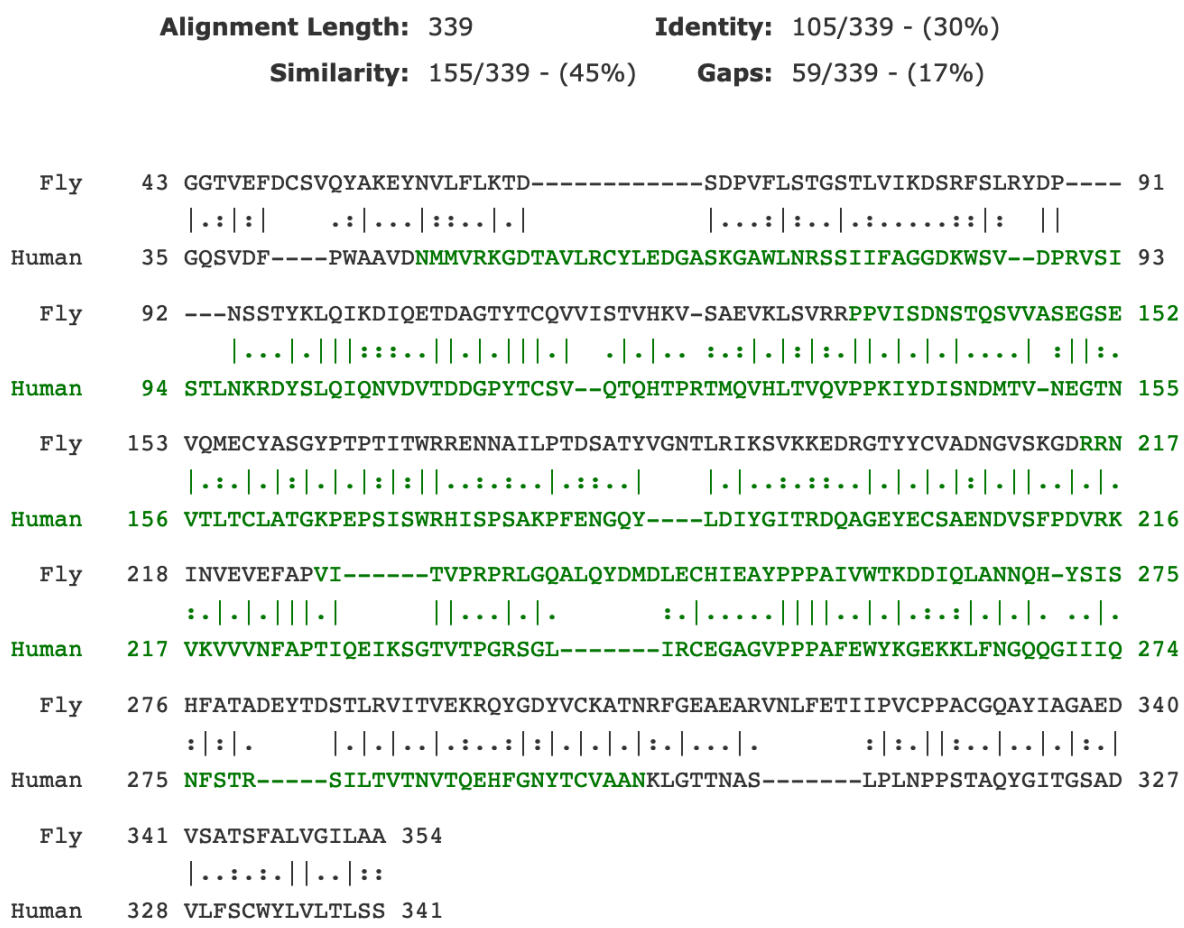

Figure 5-1 Sequence alignment between human *NEGR1* and *Drosophila Lac*

These two genes share 45% similarity and 30% identity. *NEGR1* is *Lac*'s best match human homologue.

Lac was identified and described before *NEGR1*, yet, *NEGR1* has been studied much more extensively [305]. Initially named *Kilon*, kindred of IgLON, *NEGR1* has since been fully incorporated into the IgLON family and found to be involved in correct neural development and synapse formation but is also associated with human obesity [304]. These two seemingly unrelated classes of *NEGR1* functions have recently been explored in a study where NEGR1 was found to accumulate in GABAergic inhibitory synapses in hypothalamic neurons, promoting the clustering of a GABA-synthesizing enzyme, GAD65, at the synaptic plasma membrane. Interestingly, *NEGR1* deficient mice have reduced GABAergic synapse densities and food reward responses, while

in high fat diet mice, NEGR1 and GAD65 accumulation increases abnormally [306]. With respect to its nervous system functions, in mice, it was established that NEGR1 and fibroblast growth factor receptor 2 (FGFR2) jointly influence cortical development and fundamental behaviours associated with autism spectrum disorders. *Negr1* deficiency in mice was found to be responsible for structural changes in the brain and behavioural abnormalities [288, 307]. When studied in humans, the absence of the *NEGR1* gene has been linked to conditions such as learning difficulties, intellectual disability, language impairment, developmental dyslexia and other neuropsychiatric issues [308-310].

Drosophila has their own suite of IgSF family proteins, occasionally referred to as the Wirin (wiring Ig) family, which control synaptic connectivity both structurally and functionally [299]. Wirins are suggested to have originated as a single gene in the bilaterians' last common ancestor according to phylogenetic analysis, and IgLONs in deuterostomes, including *NEGR1*, are co-orthologous to Dpr (Defective proboscis extension response), DIP (Dpr Interacting Proteins), Klingon, and Lachesin subfamilies in protostomes, all descended from an ancient progenitor [311-313]. The family is named due to the shared function among its members, specifically in guiding neuronal wiring, where the unique combinations of Wirins members serve as "identifiers" for individual nervous system cells [312, 314-319].

However, *Lac* is one of the less studied Wirins, though it has been recognised as a promising candidate for further exploration [320]. Initially identified in grasshopper and fly, it was found to be expressed during neurogenesis in the CNS and the PNS. Lac is also a member of SJs and, through SJs, it assures proper morphogenesis of the *Drosophila* tracheal system by affecting cell length through cell adhesion [305]. SJs

and, in vertebrates, TJs, are both types of occluding junctions whose role is preventing free diffusion of solutes through the intercellular space, something particularly important in the BBB, which Lac was also found to be required for [205, 321]. Interestingly, many other IgLONs, including *NEGR1*, are also expressed at the mammalian BBB [303].

The BBB is a structure aimed at protecting the complex nervous systems against uncontrolled solute, metabolite, or pathogen entry. In higher vertebrates, this barrier is made by polarised endothelial cells with extensive TJs; in contrast, lower vertebrates and invertebrates rely solely on glial cells for their BBB [210]. Given the structural similarities of IgLONs as evidenced in previous research, they might have influenced evolutionary adaptations in brain complexity, including the regulation of neural growth and BBB integrity [303]. The period of emergence of complex BBBs seems to coincide with IgLON duplication events [303, 322, 323].

Thus, *Lac* emerged as an interesting candidate to further explore, both from the previous research looking into IgLONs roles in the BBB formation, but also my own observations from the preceding chapters. Very little is known about the transport and local translation of mRNAs coding for cell adhesion proteins, specifically in BBB glia. In this chapter, I therefore wanted to investigate the functions of Lac specifically with this context in mind. Where is the *Lac* mRNA in the glial projections when compared to the BBB? Is *Lac* mRNA or protein affected in the context of structural synaptic plasticity at the *Drosophila* NMJ? Which glial cells whose projections make it to the NMJ contribute to the observed crawling phenotype, and does knocking *Lac* down in the motor neuron cause the same phenotype? Is *Lac* mRNA in the NMJ glial projections spliced or unspliced? Asking these questions could allow me to further

understand not only the function of IgSF in invertebrate BBB, but also how that function can be controlled by mRNA localisation and local translation.

5.2 Specific aims of this chapter

1. To test the specificity of the previously used *Lac*-RNAi knockdown.
2. To test the specificity of the previously used CPTI Lac::YFP line.
3. To quantify the amount of *Lac* mRNA and protein in the *Drosophila* 3rd instar NMJ before and after spaced potassium stimulation, and thus explore potential impact of structural synaptic plasticity on *Lac* mRNA transport and translation.
4. To assess whether introns are present in *Lac* mRNA molecules found in the NMJ glial projections.
5. To visualise the glial cell subtypes whose projections make it to the NMJ and determine which glial cell subtypes contribute to the previously observed impaired crawling phenotype upon *Lac*-RNAi knockdown.
6. To establish whether *Lac*-RNAi knockdown in the motor neuron causes similar phenotype to the previously observed impaired crawling phenotype upon glial *Lac*-RNAi knockdown.
7. To determine the impact of the RNAi knockdown of *Imp*, which encodes an mRNA binding protein, on the *Lac* mRNA presence at the NMJ.
8. To understand the *Lac* mRNA localisation with respect to the BBB and motor neuron axon projections at the NMJ.

5.3 Materials and methods

5.3.1 Fly stocks

For the experiments in this chapter, I used the previously mentioned *Lac*-RNAi (VDRC 35524) and Lac::YFP (CPTI001714) lines, as well as the Repo>GFP and Repo>mCherry lines. For the *Imp* knockdown in glia, I used *Imp*-RNAi (BDSC 34977). For *Lac*-RNAi and *Imp*-RNAi knockdown experiments, I used the same *mCherry*-RNAi (BDSC 35785) control cross: UAS-mCD8-GFP/+; Repo-GAL4/UAS-*mCherry*-RNAi.

I also constructed two different lines to fluorescently label SPG and PG and test if their projections reach the NMJ: Mdr65-GAL4 (gifted by Teodoro laboratory, BDSC 50472) and 46F-GAL4 (gifted by Prof Stefanie Schirmeier), respectively, driving UAS-mCD8-GFP expression (BDSC 63045). To test if WG projections reach the NMJ, I used Nrv2-GAL4, UAS-mCD8-GFP/CyoGFP line, gifted by Teodoro laboratory.

To carry out *Lac*-RNAi knockdown in the motor neuron, I used a previously constructed OK6-GAL4, UAS-mCD8-mCherry/CyoGFP line available in our laboratory and crossed it to *Lac*-RNAi (VDRC 35524). The control experiment was the same line crossed to *Luciferase*-RNAi (BSDC 35788). To label the BBB, I used Nrx-IV::GFP protein trap (CA06597), kindly gifted by Teodoro laboratory. Table 5-1 presents all lines used in the experiments described in this chapter.

Table 5-1 List of *Drosophila melanogaster* stocks used in Chapter 5

Line name	Line ID	Line source	Line description
Lac::YFP	CPTI001714	DGRC	*Lachesin* gene YFP protein trap line
Repo-GAL4	7415	BDSC	Expresses GAL4 in glia [155]
UAS-mCD8-mCherry/cyo-GFP	27391	BDSC	Expresses Cherry RFP fused to the mouse CD8 extracellular and transmembrane domains for membrane targeting under UAS control.
UAS-mCD8-GFP/cyo-GFP	63045	BDSC	Expresses GFP fused to the mouse CD8 extracellular and transmembrane domains for membrane targeting under UAS control.
Lac-RNAi	GD 35524	VDRC	Expresses dsRNA for RNAi of *Lac* under UAS control in the pUAST vector pMF3.
mCherry-RNAi	35785	BDSC	Expresses dsRNA for RNAi of *mCherry* under UAS control in the VALIUM20 vector.
Nrv2-GAL4, UAS-mCD8-GFP/CyoGFP	-	-	Recombined stock which expresses GAL4 in WG and drives expression of membrane targeted GFP, kindly gifted by Prof Rita Teodoro. Based on BDSC stocks 6800 and 63045.
46F-GAL4	-	-	Expresses GAL4 in PG[187]. Gift from Prof Stefanie Schirmeier.
Mdr65-GAL4	50472	BDSC	Expresses GAL4 in SPG.
OK6-GAL4 > UAS-mCD8 mCherry	-	Constructed in the Davis laboratory	GAL4 expressed in motor neurons, recombined with membrane targeted mCherry.
Imp-RNAi	34977	BDSC	Expresses dsRNA for RNAi of *Imp* under UAS control in the VALIUM20 vector.
Nrx-IV::GFP	CA06597	-	Carnegie collection protein trap for *neurexin IV*, labelled with GFP, kindly gifted by Prof Rita Teodoro[188].
Luciferase-RNAi	35788	BDSC	Expresses firefly Luciferase under the control of UAS in the VALIUM10 vector.

5.3.2 Driver RNAi crosses genotype abbreviations

I abbreviate the genotypes of the RNAi fly crosses created in this chapter as outlined in Table 5-2.

Table 5-2 Summary of fly line abbreviations used in Chapter 5

Full genotype	Abbreviation
UAS-mCD8-GFP/+; Repo-GAL4/UAS-*mCherry*-RNAi	Repo>Control
UAS-mCD8-GFP/+; Repo-GAL4/UAS-*Lac*-RNAi	Repo>*Lac*-RNAi
UAS-mCD8-GFP/+; Repo-GAL4/UAS-*Imp*-RNAi	Repo>*Imp*-RNAi
Nrv2-GAL4, UAS-mCD8-GFP/+; UAS-*mCherry*-RNAi/+	Nrv2>Control
Nrv2-GAL4, UAS-mCD8-GFP/+; UAS-*Lac*-RNAi/+	Nrv2>*Lac*-RNAi
46F-GAL4/+; UAS-mCD8-GFP/UAS-*mCherry*-RNAi	46F>Control
46F-GAL4/+; UAS-mCD8-GFP/UAS-*Lac*-RNAi	46F>*Lac*-RNAi
UAS-mCD8-GFP/+; Mdr65-GAL4/UAS-*mCherry*-RNAi	Mdr65>Control
UAS-mCD8-GFP/+; Mdr65-GAL4/UAS-*Lac*-RNAi	Mdr65>*Lac*-RNAi
OK6-GAL4, UAS-mCD8-mCherry/+; UAS-*Luciferase*-RNAi/+	OK6>Control
OK6-GAL4, UAS-mCD8-mCherry/+; UAS-*Lac*-RNAi/+	OK6>*Lac*-RNAi

5.3.3 Spaced High K^+ depolarisation paradigm

The spaced potassium stimulation procedure was conducted as previously detailed in Section 2.8.1. Briefly, the larvae were dissected and underwent five consecutive washes of potassium-rich solution (3 times 2 minutes), with 10-minute intervals of low potassium solution in between [197].

5.3.4 Larval locomotion behaviour assay

The larval crawling behaviour was explored using the automated tracking assay as described in Section 2.8.2.2 [199]. Briefly, 3rd instar wandering larvae were acclimated for 1 hour at room temperature, then transferred five at a time to a 9-cm 1% agarose petri dish and acclimatised for 1-minute. Larvae were recorded in 1080p at 30fps, and subsequently tracked using the BIOImageOperation software's standard tracking mode, available at https://joostdefolter.info/bio-research. Tracking ended when larvae reached the plate edge or interacted with another larva. I verified the tracking results manually by comparing them to post-filtering videos, discarding any false tracks. Clean data was processed in RStudi using the 'tidyverse' package. I quantified crawling speed (in cm/s), path straightness, as well as movement linearity (mean directional change) and irregularity (standard deviation of directional change), the latter two calculated using 'trajr' package in RStudio (Section 2.8.3) [200, 324].

5.3.4.1 Image acquisition and processing

The morphology of 3rd instar *Drosophila* NMJs was assessed using confocal microscopy (Section 2.5.2). I quantified the NMJ morphology before and after stimulation by measuring glial and motor neuron axon terminal projection areas (both expressed in μm^2), labelled with Repo-GAL4 driving UAS-mCD8-GFP and α-HRP antibody, respectively, as well as their ratios (Section 2.7.1). The measurements were

made in abdominal segments 2-5, using ImageJ, and subsequently analysed in RStudio [121, 194, 195]. I quantified the area of the BBB in the same way using the Nrx-IV::GFP labelling. The Lac::YFP protein signal intensity was calculated by subtracting the background from the sum of signal intensity and dividing that by the sum of the Lac::YFP area using ImageJ and RStudio (Section 2.7.3).

5.3.4.2 mRNA spots quantification

I detected *Lac* mRNA, either labelled with the α-*YFP* probe or α-*Lac* intron or exon probes using smFISH as previously described (Section 2.4.3) and visualised the signal in tissue using confocal microscopy (Section 2.6.1). The probe sequences can be found in the Table B-2 in the Appendix. I utilised a tailored Big-FISH approach to count smFISH spots in the images (Section 2.7.2) [196]. After background subtraction and noise reduction, the intensity threshold was set based on manual examination of representative spots. Following this, mRNA smFISH spots in each image were detected and their positions correlated with "mask" images of glial areas, axon terminal areas, or NrxIV::GFP areas. This process provided a comprehensive count of single mRNA molecules within the NMJ glia, marked by Repo>GFP, neurite (α-HRP area) or BBB area (marked by NrxIV::GFP signal).

5.4 Results

5.4.1 CPTI Lac::YFP and *Lac*-RNAi lines target Lac

Having identified *Lac* as a candidate transcript whose knockdown in glia resulted in altered larval locomotion, my objective was to explore the mechanism through which Lac acted at the NMJ. To start, I first set out to confirm that the YFP trap used in Chapter 3 indeed labels Lac protein. I designed α-*Lac* exon probes and used it

together with the same α-*YFP* probes from Chapter 3 to image 3rd instar *Drosophila* NMJs and observe whether they co-localise. The probe sequences are available in Table B-1 in the Appendix. Indeed, the probes showed the exact same pattern of expression (Figure 5-2).

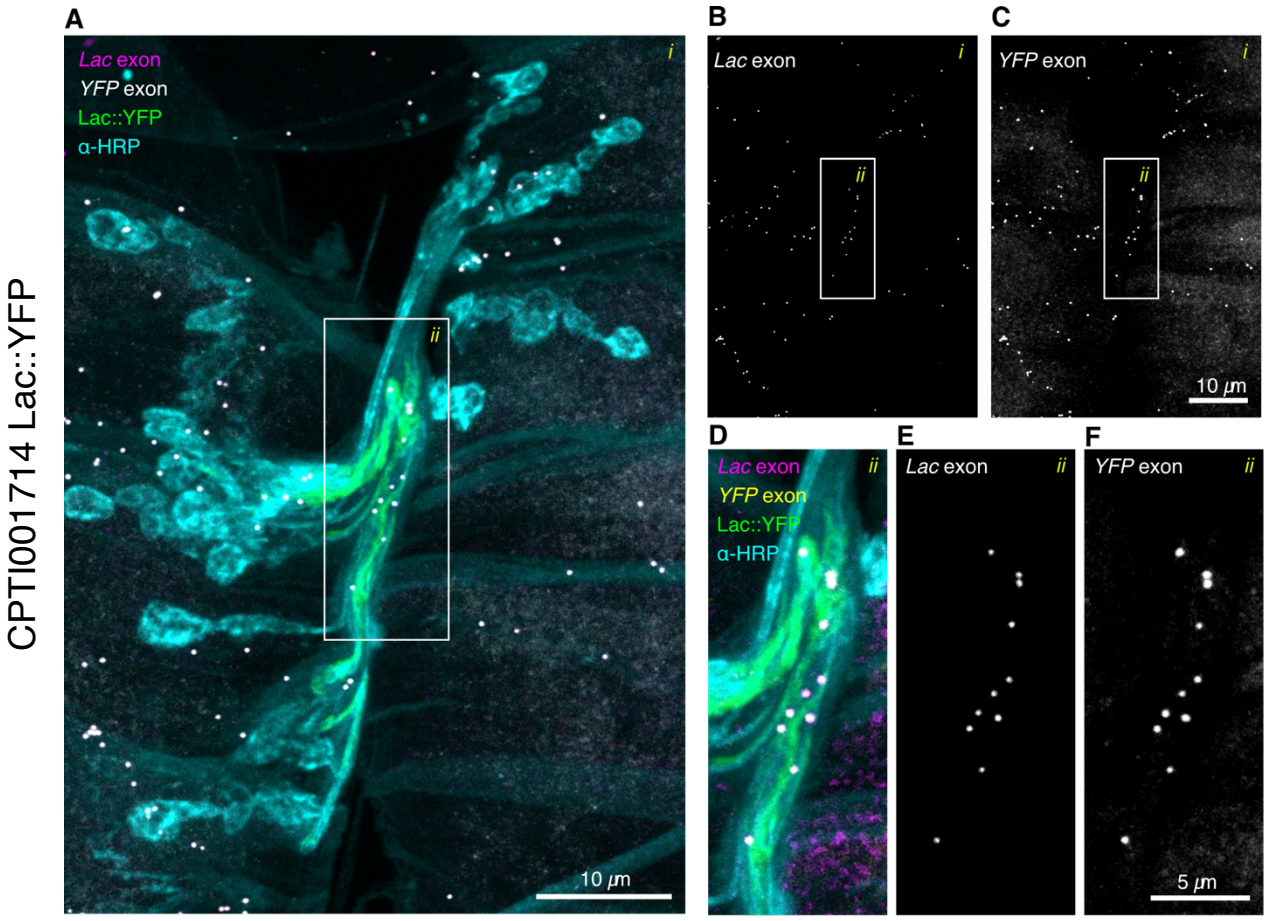

Figure 5-2 Co-localisation of *Lac::YFP* mRNA and *Lac* mRNA in *Drosophila* NMJ glia

A) A representative confocal image of the Lac::YFP CPTI line *Drosophila* 3rd instar larva NMJ (segment A3), showing the *Lac* mRNA in magenta (α-*Lac* exon probe, Alexa 568), *Lac::YFP* mRNA in white (α-*YFP* exon probe, Atto 633), Lac protein in green (Lac::YFP), and the motor neuron axon terminal projection in cyan (α-HRP antibody conjugated to Alexa 405 fluor). B-C) A single-channel view (see label) of A i) showing mRNA molecules of *Lac::YFP* and *Lac* exon in the same locations. D) A zoomed in view of ii) of A) showing a selected area of Lac::YFP protein with multiple mRNA molecules. E-F) A single-channel view (see label) of D (A ii)) showing that *Lac* exon and *Lac::YFP* exon molecules are in the exact same locations. Scale bars: A-C - 10 μm, D-F – 5 μm.

In order to determine if Lac::YFP area could be used as a proxy for glial area, I wanted to compare what proportion of the glial projection area, as labelled by Repo>mCherry, Lac::YFP protein occupies. I crossed the Repo>mCherry line to the CPTI Lac::YFP line and quantified the respective areas. There was no significant difference (Wilcoxon rank sum test, p = 0.0616, Figure 5-3) between the areas of glial membrane marked by Repo>mCherry and Lac::YFP, suggesting that Lac protein fills the glial cell projection nearly completely.

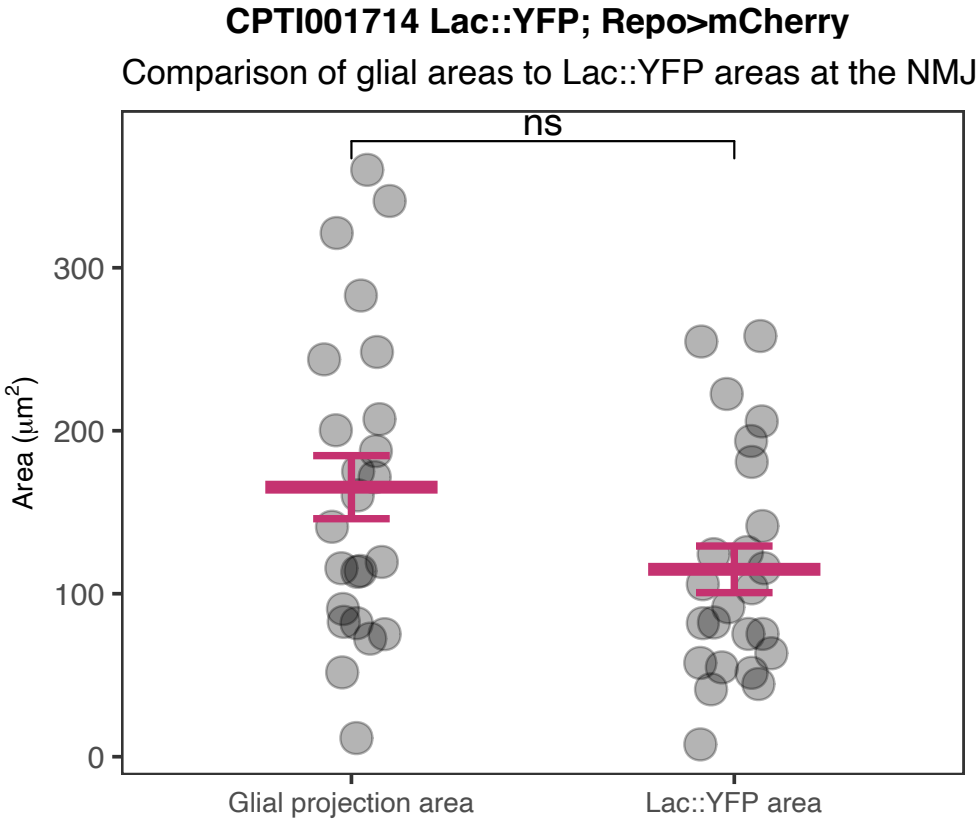

Figure 5-3 Lac::YFP area is similar in size to glial projections area

Quantification of the glial projection areas, labelled with Repo>mCherry, and Lac protein areas, marked with Lac::YFP. Wilcoxon rank sum test p-value is reported (p = 0.0616, N. S.).

I next wanted to confirm whether the RNAi knockdown line (VDRC 35524) which I used in Chapter 4 indeed targets *Lac*. I therefore used smFISH to visualise the *Lac* mRNA molecules in control and *Lac*-RNAi knockdown larval 3rd instar NMJ glia (Figure

5-4). The glial projections of the *Lac*-RNAi knockdown NMJs seemed to have almost no *Lac* mRNA molecules. I then confirmed through quantification that the numbers of *Lac* mRNA molecules were significantly decreased in the *Lac*-RNAi NMJs (Wilcoxon rank sum test, $p < 0.001$, Figure 5-5). Therefore, VDRC 35524 *Lac*-RNAi line previously used targets *Lac*, and the observed phenotypes can be attributed to *Lac* knockdown.

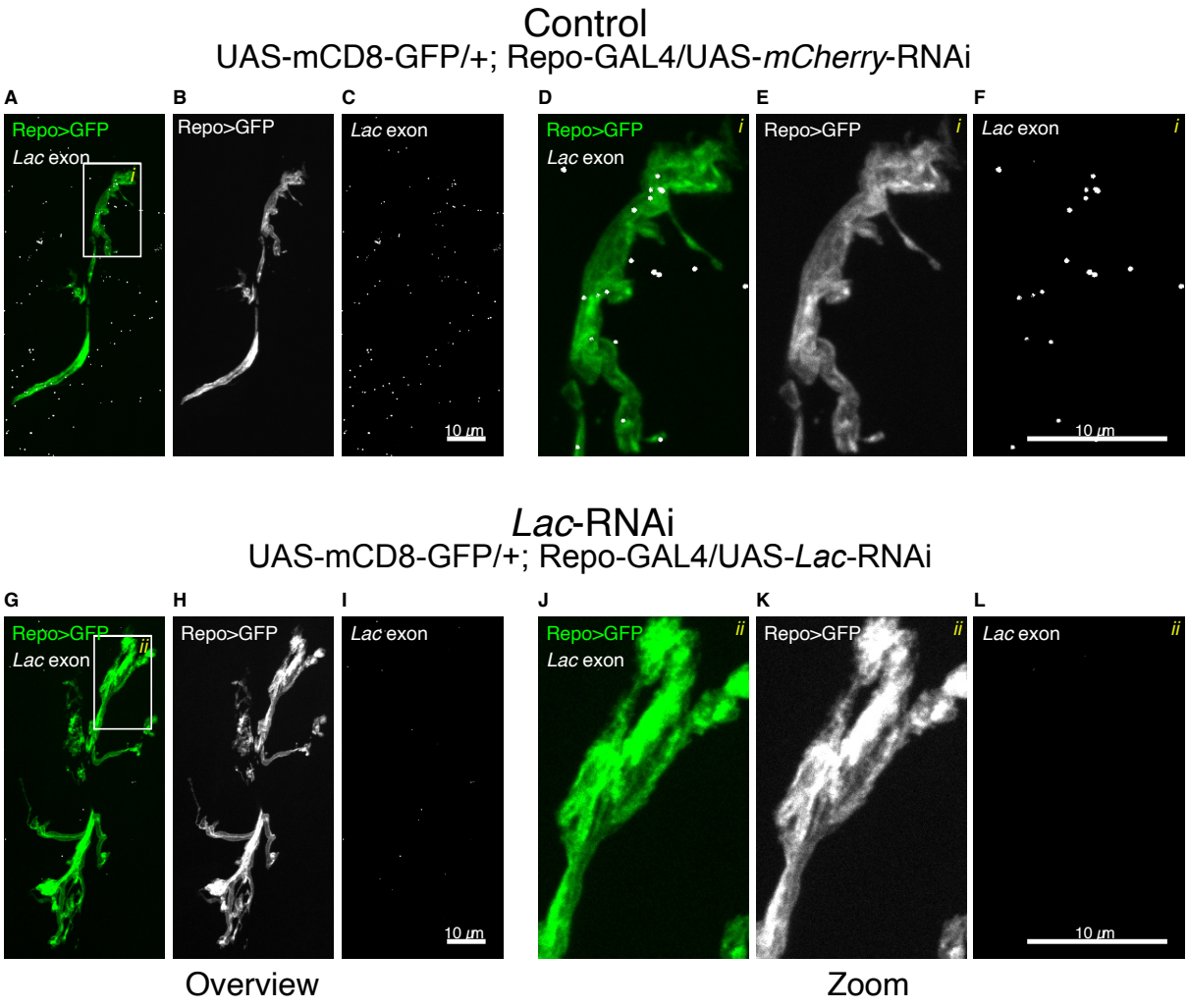

Figure 5-4 *Lac* mRNA in absent in *Lac*-RNAi Drosophila glia

A-F: control. G-L: *Lac*-RNAi glial knockdown. D-F and J-L are zoomed in areas of i) in A and ii) in G, respectively. A, D, G, J) Confocal images of the *Drosophila* 3rd instar larval NMJs, showing *Lac* mRNA in white (α-*Lac* exon probe, Alexa 568), and glial membrane of perisynaptic glia labelled with Repo>GFP in green. B, E, H, K) A single-channel view of A, D, G, J respectively, showing only the glial membrane of perisynaptic glia. C, F, I, L) A single-channel view of A, D, G, J respectively, showing only *Lac* mRNA. Scale bar: 10 μm.

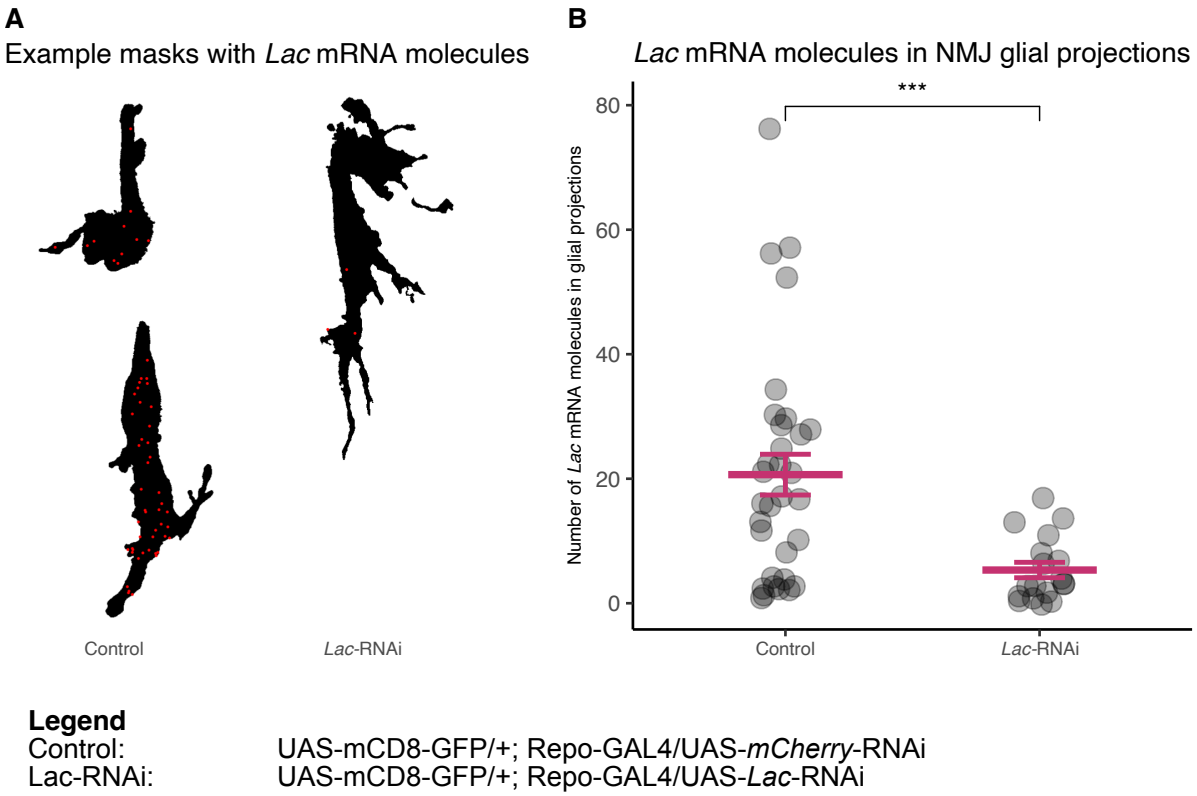

Legend
Control: UAS-mCD8-GFP/+; Repo-GAL4/UAS-*mCherry*-RNAi
Lac-RNAi: UAS-mCD8-GFP/+; Repo-GAL4/UAS-*Lac*-RNAi

Figure 5-5 Number of *Lac* mRNA molecules is significantly reduced in *Lac*-RNAi glia

A) Example masks showing the overlay of the detected mRNA molecules (red) in the control (left) and *Lac*-RNAi (right) NMJ glia (black binary mask of Repo>GFP area acquired using ImageJ). B) Quantification of the number of *Lac* mRNA molecules within glia shows a significant ($p < 0.001$) decrease of the number of mRNA molecules in the *Lac*-RNAi knockdown NMJs. Wilcoxon rank sum test p-value is reported. See legend for genotype details.

5.4.2 *Lac*-RNAi NMJ phenotype exploration

Having confirmed the successful knockdown of *Lac* with the previously utilised RNAi line (VDRC 35524), I wanted to further explore the previously observed NMJ phenotype. Particularly, I set out to image the glial projections at the NMJ in control (Figure 5-6) and RNAi (Figure 5-7) conditions, after high potassium stimulation.

Glial projections in control NMJs are predominantly simple and not overly branched. They most often take a form of an extended thin "filament" of glial membrane ending in a structure similar to a "ghost bouton" (Figure 5-6 Ai) or are blunt and in direct

contact with a synaptic bouton (Figure 5-6 Aii), which has been described before [121]. They are also known to interact with motor neuron “ghost boutons” (Figure 5-6 Bii, Ci) and the trachea (Figure 5-6D) [204]. Interestingly, many are independent structures with *Lac* mRNA molecules localised to their very periphery (Figure 5-6 Ai, Bi, Cii).

In contrast, the glial projections in the *Lac*-RNAi condition are extensive and form structures not seen in the control condition, making them appear disordered and chaotic (Figure 5-7). Some seem to form “glial ghost boutons” which present as untethered round structures akin to neuronal “ghost boutons” with no neurite attached to them (Figure 5-7 Ai, Bi). Others make projections ending in boutons like those seen in the control (Figure 5-6 Ai), but much more numerous and extensive (Figure 5-7 Aii, B). They often co-exist with neuronal “ghost boutons” and occasionally seem to “compete” with them (Figure 5-7 Biii-iv) or enwrap them (Figure 5-7 Bii, Ciii). The glial membrane branches observed in *Lac*-RNAi are more extensive, too. Some wrap the tracheas (Figure 5-7 Ci), like in control (Figure 5-6 D), others extend seemingly aimlessly over the muscle surface (Figure 5-7 E). Some branches give rise to numerous processes and boutons which do not interact with any other structures (Figure 5-7 Cii, D).

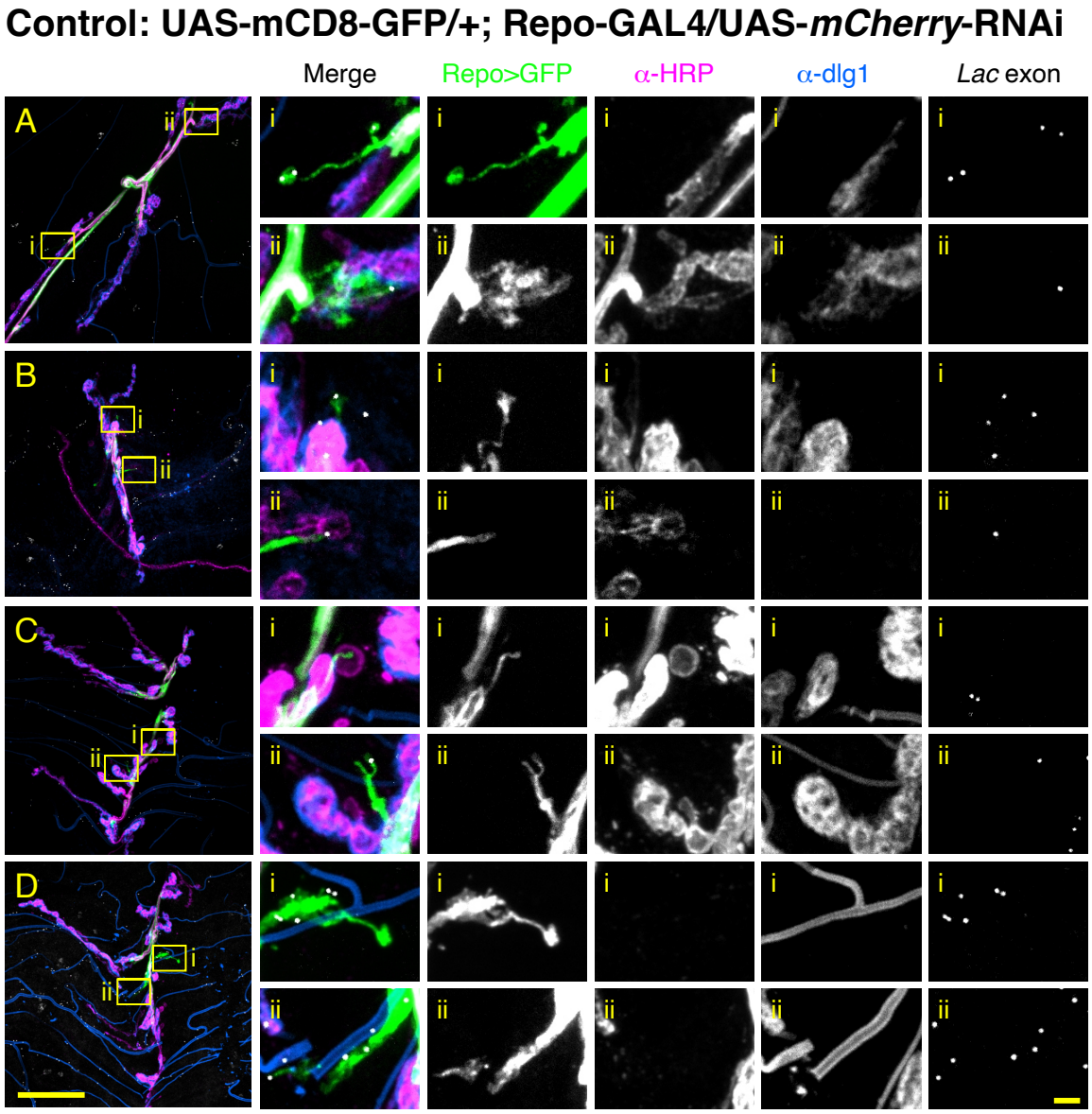

Figure 5-6 *Lac* mRNA localises to the tips of distal projections made by perisynaptic glia

A-D) Confocal images of control *Drosophila* 3rd instar larval NMJs showing Repo>GFP signal in green (Repo>GFP, *mCherry*-RNAi), motor neuron axon terminal in magenta (α-HRP antibody conjugated to Alexa 568 fluor), postsynaptic density in blue (α-dlg1 antibody, Alexa 405 fluor, trachea is auto-fluorescent) and *Lac* mRNA in white (α-*Lac* exon probe, Atto 633). Scale bar: 25 μm. i-ii) A zoomed in view of A-D. See labels for details. Scale bar: 2 μm. A) Glia form processes which elongate along muscle surface (Ai) or terminate bluntly before the proximal bouton (Aii). *Lac* mRNA is localised to the very edge of both. B) Glial processes can be independent structures (Bi) or can interact with "ghost boutons" (Bii), where *Lac* mRNA is located at the contact site between the glial and the neural membrane. C) More examples of glial projections interacting with a large "ghost bouton" (Ci) and creating an interesting, forked structure (Cii) with *Lac* mRNA located to its very edge. D) Glial projections filled with *Lac* mRNA molecules interact with the trachea (Di, Dii).

Lac-RNAi: UAS-mCD8-GFP/+; Repo-GAL4/UAS-*Lac*-RNAi

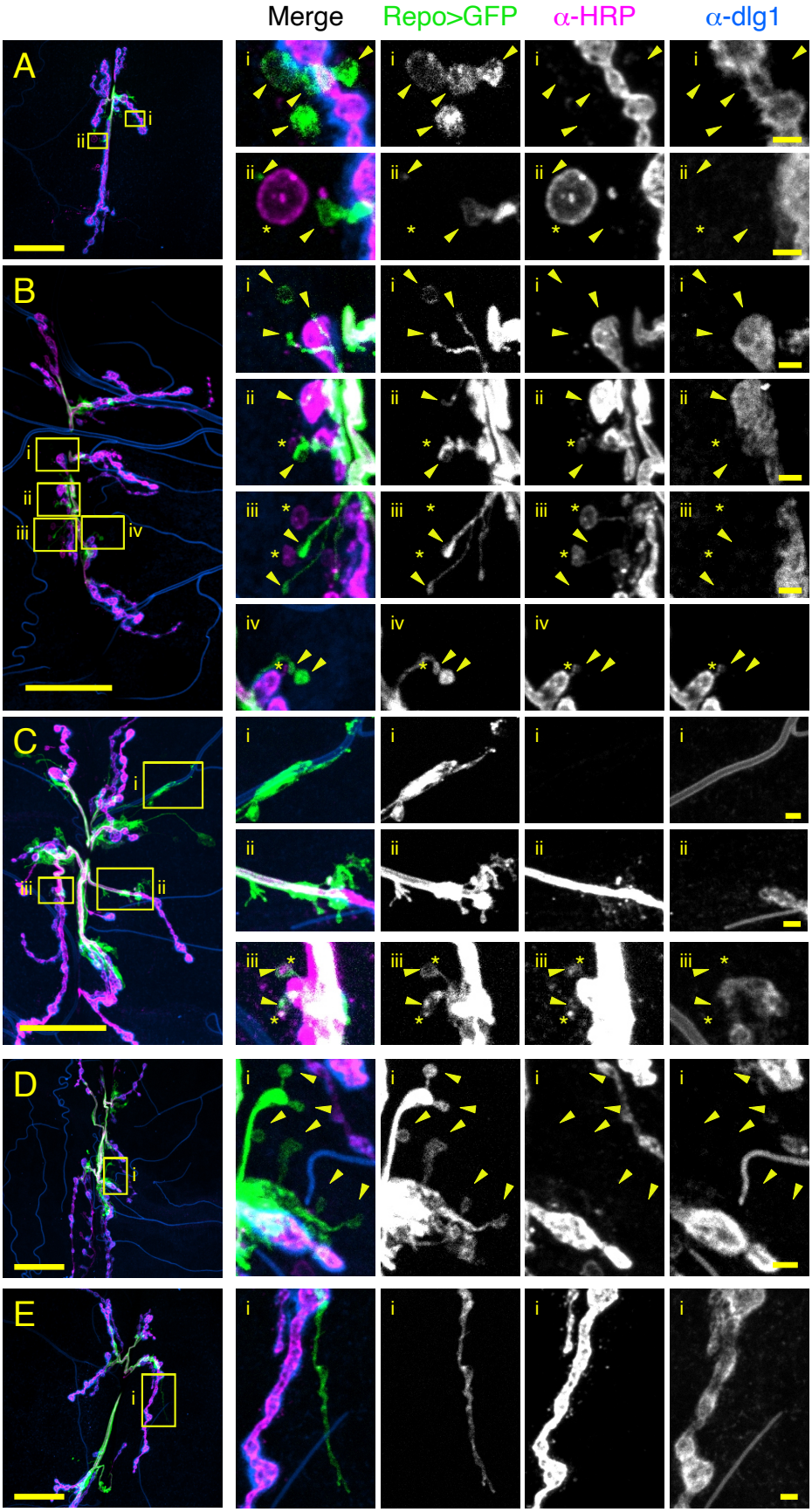

Figure 5-7 *Lac*-RNAi knockdown driven emergence of disordered glial structures

Previous page: A-E) Confocal images of *Lac*-RNAi *Drosophila* 3rd instar larval NMJs showing Repo>GFP signal in green (Repo>GFP, *Lac*-RNAi), motor neuron axon terminal in magenta (α-HRP antibody conjugated to Alexa 568 fluor) and the postsynaptic density in blue (α-dlg1 antibody, Alexa 405 fluor, trachea is auto-fluorescent). Scale bar: 25 μm. i-iv) A zoomed in view of A-E. See labels for details. Scale bar: 2 μm. Glial membrane indicated with a yellow arrow, neuronal membrane with a yellow asterisk. A) *Lac*-RNAi glia form boutons independent from neuronal "ghost boutons" (Ai, Aii). B) Glial boutons in *Lac*-RNAi interact closely with neuronal structures. C) Glial branches wrap around trachea (Ci) and form independent structures (Cii). Glial boutons wrap around "ghost boutons" (Ciii). D) *Lac*-RNAi glia create numerous glial boutons. E) *Lac*-RNAi glia create unbranched, long projections.

5.4.3 *Lac* exon, but not intron, are present at the NMJ

I next wanted to verify whether *Lac* molecules observed at the NMJ are pre-mRNA or mRNA. I designed α-*Lac* intron probes (Table B-1 in the Appendix) and used smFISH to visualise them together with α-*Lac::YFP* probes (Figure 5-8). I did not observe any *Lac* intron signal at the NMJ, but I did observe *Lac::YFP* exon signal. I however observed intron signal in the brain cell nuclei, overlapping with the exon signal. Thus, I concluded that pre-mRNA of *Lac* is not present at the NMJ.

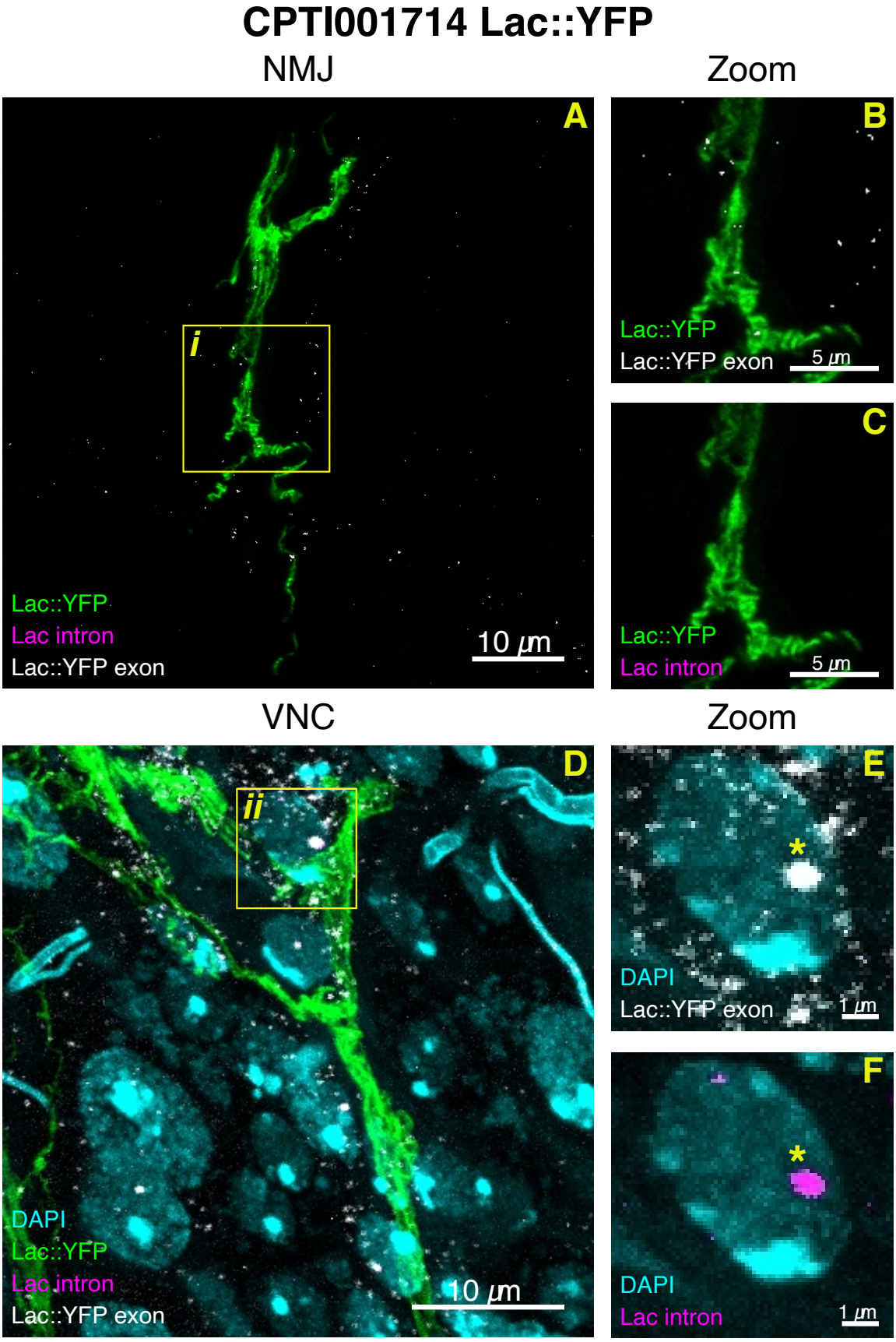

Figure 5-8. *Lac* intron and *Lac::YFP* exon in the NMJ and VNC

Previous page: A) Confocal image of the *Drosophila* 3rd instar larval NMJ, showing Lac::YFP protein signal in green, *Lac* intron in magenta (α-*Lac* intron probe, Alexa 568) and *Lac::YFP* exon in white (α-*YFP probe,* Atto 633). Scale bar: 10 μm. B) A zoomed-in view (see label) of the region marked i) in A showing the *Lac::YFP* mRNA exon molecules overlapping with the Lac::YFP protein area. Scale bar: 5 μm. C) A zoomed-in view (see label) of the region marked i) in A showing the absence of *Lac* intron mRNA signal in the Lac::YFP protein area. Scale bar: 5 μm. D) Confocal image of the *Drosophila* 3rd instar larval VNC showing Lac::YFP protein signal in green, *Lac* intron in magenta (α-*Lac* intron probe, Alexa 568) and Lac::YFP exon in white (α-*YFP probe,* Atto 633). Scale bar: 10 μm. B) A zoomed-in view (see label) of the region marked ii) in D showing the *Lac::YFP* mRNA exon molecules near and in a selected VNC nucleus. The overlap area is marked with a yellow asterisk. Scale bar: 1 μm. C) A zoomed-in view (see label) of the region marked ii) in D showing the overlap of *Lac* intron mRNA signal with the *Lac::YFP* mRNA exon, marked with the yellow asterisk. Scale bar: 1 μm.

5.4.4 Lac::YFP area decreases after stimulation, but mRNA and protein are unaffected

I next performed a spaced potassium simulation experiment with the use of Lac::YFP line to observe the dynamics of *Lac::YFP* mRNA and protein at the *Drosophila* NMJ in the context of structural synaptic plasticity (Figure 5-9). Lac::YFP protein is present in fine “projections” both at unstimulated (Figure 5-9 A, B) and stimulated (Figure 5-9 C, D) NMJs. These projections interact with each other and motor neuron branches (Figure 5-9 i, ii) as well as mature (Figure 5-9 iii) and “ghost” synaptic boutons (Figure 5-9 iv). *Lac::YFP* mRNA molecules are localised to the periphery of those Lac::YFP protein filaments.

I then quantified the area occupied by the Lac::YFP protein, Lac::YFP protein signal density, and the motor neuron axon projection area before and after the potassium stimulation as described in Sections 2.7.3 and 2.7.1 to try to examine possible changes in the area occupied by Lac::YFP, or increase in the amount of Lac::YFP protein, possibly thanks to local translation caused by the stimulation. I expected that

Lac::YFP protein signal intensity or Lac::YFP area could increase if stimulation caused local translation, but the motor neuron axon projection area should not change significantly. The results obtained indicate no significant changes in the Lac::YFP protein signal density or the motor neuron axon projection area (Wilcoxon rank sum test, $p = 0.498$), but the Lac::YFP protein area is decreased after stimulation, in contrast to what I hypothesised (Wilcoxon rank sum test, $p < 0.05$, Figure 5-10). I also quantified the number of *Lac::YFP mRNA* molecules in the different NMJ compartments, namely the Lac::YFP area, or the approximate "glial projection" area, and the α-HRP area, the neuronal projection area. I suspected that if *Lac* mRNA is required in glia for structural synaptic plasticity of the neighbouring motor neuron, the stimulation might induce increased transport of *Lac* mRNA to the glial periphery. However, neither "glial", nor neuronal projection *Lac* mRNA molecule numbers were significantly changed after the spaced potassium stimulation (Wilcoxon rank sum test, $p = 0.401$ & 0.162, Figure 5-11 A). Yet, both before and after stimulation, the number of *Lac::YFP* mRNA molecules in the α-HRP area was significantly higher than in glial domain, where I used Lac::YFP area as a proxy (Wilcoxon rank sum test, $p<0.0001$ in both cases, Figure 5-11 B).

Intrigued by these results, I wondered if decreased Lac::YFP areas (Figure 5-10 A) and unaffected number of mRNA molecules (Figure 5-11 A) translate to an overall increase in the concentration of *Lac::YFP* mRNA molecules per unit of Lac::YFP area. I quantified the numbers of mRNA molecules per μm^2 of Lac::YFP area for unstimulated and stimulated NMJs, and determined that the difference was not significant (Wilcoxon rank sum test, $p=0.85$, Figure 5-12).

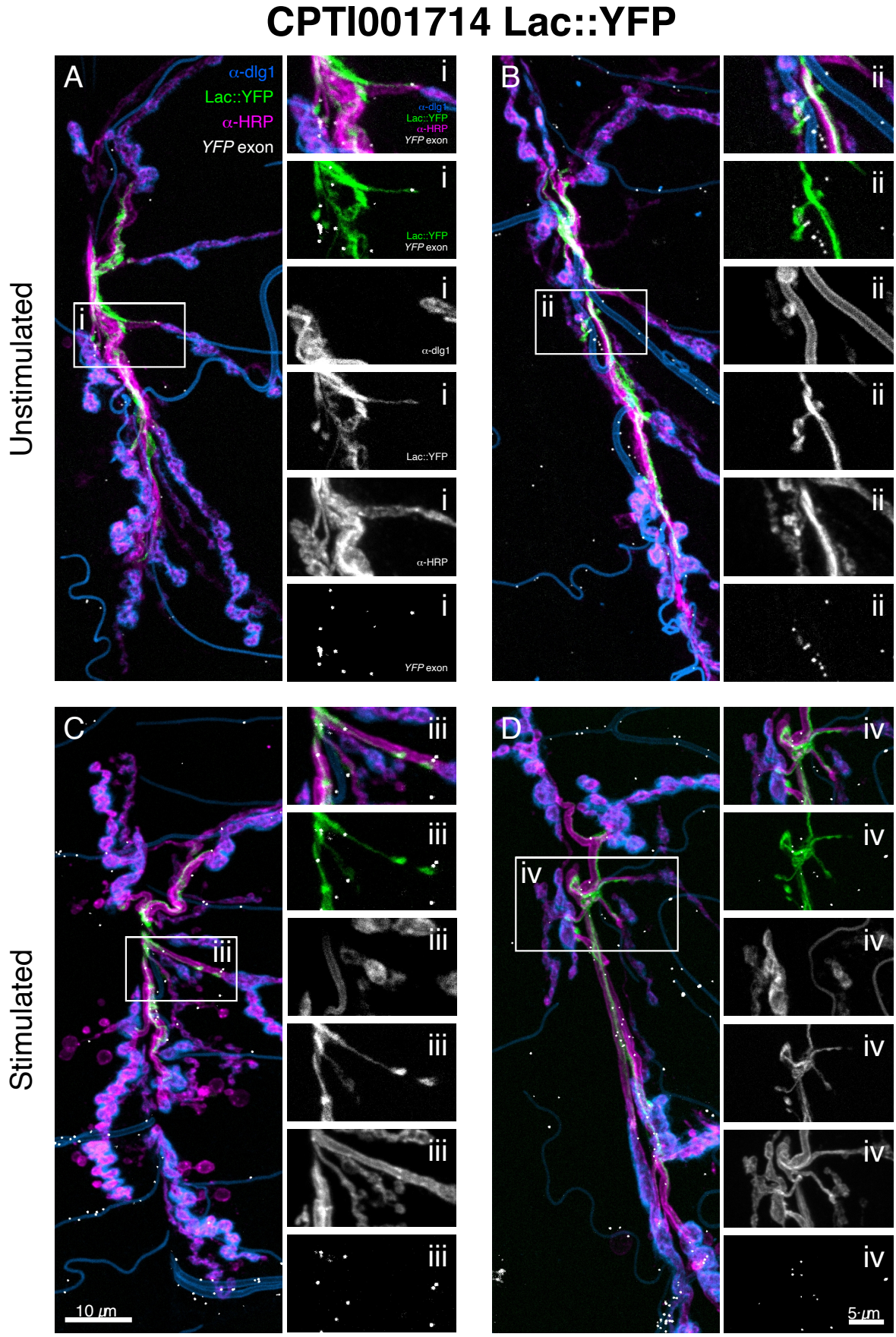

Figure 5-9 The dynamics of *Lac::YFP* mRNA and protein before and after stimulation

Previous page: A-D) Confocal images of CPTI Lac::YFP *Drosophila* 3rd instar larval NMJs, showing Lac::YFP signal in green, motor neuron axon terminal in magenta (α-HRP antibody conjugated to Alexa 568 fluor), the postsynaptic density in blue (α-dlg1 antibody, Alexa 405 fluor, trachea is auto-fluorescent in this channel) and *Lac::YFP* mRNA in white (α-*YFP* probe, Atto 633). Scale bar: 10 μm. i-iv) Zoomed in view of the respective ROI from A-D. See labels for details. Scale bar: 5 μm. A-B) Examples of unstimulated Lac::YFP NMJs showing fine Lac::YFP filaments with *Lac::YFP* mRNA localised to their periphery (i, ii). C-D) Examples of stimulated Lac::YFP NMJs showing Lac::YFP "projections" elongating along the motor neuron branches (iii) and interacting with "ghost boutons" (iv).

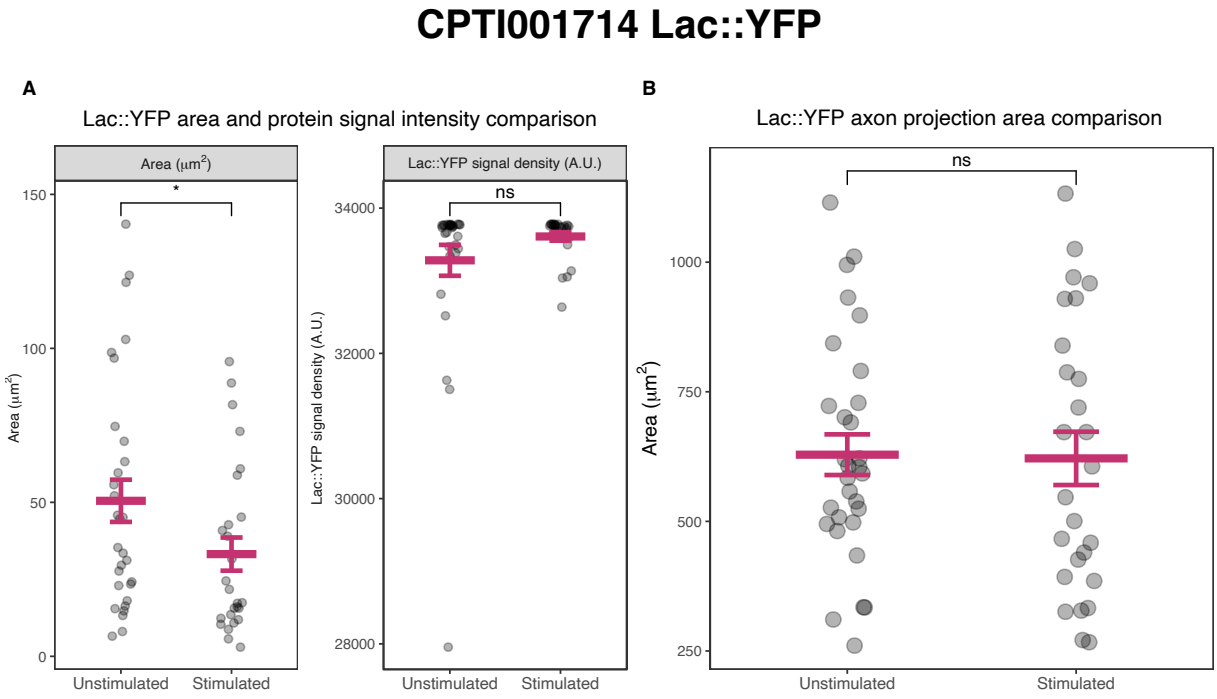

Figure 5-10 Only Lac::YFP area changes after stimulation

A). Comparison of Lac::YFP area and protein signal intensity. While the areas covered by Lac::YFP are lower ($p < 0.05$) after stimulation, the protein intensity signal is not significantly affected ($p = 0.498$). B). The area covered by the axon projection of the motor neuron is not significantly affected by the spaced potassium stimulation protocol on Lac::YFP larvae ($p = 0.913$). Wilcoxon rank sum test p-values are reported for both A and B.

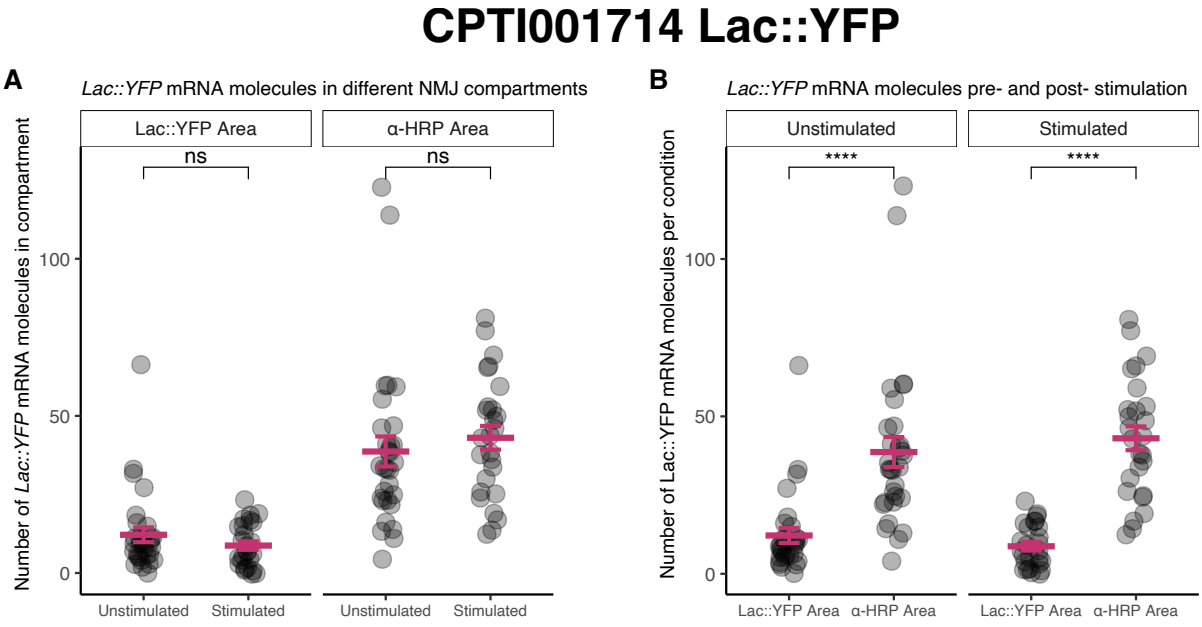

Figure 5-11 *Lac::YFP mRNA* molecules distribution does not change with stimulation

A). Quantification of mRNA molecules of *Lac::YFP* in the Lac::YFP and α-HRP areas pre- and post-spaced potassium. No significant differences were observed (Lac::YFP area p = 0.401, α-HRP p = 0.162). B). Quantification of mRNA molecules of *Lac::YFP* in the Lac::YFP and α-HRP areas shows a significant difference between the numbers of molecules both pre- ($p<0.0001$) and post-stimulation ($p<0.0001$). Wilcoxon rank sum test Bonferroni adjusted p-values are reported for both A and B.

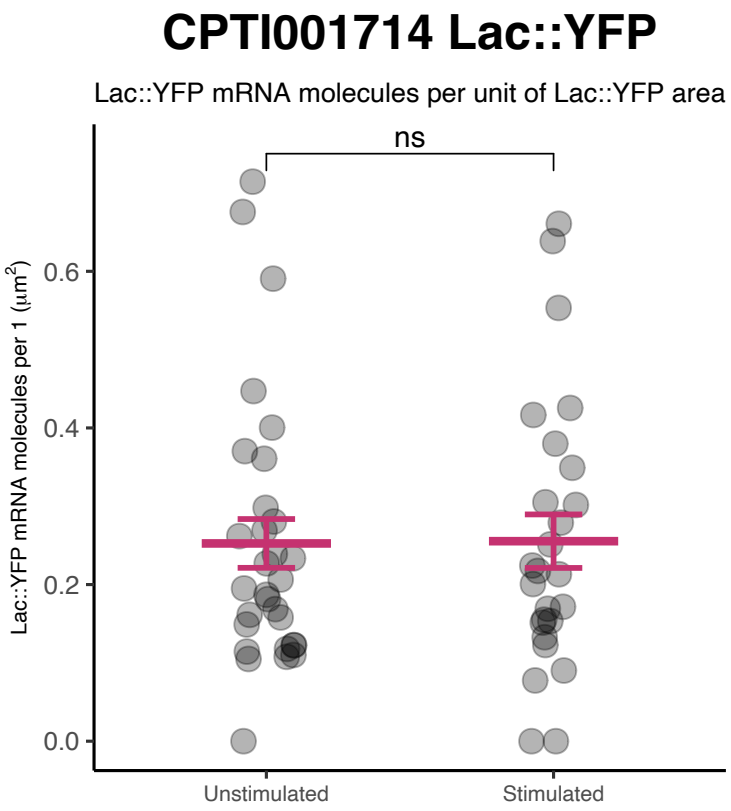

Figure 5-12 *Lac::YFP* mRNA molecules concentration does not change with stimulation

There is no significant difference when comparing the numbers of *Lac::YFP* mRNA molecules per µm^2 of Lac::YFP area, approximating "glial" area, for unstimulated and stimulated conditions (p = 0.85). Wilcoxon rank sum test p-value is reported.

I wanted to further explore the results obtained when quantifying the Lac::YFP area and observe whether the overall glial projection area at the NMJ also decreases after stimulation, without using Lac::YFP as proxy. I therefore performed a spaced potassium simulation assay on Repo>GFP line in control and *Lac*-RNAi knockdown conditions to compare what happens to glial projections before and after stimulation (Figure 5-13). Interestingly, in the control condition, axon terminal projection areas are unaffected and glial areas are decreased post-stimulation, much like for Lac::YFP (Figure 5-10), while for glial *Lac*-RNAi knockdown, neuronal areas are increased, and glial areas are unchanged after stimulation.

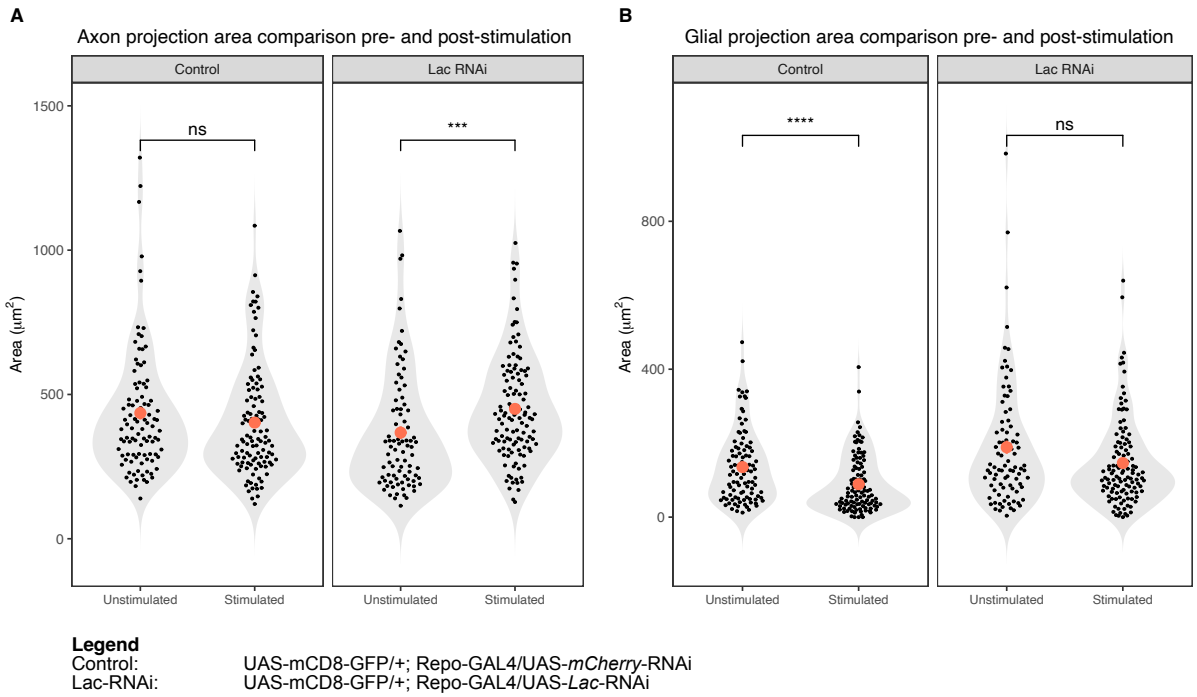

Figure 5-13 Neuronal and glial areas before and after spaced potassium stimulation

A) Quantification of axon projection areas pre- and post-stimulation. In control, there is no significant difference for the axon projection area (p = 0.227) before and after stimulation. For *Lac*-RNAi in glia using pan-glial driver Repo-GAL4, the neuronal areas are significantly increased after stimulation (p<0.001). B) Quantification of glial projection areas pre- and post-stimulation. Glial areas are significantly decreased post-stimulation in control condition (p<0.0001), and not affected in *Lac*-RNAi (p glia = 0.0716). Wilcoxon rank sum test Bonferroni adjusted p-values are reported for both A and B. See legend for genotype details.

5.4.5 *Lac* mRNA molecules associate with the BBB

I wanted to understand the relationship between *Lac* mRNA at the NMJ and the *Drosophila* BBB, specifically considering the importance of IgLONs at the mammalian BBB discussed in the introduction of this chapter. Several SJ proteins mark the location of the BBB in the *Drosophila* NMJ, including Atpα, Nrg, nrv2, NrxIV and Cora [210, 325]. Using a NrxIV::GFP trap kindly gifted by Professor Rita Teodoro's lab, I performed *Lac* smFISH to observe where *Lac* mRNA molecules are with respect to the BBB (Figure 5-14). I confirmed that many *Lac* mRNA molecules localise to

NrxIV::GFP area, further supporting that Lac may be a component of SJs. Interestingly, I observed individual *Lac* mRNA molecules localised to fine BBB "projections", as demarcated by NrxIV::GFP. Notably, several *Lac* mRNA molecules are situated at the BBB edge, where the NrxIV::GFP signal terminates, suggesting that they could be primed for translation potentially linked to ongoing BBB maintenance or function (Figure 5-14, C-K). This observation led me to the hypothesis that mRNA molecules encoding SJ proteins, some of which I also studied in Chapter 3, might play roles in the repair of SJs, their proliferation, or the overall maintenance of the BBB, especially during neural or glial remodelling.

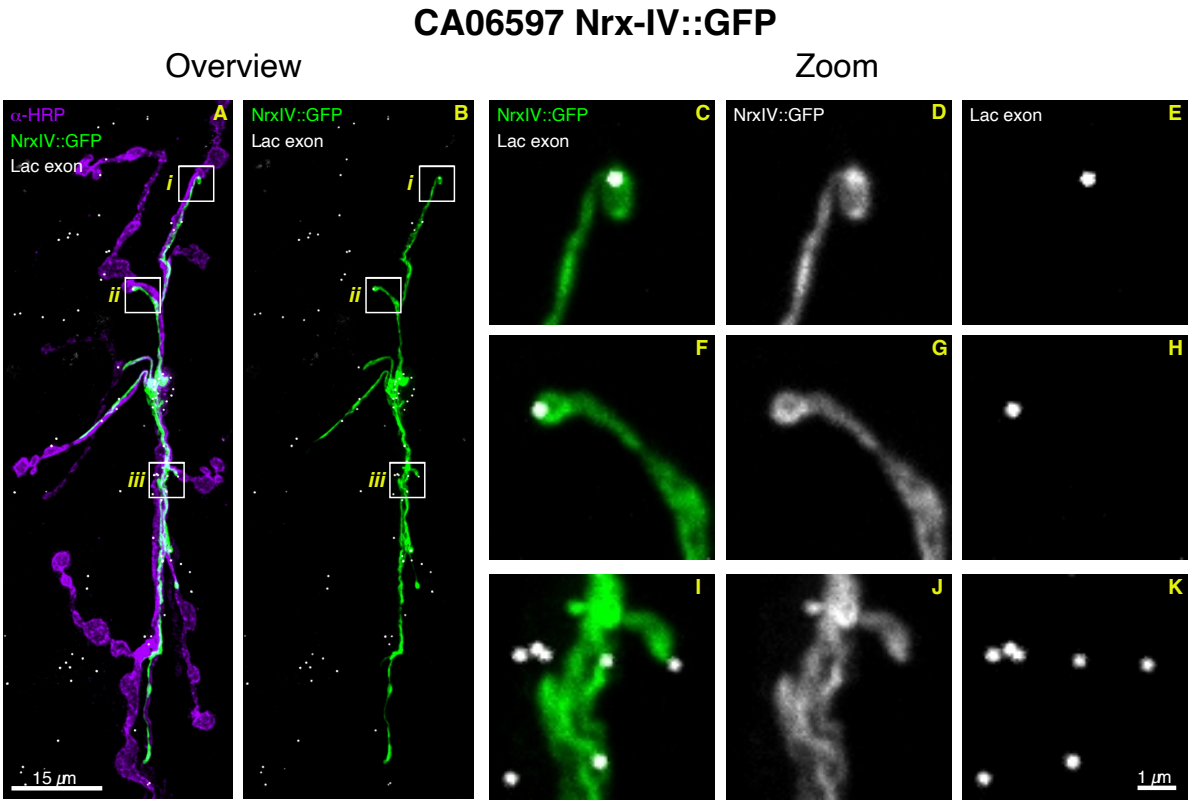

Figure 5-14 *Lac* mRNA overlaps with BBB and localises to its fine structures

A-B) Confocal image of the *Drosophila* 3rd instar larval NMJ, showing motor neuron axon terminal projections in purple (α-HRP antibody conjugated to Alexa 568, A only), NrxIV::GFP protein signal in green and *Lac* exon in white (α-*Lac* exon probe, Atto 633). Scale bar: 15 μm. C-E, F-H, I-K) A zoomed-in view (see label) of A i), ii) and iii), respectively, showing the *Lac* mRNA molecules association with fine distant regions of the BBB, marked by NrxIV::GFP. Scale bar: 1 μm.

I then aimed to determine the distribution pattern of *Lac* mRNA molecules within motor neuron axon terminal projections relative to the BBB. Given that the BBB labelling overlaps with that of the motor neuron axon terminal projections, I hypothesised that if *Lac* mRNA molecules were evenly distributed across both structures, the ratio of their distribution would mirror the ratio of the areas occupied by the BBB and the motor neuron axon terminal projection. However, the ratios of the numbers of *Lac* mRNA molecules present in the BBB to the numbers of *Lac* mRNA molecules in motor neuron axon terminal projection are significantly higher than the area ratios (Wilcoxon rank sum test, $p < 0.01$, Figure 5-15). This discrepancy led me to conclude that the area near the BBB is more densely populated with *Lac* mRNA molecules than the motor neuron axon terminal projection.

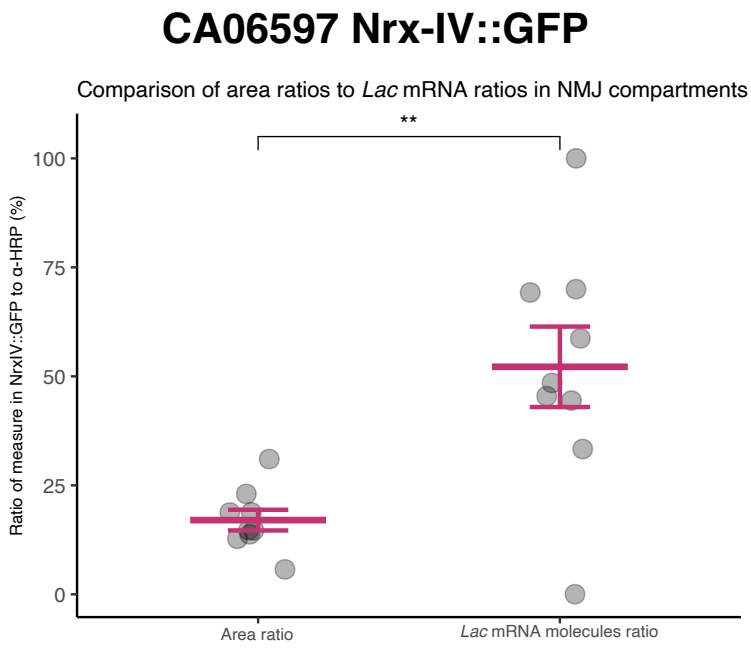

Figure 5-15 *Lac* mRNA molecules are associated with the BBB

Comparison of ratios of BBB (NrxIV::GFP) to motor neuron terminal (α-HRP) areas and numbers of *Lac* mRNA molecules in those areas. BBB to α-HRP area ratios are significantly lower ($p<0.01$) than *Lac* mRNA molecules in BBB area to *Lac* mRNA molecules in α-HRP area ratios. Thus, *Lac* mRNA molecules are preferentially associated with the BBB area within the α-HRP area. Wilcoxon rank sum test p-value reported.

5.4.6 Loss of glial projections at the NMJ following *Imp*-RNAi knockdown

I wanted to explore whether mRNA knockdown of RNA binding proteins which could be involved in *Lac* mRNA transport to the glial periphery at the NMJ affects the numbers of mRNA molecules of Lac in the NMJ glia. Previous results from an individual-nucleotide resolution CrossLinking and ImmunoPrecipitation (iCLIP) experiment conducted in our laboratory focused on the IGF-II mRNA-binding protein (Imp) and showed that Imp protein targets *Lac* (Jeffrey Y Lee, Davis lab, unpublished). Using RBPmap database, putative Imp binding sites across *Lac* transcripts were also predicted (Dominika Syska, Davis lab, unpublished) (Figure 5-16).

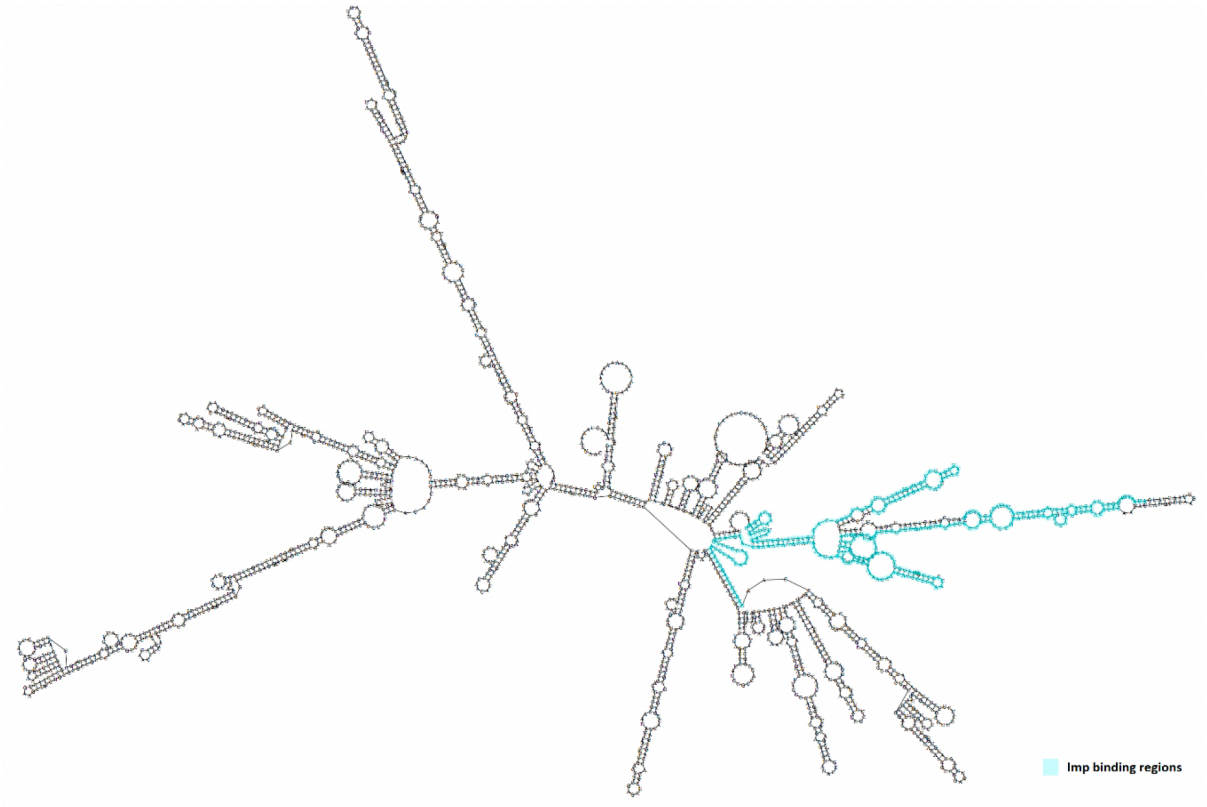

Figure 5-16 Imp binds *Lac* mRNA

Imp binding sites (cyan) determined by the Imp iCLIP experiment (Jeffrey Y Lee, Davis lab, unpublished). Visuals generated by Dominika Syska, Davis lab.

Imp, or IGF-II mRNA-binding protein, can affect the stability, transport and translation of its target transcripts, and it is known to affect axonal transport and remodelling, as well as synaptogenesis, in the developing nervous system [326-328]. Therefore, based on the previous results and its known importance in the nervous system, I set out to investigate the consequences of *Imp*-RNAi knockdown in glial cells using the Repo-GAL4 pan-glial driver on the numbers of *Lac* mRNA molecules in the NMJ glial projections.

Upon *Imp*-RNAi knockdown, I observed that no glial projections were extending to the NMJ area (Figure 5-17). The larvae used for this experiment were selected based on the GFP fluorescence of their brains, as both control (*mCherry*-RNAi) and *Imp*-RNAi were being driven by Repo>GFP line. Therefore, glial cells could not be completely ablated, but did not make projections to the NMJ. I thus could not quantify the impact of *Imp*-RNAi knockdown on the number of *Lac* mRNA molecules in NMJ glia. This observation alone is a notable phenotype, to my knowledge previously unreported in literature.

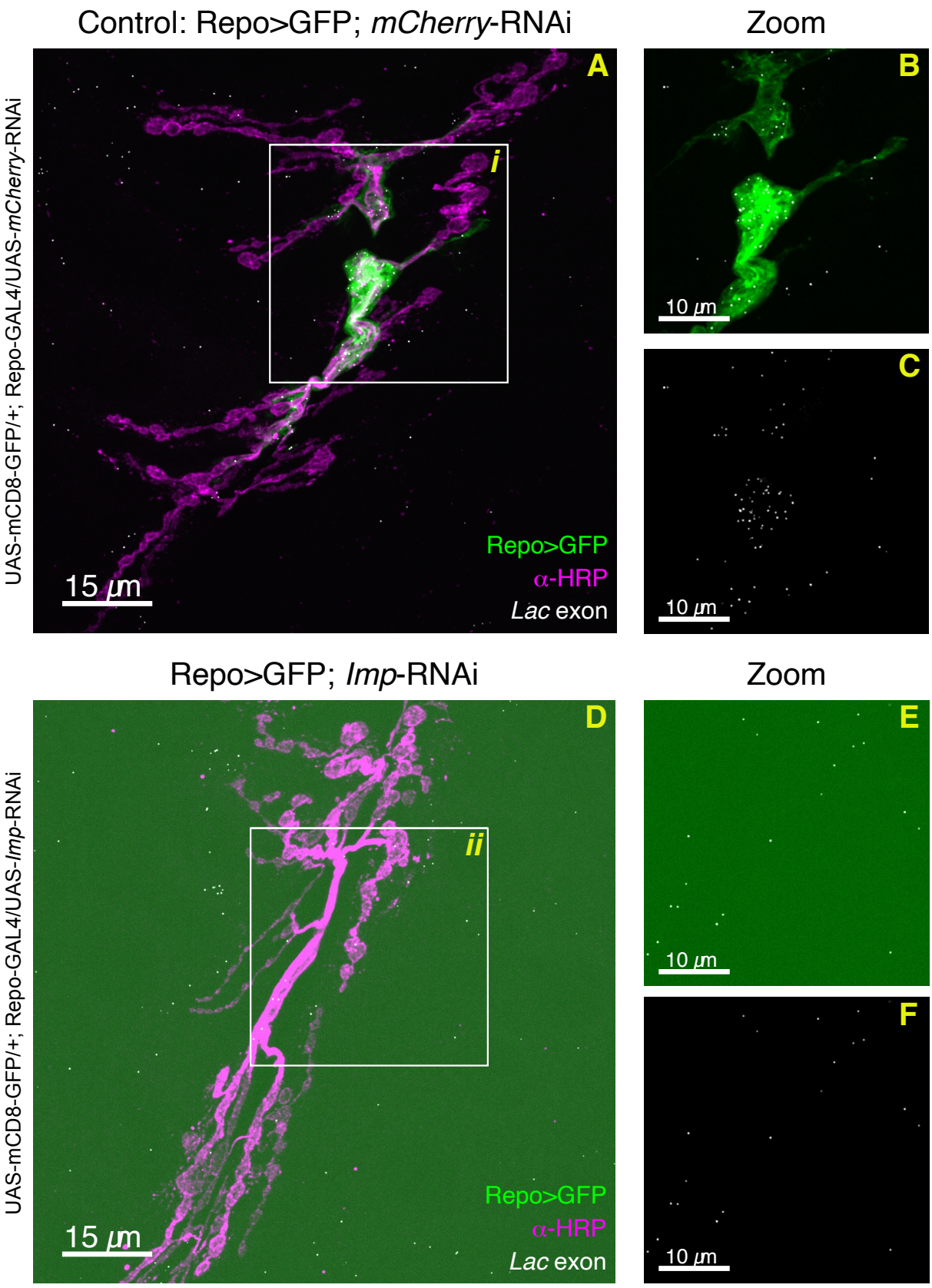

Figure 5-17 *Imp*-RNAi knockdown in glia causes loss of NMJ glial projections

Previous page: A) Confocal image of the *Drosophila* 3rd instar larval NMJ from the control condition, showing motor neuron axon terminal projections in magenta (α-HRP antibody conjugated to Alexa-568), glial projections labelled with Repo>GFP line, and *Lac* exon in white (α-*Lac* exon probe, Atto 633). Scale bar: 15 μm. B-C) A zoomed-in view (see label) of A i), showing the *Lac* mRNA molecules in glia (B), and a single-channel view of *Lac* mRNA molecules (C). Scale bar: 10 μm. D) Confocal image of the Imp-RNAi knockdown *Drosophila* 3rd instar larval NMJ, showing motor neuron axon terminal projections in magenta (α-HRP antibody conjugated to Alexa 568), lack of glial projections labelled with Repo>GFP line, and *Lac* exon in white (Atto 633). Scale bar: 15 μm. E-F) A zoomed-in view (see label) of D ii), showing the *Lac* mRNA molecules against the empty glial channel (E), and a single-channel view of *Lac* mRNA molecules (F). Scale bar: 10 μm.

5.4.7 Quantifying the impact of *Lac*-RNAi knockdown in specific glial cell subtypes

I next set out to explore the effects of the RNAi knockdown of *Lac* in specific glial cell subtypes. Since the pan-glial promoter Repo drives expression in all larval glia, I wanted to explore specifically which glial subtype projections make it to the NMJ, and whether *Lac* mRNA was preferentially localised to one of the subtypes. Although some literature exists on the topic, conflicting reports are made about the specific subtypes and drivers to use. Specifically, most publications suggest that PG and SPG projections are the ones which are present at the NMJ, however, some publications also mention that WG extend their projections to the NMJs [111, 114, 118, 119, 126, 329, 330].

I therefore used known drivers targeting all three cell types. These were: 46F-GAL4, kindly gifted by Prof. Stefanie Schirmeier's laboratory, driving expression in PG [187, 331], Mdr65-GAL4, kindly gifted by Prof. Rita Teodoro's laboratory (available for purchase from BSDC, ID 50472), driving expression in SPG and Nrv2-GAL4, driving expression in WG (BDSC, ID 6800), already recombined with membrane targeted GFP. I crossed PG and SPG lines to the same UAS-mDC8-GFP line previously used

to visualise the glial membrane. I subsequently refer to the lines as 46F>GFP, Mdr65>GFP, Nrv2>GFP, respectively.

I imaged control and *Lac*-RNAi knockdown NMJs crossed to all drivers, including Repo-GAL4 as positive control (Figure 5-18). I aimed both to verify which glial cell types make the NMJ projections, but, additionally, to observe any potential impact of *Lac*-RNAi knockdown on their morphology. I observed that PG (Figure 5-19) and SPG (Figure 5-20) created extensive projections at the NMJs, while WG made minimal or no projections at the NMJs (Figure 5-21). The hypermorphic NMJ phenotype previously observed for *Lac*-RNAi knockdown using Repo-GAL4 was not observed for Nrv2-GAL4 (Figure 5-21) or 46F-GAL4 (Figure 5-19), but was observed for Mdr65-GAL4 (Figure 5-20), albeit to a much lesser extent when compared to Repo-GAL4 (Figure 5-18).

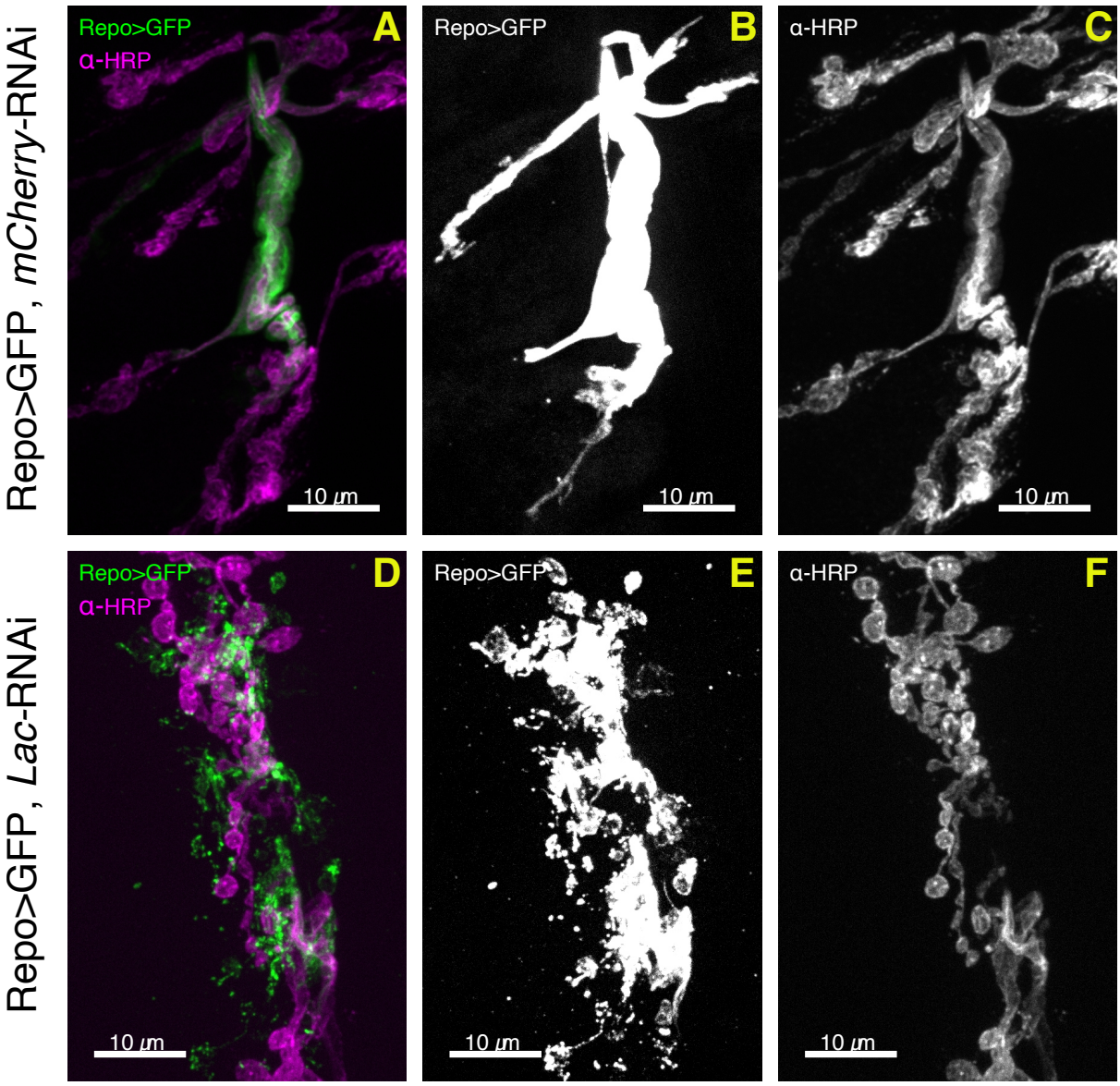

Figure 5-18 Hypermorphic glial projections in Repo-GAL4 driven *Lac*-RNAi knockdown

A) Confocal image of the *Drosophila* 3rd instar larval NMJ from the control condition for Repo-GAL4, showing motor neuron axon terminal projections in magenta (α-HRP antibody conjugated to Alexa-568) and glial projections labelled with Repo>GFP. Scale bar: 10 μm. B-C) A single-channel view (see label) of A. D) Confocal image of the *Lac*-RNAi knockdown *Drosophila* 3rd instar NMJ, showing motor neuron axon terminal projections in magenta (α-HRP antibody conjugated to Alexa-568) and hypermorphic, altered glial projections labelled with Repo>GFP. Scale bar: 10 μm. E-F) A zoomed-in view (see label) of D. Scale bar: 10 μm. See legend for genotype details.

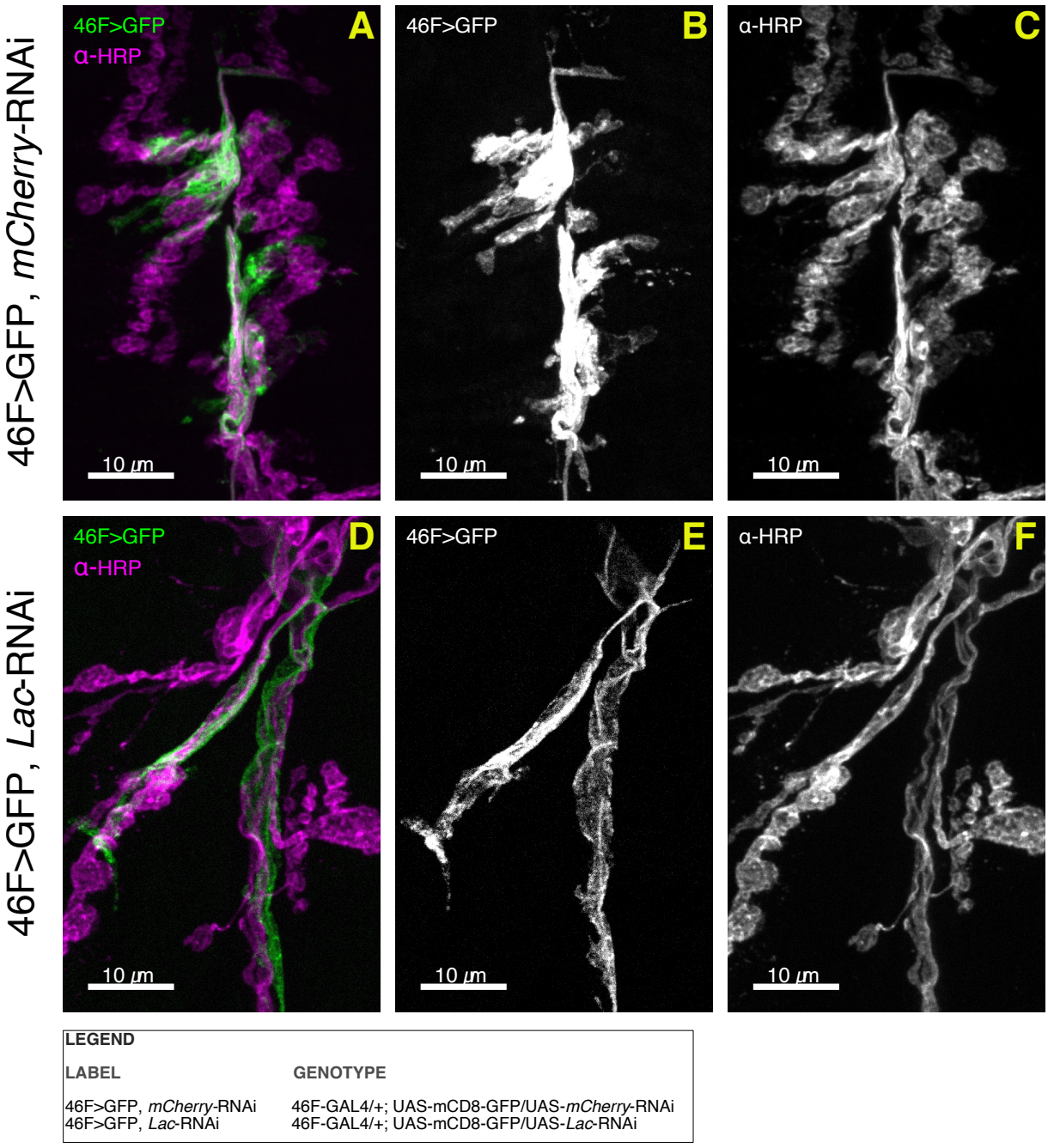

Figure 5-19 Glial projections in 46F-GAL4 driven *Lac*-RNAi knockdown

A) Confocal image of the *Drosophila* 3rd instar larval NMJ from the control condition for PG, showing motor neuron axon terminal projections in magenta (α-HRP antibody conjugated to Alexa 568) and glial projections labelled with 46F>GFP. Scale bar: 10 μm. B-C) A single-channel view (see label) of A. D) Confocal image of the *Lac*-RNAi knockdown *Drosophila* 3rd instar NMJ in PG using 46F>GFP line, showing motor neuron axon terminal projections in magenta (α-HRP antibody conjugated to Alexa-568) and glial projections labelled with 46F>GFP. Scale bar: 10 μm. E-F) A single-channel view (see label) of D. Scale bar: 10 μm. See legend for genotype details.

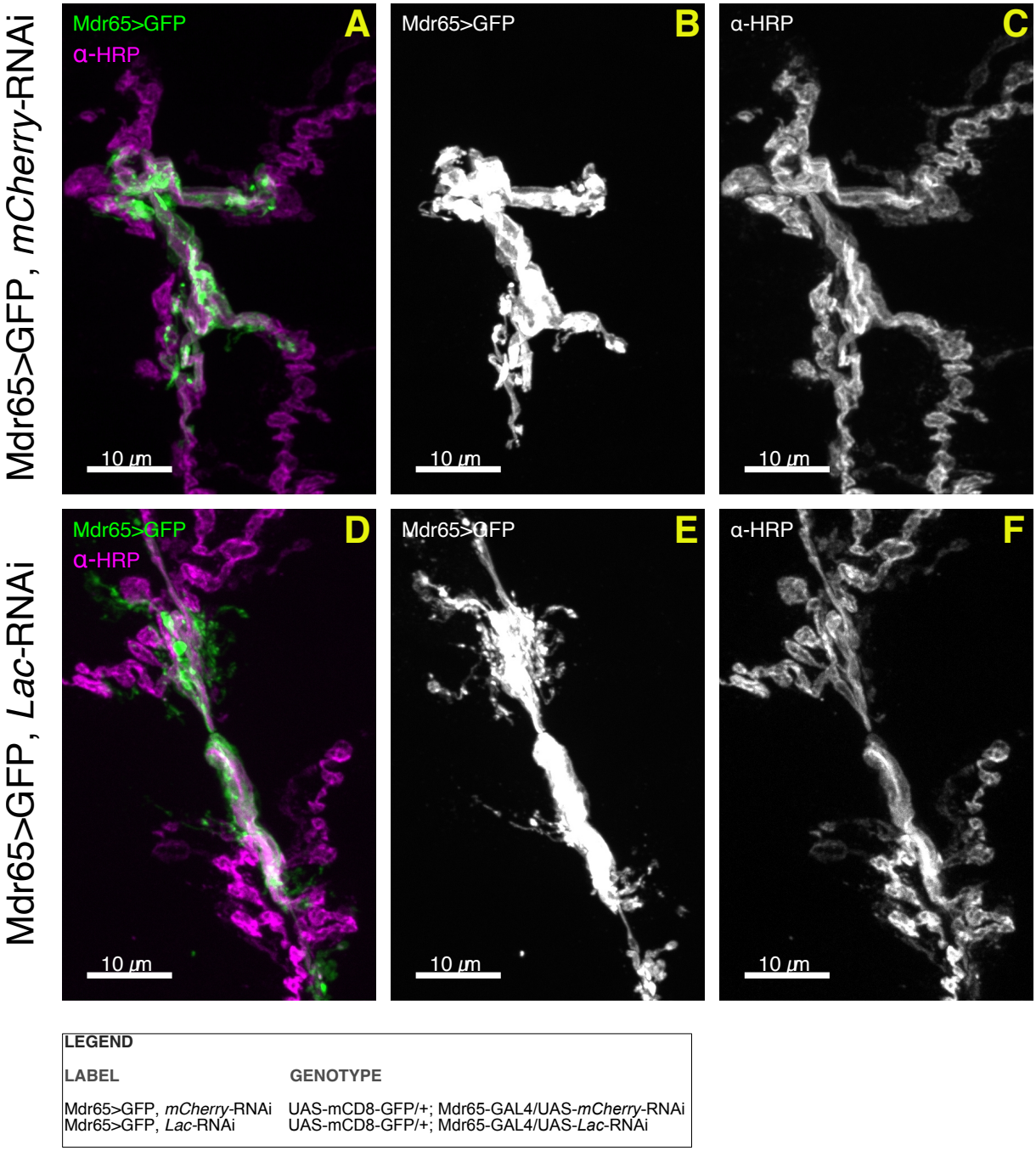

Figure 5-20 Glial projections in Mdr65-GAL4 driven *Lac*-RNAi knockdown

A) Confocal image of the *Drosophila* 3rd instar larval NMJ from the control condition for SPG, showing motor neuron axon terminal projections in magenta (α-HRP antibody conjugated to Alexa-568) and glial projections labelled with Mdr65>GFP. Scale bar: 10 μm. B-C) A single-channel view (see label) of A. D) Confocal image of the *Lac*-RNAi knockdown *Drosophila* 3rd instar NMJ in SPG using Mdr65>GFP line, showing motor neuron axon terminal projections in magenta (α-HRP antibody conjugated to Alexa-568) and glial processess, which have some unusual projections, labelled with Mdr65>GFP line. Scale bar: 10 μm. E-F) A single-channel view (see label) of D. Scale bar: 10 μm. See legend for genotype details.

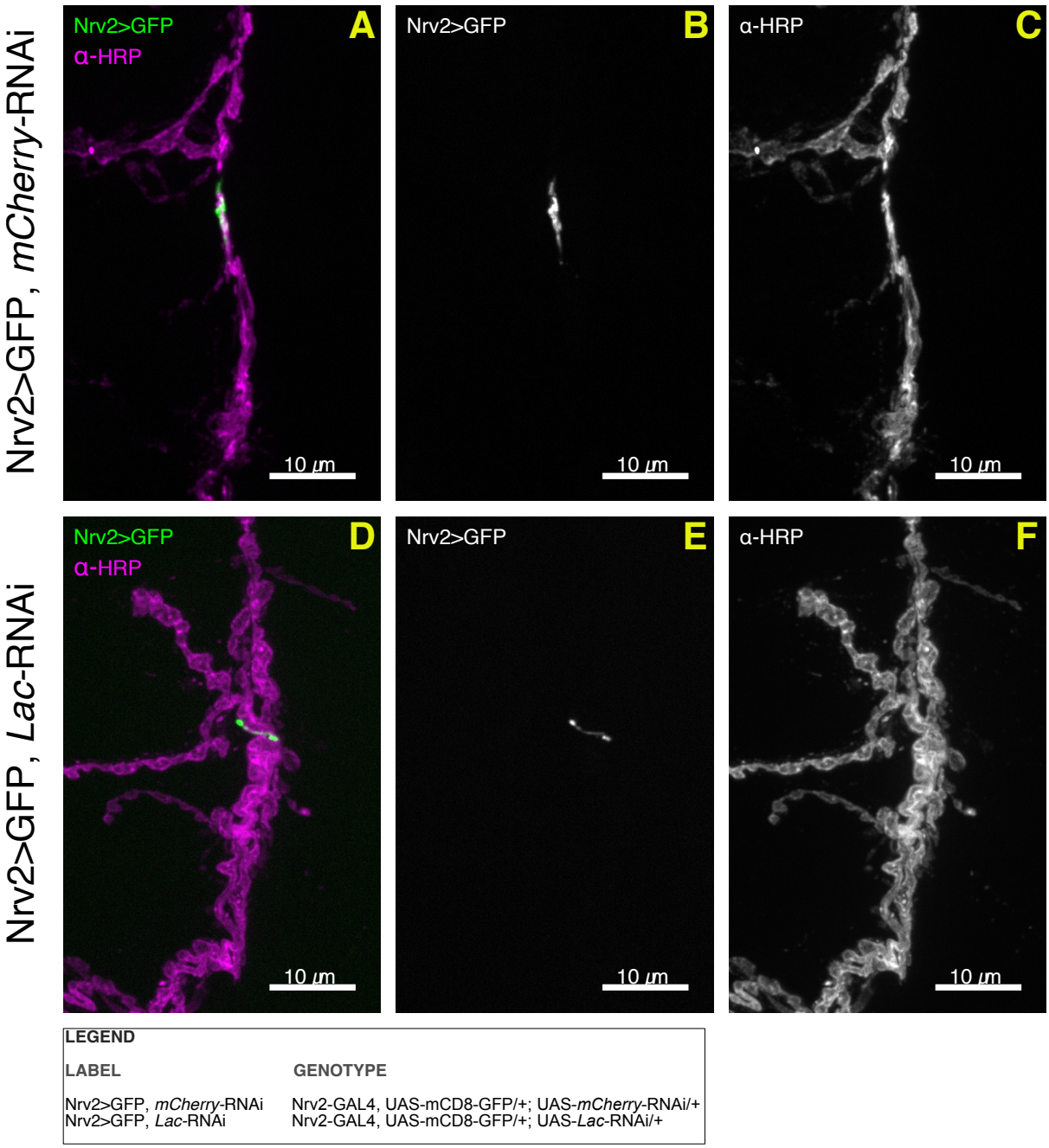

Figure 5-21 Glial projections in Nrv2-GAL4 driven *Lac*-RNAi knockdown

A) Confocal image of the *Drosophila* 3rd instar larval NMJ from the control condition for WG, showing motor neuron axon terminal projections in magenta (α-HRP antibody conjugated to Alexa-568) and glial projections labelled with Nrv2>GFP. Scale bar: 10 μm. B-C) A single-channel view (see label) of A. D) Confocal image of the *Lac*-RNAi knockdown *Drosophila* 3rd instar NMJ in WG using Nrv2>GFP line, showing motor neuron axon terminal projections in magenta (α-HRP antibody conjugated to Alexa-568) and glial projections labelled with Nrv2>GFP. Scale bar: 10 μm. E-F) A single-channel view (see label) of D. Scale bar: 10 μm. See legend for genotype details.

After confirming the presence of projections from all three glial cell subtypes at the NMJ, I performed the larval locomotion analysis assay accompanied by NMJ morphometrics quantification with all three drivers. The aim of this experiment was to answer the question: which specific glial cell subtype plays the most significant role in the previously observed *Lac*-RNAi knockdown phenotype associated with the pan-glial driver, Repo-GAL4? For each driver, I included Repo-GAL4 as a positive control and quantified glial and motor neuron axon terminal projection areas and their ratios. Additionally, I tested locomotor activity of the larvae by quantifying crawling speed, movement linearity, path straightness and movement irregularity, as defined in Section 2.8.3.

I observed virtually no differences in larval crawling and NMJ morphometrics for *Lac*-RNAi knockdown using the 46F>GFP line when compared to its control (Figure 5-22 – 25). Comparing Nrv2>*Lac*-RNAi to Nrv2>Control (Figure 5-26), I observed that 3 parameters were significantly affected: motor neuron axon terminal projection areas ($p < 0.0001$) (Figure 5-27), movement linearity ($p < 0.01$) (Figure 5-29 B) and movement irregularity ($p < 0.01$) (Figure 5-29 D). The neuronal and glial area ratios were not affected (Figure 5-28). Finally, when knocking down *Lac* with Mdr65>GFP line (Figure 5-30), all crawling parameters were significantly affected (Figure 5-33 A-D) (crawling speed: $p < 0.0001$, movement linearity: $p < 0.0001$, path straightness: $p < 0.05$, movement irregularity: $p < 0.0001$). Interestingly, despite observing a slight manifestation of the hypermorphic glial projection phenotype using microscopy (Figure 5-20 E), this did not correlate with quantitative differences (Figure 5-31, Figure 5-32).

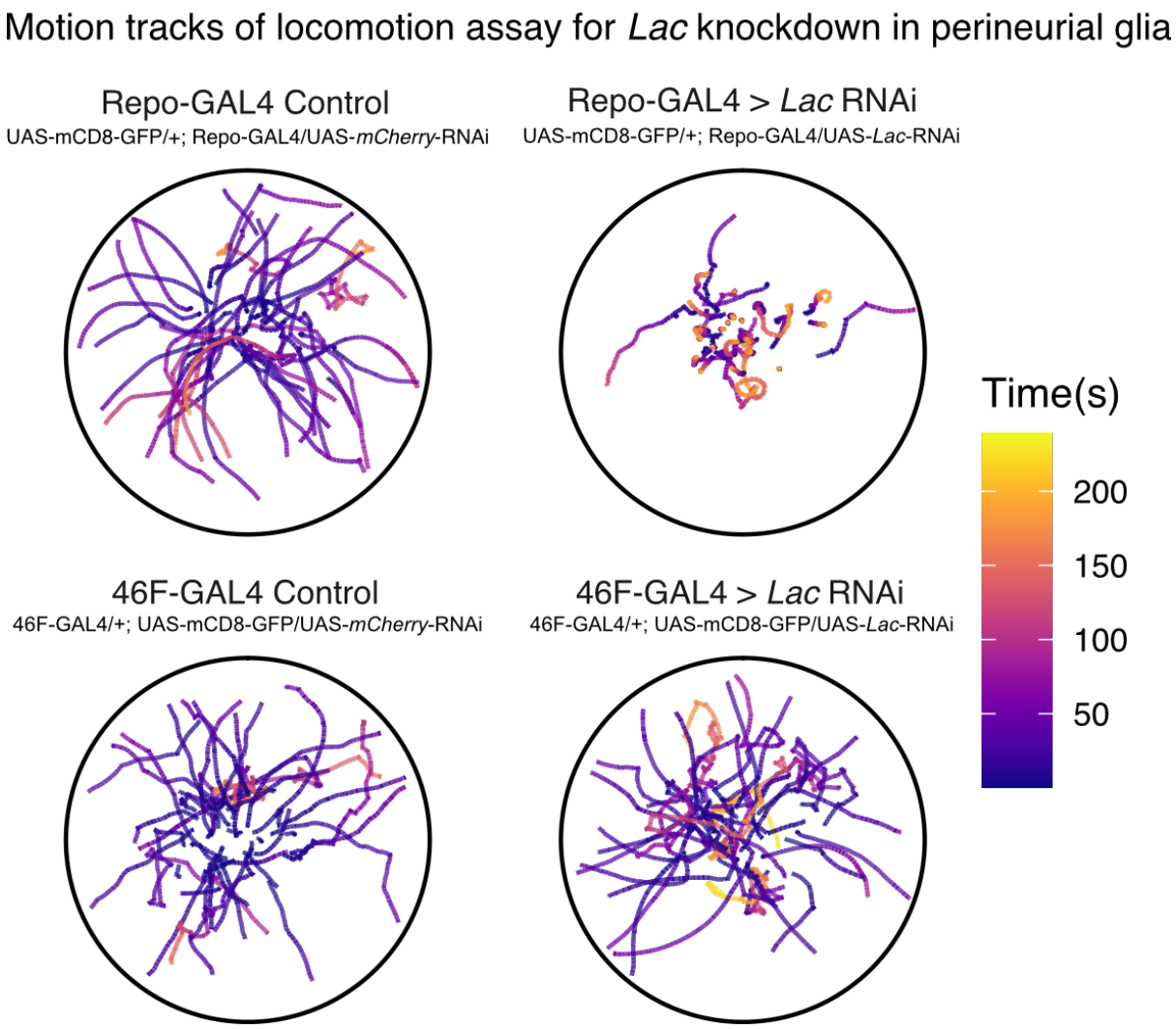

Figure 5-22 Motion tracks of locomotion assay for *Lac* knockdown in perineurial glia

Color-coded trajectories representing the motion of free crawling 3rd instar larvae of different genotypes (see labels above) over time (n = 44 (Repo-GAL4 Control), 42 (Repo-GAL4 > *Lac*-RNAi), 44 (46F-GAL4 Control), 43 (46F-GAL4 > *Lac*-RNAi)).

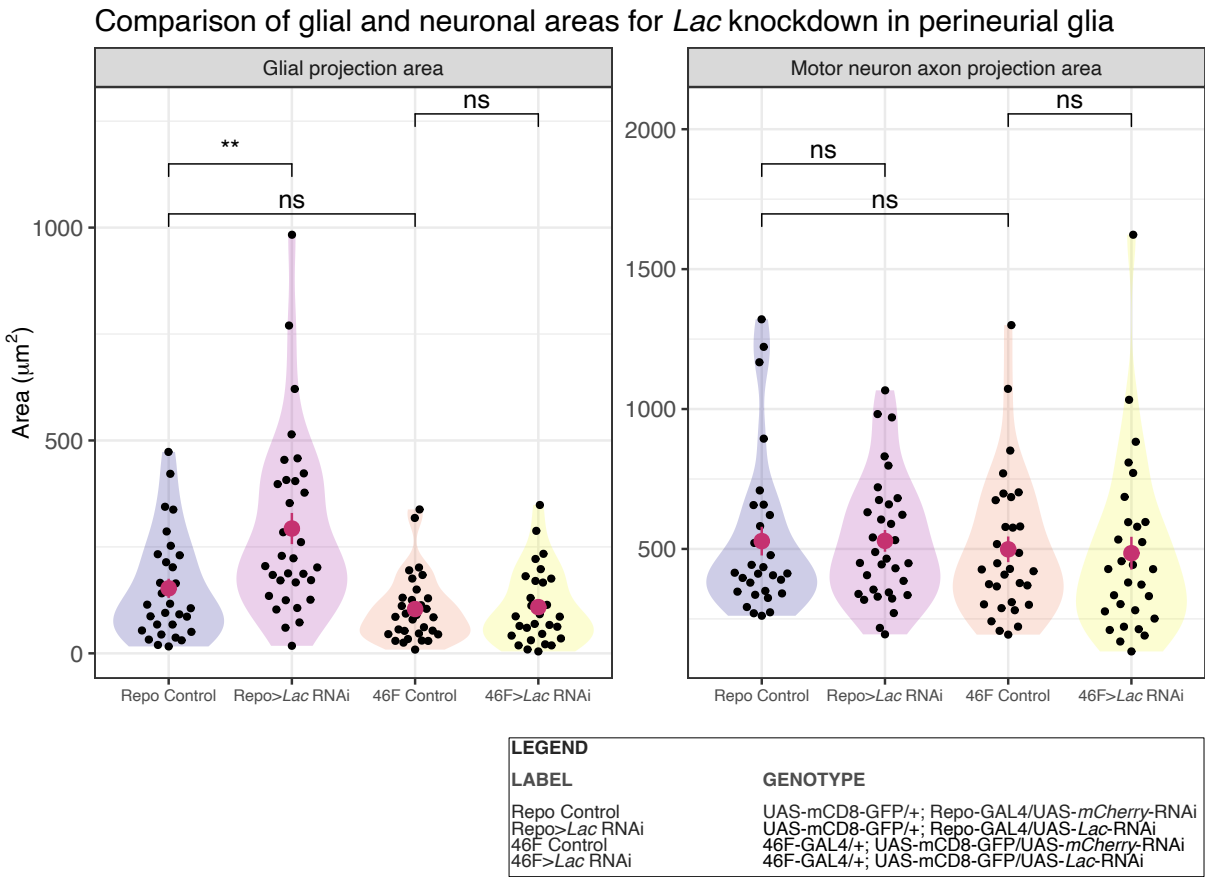

Figure 5-23 Comparison of glial and neuronal areas for *Lac* knockdown in perineurial glia

Comparison of glial (left) and neuronal (right) projection areas between all glia and PG in control and *Lac*-RNAi conditions (n = 30 (Repo Control), 33 (Repo>*Lac*-RNAi), 31 (46F Control), 29 (46F>*Lac*-RNAi)). Significance levels are denoted as follows: **p < 0.01; ****p < 0.0001. Dunnett's Test (Holm Adjusted) p-values are reported for all panels. See legend for genotype details.

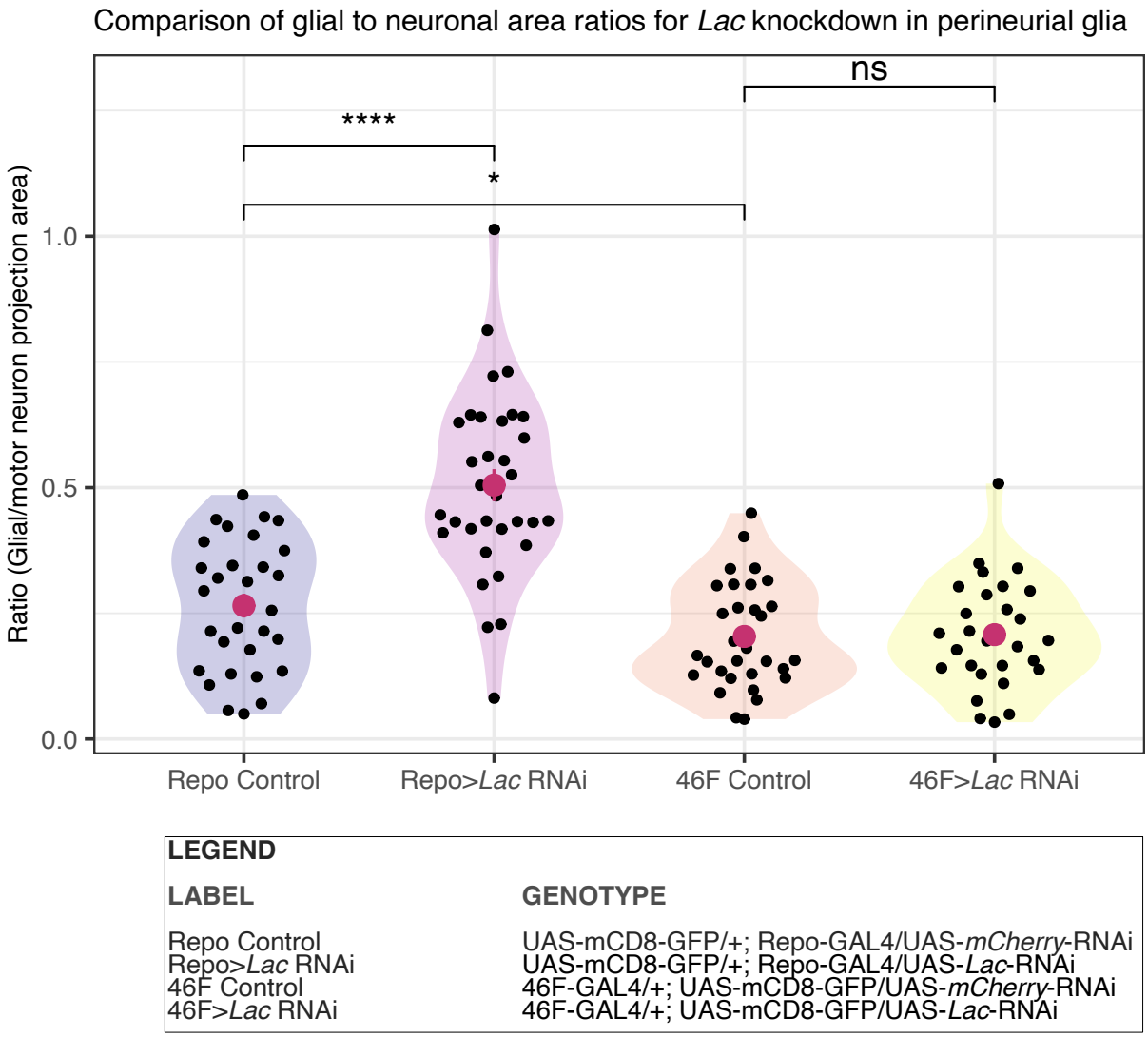

Figure 5-24 Comparison of glial to neuronal area ratios for *Lac* knockdown in perineurial glia

Comparison of glial (left) and neuronal (right) area ratios between all glia and PG in control and *Lac*-RNAi conditions (n = 30 (Repo Control), 33 (Repo>*Lac*-RNAi), 31 (46F Control), 29 (46F>*Lac*-RNAi)). Significance levels are denoted as follows: **p < 0.01; ****p < 0.0001. Dunnett's Test (Holm Adjusted) p-values are reported. See legend for genotype details.

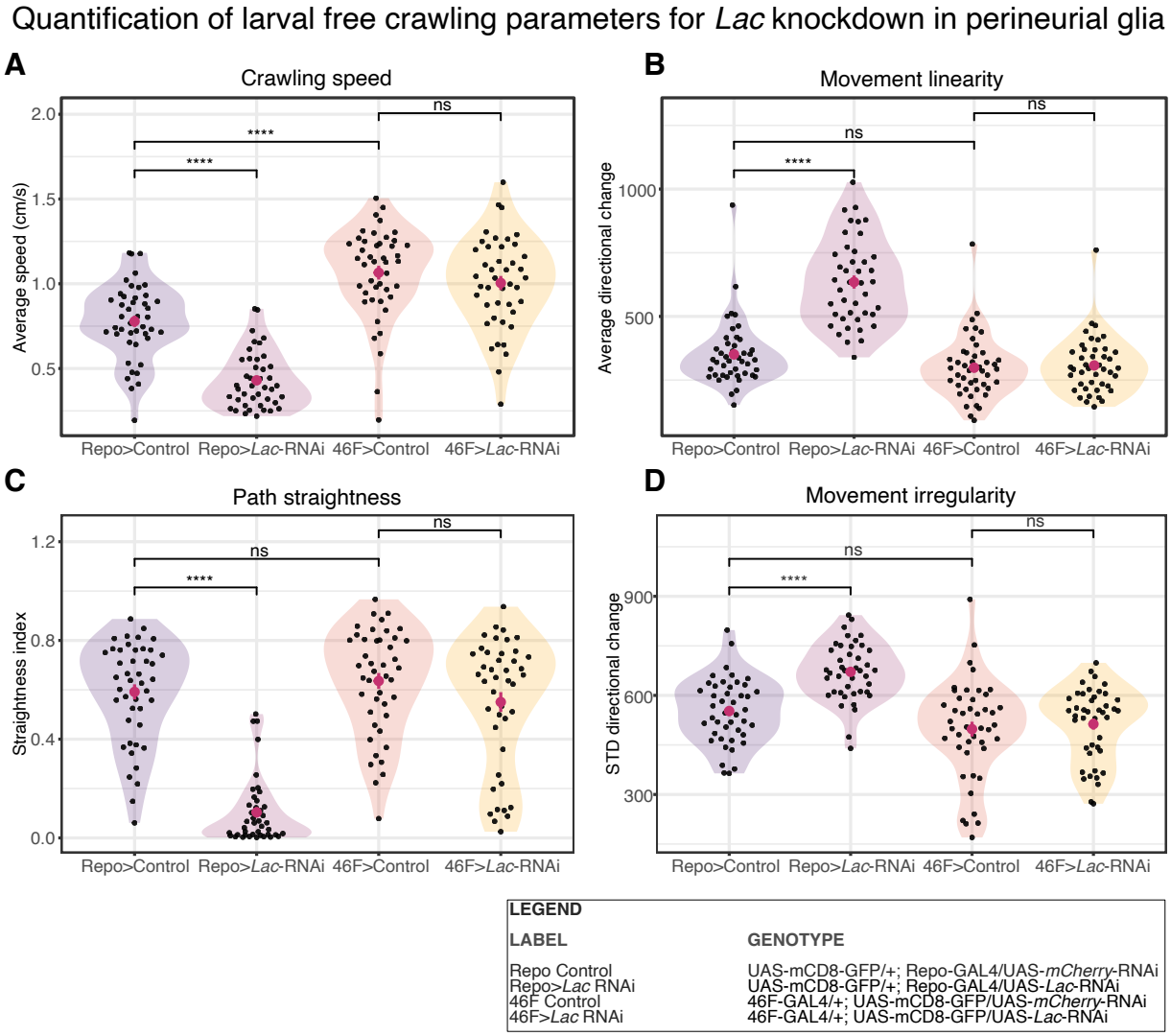

Figure 5-25 Quantification of larval free crawling parameters for *Lac* RNAi in perineurial glia

Larval free-crawling parameters quantification (see Materials and Methods Section 2.8.3) (n = 44 (Repo-GAL4 Control), 42 (Repo-GAL4 > *Lac*-RNAi), 44 (46F-GAL4 Control), 43 (46F-GAL4 > *Lac*-RNAi)). Significance levels are denoted as follows: **p < 0.01; ****p < 0.0001. Dunnett's Test (Holm Adjusted) p-values are reported for all panels. See legend for genotype details.

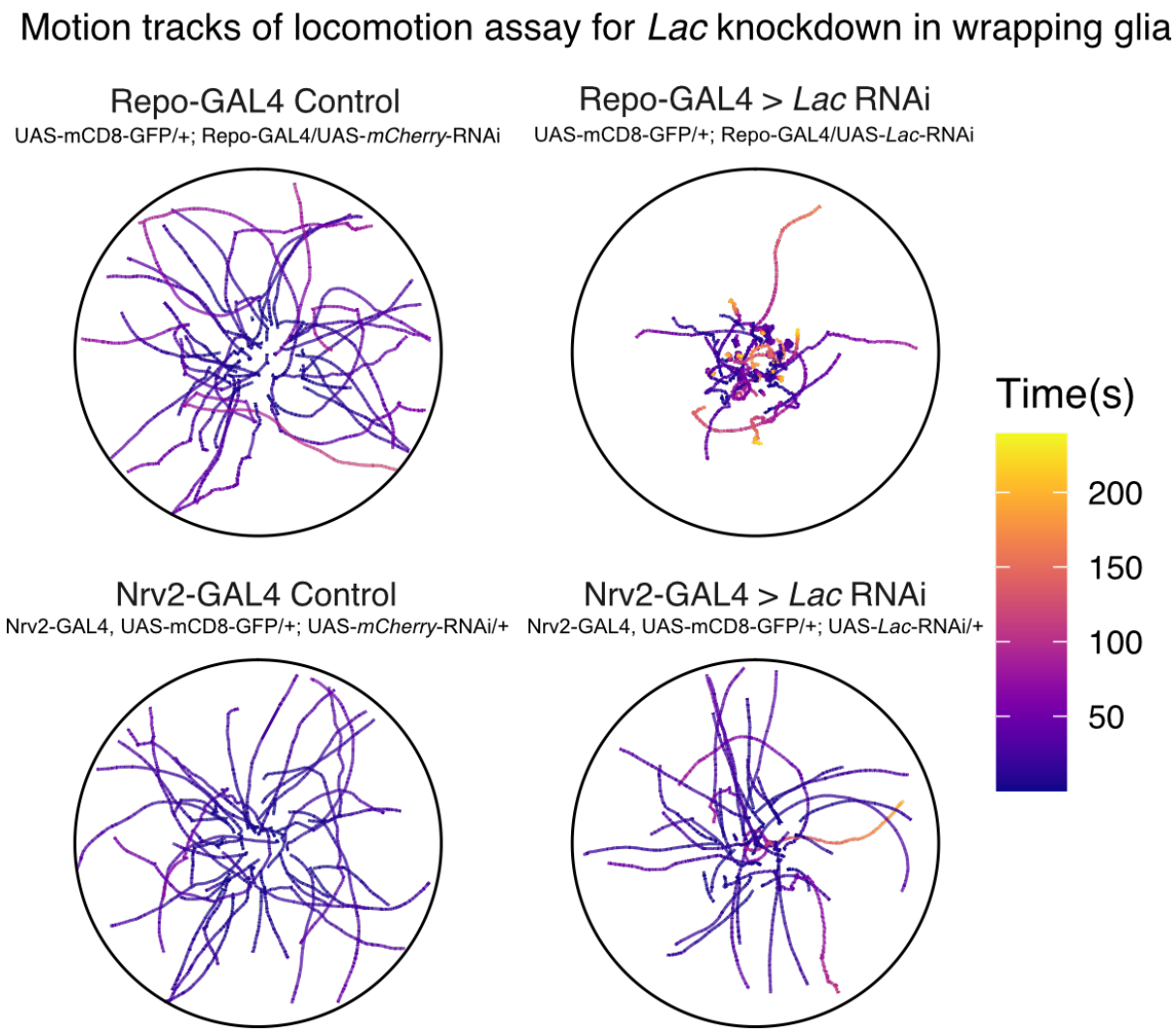

Figure 5-26 Motion tracks of locomotion assay for *Lac* knockdown in wrapping glia

Color-coded trajectories representing the motion of free crawling 3rd instar larvae of different genotypes (see labels above) over time (n = 45 (Repo Control), 44 (Repo>*Lac*-RNAi), 44 (Nrv2 Control), 40 (Nrv2>*Lac*-RNAi)).

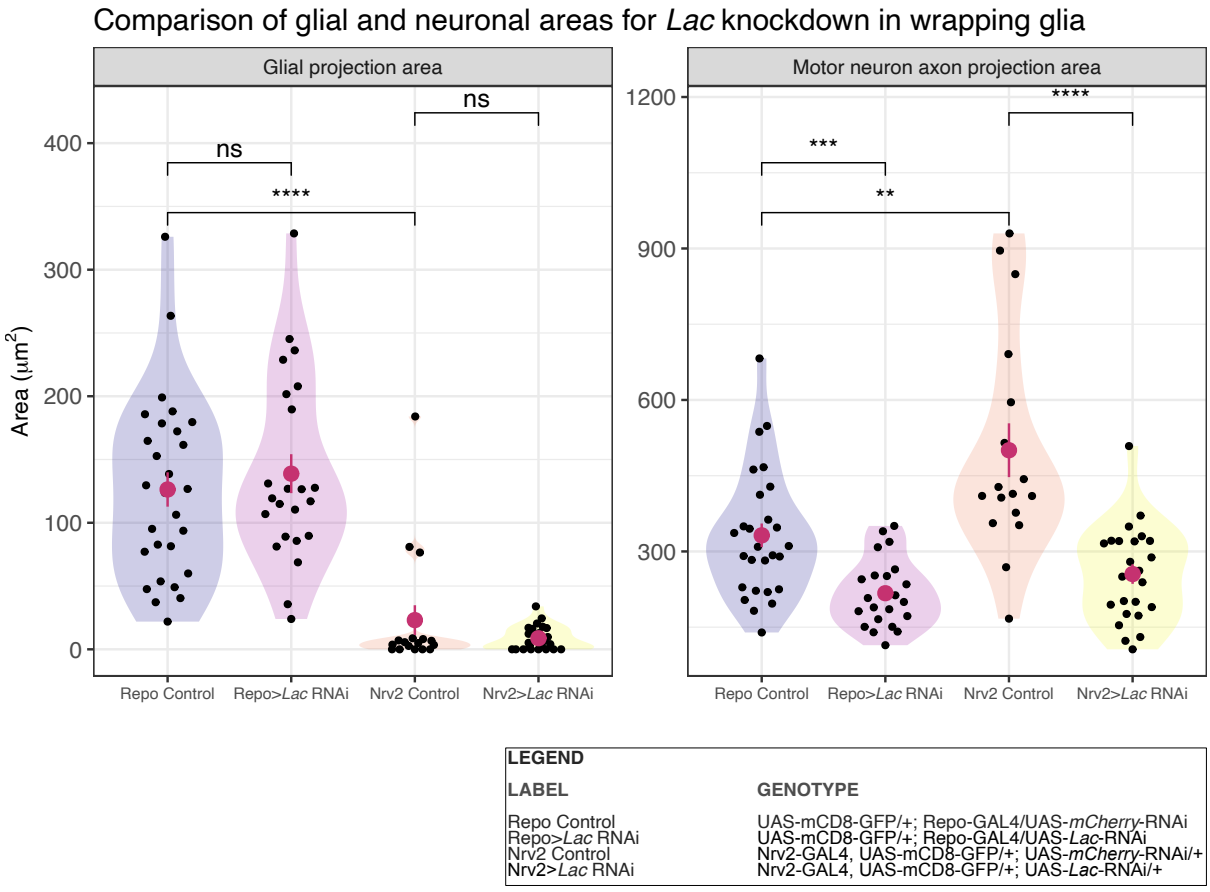

Figure 5-27 Comparison of glial and neuronal areas for *Lac* knockdown in wrapping glia

Comparison of glial (left) and neuronal (right) projection areas between all glia and WG in control and Lac-RNAi conditions (n = 28 (Repo Control), 23 (Repo>Lac-RNAi), 17 (Nrv2 Control), 24 (Nrv2>Lac-RNAi)). Significance levels are denoted as follows: **p < 0.01; ****p < 0.0001. Dunnett's Test (Holm Adjusted) p-values are reported for all panels. See legend for genotype details.

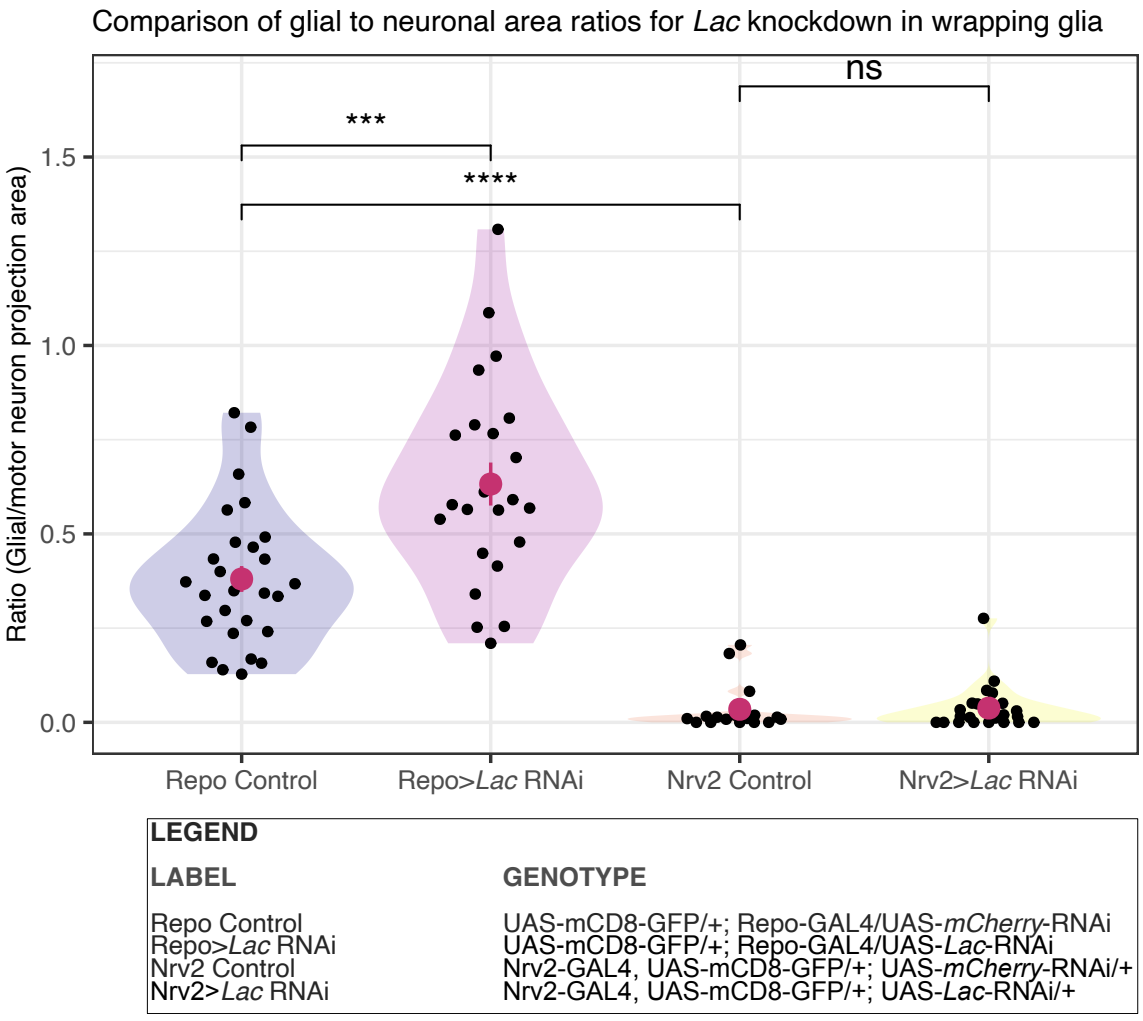

Figure 5-28 Comparison of glial to neuronal area ratios for *Lac* knockdown in wrapping glia

Comparison of glial (left) and neuronal (right) area ratios between all glia and WG in control and *Lac*-RNAi conditions (n = 28 (Repo Control), 23 (Repo>*Lac*-RNAi), 17 (Nrv2 Control), 24 (Nrv2>*Lac*-RNAi)). Significance levels are denoted as follows: **p < 0.01; ****p < 0.0001. Dunnett's Test (Holm Adjusted) p-values are reported. See legend for genotype details.

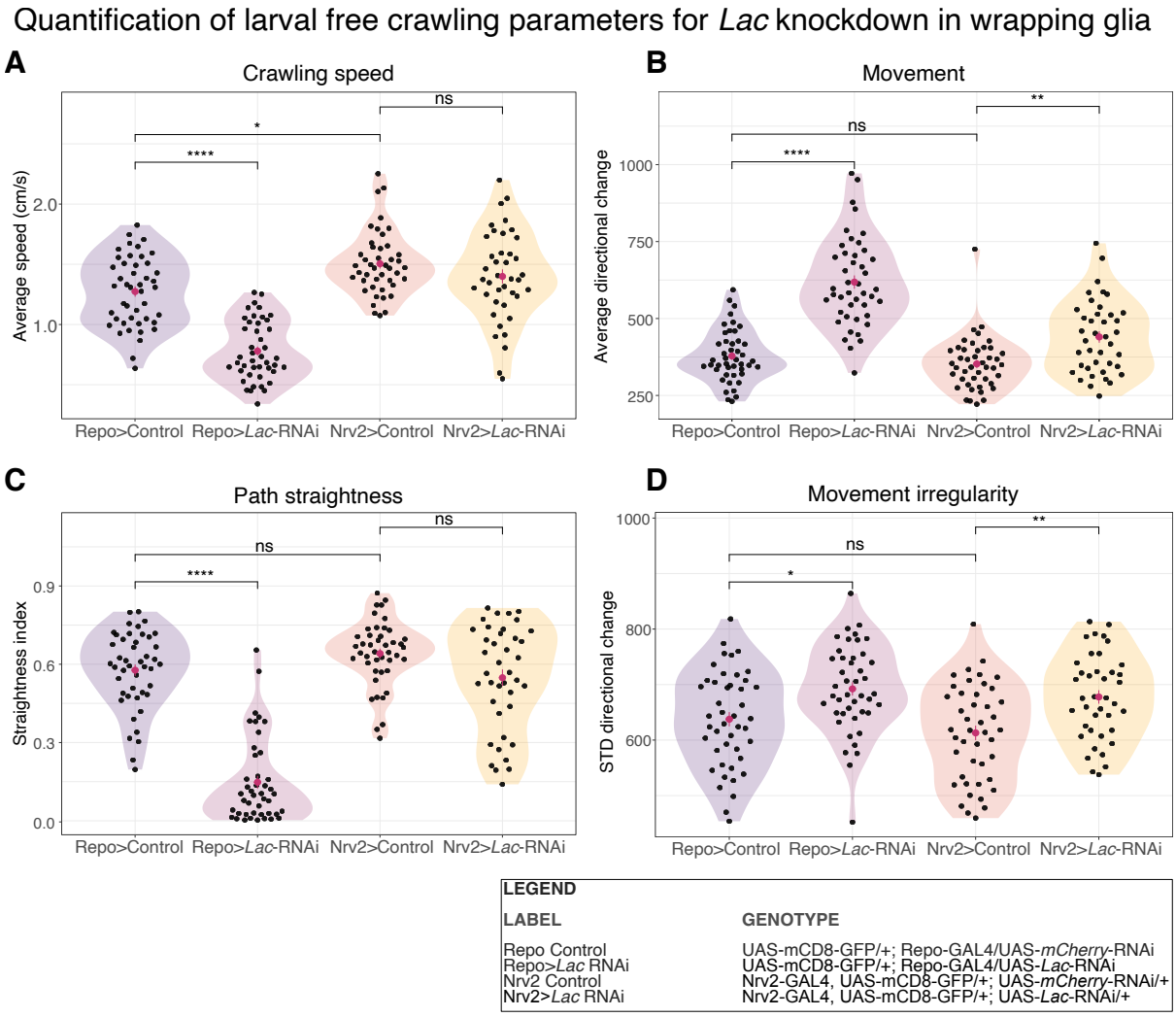

Figure 5-29 Quantification of larval free crawling parameters for *Lac* RNAi in wrapping glia

Larval free-crawling parameters quantification (see Materials and Methods Section 2.8.3) ((n = 45 (Repo Control), 44 (Repo>*Lac*-RNAi), 44 (Nrv2 Control), 40 (Nrv2>*Lac*-RNAi)). Significance levels are denoted as follows: **p < 0.01; ****p < 0.0001. Dunnett's Test (Holm Adjusted) p-values are reported for all panels. See legend for genotype details.

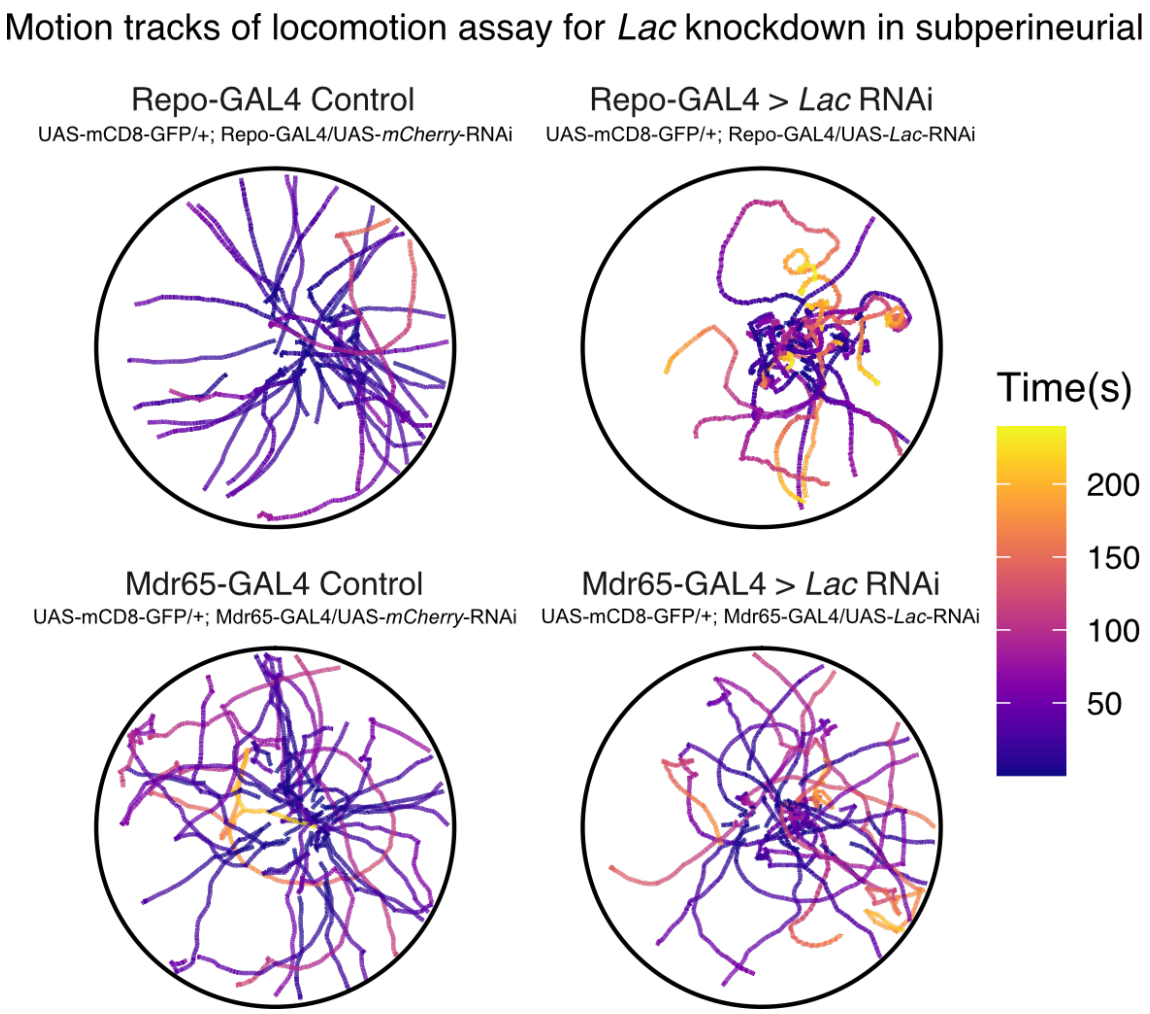

Figure 5-30 Motion tracks of locomotion assay for *Lac* knockdown in subperineurial glia

Color-coded trajectories representing the motion of free crawling 3rd instar larvae of different genotypes (see labels above) over time (n = 43 (Repo Control), 45 (Repo>*Lac*-RNAi), 37 (Mdr65 Control), 41 (Mdr65>*Lac*-RNAi)).

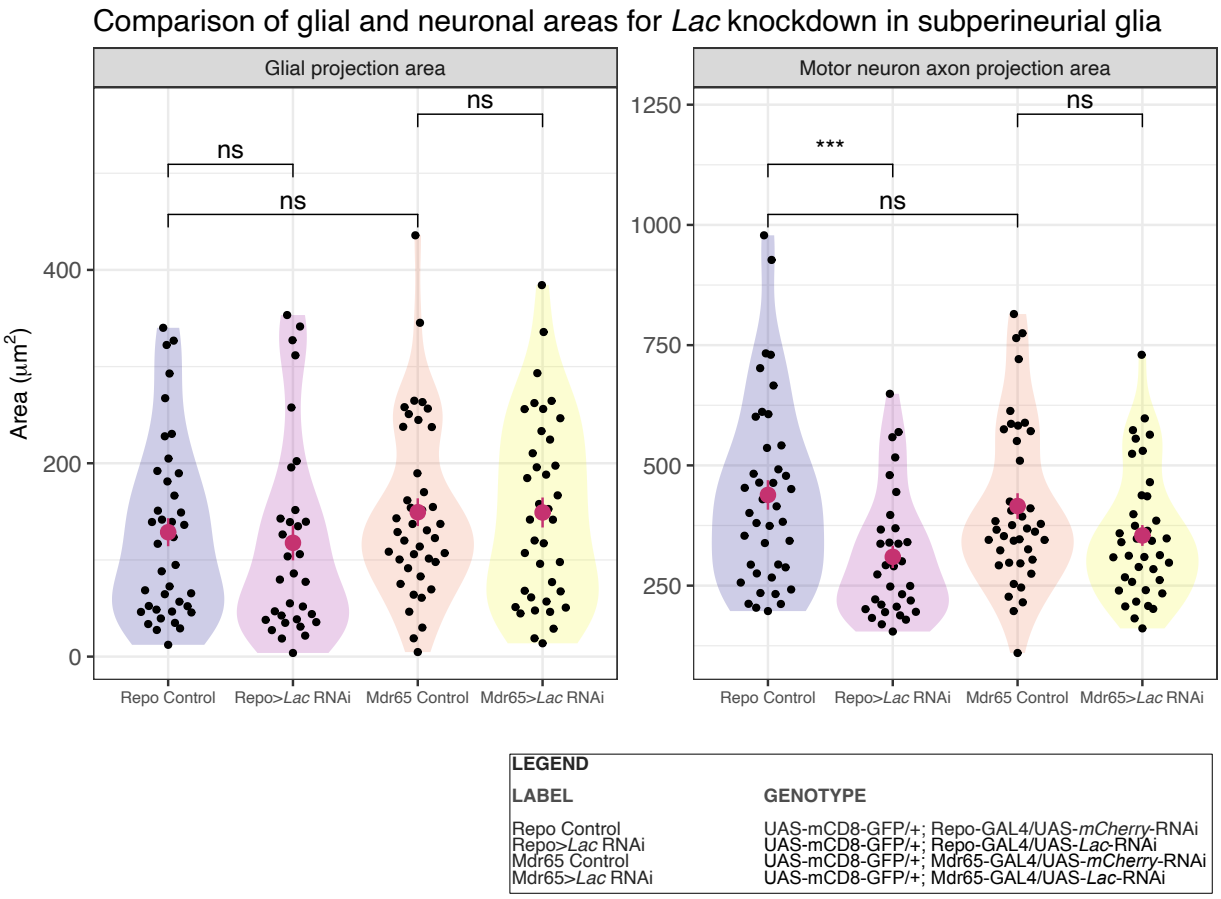

Figure 5-31 Comparison of glial and neuronal areas for *Lac* knockdown in subperineurial glia

Comparison of glial (left) and neuronal (right) projection areas between all glia and SPG in control and Lac-RNAi conditions (n = 40 (Repo Control), 32 (Repo>Lac-RNAi), 40 (Mdr65 Control), 38 (Mdr65>Lac-RNAi)). Significance levels are denoted as follows: **p < 0.01; ****p < 0.0001. Dunnett's Test (Holm Adjusted) p-values are reported for all panels. See legend for genotype details.

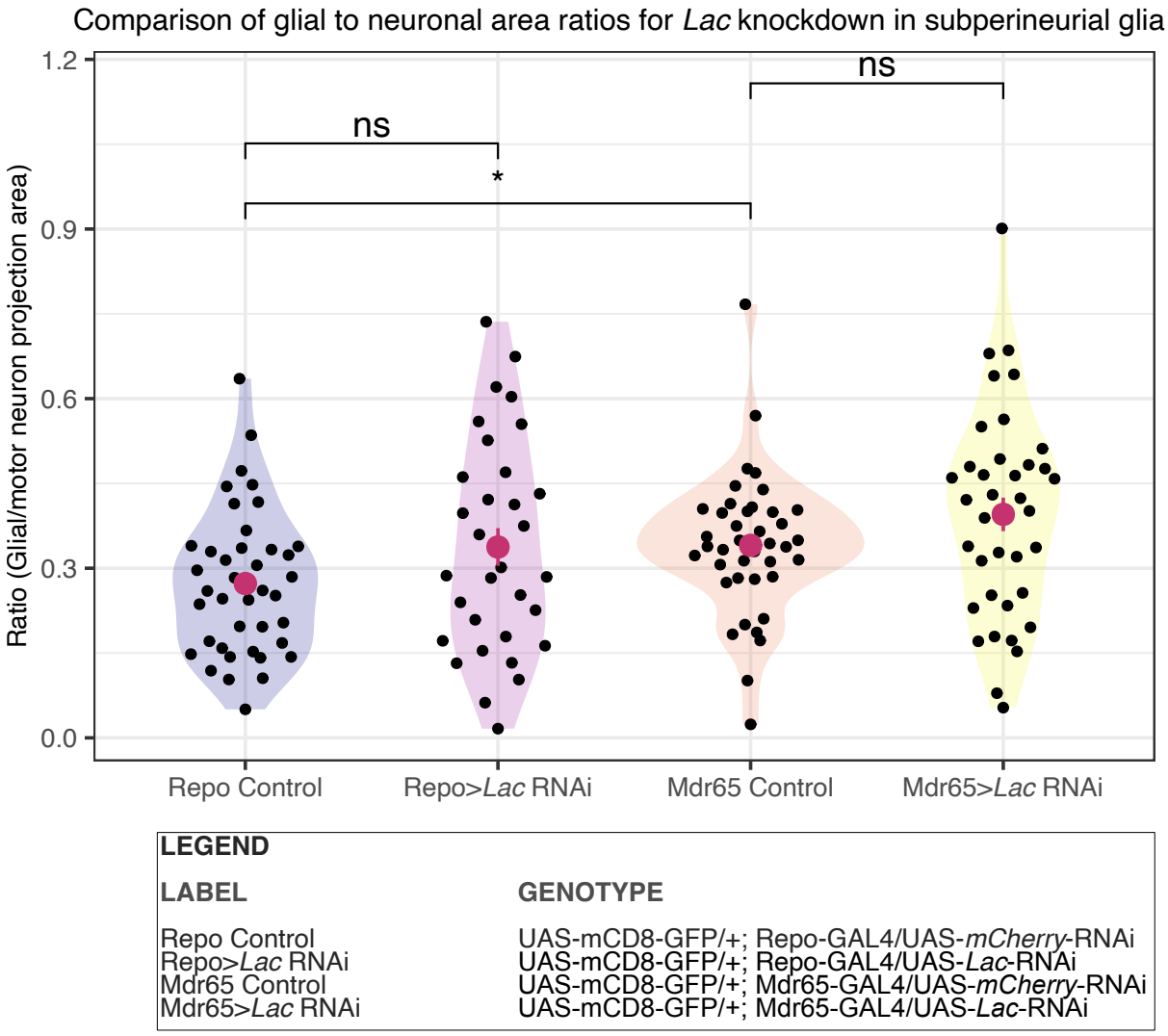

Figure 5-32 Comparison of glial to neuronal area ratios for Lac knockdown in subperineurial glia

Comparison of glial (left) and neuronal (right) projection area ratios between all glia and SPG in control and Lac-RNAi conditions (n = 40 (Repo Control), 32 (Repo>Lac-RNAi), 40 (Mdr65 Control), 38 (Mdr65>Lac-RNAi)). Significance levels are denoted as follows: **p < 0.01; ****p < 0.0001. Dunnett's Test (Holm Adjusted) p-values are reported for all panels. See legend for genotype details.

Quantification of larval free crawling parameters for *Lac* knockdown in subperineurial glia

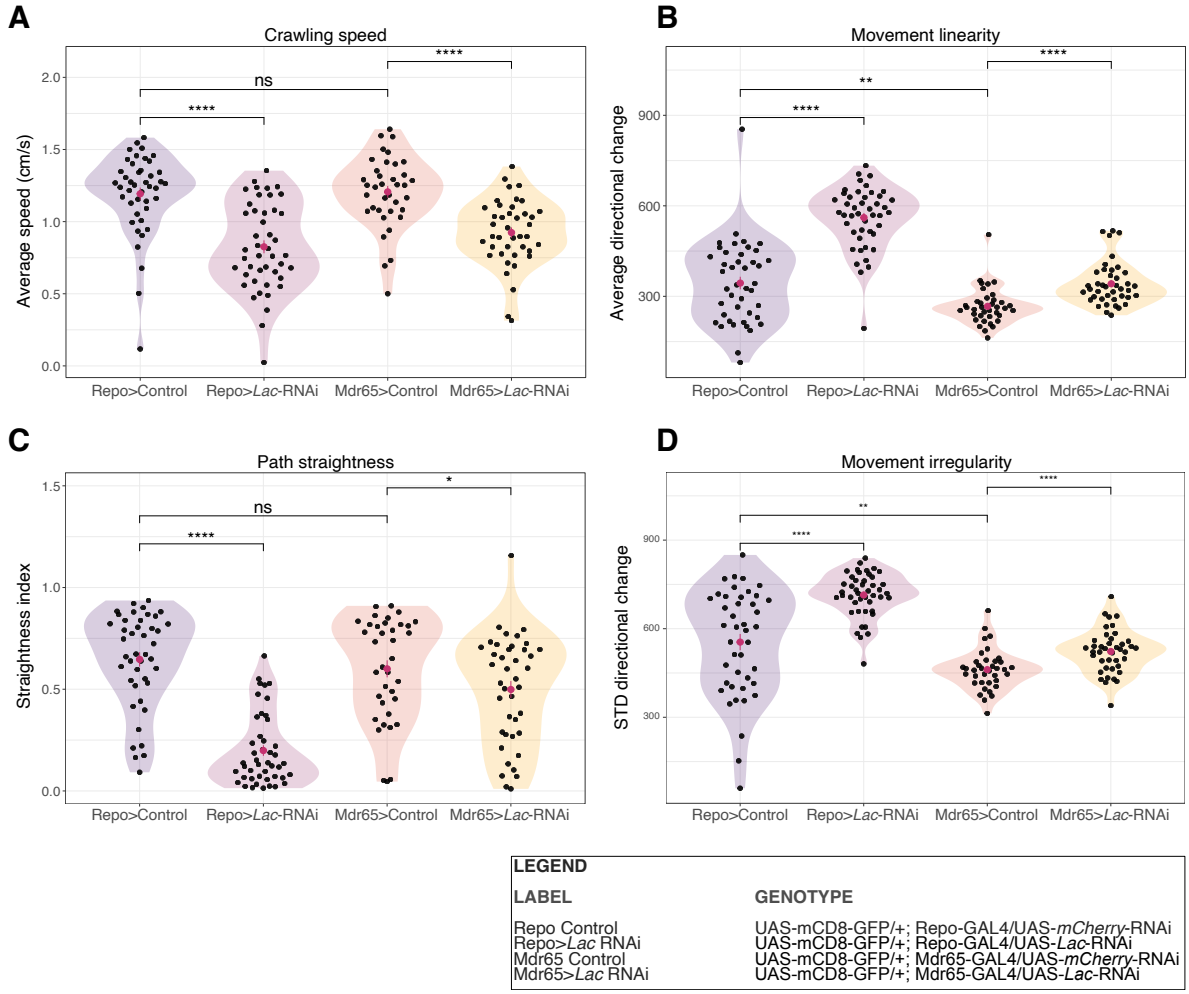

Figure 5-33 Quantification of larval free crawling parameters for *Lac* RNAi in subperineurial glia

Larval free-crawling parameters quantification (see Materials and Methods Section 2.8.3) n = 43 (Repo Control), 45 (Repo>*Lac*-RNAi), 37 (Mdr65 Control), 41 (Mdr65>*Lac*-RNAi)). Significance levels are denoted as follows: **p < 0.01; ****p < 0.0001. Dunnett's Test (Holm Adjusted) p-values are reported for all panels. See legend for genotype details.

Figure 5-34 provides a summary of various NMJ morphometric measurements associated with each glial cell driver. Among these measurements, all three metrics show significant changes in the Repo>*Lac*-RNAi knockdown condition.

However, the only glial driver that partially replicates these observed changes is Nrv2-GAL4. Specifically, Nrv2-GAL4 knockdown of *Lac* leads to a significant decrease in neurite projection area. This suggests that no single glial driver appears to be primarily

responsible for the observed phenotype when Repo-GAL4 is used. Instead, it indicates the possibility of a cumulative or compounding effect of *Lac*-RNAi knockdown on NMJ morphometrics, involving contributions from multiple glial cell subtypes.

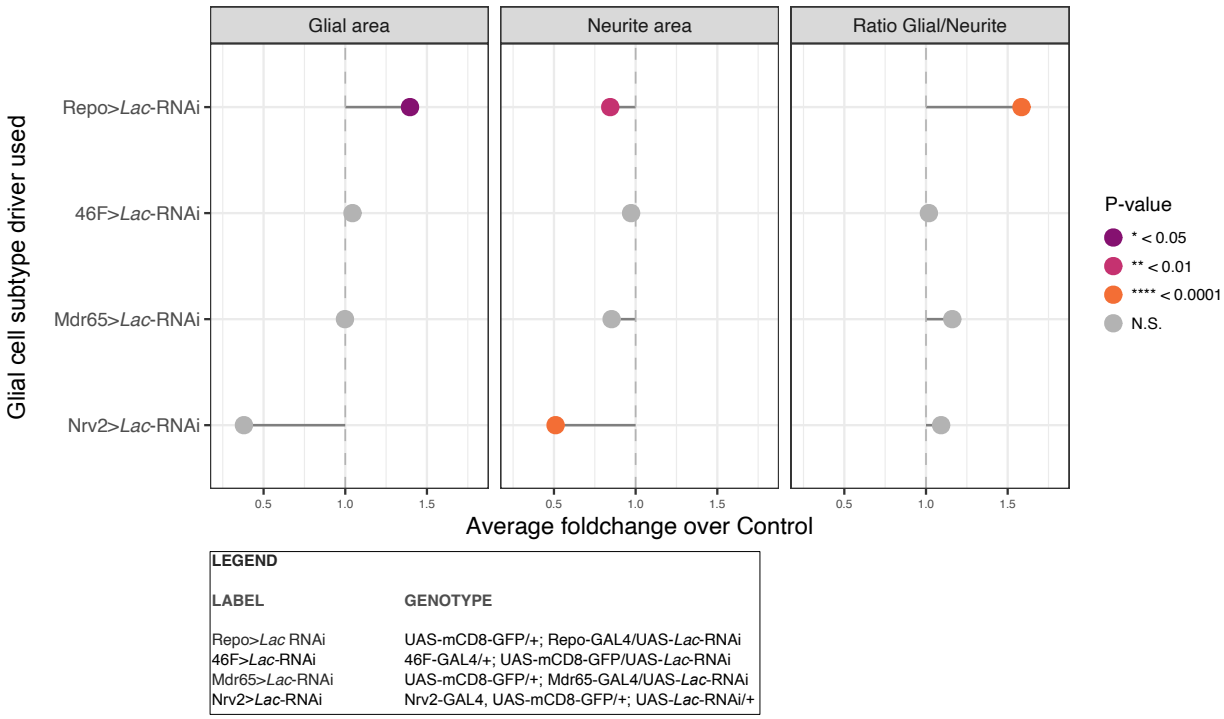

Figure 5-34 Only Nrv2-GAL4 driven knockdown of *Lac* affects NMJ morphometrics

Foldchange in glial protrusion area, neurite area and their ratio upon knockdown of *Lac* in unstimulated NMJs using various glial cell subtype drivers. Data from figures 16-18 is replotted for easier visualisation purposes. Data represents average foldchange for each gene. Wilcoxon rank sum test p-values are reported (n = 98 (Repo Control), 88 (Repo>*Lac*-RNAi), 31 (46F Control), 29 (46F>*Lac*-RNAi), 40 (Mdr65 Control), 38 (Mdr65>*Lac*-RNAi), 17 (Nrv2 Control), 24 (Nrv2>*Lac*-RNAi). See legend for genotype details.

5.4.8 *Lac* knockdown in glia does not affect motor neuron "ghost bouton" numbers

Additionally, to obtain potential insights into putative defects in synaptic development, I quantified the numbers of "ghost boutons" in unstimulated NMJs in control and *Lac*-RNAi conditions using all glial drivers (Figure 5-35). "Ghost boutons" at 3rd instar NMJs

are transient structures destined to be stabilised into mature boutons or else eliminated. Increased “ghost bouton” numbers in a gene mutant or knockdown could indicate that this gene plays a role in the proper maturation of “ghost boutons” and the formation of synapses with correct structural attributes [267, 332-334]. I observed no significant differences in the numbers of “ghost boutons” observed in unstimulated NMJs for any of the glial driver used to knock *Lac* down (Figure 5-35), indicating that glial knockdown of *Lac* does not affect the “ghost bouton” maturation process.

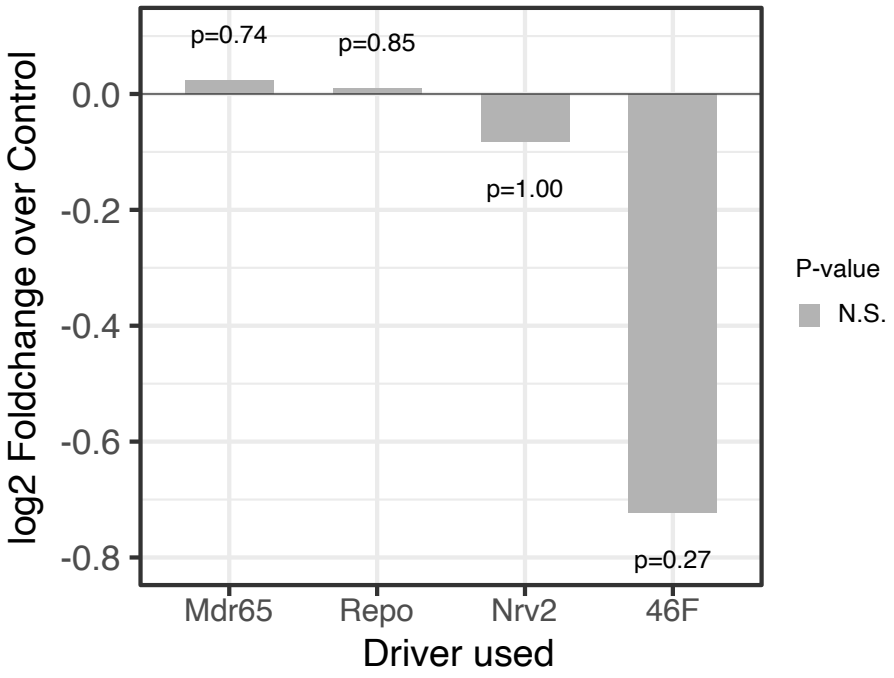

LEGEND	
LABEL	**GENOTYPE**
Repo	UAS-mCD8-GFP/+; Repo-GAL4/UAS-*Lac*-RNAi
46F	46F-GAL4/+; UAS-mCD8-GFP/UAS-*Lac*-RNAi
Mdr65	UAS-mCD8-GFP/+; Mdr65-GAL4/UAS-*Lac*-RNAi
Nrv2	Nrv2-GAL4, UAS-mCD8-GFP/+; UAS-*Lac*-RNAi/+

Figure 5-35 Knockdowns of *Lac* in glia do not affect developmental “ghost bouton” numbers

Bar graph represents average log2 FoldChange of “ghost bouton” counts compared to RNAi controls using varying glial drivers. Wilcoxon rank sum test p-values are reported (n = 98 (Repo>GFP control), 87 (Repo>*Lac*-RNAi), 31 (46F>Control), 29 (46F>*Lac*-RNAi), 40 (Mdr65>Control), 38 (Mdr65>*Lac*-RNAi), 17 (Nrv2>Control), 24 (Nrv2>*Lac*-RNAi). See legend for genotype details.

5.4.9 *Lac*-RNAi knockdown in motor neuron affects the larval crawling behaviour

I wanted to verify whether any of the phenotypes observed upon *Lac*-RNAi knockdown in glia are replicated upon *Lac*-RNAi knockdown in the motor neuron. Using OK6-GAL4 line recombined with UAS-mCD8-mCherry expression, I knocked down *Lac* and performed the crawling assay (Figure 5-36). Since mCherry was expressed by these larvae, *Luciferase*-RNAi was used as a control instead. The larval locomotor behaviour was altered for 3 of the 4 quantified crawling parameters for *Lac*-RNAi when compared to OK6>Control (Figure 5-36 B-E).

Motor neuron (OK6-GAL4)

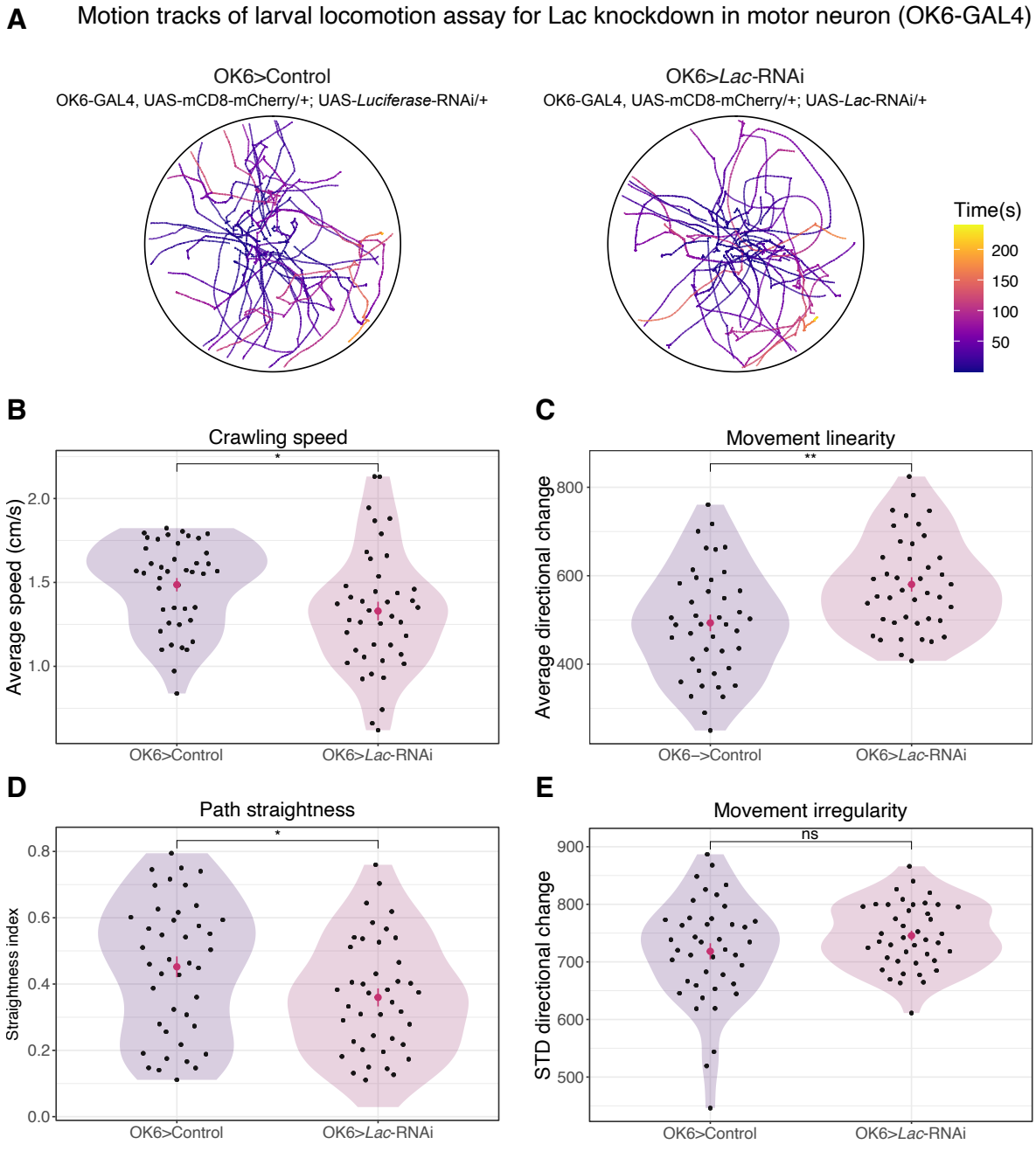

Figure 5-36 Alterations in locomotor behaviour in OK6-GAL4>*Lac*-RNAi larvae

Significance levels are denoted as follows: *p < 0.05; **p < 0.01. Dunnett's Test (Holm Adjusted) p-values are reported for all panels. A) Color-coded trajectories representing the motion of free crawling 3rd instar larvae of different genotypes (see labels above) over time (n = 42 (OK6>Control which was UAS-*Luciferase*-RNAi), 42 (OK6>*Lac*-RNAi)). B-E) Larval free-crawling parameters quantification (see Materials and Methods Section 2.8.3).

5.4.10 *Lac* knockdown using Mdr65-GAL4 most closely replicates Repo phenotype

Having tested various drivers, I wanted to determine which one of them most closely replicated the Repo-driven crawling phenotype when used for *Lac*-RNAi knockdown. I therefore pooled all data from figures 16-18 and 21 to combine the crawling assay results for easier visualisation purposes (Figure 5-37). *Lac* knockdown using Mdr65-GAL4, the SPG driver, most closely resembles the Repo-GAL4 driven knockdown with regards to crawling parameters, with all four measures quantified affected significantly and in the same way as Repo-GAL4 driven knockdown.

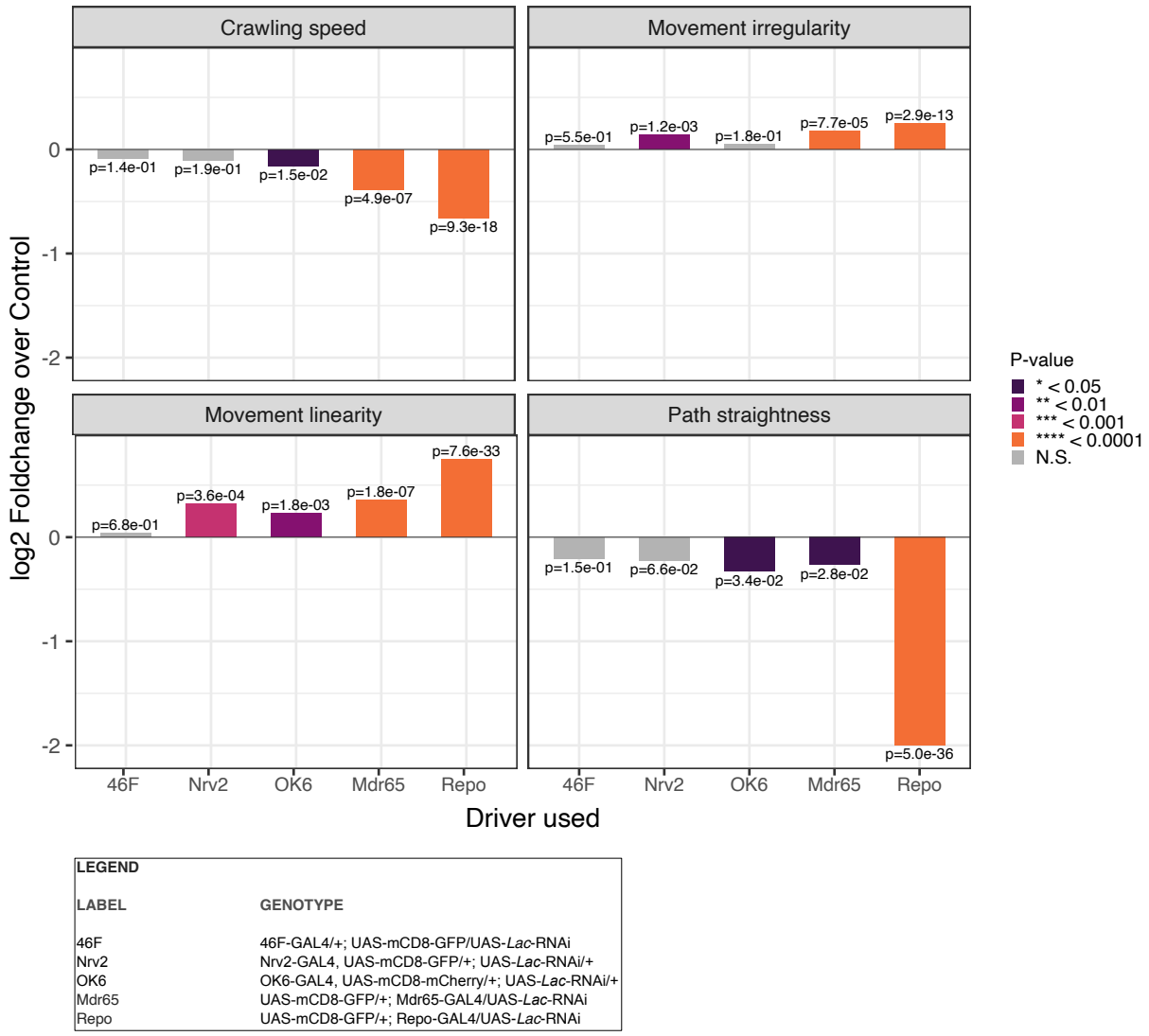

LEGEND	
LABEL	GENOTYPE
46F	46F-GAL4/+; UAS-mCD8-GFP/UAS-*Lac*-RNAi
Nrv2	Nrv2-GAL4, UAS-mCD8-GFP/+; UAS-*Lac*-RNAi/+
OK6	OK6-GAL4, UAS-mCD8-mCherry/+; UAS-*Lac*-RNAi/+
Mdr65	UAS-mCD8-GFP/+; Mdr65-GAL4/UAS-*Lac*-RNAi
Repo	UAS-mCD8-GFP/+; Repo-GAL4/UAS-*Lac*-RNAi

Figure 5-37 Larval crawling parameters upon knockdown of *Lac* using various drivers

Data from figures 16-18 and 21 is replotted for easier visualisation purposes. Bar graphs represent average log2 FoldChange of specified parameters describing larval free-crawling behaviours (see label above). Driver used is specified on the x axis. Statistically significant changes are highlighted in colour. Wilcoxon rank sum test p-values are reported (n = 44 (46F>Control), 43 (46F>*Lac*-RNAi), 44 (Nrv2>Control), 40 (Nrv2>*Lac*-RNAi), 42 (OK6>Control), 42 (OK6>*Lac*-RNAi), 37 (Mdr65>Control), 41 (Mdr65>*Lac*-RNAi), 132 (Repo>Control), 131 (Repo>*Lac*-RNAi)). See legend for genotype details.

I also wanted to explore the severity of each phenotype observed comparatively, since some showed a higher level of significance. I therefore used a heatmap of p-values to achieve that, which again showed that the Mdr65-GAL4 driven RNAi knockdown of *Lac* resulted in the most severe phenotypes (Figure 5-38).

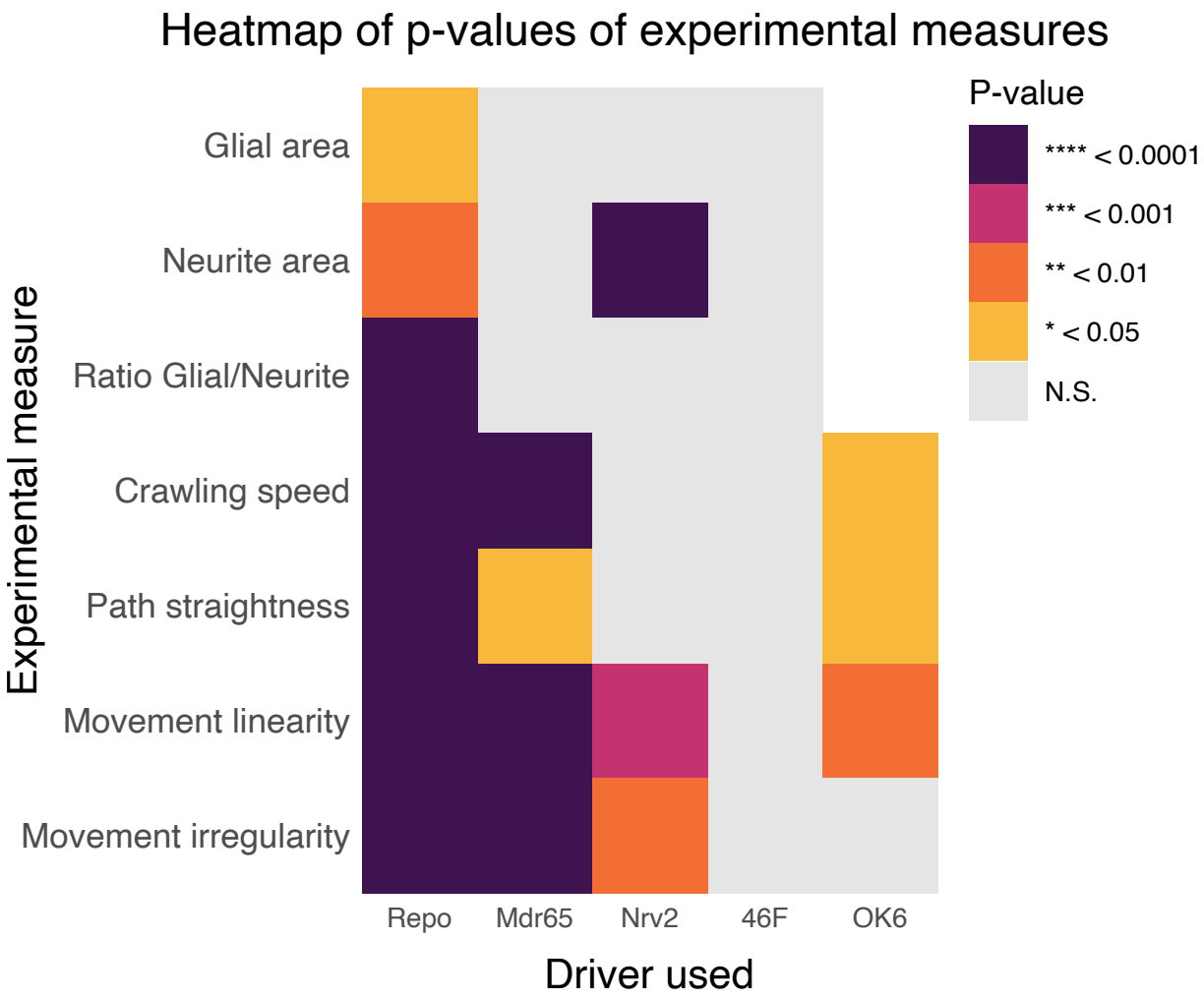

LEGEND	
LABEL	**GENOTYPE**
46F	46F-GAL4/+; UAS-mCD8-GFP/UAS-*Lac*-RNAi
Nrv2	Nrv2-GAL4, UAS-mCD8-GFP/+; UAS-*Lac*-RNAi/+
OK6	OK6-GAL4, UAS-mCD8-mCherry/+; UAS-*Lac*-RNAi/+
Mdr65	UAS-mCD8-GFP/+; Mdr65-GAL4/UAS-*Lac*-RNAi
Repo	UAS-mCD8-GFP/+; Repo-GAL4/UAS-*Lac*-RNAi

Figure 5-38 Experimental measures p-values heatmap for different drivers

Data from figures 16-18 and 21 is replotted for easier visualisation purposes and comparison. Driver used is specified on the x axis, experimental measure is specified on the y axis. See legend for genotype details.

5.5 Discussion

5.5.1 Insights into molecular *Lac* mRNA dynamics and knockdown phenotype

In this chapter, I set out on an in-depth exploration of *Lac,* a candidate gene that exhibited mRNA localisation in glial protrusions, as seen in Chapter 3 (Figure 3-21) and whose knockdown in glia resulted in altered larval locomotion, as shown in Chapter 4 (Figure 4-12). Thus, *Lac* was a promising gene to explore in-depth in the context of the potential importance of its mRNA localised to glial protrusions being involved in the structural synaptic plasticity of the neighbouring motor neuron at the 3rd instar *Drosophila* NMJ.

Although *Lac* has been known to be present in the genome of insects, such as the fly, since the 1990s, its role in *Drosophila* is less defined compared to mammals [204, 205, 305]. Our understanding in mammals is also limited, primarily focusing on the gene's functions based on its structure and its inclusion in the IgLONs family, rather than specifics about the gene itself [299, 302]. Nevertheless, Single Nucleotide Polymorphism (SNP) analyses and animal model studies underscore its importance for neuronal development and morphogenesis [288, 302, 306, 307]. My research complements this knowledge and investigates a parallel yet underemphasised aspect by highlighting its importance in glial cells for correct synapse morphology and crawling behaviour of *Drosophila* larvae.

Why does this aspect have the potential to be insightful? Since most research so far focused on IgLONs role as cis- or trans-synaptic adhesion molecules, the possibility of IgLONs interacting with glial cells in a similar manner is only recently starting to be explored [77, 303]. Moreover, the genesis of my research question and design was the localisation of the mRNA of *Lac* and other candidate molecules, many of them

connected to cell adhesion, to the glial cell periphery. It is therefore plausible that many disease phenotypes identified in IgLON studies, previously attributed to or explored as neuronal dysfunction, might at least partly arise from the glial functions of IgLONs instead [303]. Some of these functions may be mediated by the localisation of mRNA and its local translation at the glial periphery, as has been observed for other proteins and transcripts in neurons, astrocytes, oligodendrocytes, and radial glia [34, 48-50, 79, 164, 280, 335, 336].

My results highlighted the properties of the *Lac* gene related to the microscopic localisation of its mRNA and protein at the NMJ synapse in the context of structural synaptic plasticity (Figure 5-9 – 14), BBB (Figure 5-14), but also to the micro- and macroscopic consequences of its absence caused by its glial RNAi-mediated knockdown (Figure 5-6 and Figure 5-13).

An observation which I made in Chapter 3 and expanded on significantly in this chapter was that *Lac* mRNA and protein are intimately associated with some of the most distant and fine structures created by the glial cells present at the NMJ (Figure 5-9). What is unclear is whether the presence of *Lac* mRNA means that *Lac* mRNA is actively transported to the glial periphery and translated there. Experiments employing selective mutations in the *Lac* 3'UTR mRNA localisation sequences, combined with techniques like Fluorescence Assay to Detect Ribosome Interactions With mRNA (FLARIM), or SUperNova (SunTag) and MS2–MCP (MS2 coat protein) mRNA tagging could help to identify the specific *Lac* sequence responsible for its mRNA localisation, the RNA binding proteins involved in its transport, and whether *Lac* is locally translated at the glial periphery [337-339]. These experiments could also aim to determine if the observed effects of the absence of *Lac* mRNA and protein are due to its unfulfilled

localised function at the glial cell periphery or a broader deficiency throughout the entire cell. While these studies fall outside the scope of my thesis, they are currently being pursued by other members of the Davis laboratory.

5.5.2 NMJ neuronal and glial area ratios in *Lac*-RNAi

A key finding of this chapter was an observation initially made for Lac::YFP protein area and later confirmed with Repo>GFP marked glial projections areas in the context of structural synaptic plasticity. Lac::YFP protein area (Figure 5-10) and glial projections areas (Figure 5-13) decrease after spaced potassium stimulation, but remain unchanged when *Lac* is knocked down in glia. Moreover, the motor neuron terminal area is not affected after potassium stimulation in Repo>GFP control (Figure 5-13) or Lac::YFP (Figure 5-10) larvae, but is significantly increased after potassium stimulation in *Lac*-RNAi NMJs. Therefore, it could be concluded that in baseline conditions, the glial projection area is supposed to decrease when structural synaptic plasticity occurs, and the neuronal area should not change, indicating that it is perhaps remodelled by the emergence of “ghost boutons”, but not significantly increased or decreased. However, in the absence of *Lac*, the glial projection area remains unchanged, and the neuronal area is increased significantly.

Therefore, it appears that the NMJ neuronal and glial areas are dependent on one-another and change proportionately, in equilibrium. This has been demonstrated before, but not directly in the context of structural synaptic plasticity and crawling defects [121]. It appears that if the neuronal area is unchanged upon structural synaptic plasticity, glial area must decrease, but if glial area cannot decrease, something which I hypothesise could be caused by the absence of Lac on the glial

membrane, neuronal projections must “accommodate” those disordered glial projections by expanding themselves.

The observations from the spaced potassium stimulation experiment using Lac::YFP seem to support this hypothesis. None of the measures apart from the Lac::YFP area quantification were affected (Figure 5-10), and the Lac::YFP area was decreased post-stimulation. Considering that neither the absolute nor the area-proportional counts of mRNA molecules change significantly with potassium stimulation (Figure 5-11, Figure 5-12), it could be hypothesised that maintenance of a consistent level of *Lac* mRNA in glial cell projections, which Lac::YFP area approximates (Figure 5-3), is required for the maintenance of the glial to neuronal area equilibrium. Such homeostasis could be essential for glial cell function or response during structural synaptic plasticity, and Lac protein, whose area and intensity levels are also unchanged, might play a role in regulating the morphological changes of glial cell projections post-structural synaptic plasticity. Those morphological changes could include expanding the BBB to also cover the new axon terminal areas formed as a result of structural synaptic plasticity. This implies that it is not the ratio of the area of the glial to neural projections, but rather the level of contact between the two cells, the number of SJs, or the BBB area, that are tightly controlled.

5.5.3 Importance of Lac in SPG and the BBB

My study assessed the role of specific glial cell subtype drivers on the *Lac*-RNAi knockdown phenotype associated with the pan-glial driver, Repo-GAL4. I determined that Mdr65-GAL4 knockdown of *Lac* most closely resembled the phenotype observed with Repo-GAL4 (Figure 5-30, Figure 5-32, Figure 5-37, Figure 5-38), but Nrv2-GAL4 knockdown also has measurable effects. The larval crawling assay results also

indicate that *Lac* knockdown in motor neuron affects the larval crawling behaviour, albeit to a lesser extent (Figure 5-36). *Lac* knockdown in the motor neuron causing behavioural issues is much more understandable in the context of mammalian evidence [288, 306, 307]. To further explore the role or Lac in the motor neuron, future research could employ various motor neuron drivers. While OK6-GAL4 is one option, there are other available drivers. Some of these not only target motor neurons but also sensory neurons, which have been identified as influencers of larval crawling behaviour [340, 341]. Moreover, I did not have the possibility to quantify the impact of OK6-GAL driven knockdown of *Lac* on the glial morphology. An experiment with dual labelling of glia and neuron followed by the NMJ morphometrics quantification could be designed with the use of LexA-*lexAop* or another similar system [342, 343].

However, while OK6-GAL4 knockdown produced a phenotype, it was not as severe as that observed with the use of Mdr65-GAL4, and the use of Nrv2-GAL4 also caused crawling and morphological defects. Therefore, it is possible to hypothesise that the effects observed upon *Lac* knockdown using Repo-GAL4 are a compound effect of the absence of *Lac* in more than one glial cell subtype, with the main contributor being the BBB-forming SPG. This would suggest that the BBB glia regulate the synaptic transmission to a high extent.

The idea that BBB can be involved in regulating structural synaptic plasticity is not new. The BBB's main role is to maintain the neuronal microenvironment, including its chemical composition homeostasis which is required for proper functioning of structural synaptic plasticity, neuronal circuit conductivity and synaptic remodelling [344, 345]. It has also been documented that impaired interactions between the neurovascular unit (NVU), formed of different types of glia, blood vessels and neurons,

and the BBB, play roles in astroglial dysfunction, epileptogenesis, neuroinflammation, ageing-related disfunction and neurodegeneration [346-349]. Though the mammalian BBB is formed by the epithelium, in *Drosophila* it is exclusively constituted by SPG, which could therefore be assumed to perform largely the same roles [210, 350].

5.5.4 Lac and its role from molecular function to larval locomotion

What is the molecular and cellular role of Lac in mediating structural synaptic plasticity at the *Drosophila* NMJ? The NMJ glial projections of control larvae, marked with Repo-GAL4, are simple and appear strictly targeted to specific structures like “ghost” or synaptic boutons. Often, they have a single molecule of *Lac* mRNA localised to their periphery (Figure 5-6). Lac::YFP protein is similarly observed in specific and limited locations at the synapse (Figure 5-9). In *Lac*-RNAi condition, the projections appeared chaotic and disordered, as if they cannot recognise their target structure (Figure 5-7), or cannot stabilise their projections, which is similar to existing evidence where Lac was shown to have a role in regulating cell size and cell adhesion in morphogenesis [204]. Could *Lac*-RNAi glial projections be “blind” to other structures due to the inability to bind them intercellularly through Lac? The examination of the *Lac* mRNA molecules in relation to the *Drosophila* BBB certainly seems to support such interpretation, indicating their localisation and concentration near SJ as marked by NrxIV::GFP, thus suggesting their potential roles in BBB maintenance. Furthermore, the crawling phenotype I observed appears as a milder manifestation of a previously noted phenotype from a homozygous *Lac* mutation [205]. In the prior case, embryos showed an initial phase of increased activity marked by erratic muscle contractions, progressing to paralysis and inability to hatch, while Repo>*Lac*-RNAi larvae in my study also appeared to be unable to move or were moving slowly and erratically.

Previously, this was determined to be caused by the disrupted ultrastructure of SJ in both CNS and PNS BBB glia. Additionally, the neuronal fibres within the neuropil (the CNS synaptic region) exhibited notable enlargement, which I also observed for the *Lac*-RNAi axon terminal projection after spaced potassium stimulation, a period of increased structural synaptic plasticity and activity.

Based on the information presented in this chapter and the available literature, I have formed a hypothesis for the connection between Lac and its molecular function, glial morphology, and larval crawling behaviour. Lac deficiency at the periphery of NMJ glial cells resulting in aberrant glial cell morphology could lead to altered structural synaptic plasticity in motor neurons and subsequently result in aberrant locomotor behaviour due to disruptions in glial-neuronal communication, the BBB function and maintenance, altered neurotransmitter homeostasis, and changes in synaptic strength (Figure 5-39).

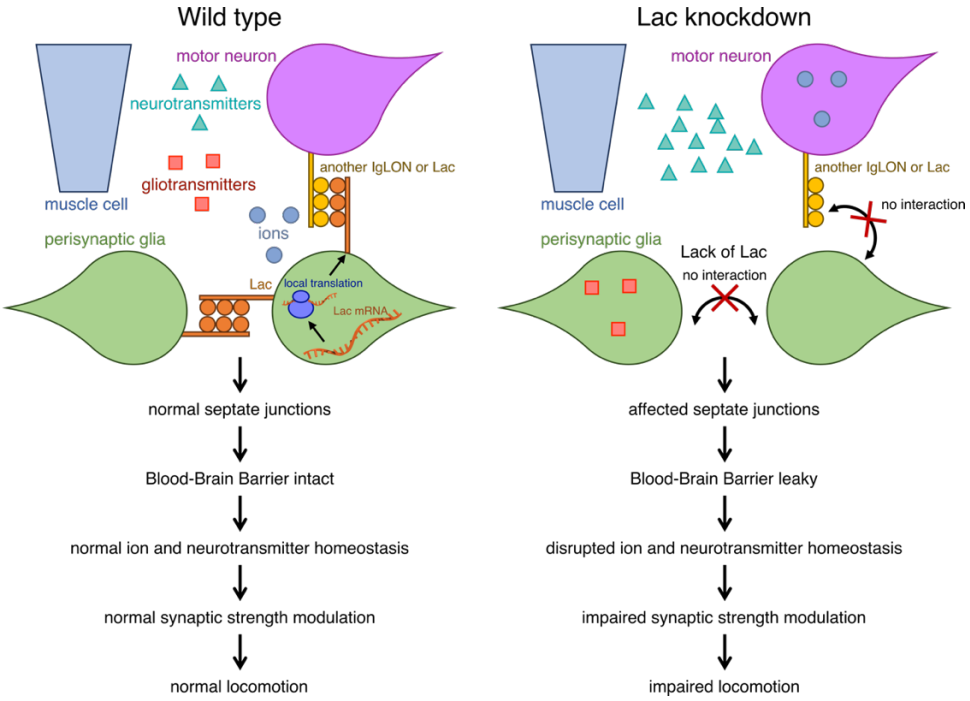

Figure 5-39 Hypothesis: Lac and its role from molecular function to larval locomotion

Hypothesised role of Lac in larval locomotion derived from its molecular function at the NMJ synapse and in the BBB formation.

According to this hypothesis, the absence of Lac in glia would prevent glial-glial cell homophilic binding [204, 205]. This binding would be impaired from the beginning of development. That would mean improper development of SJs, not only between glial cells at earlier developmental stages, but also between neurons and glia at later stages, which have before been observed in the larval CNS, considering that Lac is expressed in both neurons and glia [305, 351, 352]. SJs necessitate the assembly of multiprotein complexes between two adjacent cells. Given that Lac is a homophilic cell adhesion protein, it might act as a key component, or even the final piece, in ensuring this assembly [202]. Furthermore, Lac is suspected of being able to form heterophilic bonds with similar proteins based on its membership in the IgLON family, thus further expanding the possibility of Lac connecting different cells in different contexts, including that of development and synaptic plasticity [299, 302-304].

Assuming improper SJ assembly and altered BBB formation or maintenance caused by Lac absence, impaired ion and neurotransmitter homeostasis would be the basis of affected synaptic transmission, not only at the NMJ, but also throughout the nervous system. At this point, it would be hard to directly determine the cause of the impaired transmission at the NMJ alone, considering the vast synaptic circuitry which contributes to crawling behaviour [341]. Overall, uncontrolled ion flow if the BBB does not operate properly would impact both the glial and neuronal function, possibly causing uncontrolled release of neurotransmitters and gliotransmitters, thus affecting the synaptic strength, modulation, and, as a result, synaptic plasticity. The beta subunits of *Drosophila* Na/K ATPase (nrv2 and ATPα, whose mRNAs were also present on the original glial protrusion-localised transcript list), are important for maintenance of the correct ion concentrations inside and outside neurons; they, too,

are required for correct SJ formation, further supporting this hypothesis [214, 222, 353].

Altogether, I provided evidence in favour of certain aspects of this hypothesis, but a more comprehensive investigation is needed to fully explain the role of Lac in structural synaptic plasticity at the *Drosophila* NMJ. Specifically, additional experiments should focus on the ultrastructure of SJs, BBB permeability, variations in ion, gliotransmitter, and neurotransmitter levels, as well as the potential homophilic or heterophilic binding of Lac. Identification of any potential IgLON-like binding partners of Lac or evidence of *Lac* mRNA transport and translation in response to synaptic activity could further explain the molecular basis of the phenotypes which I observed. Furthermore, the role of *Lac* mRNA and its absence in the synapse maturation process would have to be explored, as the decreased emergence of “ghost boutons” observed upon *Lac* RNAi-mediated knockdown only points to active zone formation impairment, not synapse maturation impairment. Investigating these detailed questions is beyond the scope of my thesis, but it would allow the deepening of the understanding of glia, mRNA, and structural synaptic plasticity in both health and disease.

CHAPTER 6

6 Discussion

6.1 Background

The molecular basis of learning and memory is one of the greatest mysteries of modern biology. Much of the neuroscientific research of the second half of the 20th century has focused on trying to understand these phenomena, with the specific roles of specialised nervous system cells and their molecular, cellular and physiological interplay being explored in great detail. Particularly, numerous significant studies started drawing attention to the astounding breadth of contacts made by neurons, but also glial cells like astrocytes and oligodendrocytes [73, 354]. These cells are extremely polarised and create fine projections to achieve distal local regulation and specificity, often through mRNA localisation, enabling localised protein production [355]. In neurons, it is well documented that regional specialisations are often achieved via protein sorting or mRNA transport coupled with localised translation [151, 154, 356-358]. Yet, this type of regulation is only starting to be explored in glial cells, which have been side-lined in research and considered passive for years [1, 34, 74]. The identification of glial cells as components of tripartite synapses in the 1990s spurred heightened interest in their functions within the nervous system. This led to significant findings about glial involvement in regulating essential neuronal functions such as synaptic plasticity and neurotransmitter homeostasis, as well as their distinct roles apart from neurons [13, 17, 18, 33, 359]. Additionally, research is delving into the role of glia in mRNA localisation, especially in their fine processes that interact with synapses. Studies have shown that fear conditioning modifies the transcriptome, translatome, and proteome of these peripheral processes [34, 45, 46, 53, 74]. Previous studies in our laboratory suggested that numerous transcripts might be localised to

the periphery of glial cells extending to the NMJ of the *Drosophila* 3rd instar wandering larvae [181]. This raises several questions: Are these transcripts truly present in the NMJ glia? What is their role at the NMJ? Are they vital for the structural synaptic plasticity of the NMJ? Consequently, I began exploring the answers to these questions.

6.2 mRNA is localised to the glial projections of the *Drosophila* 3rd instar NMJ

In Chapter 3, I performed smFISH on YFP trap lines of the nineteen candidate genes suggested as promising candidates with glial localisation of their mRNA. I confirmed that all genes had mRNA localised within the boundary of the glial labelling at the NMJ using Repo-GAL4 pan-glial driver [155, 329]. Many of these genes code for proteins whose functions pertain to cell junction formation and cell-cell adhesion [201-206, 208, 360]. The presence of their mRNAs might suggest a requirement for localised translation, facilitating glial cell functions associated with adhesion and membrane reshaping.

Not all the candidate genes showed protein expression at the NMJ. I excluded one of the candidate genes, ORMDL, based on the observation that it did not have any protein expression and an extremely high mRNA expression by designing a probe against its gene sequence and comparing its localisation with the *YFP* exon localisation, and observing that they did not match. I further explored the ORMDL::YFP trap by performing a RT-PCR experiment and determining that *YFP* sequence is present, but most likely not where it is stated it is on FlyBase and in the original publication [361].

For the remaining eighteen genes, I observed widely varying numbers of mRNA molecules in the NMJ perisynaptic glia, ranging from one or two to tens. For several genes, like *nrv2, Gli, Flo2, Atpα, Lac, cold, CG42342* and *sdk*, the mRNA appeared to be mostly inside the glial membrane, while for other genes it was also abundantly present in the surrounding muscle cells. Gs2 stood out as an interesting example because of the localisation of its mRNA to “glial boutons”, or regions showing glial labelling that were distinct and separate from the axon terminal boutons. Therefore, I moved on with the exploration of eighteen genes that I wanted to investigate further to begin understanding the functional implications of the localisation of their mRNA within the NMJ glia.

6.3 Glial localised mRNAs knockdown affects structural synaptic plasticity

In Chapter 4, I then asked how RNAi-mediated knockdown of the candidate genes affects the overall development and NMJ morphology of unstimulated and stimulated *Drosophila* 3rd instar wandering larvae. Knocking down the candidate glial protrusion-localised transcripts in all glial cells, I noted larval or adult lethality for 5 of the transcripts. Many also showed NMJ morphology changes, both before and after potassium stimulation. Overall, these findings reinforce the notion that the candidate glial protrusion-localised transcripts, for which phenotypes were noted, have crucial but diverse roles in the proper development of glial cells. Consequently, these roles directly and indirectly affect the functions these cells perform during development and plasticity, both in the CNS and PNS.

Some of the notable observations made in this chapter included a phenotype observed upon *Vha55*-RNAi knockdown that, to my knowledge, has not been reported before [248]. This manifested as a significant reduction in the size of the larval brain

hemispheres. *Lac* and *cold* knockdowns also had effects on the larval brain anatomy. While the elongated VNC phenotype following knockdown has been documented before, it had not been previously associated with these two genes [277-279]. Notable NMJ morphology phenotypes emerged, too, with *Lac*-RNAi NMJ glial projections being markedly expanded and hypermorphic when compared to control, while *shot*-RNAi glial projections appeared non-existent.

I then performed spaced potassium stimulation, a widely recognised assay used to induce the rapid formation of new synaptic boutons, known as “ghost boutons”. This method therefore facilitates the measurement of activity-induced structural synaptic plasticity by quantifying the emergence of these structures [191, 197, 273, 333]. Having quantified the “ghost bouton” counts, I established that they increased for two transcripts (*Pdi*, *CG1648*) and decreased for two (*CG42342*, *Lac*) when compared to their respective controls. Therefore, I demonstrated that knocking down these candidate protrusion-localised transcripts in the perisynaptic glial cells affects the structural synaptic plasticity in the neighbouring neuron. This observation underscores the complex interplay between glial cells and neuronal structural synaptic plasticity, emphasizing the fundamental role of glia in supporting neuronal function.

By employing a crawling assay to evaluate larval locomotor behaviour, I found that the *Lac*-RNAi larvae exhibited significantly reduced crawling. In contrast, other larvae where glial protrusion-localised transcripts had been knocked down and had previously shown “ghost bouton” phenotypes displayed normal crawling behaviour. I thus correlated the observed brain anatomy and NMJ morphology abnormalities with an observable behavioural phenotype, this being compromised crawling.

Consequently, I chose to concentrate on *Lac* and investigate further the effects of knocking down its mRNA in glial protrusions on both glia and neurons at the NMJ.

6.4 Lac is important in SPG and BBB

In Chapter 5, I presented the confirmation that the *Lac*-RNAi knockdown line, as well as the Lac::YFP trap previously used, target *Lac* specifically, and that *Lac* exon, not intron, is present in the *Lac* mRNA found at the NMJ. I next examined the localisation of *Lac* mRNA and protein at the NMJ extensively. I confirmed that the Lac::YFP protein almost entirely fills the glial projections, forms structures that resemble fine filaments, and is expressed in close proximity to both “ghost boutons” and mature boutons of the motor neuron. Additionally, *Lac::YFP* mRNA is often found at the outermost edges of the glial projections.

I next asked: what happens to Lac protein and mRNA when the NMJ undergoes structural synaptic plasticity? I used the spaced potassium stimulation paradigm again and determined that the intensity of the Lac protein and the number of mRNA molecules remain unaffected by this assay. However, the area covered by Lac::YFP diminishes, mirroring the reduction seen in glial projections as marked by Repo-GAL4 driving a membrane-targeted GFP. This suggests that, in the wild type, glial projections should shrink as a result of structural synaptic plasticity. Moreover, the proportion of *Lac* mRNA molecules in the BBB area (as marked by NrxIV::GFP) to the proportion of *Lac* mRNA molecules in motor neuron axon projection area is higher than the proportion of the areas themselves [202, 325, 360]. *Lac* mRNA, therefore ,is preferentially localised in the BBB at the NMJ.

I finally determined that Mdr65-GAL4 driven knockdown of *Lac* most closely resembles the crawling phenotype elicited upon Repo-GAL4 driven knockdown, but Nrv2-GAL4 and OK6-GAL4 also affect the larval crawling and, in the case of Nrv2-GAL4, the NMJ morphology. Based on my results and existing literature, I then formulated a hypothesis regarding the link between Lac, its molecular function, glial morphology, and larval crawling behaviour. A deficiency of Lac at the peripheral regions of NMJ glial cells could lead to incorrect formation or potentially complete absence of SJs [204, 205]. This disruption could cause compromised glial-glial and glial-neuronal communication due to the lack of homophilic and speculated heterophilic adhesion through Lac, resulting in impacted BBB functionality and maintenance. Imbalanced neurotransmitter homeostasis and variations in synaptic strength stemming from BBB impairment might, in turn, influence synaptic plasticity in motor neurons, potentially causing deviations in locomotor behaviour [114, 325, 344, 347, 348].

6.5 Limitations

6.5.1 Chapter 3 limitations

Instead of directly detecting the sequence of the target gene, the mRNA was detected using a *YFP* probe, identifying the *YFP* sequence inserted into the gene sequence. A case in point is the *ORMDL* gene, where the α-*YFP* probe failed to detect the intended protein. While the insertions in the remaining genes seemed correct, I cannot assert with confidence that none were similar to *ORMDL*, and thus I explored the mRNA localisation of some other gene than reported. Notably, that should not be the case for Lac, whose *YFP* and exon probe co-localisation were confirmed in Chapter 5. Furthermore, some of the *YFP* traps are heterozygous, hence only half of the mRNA molecules might be visualised. This could potentially skew the perceived quantity,

though the primary focus of Chapter 3 was on presence in glia. Finally, the analysis of presence was restricted to the periphery of the glial cell, not its entirety. The assessment of mRNA in projections was qualitative and performed in 2D. Given that the projection and cell are volumetric, a 3D assessment would be beneficial, particularly for the mRNAs where only a few molecules were detected.

6.5.2 Chapter 4 limitations

The driver employed, Repo-GAL4, was pan-glial, thus driving expression of *Lac*-RNAi in all larval glia. This raises questions about whether an NMJ phenotype is directly caused by the lack of mRNA localisation and protein presence specifically at the glial periphery at the NMJ, or if it is a secondary effect stemming from prior improper development caused by the knockdown, which might have impacted other glial cells, such as those in the CNS. Another limitation is that the RNAi lines may inadvertently target unintended genes, as I have not verified this for every line used, but only for *Lac*-RNAi line.

Furthermore, the spaced potassium stimulation protocol does not measure synaptogenesis, but immature synapse formation, as quantified by the emergence of “ghost boutons”. Synapse maturation experiments would have to be performed to understand the detailed role of the candidate transcript knockdown in glia on both the active zone formation, but also synapse maturation. Additionally, the spaced potassium stimulation protocol showed significant variability during my experiments. Observing a fluctuation in “ghost bouton” numbers from a given experiment does not guarantee, in my experience, that I have captured all potential phenotypes for various genes. Similarly, area quantifications might be affected by variability in selecting 3rd

instar larvae. That said, I supplemented my observations with the crawling assay, which increased my confidence when selecting *Lac* as the gene to focus on.

Finally, in Chapter 4, knockdown of several transcripts resulted in intriguing phenotypes. However, due to time constraints and limited resources, with me being the primary researcher, not all were explored in depth. For example, the *Vha55*-RNAi brain phenotype has yet to be fully investigated.

6.5.3 Chapter 5 Limitations

The quantification from the Lac::YFP spaced potassium stimulation experiment does not conclusively reflect variations in *Lac* translation or protein synthesis. When using a confocal microscope, subtle changes in signal intensity due to variations in translation might go undetected. Employing super-resolution microscopy would provide a more definitive assessment of such changes. Moreover, the mere consistency of mRNA levels does not preclude altered mRNA transport and translation dynamics. To genuinely observe if mRNA transport and translation occurs, one could use experiments employing techniques like MS2-MCP tagging to track mRNA transport live, and SunTag or FLARIM to detect translation [338, 339, 362]. Similarly, the association of *Lac* mRNA molecules with the BBB area does not inherently signify their higher concentration near on in these structures, especially since these areas were observed in 2D. Super-resolution microscopy could, again, demonstrate how close those molecules are to the BBB.

When I tried to explore the possibility that the mRNA binding protein Imp transports *Lac* mRNA, I observed that *Imp*-RNAi knockdown in glia abolishes glial NMJ projections. This in itself is an interesting phenotype worth exploring, but I did not have an opportunity and time to do that. Similar limitation applies to the observation that *Lac*

exon, and not intron, is present at the glial periphery. Assuming *Lac* mRNA transport to the periphery leads to its translation, based on the fact that mature mRNA and not pre-mRNA is transported to the periphery, it would be worth exploring whether ribosomes are present at the glial cell periphery, and if there is scope for any newly translated protein to acquire post-translational modifications at the periphery, something which I did not have the opportunity to do.

Glial subtype experiments and the phenotypes which I observed had their own set of challenges. The strength of drivers might differ, and some glial drivers might influence glial subtypes other than their intended targets [111]. Simultaneously, both for Repo-GAL4 and the glial subtype specific drivers, *Lac* was knocked down since hatching, which means developmental defects cannot be differentiated from structural synaptic plasticity defects. This is something which has been discussed both in the context of Chapter 4 and Chapter 5 experiments, though other Davis lab members have now performed temperature sensitive knockdown of *Lac*, confirming that the phenotype was much milder, thus suggesting the predominantly developmental nature of the observed defects (Dominika Syska, Davis lab, unpublished). Yet, to explore purely structural synaptic plasticity related effects purely related to the NMJ, one would have to design a complex experiment to impede the mRNA transport by 3'UTR or motor protein manipulations, preferably in a temperature-sensitive manner, something which I did not have the opportunity to do. Finally, in my hypothesis about Lac function, I tried to link the crawling phenotype observed to the observed NMJ morphology, but I established in Chapter 4 that *Lac*-RNAi larval brain anatomy is also affected. Thus, it might be that NMJ morphology and physiology are not the only causes of the observed crawling defects, and brain circuitry related to crawling behaviours is also affected [341]. Moreover, the same limitation mentioned in Chapter 4 limitations section (6.5.2)

applies to the spaced potassium stimulation experiments employed in this chapter, in that they measure active zones formation, not synaptogenesis, and thus conclusions cannot be drawn directly in relation to the synapse maturation process with regards to *Lac* RNAi knockdown.

To summarise, in addressing these limitations, I approach them with a problem-solving mindset for future studies, some already underway in our laboratory. This will aid in refining experimental protocols and generating more conclusive results. I would like to expand on the promising future experimental avenues next.

6.6 Future directions

Throughout my experiments, I have explored questions surrounding the role of glial cells in structural synaptic plasticity. Nevertheless, several queries remain, and numerous interesting experiments can be designed based on the research described in this study. Many more of the candidate transcripts I explored in Chapter 4 merit in-depth studies. Investigating the other SJ proteins which I worked on, like Nrv2, Gli, Atpα, cold and Nrg, could be the starting point, especially considering their potential as IgLON-like partners for Lac. Examining heterophilic adhesion between these proteins and Lac, or their own homophilic adhesion, would be a good approach. A similar idea has been explored by Strigini et al. before, based on their exploration of Gli [205]. Even though they did not find any evidence supporting Gli binding Lac, they noted that Gli is a type of electrotactin, much like *Drosophila* Neurotactin (Nrt) and vertebrate Neuroligins. Since Nrt has been identified to facilitate different types of cell adhesion with Amalgam, and Amalgam has a significant resemblance in its amino acid sequence to Lac, exploring the potential interactions of other electrotactins with Lac could be worthwhile [205, 299, 303, 305, 363-365].

My research also merits further exploration of brain phenotypes, particularly the extended VNC phenotype seen in *Lac-RNAi* and *cold*-RNAi. Since it is a documented phenomenon, understanding its correlation with cellular size adjustment, akin to the tracheal system, would further clarify the molecular role of Lac in the development of these two seemingly unrelated anatomical structures [204, 277-279]. The absence of glial projections at the NMJ in *shot*-RNAi, given the role of shot as a cytoskeletal linker, similarly warrants further exploration. Assessing actin and microtubule differences in control versus *shot*-RNAi or *shot* mutant NMJ would be a starting point to understand the cause of this glial phenotype.

For Lac-specific investigations, I would proceed with previously mentioned experiments, including the attempt to identify the mRNA localisation signal sequences in *Lac* 3' or 5'UTR. A particularly promising experiment aiming to address this, which I considered and designed, but was unable to execute, is currently being undertaken by a lab colleague. In it, GFP replaces the *Lac* sequence and such construct is placed under UAS control for selective expression in glial cells, potentially illuminating the *Lac* mRNA localisation signal within 3'UTR or 5'UTR (Figure 6-1). Beyond this, electrophysiology assessments on *Lac* knockdown or mutant could help to gauge the impact of the absence of Lac on synaptic potentiation. Super-resolution imaging of SJs in *Lac* knockdown or mutant can also provide insights into the *Lac* mRNA's position or SJ ultrastructure impairment in the absence of Lac.

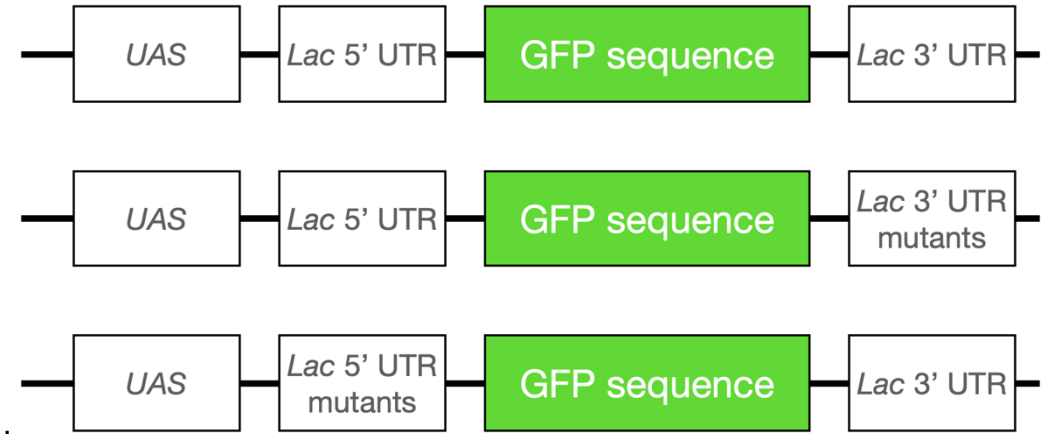

Figure 6-1 Suggested future experiment to test *Lac* mRNA localisation signal

An example of an experimental design to test the role of Lac 3'UTR and 5'UTR mutations on the mRNA localisation. Lac is replaced with GFP sequence to be able to verify the protein presence at cell periphery. The construct is placed under UAS control for selective expression in glial cells under the control of a given driver. The top construct is used to determine whether such construct is stable, something which can also be confirmed using qPCR against GFP sequence. The middle and bottom constructs are schematic representations of numerous constructs which could then be designed to be compared to the top construct in their mRNA and GFP signal location. If one of the mutants affects the localisation sequence, it should not be localised to the same regions as the control - top construct. Though a representation, this schematic shows how *Lac* mRNA localisation sequence could be determined experimentally. An extended version of this experiment is already underway in our laboratory.

Lastly, to study whether *Lac* is transported upon spaced potassium stimulation, the assay could be followed by imaging of MS2-MCP tagged *Lac* transcripts. Finally, using FLARIM, which is a technique that adapts smFISH and fluorescent labelling to detect interactions between ribosomes and mRNA of interest, could clarify whether *Lac* is locally translated at the NMJ. If it was detected that translation occurs, the molecular machinery present at the glial cell periphery to facilitate that could be explored to provide a fine-scale view of translation dynamics.

Often in research, broad questions lead to specialised niches; my journey took me into the specific domain of *Drosophila* BBB, SJs, localised mRNA and their importance in the structural synaptic plasticity of the NMJ. These are not the only important aspects of glial biology relevant to synaptic plasticity, and more questions remain to be answered. How consistent and widespread is the interaction between glia and synapses? It is known that astrocytes and PSCs are members of tripartite synapses, but what about other glial cell subtypes? Beyond homeostasis and the regulation of ions, neurotransmitters, and gliotransmitters, do glial cells actively transmit signals? While calcium waves in glia are well-documented, their potential to send electrical signals remains a topic for exploration [13, 30, 33, 96-98, 366]. Do glial cells have distinct subpopulations which release specific sets of gliotransmitters or ions, much like neurons? Naturally, we are aware of distinct glial cell subtypes, like among astrocytes, but it is also known that not all astrocytes perform the same functions. The extent of their specialisation could be a fascinating topic of exploration.

The mRNA localisation and local translation in glial cells fit well into these considerations, and those topics are also in their infancy, with more progress being made in recent years. The open questions which remain are: Do the molecular mechanisms governing mRNA localisation in various glial types mirror those seen in oligodendrocytes, described in the Introduction chapter (Figure 1-5), or do they differ? If they differ, how? And would such mechanisms be conserved between species, for example between invertebrates like *Drosophila* and humans? Furthermore, can these mechanisms or the types of localised mRNAs be disrupted themselves in neurodegenerative and neuropsychiatric conditions? The simplicity of *Drosophila* makes it an ideal model for such investigations, offering a clearer view of individual

glial cell projections, ease of dissection and live imaging, and a plethora of genetic and neuroscientific tools at the researcher's disposal.

References

[1] D. S. Gala, J. S. Titlow, R. O. Teodoro, and I. Davis, "Far from home: the role of glial mRNA localization in synaptic plasticity," (in eng), *RNA,* vol. 29, no. 2, pp. 153-169, Feb 2023, doi: 10.1261/rna.079422.122.

[2] J. Y. Lee *et al.*, "Absolute quantitation of individual SARS-CoV-2 RNA molecules provides a new paradigm for infection dynamics and variant differences," (in eng), *Elife,* vol. 11, Jan 20 2022, doi: 10.7554/eLife.74153.

[3] G. Santoro, M. D. Wood, L. Merlo, G. P. Anastasi, F. Tomasello, and A. Germanò, "THE ANATOMIC LOCATION OF THE SOUL FROM THE HEART, THROUGH THE BRAIN, TO THE WHOLE BODY, AND BEYOND: A JOURNEY THROUGH WESTERN HISTORY, SCIENCE, AND PHILOSOPHY," *Neurosurgery,* vol. 65, no. 4, pp. 633-643, 2009, doi: 10.1227/01.neu.0000349750.22332.6a.

[4] F. López-Muñoz, G. Rubio, J. D. Molina, and C. Alamo, "The pineal gland as physical tool of the soul faculties: A persistent historical connection," *Neurología (English Edition),* vol. 27, no. 3, pp. 161-168, 2012/04/01/ 2012, doi: https://doi.org/10.1016/j.nrleng.2012.04.007.

[5] F. G. Barker, "Phineas among the phrenologists: the American crowbar case and nineteenth-century theories of cerebral localization," (in eng), *J Neurosurg,* vol. 82, no. 4, pp. 672-82, Apr 1995, doi: 10.3171/jns.1995.82.4.0672.

[6] F. López-Muñoz, J. Boya, and C. Alamo, "Neuron theory, the cornerstone of neuroscience, on the centenary of the Nobel Prize award to Santiago Ramón y Cajal," (in eng), *Brain Res Bull,* vol. 70, no. 4-6, pp. 391-405, Oct 16 2006, doi: 10.1016/j.brainresbull.2006.07.010.

[7] C. Sotelo, "The History of the Synapse," (in eng), *Anat Rec (Hoboken),* vol. 303, no. 5, pp. 1252-1279, May 2020, doi: 10.1002/ar.24392.

[8] B. W. Connors and M. A. Long, "Electrical synapses in the mammalian brain," (in eng), *Annu Rev Neurosci,* vol. 27, pp. 393-418, 2004, doi: 10.1146/annurev.neuro.26.041002.131128.

[9] L. F. Abbott and S. B. Nelson, "Synaptic plasticity: taming the beast," *Nature Neuroscience,* vol. 3, no. 11, pp. 1178-1183, 2000/11/01 2000, doi: 10.1038/81453.

[10] M. F. Bear and R. C. Malenka, "Synaptic plasticity: LTP and LTD," *Current Opinion in Neurobiology,* vol. 4, no. 3, pp. 389-399, 1994/06/01/ 1994, doi: https://doi.org/10.1016/0959-4388(94)90101-5.

[11] W. B. Smith, G. Aakalu, and E. M. Schuman, "Local protein synthesis in neurons Girish Aakalu and," *Current Biology,* pp. 901-903, 2001.

[12] B. L. Lichterman, "Nerve Endings: The Discovery of the Synapse," *BMJ,* 2006, doi: 10.1136/bmj.332.7536.308.

[13] A. Araque, V. Parpura, R. P. Sanzgiri, and P. G. Haydon, "Tripartite synapses: Glia, the unacknowledged partner," *Trends in Neurosciences,* vol. 22, no. 5, pp. 208-215, 1999, doi: 10.1016/S0166-2236(98)01349-6.

[14] E. A. Newman, "New roles for astrocytes: Regulation of synaptic transmission," ed, 2003.

[15] M. M. Halassa, T. Fellin, and P. G. Haydon, "The tripartite synapse: roles for gliotransmission in health and disease," *Trends in Molecular Medicine,* vol. 13, no. 2, pp. 54-63, 2007, doi: 10.1016/j.molmed.2006.12.005.

[16] G. Perea, M. Navarrete, and A. Araque, "Tripartite synapses: astrocytes process and control synaptic information," ed, 2009.

[17] A. Pérez-Alvarez and A. Araque, "Astrocyte-Neuron Interaction at Tripartite Synapses," *Current Drug Targets,* 2013, doi: 10.2174/13894501113149990203.

[18] A. Panatier and R. Robitaille, "Astrocytic mGluR5 and the tripartite synapse," ed, 2016.

[19] E. A. Newman, "Glia and Synaptic Transmission," 2013.

[20] U. Ndubaku and M. E. de Bellard, "Glial cells: old cells with new twists," (in eng), *Acta Histochem,* vol. 110, no. 3, pp. 182-95, 2008, doi: 10.1016/j.acthis.2007.10.003.

[21] N. J. Allen and B. A. Barres, "Glia — more than just brain glue," *Nature,* vol. 457, no. 7230, pp. 675-677, 2009/02/01 2009, doi: 10.1038/457675a.

[22] M. R. Freeman and D. H. Rowitch, "Evolving concepts of gliogenesis: a look way back and ahead to the next 25 years," (in eng), *Neuron,* vol. 80, no. 3, pp. 613-23, Oct 30 2013, doi: 10.1016/j.neuron.2013.10.034.

[23] C. I. De Zeeuw and T. M. Hoogland, "Reappraisal of Bergmann glial cells as modulators of cerebellar circuit function," (in eng), *Front Cell Neurosci,* vol. 9, p. 246, 2015, doi: 10.3389/fncel.2015.00246.

[24] A. Bringmann *et al.*, "Müller cells in the healthy and diseased retina," (in eng), *Prog Retin Eye Res,* vol. 25, no. 4, pp. 397-424, Jul 2006, doi: 10.1016/j.preteyeres.2006.05.003.

[25] M. Bradl and H. Lassmann, "Oligodendrocytes: biology and pathology," (in eng), *Acta Neuropathol,* vol. 119, no. 1, pp. 37-53, Jan 2010, doi: 10.1007/s00401-009-0601-5.

[26] M. Andoh and R. Koyama, "Microglia regulate synaptic development and plasticity," *Developmental Neurobiology,* vol. 81, no. 5, pp. 568-590, 2021, doi: 10.1002/dneu.22814.

[27] W. Wittkowski, "Tanycytes and pituicytes: morphological and functional aspects of neuroglial interaction," (in eng), *Microsc Res Tech,* vol. 41, no. 1, pp. 29-42, Apr 01 1998, doi: 10.1002/(SICI)1097-0029(19980401)41:1<29::AID-JEMT4>3.0.CO;2-P.

[28] M. R. Del Bigio, "Ependymal cells: biology and pathology," (in eng), *Acta Neuropathol,* vol. 119, no. 1, pp. 55-73, Jan 2010, doi: 10.1007/s00401-009-0624-y.

[29] K. R. Jessen, R. Mirsky, and A. C. Lloyd, "Schwann cells: Development and role in nerve repair," *Cold Spring Harbor Perspectives in Biology,* vol. 7, no. 7, pp. 1-15, 2015, doi: 10.1101/cshperspect.a020487.

[30] P. Alvarez-Suarez, M. Gawor, and T. J. Prószyński, "Perisynaptic schwann cells - The multitasking cells at the developing neuromuscular junctions," *Seminars in Cell and Developmental Biology,* no. December 2019, pp. 0-1, 2020, doi: 10.1016/j.semcdb.2020.02.011.

[31] M. Hanani, "Satellite glial cells in sympathetic and parasympathetic ganglia: in search of function," (in eng), *Brain Res Rev,* vol. 64, no. 2, pp. 304-27, Sep 24 2010, doi: 10.1016/j.brainresrev.2010.04.009.

[32] V. Grubišić and B. D. Gulbransen, "Enteric glia: the most alimentary of all glia," (in eng), *J Physiol,* vol. 595, no. 2, pp. 557-570, 01 15 2017, doi: 10.1113/JP271021.

[33] A. Araque, G. Carmignoto, and P. G. Haydon, "Dynamic signaling between astrocytes and neurons," (in eng), *Annu Rev Physiol,* vol. 63, pp. 795-813, 2001, doi: 10.1146/annurev.physiol.63.1.795.

[34] M. Blanco-Urrejola *et al.*, "RNA Localization and Local Translation in Glia in Neurological and Neurodegenerative Diseases: Lessons from Neurons," *Cells,* 2021, doi: 10.3390/cells10030632.

[35] A. J. Barker and E. M. Ullian, "Astrocytes and synaptic plasticity," *Neuroscientist,* vol. 16, no. 1, pp. 40-50, 2010, doi: 10.1177/1073858409339215.

[36] M. De Pittà, N. Brunel, and A. Volterra, "Astrocytes: Orchestrating synaptic plasticity?," *Neuroscience,* vol. 323, pp. 43-61, 2016, doi: 10.1016/j.neuroscience.2015.04.001.

[37] R. Min, M. Santello, and T. Nevian, "The computational power of astrocyte mediated synaptic plasticity," *Frontiers in Computational Neuroscience,* vol. 6, no. OCTOBER 2012, pp. 1-15, 2012, doi: 10.3389/fncom.2012.00093.

[38] Y. Ota, A. T. Zanetti, and R. M. Hallock, "The role of astrocytes in the regulation of synaptic plasticity and memory formation," *Neural Plasticity,* vol. 2013, 2013, doi: 10.1155/2013/185463.

[39] Y. Zhou, A. Shao, Y. Yao, S. Tu, Y. Deng, and J. Zhang, "Dual roles of astrocytes in plasticity and reconstruction after traumatic brain injury," *Cell Communication and Signaling,* vol. 18, no. 1, pp. 1-16, 2020, doi: 10.1186/s12964-020-00549-2.

[40] N. A. Perez-Catalan, C. Q. Doe, and S. D. Ackerman, "The role of astrocyte-mediated plasticity in neural circuit development and function," *Neural Development,* vol. 16, no. 1, pp. 1-14, 2021, doi: 10.1186/s13064-020-00151-9.

[41] J. Wahis, M. Hennes, L. Arckens, and M. G. Holt, "Star power: the emerging role of astrocytes as neuronal partners during cortical plasticity," *Current Opinion in Neurobiology,* vol. 67, pp. 174-182, 2021, doi: 10.1016/j.conb.2020.12.001.

[42] F. Petrelli and P. Bezzi, "Novel insights into gliotransmitters," *Current Opinion in Pharmacology,* vol. 26, no. Table 1, pp. 138-145, 2016, doi: 10.1016/j.coph.2015.11.010.

[43] K. Bohmbach, M. K. Schwarz, S. Schoch, and C. Henneberger, "The structural and functional evidence for vesicular release from astrocytes in situ," *Brain Research Bulletin,* vol. 136, pp. 65-75, 2018, doi: 10.1016/j.brainresbull.2017.01.015.

[44] A. Lebedeva, A. Plata, O. Nosova, O. Tyurikova, and A. Semyanov, "Activity-dependent changes in transporter and potassium currents in hippocampal astrocytes," *Brain Research Bulletin,* vol. 136, no. May 2017, pp. 37-43, 2018, doi: 10.1016/j.brainresbull.2017.08.015.

[45] N. Mazaré *et al.*, "Local Translation in Perisynaptic Astrocytic Processes Is Specific and Changes after Fear Conditioning," *Cell Reports,* 2020, doi: 10.1016/j.celrep.2020.108076.

[46] D. Sapkota *et al.*, "Activity-dependent translation dynamically alters the proteome of the perisynaptic astrocyte process," (in eng), *Cell Rep,* vol. 41, no. 3, p. 111474, Oct 18 2022, doi: 10.1016/j.celrep.2022.111474.

[47] B. R. D'Arcy and D. L. Silver, "Local gene regulation in radial glia: Lessons from across the nervous system," (in eng), *Traffic,* vol. 21, no. 12, pp. 737-748, 12 2020, doi: 10.1111/tra.12769.

[48] S. Medrano and O. Steward, "Differential mRNA localization in astroglial cells in culture," *Journal of Comparative Neurology,* vol. 430, no. 1, pp. 56-71, 2001, doi: 10.1002/1096-9861(20010129)430:1<56::AID-CNE1014>3.0.CO;2-Y.

[49] K. Sakers *et al.*, "Astrocytes locally translate transcripts in their peripheral processes," *Proceedings of the National Academy of Sciences of the United States of America,* vol. 114, no. 19, pp. E3830-E3838, 2017, doi: 10.1073/pnas.1617782114.

[50] K. Sakers *et al.*, "Loss of Quaking RNA binding protein disrupts the expression of genes associated with astrocyte maturation in mouse brain," (in eng), *Nat Commun,* vol. 12, no. 1, p. 1537, 03 09 2021, doi: 10.1038/s41467-021-21703-5.

[51] O. de Faria, H. Pivonkova, B. Varga, S. Timmler, K. A. Evans, and R. T. Káradóttir, "Periods of synchronized myelin changes shape brain function and plasticity," (in eng), *Nat Neurosci,* vol. 24, no. 11, pp. 1508-1521, 11 2021, doi: 10.1038/s41593-021-00917-2.

[52] R. D. Fields and O. Bukalo, "Myelin makes memories," (in eng), *Nat Neurosci,* vol. 23, no. 4, pp. 469-470, 04 2020, doi: 10.1038/s41593-020-0606-x.

[53] S. Pan, S. R. Mayoral, H. S. Choi, J. R. Chan, and M. A. Kheirbek, "Preservation of a remote fear memory requires new myelin formation," (in eng), *Nat Neurosci,* vol. 23, no. 4, pp. 487-499, 04 2020, doi: 10.1038/s41593-019-0582-1.

[54] C. M. Bacmeister *et al.*, "Motor learning promotes remyelination via new and surviving oligodendrocytes," (in eng), *Nat Neurosci,* vol. 23, no. 7, pp. 819-831, 07 2020, doi: 10.1038/s41593-020-0637-3.

[55] A. N. Hughes and B. Appel, "Oligodendrocytes express synaptic proteins that modulate myelin sheath formation," (in eng), *Nat Commun,* vol. 10, no. 1, p. 4125, 09 11 2019, doi: 10.1038/s41467-019-12059-y.

[56] M. Jang, E. Gould, J. Xu, E. J. Kim, and J. H. Kim, "Oligodendrocytes regulate presynaptic properties and neurotransmission through bdnf signaling in the mouse brainstem," *eLife,* vol. 8, pp. 1-26, 2019, doi: 10.7554/eLife.42156.

[57] S. J. Raiker, H. Lee, K. T. Baldwin, Y. Duan, P. Shrager, and R. J. Giger, "Oligodendrocyte-myelin glycoprotein and nogo negatively regulate activity-dependent synaptic plasticity," *Journal of Neuroscience,* vol. 30, no. 37, pp. 12432-12445, 2010, doi: 10.1523/JNEUROSCI.0895-10.2010.

[58] R. Káradóttir, N. B. Hamilton, Y. Bakiri, and D. Attwell, "Spiking and nonspiking classes of oligodendrocyte precursor glia in CNS white matter," (in eng), *Nat Neurosci,* vol. 11, no. 4, pp. 450-6, Apr 2008, doi: 10.1038/nn2060.

[59] Y. Yamazaki *et al.*, "Modulatory effects of oligodendrocytes on the conduction velocity of action potentials along axons in the alveus of the rat hippocampal CA1 region," (in eng), *Neuron Glia Biol,* vol. 3, no. 4, pp. 325-34, Nov 2007, doi: 10.1017/S1740925X08000070.

[60] S. Hofstetter, I. Tavor, S. Tzur Moryosef, and Y. Assaf, "Short-term learning induces white matter plasticity in the fornix," (in eng), *J Neurosci,* vol. 33, no. 31, pp. 12844-50, Jul 31 2013, doi: 10.1523/JNEUROSCI.4520-12.2013.

[61] J. Scholz, M. C. Klein, T. E. Behrens, and H. Johansen-Berg, "Training induces changes in white-matter architecture," (in eng), *Nat Neurosci,* vol. 12, no. 11, pp. 1370-1, Nov 2009, doi: 10.1038/nn.2412.

[62] C. Sampaio-Baptista *et al.*, "Motor skill learning induces changes in white matter microstructure and myelination," (in eng), *J Neurosci,* vol. 33, no. 50, pp. 19499-503, Dec 11 2013, doi: 10.1523/JNEUROSCI.3048-13.2013.

[63] M. È. Tremblay and A. K. Majewska, "A role for microglia in synaptic plasticity?," *Communicative and Integrative Biology,* vol. 4, no. 2, pp. 220-222, 2011, doi: 10.4161/cib.4.2.14506.

[64] D. P. Schafer *et al.*, "Microglia sculpt postnatal neural circuits in an activity and complement-dependent manner," (in eng), *Neuron,* vol. 74, no. 4, pp. 691-705, May 24 2012, doi: 10.1016/j.neuron.2012.03.026.

[65] M. Ě. Tremblay, R. L. Lowery, and A. K. Majewska, "Microglial interactions with synapses are modulated by visual experience," *PLoS Biology,* vol. 8, no. 11, 2010, doi: 10.1371/journal.pbio.1000527.

[66] G. O. Sipe, R. L. Lowery, M. Tremblay, E. A. Kelly, C. E. Lamantia, and A. K. Majewska, "Microglial P2Y12 is necessary for synaptic plasticity in mouse visual cortex," *Nature Communications,* vol. 7, 2016, doi: 10.1038/ncomms10905.

[67] M. É. Tremblay, "The role of microglia at synapses in the healthy CNS: Novel insights from recent imaging studies," *Neuron Glia Biology,* vol. 7, no. 1, pp. 67-76, 2012, doi: 10.1017/S1740925X12000038.

[68] G. P. Morris, I. A. Clark, R. Zinn, and B. Vissel, "Microglia: A new frontier for synaptic plasticity, learning and memory, and neurodegenerative disease research," *Neurobiology of Learning and Memory,* vol. 105, pp. 40-53, 2013, doi: 10.1016/j.nlm.2013.07.002.

[69] Y. Wu, L. Dissing-Olesen, B. A. MacVicar, and B. Stevens, "Microglia: Dynamic Mediators of Synapse Development and Plasticity," *Trends in Immunology,* vol. 36, no. 10, pp. 605-613, 2015, doi: 10.1016/j.it.2015.08.008.

[70] Y. Zaki and D. J. Cai, "Creating Space for Synaptic Formation—A New Role for Microglia in Synaptic Plasticity," *Cell,* vol. 182, no. 2, pp. 265-267, 2020, doi: 10.1016/j.cell.2020.06.042.

[71] B. Stevens *et al.*, "The classical complement cascade mediates CNS synapse elimination," (in eng), *Cell,* vol. 131, no. 6, pp. 1164-78, Dec 14 2007, doi: 10.1016/j.cell.2007.10.036.

[72] P. Gasque *et al.*, "The receptor for complement anaphylatoxin C3a is expressed by myeloid cells and nonmyeloid cells in inflamed human central nervous system: analysis in multiple sclerosis and bacterial meningitis," (in eng), *J Immunol,* vol. 160, no. 7, pp. 3543-54, Apr 01 1998.

[73] N. J. Allen and D. A. Lyons, "Glia as architects of central nervous system formation and function," (in eng), *Science,* vol. 362, no. 6411, pp. 181-185, 10 12 2018, doi: 10.1126/science.aat0473.

[74] L. M. Meservey, V. V. Topkar, and M. m. Fu, "mRNA Transport and Local Translation in Glia," *Trends in Cell Biology,* vol. 31, no. 6, pp. 419-423, 2021, doi: 10.1016/j.tcb.2021.03.006.

[75] M. Oudart, R. Tortuyaux, P. Mailly, N. Mazaré, A. C. Boulay, and M. Cohen-Salmon, "AstroDot - A new method for studying the spatial distribution of mRNA in astrocytes," *Journal of Cell Science,* vol. 133, no. 7, 2020, doi: 10.1242/jcs.239756.

[76] M. J. Vasek, J. D. Deajon-jackson, Y. Liu, H. W. Crosby, and S. L. Mo, "Microglia perform local protein synthesis at perisynaptic and phagocytic structures Affiliations : Department of Genetics , Washington University School of Medicine , 660 S . Euclid Ave , Department of Psychiatry , Washington University School of Medicine," 2021.

[77] Y. Zhang *et al.*, "An RNA-sequencing transcriptome and splicing database of glia, neurons, and vascular cells of the cerebral cortex," (in eng), *J Neurosci,* vol. 34, no. 36, pp. 11929-47, Sep 03 2014, doi: 10.1523/JNEUROSCI.1860-14.2014.

[78] K. Campbell and M. Götz, "Radial glia: multi-purpose cells for vertebrate brain development," (in eng), *Trends Neurosci,* vol. 25, no. 5, pp. 235-8, May 2002, doi: 10.1016/s0166-2236(02)02156-2.

[79] L. J. Pilaz, A. L. Lennox, J. P. Rouanet, and D. L. Silver, "Dynamic mRNA Transport and Local Translation in Radial Glial Progenitors of the Developing Brain," *Current Biology,* 2016, doi: 10.1016/j.cub.2016.10.040.

[80] C. Xu *et al.*, "Radial Glial Cell-Neuron Interaction Directs Axon Formation at the Opposite Side of the Neuron from the Contact Site," (in eng), *J Neurosci,* vol. 35, no. 43, pp. 14517-32, Oct 28 2015, doi: 10.1523/JNEUROSCI.1266-15.2015.

[81] M. Sild and E. S. Ruthazer, "Radial glia: progenitor, pathway, and partner," (in eng), *Neuroscientist,* vol. 17, no. 3, pp. 288-302, Jun 2011, doi: 10.1177/1073858410385870.

[82] J. B. Angevine and R. L. Sidman, "Autoradiographic study of cell migration during histogenesis of cerebral cortex in the mouse," (in eng), *Nature,* vol. 192, pp. 766-8, Nov 25 1961, doi: 10.1038/192766b0.

[83] A. J. Fischer and T. A. Reh, "Potential of Müller glia to become neurogenic retinal progenitor cells," (in eng), *Glia,* vol. 43, no. 1, pp. 70-6, Jul 2003, doi: 10.1002/glia.10218.

[84] T. Watanabe, Y. Mio, F. B. Hoshino, S. Nagamatsu, K. Hirosawa, and K. Nakahara, "GLUT2 expression in the rat retina: localization at the apical ends of Müller cells," (in eng), *Brain Res,* vol. 655, no. 1-2, pp. 128-34, Aug 29 1994, doi: 10.1016/0006-8993(94)91606-3.

[85] A. G. van Rossum *et al.*, "Pals1/Mpp5 is required for correct localization of Crb1 at the subapical region in polarized Muller glia cells," (in eng), *Hum Mol Genet,* vol. 15, no. 18, pp. 2659-72, Sep 15 2006, doi: 10.1093/hmg/ddl194.

[86] P. V. Sarthy, M. Fu, and J. Huang, "Subcellular localization of an intermediate filament protein and its mRNA in glial cells," *Molecular and Cellular Biology,* vol. 9, no. 10, pp. 4556-4559, 1989, doi: 10.1128/mcb.9.10.4556.

[87] V. Sarthy and H. Egal, "Transient induction of the glial intermediate filament protein gene in Müller cells in the mouse retina," (in eng), *DNA Cell Biol,* vol. 14, no. 4, pp. 313-20, Apr 1995, doi: 10.1089/dna.1995.14.313.

[88] J. M. Luque and J. G. Richards, "Expression of NMDA 2B receptor subunit mRNA in Bergmann glia," (in eng), *Glia,* vol. 13, no. 3, pp. 228-32, Mar 1995, doi: 10.1002/glia.440130309.

[89] T. López, A. M. López-Colomé, and A. Ortega, "AMPA/KA receptor expression in radial glia," (in eng), *Neuroreport,* vol. 5, no. 4, pp. 504-6, Jan 12 1994, doi: 10.1097/00001756-199401120-00034.

[90] T. López, A. M. López-Colomé, and A. Ortega, "Changes in GluR4 expression induced by metabotropic receptor activation in radial glia cultures," (in eng), *Brain Res Mol Brain Res,* vol. 58, no. 1-2, pp. 40-6, Jul 15 1998, doi: 10.1016/s0169-328x(98)00094-1.

[91] R. Riquelme, C. P. Miralles, and A. L. De Blas, "Bergmann glia GABA(A) receptors concentrate on the glial processes that wrap inhibitory synapses," (in eng), *J Neurosci,* vol. 22, no. 24, pp. 10720-30, Dec 15 2002.

[92] A. Nimmerjahn, E. A. Mukamel, and M. J. Schnitzer, "Motor behavior activates Bergmann glial networks," (in eng), *Neuron,* vol. 62, no. 3, pp. 400-12, May 14 2009, doi: 10.1016/j.neuron.2009.03.019.

[93] E. López-Bayghen, S. Rosas, F. Castelán, and A. Ortega, "Cerebellar Bergmann glia: an important model to study neuron-glia interactions," (in eng), *Neuron Glia Biol,* vol. 3, no. 2, pp. 155-67, May 2007, doi: 10.1017/S1740925X0700066X.

[94] T. R. Shanthaveerrappa and G. H. Bourne, "Nature and Origin of Perispaptic Cells of the Motor End Plate," *International Review of Cytology,* 1967, doi: 10.1016/S0074-7696(08)60816-5.

[95] D. S. Auld and R. Robitaille, "Perisynaptic Schwann cells at the neuromuscular junction: Nerve- and activity-dependent contributions to synaptic efficacy, plasticity, and reinnervation," ed, 2003.

[96] A. Colomar and R. Robitaille, "Glial modulation of synaptic transmission at the nearomuscular junction," ed, 2004.

[97] C. P. Ko and R. Robitaille, "Perisynaptic Schwann Cells at the Neuromuscular Synapse: Adaptable, Multitasking Glial Cells," (in eng), *Cold Spring Harb Perspect Biol,* vol. 7, no. 10, p. a020503, Aug 20 2015, doi: 10.1101/cshperspect.a020503.

[98] Y. Sugiura and W. Lin, "Neuron-glia interactions: the roles of Schwann cells in neuromuscular synapse formation and function," (in eng), *Biosci Rep,* vol. 31, no. 5, pp. 295-302, Oct 2011, doi: 10.1042/BSR20100107.

[99] I. W. Smith, M. Mikesh, Y. I. Lee, and W. J. Thompson, "Terminal Schwann cells participate in the competition underlying neuromuscular synapse elimination," *Journal of Neuroscience,* vol. 33, no. 45, pp. 17724-17736, 2013, doi: 10.1523/JNEUROSCI.3339-13.2013.

[100] R. Castro *et al.*, "Specific labeling of synaptic schwann cells reveals unique cellular and molecular features," *eLife,* 2020, doi: 10.7554/eLife.56935.

[101] S. Aldridge and S. A. Teichmann, "Single cell transcriptomics comes of age," (in eng), *Nat Commun,* vol. 11, no. 1, p. 4307, Aug 27 2020, doi: 10.1038/s41467-020-18158-5.

[102] V. Marx, "Method of the Year: spatially resolved transcriptomics," (in eng), *Nat Methods,* vol. 18, no. 1, pp. 9-14, Jan 2021, doi: 10.1038/s41592-020-01033-y.

[103] J. Sun *et al.*, "Heterogeneity and Molecular Markers for CNS Glial Cells Revealed by Single-Cell Transcriptomics," (in eng), *Cell Mol Neurobiol,* Oct 26 2021, doi: 10.1007/s10571-021-01159-3.

[104] H.-C. Chen, "Boyden Chamber Assay," in *Cell Migration: Developmental Methods and Protocols*, J.-L. Guan Ed. Totowa, NJ: Humana Press, 2005, pp. 15-22.

[105] K. Scott *et al.*, "A chemosensory gene family encoding candidate gustatory and olfactory receptors in Drosophila," (in eng), *Cell,* vol. 104, no. 5, pp. 661-73, Mar 09 2001, doi: 10.1016/s0092-8674(01)00263-x.

[106] M. R. Freeman and J. Doherty, "Glial cell biology in Drosophila and vertebrates," (in eng), *Trends Neurosci,* vol. 29, no. 2, pp. 82-90, Feb 2006, doi: 10.1016/j.tins.2005.12.002.

[107] N. S. Tolwinski, "Introduction: Drosophila-A Model System for Developmental Biology," (in eng), *J Dev Biol,* vol. 5, no. 3, Sep 20 2017, doi: 10.3390/jdb5030009.

[108] H. Keshishian, K. Broadie, A. Chiba, and M. Bate, "The drosophila neuromuscular junction: a model system for studying synaptic development and function," (in eng), *Annu Rev Neurosci,* vol. 19, pp. 545-75, 1996, doi: 10.1146/annurev.ne.19.030196.002553.

[109] J. Brent, K. Werner, and B. D. McCabe, "Drosophila larval NMJ immunohistochemistry," (in eng), *J Vis Exp,* no. 25, Mar 28 2009, doi: 10.3791/1108.

[110] D. H. Rowitch and A. R. Kriegstein, "Developmental genetics of vertebrate glial-cell specification," *Nature,* vol. 468, no. 7321, pp. 214-222, 2010, doi: 10.1038/nature09611.

[111] K. Yildirim, J. Petri, R. Kottmeier, and C. Klämbt, "Drosophila glia: Few cell types and many conserved functions," *Glia,* vol. 67, no. 1, pp. 5-26, 2019, doi: 10.1002/glia.23459.

[112] M. K. DeSalvo *et al.*, "The Drosophila surface glia transcriptome: evolutionary conserved blood-brain barrier processes," (in eng), *Front Neurosci,* vol. 8, p. 346, 2014, doi: 10.3389/fnins.2014.00346.

[113] M. R. Freeman, "Drosophila Central Nervous System Glia," (in eng), *Cold Spring Harb Perspect Biol,* vol. 7, no. 11, Feb 26 2015, doi: 10.1101/cshperspect.a020552.

[114] J. Bittern *et al.*, "Neuron-glia interaction in the Drosophila nervous system," (in eng), *Dev Neurobiol,* vol. 81, no. 5, pp. 438-452, Jul 2021, doi: 10.1002/dneu.22737.

[115] S. D. Ackerman, N. A. Perez-Catalan, M. R. Freeman, and C. Q. Doe, "Astrocytes close a motor circuit critical period," (in eng), *Nature,* vol. 592, no. 7854, pp. 414-420, 04 2021, doi: 10.1038/s41586-021-03441-2.

[116] H. Liu *et al.*, "Astrocyte-like glial cells physiologically regulate olfactory processing through the modification of ORN-PN synaptic strength in Drosophila," (in eng), *Eur J Neurosci,* vol. 40, no. 5, pp. 2744-54, Sep 2014, doi: 10.1111/ejn.12646.

[117] J. Doherty, M. A. Logan, O. E. Taşdemir, and M. R. Freeman, "Ensheathing glia function as phagocytes in the adult Drosophila brain," (in eng), *J Neurosci,* vol. 29, no. 15, pp. 4768-81, Apr 15 2009, doi: 10.1523/JNEUROSCI.5951-08.2009.

[118] R. Kottmeier *et al.*, "Wrapping glia regulates neuronal signaling speed and precision in the peripheral nervous system of Drosophila," (in eng), *Nat Commun,* vol. 11, no. 1, p. 4491, 09 08 2020, doi: 10.1038/s41467-020-18291-1.

[119] T. Matzat, F. Sieglitz, R. Kottmeier, F. Babatz, D. Engelen, and C. Klämbt, "Axonal wrapping in the Drosophila PNS is controlled by glia-derived neuregulin homolog Vein," (in eng), *Development,* vol. 142, no. 7, pp. 1336-45, Apr 01 2015, doi: 10.1242/dev.116616.

[120] J. F. Silva-Rodrigues *et al.*, "Peripheral axonal ensheathment is regulated by RalA GTPase and the exocyst complex," (in eng), *Development,* vol. 147, no. 3, 02 04 2020, doi: 10.1242/dev.174540.

[121] D. L. Brink, M. Gilbert, X. Xie, L. Petley-Ragan, and V. J. Auld, "Glial processes at the Drosophila larval neuromuscular junction match synaptic growth," *PLoS ONE,* 2012, doi: 10.1371/journal.pone.0037876.

[122] E. Bier *et al.*, "Searching for pattern and mutation in the Drosophila genome with a P-lacZ vector," *Genes & development,* vol. 3, no. 9, pp. 1273-1287, 1989, doi: 10.1101/gad.3.9.1273.

[123] J. R. Fredieu and A. P. Mahowald, "Glial interactions with neurons during Drosophila embryogenesis," *Development,* vol. 106, no. 4, pp. 739-748, 1989.

[124] J. R. Jacobs and C. S. Goodman, "Embryonic development of axon pathways in the Drosophila CNS. I. A glial scaffold appears before the first growth cones," *Journal of Neuroscience,* vol. 9, no. 7, pp. 2402-2411, 1989, doi: 10.1523/jneurosci.09-07-02402.1989.

[125] D. J. Montell and C. S. Goodman, "Drosophila laminin: Sequence of B2 subunit and expression of all three subunits during embryogenesis," *Journal of Cell Biology,* vol. 109, no. 5, pp. 2441-2453, 1989, doi: 10.1083/jcb.109.5.2441.

[126] K. J. Sepp, J. Schulte, and V. J. Auld, "Developmental dynamics of peripheral glia in Drosophila melanogaster," *Glia,* vol. 30, no. 2, pp. 122-133, 2000, doi: 10.1002/(SICI)1098-1136(200004)30:2<122::AID-GLIA2>3.0.CO;2-B.

[127] E. M. Carpenter and M. Hollyday, "The distribution of neural crest-derived Schwann cells from subsets of brachial spinal segments into the peripheral nerves innervating the chick forelimb," (in eng), *Dev Biol,* vol. 150, no. 1, pp. 160-70, Mar 1992, doi: 10.1016/0012-1606(92)90015-9.

[128] T. Schwabe, A. C. Gontang, and T. R. Clandinin, "More than just glue: The diverse roles of cell adhesion molecules in the Drosophila nervous system," *Cell Adhesion and Migration,* vol. 3, no. 1, pp. 36-42, 2009, doi: 10.4161/cam.3.1.6918.

[129] T. Rival, L. Soustelle, D. Cattaert, C. Strambi, M. Iché, and S. Birman, "Physiological requirement for the glutamate transporter dEAAT1 at the adult Drosophila neuromuscular junction," *Journal of Neurobiology,* 2006, doi: 10.1002/neu.20270.

[130] P. K. Rivlin, R. M. St. Clair, I. Vilinsky, and D. L. Deitcher, "Morphology and Molecular Organization of the Adult Neuromuscular Junction of Drosophila," *Journal of Comparative Neurology,* vol. 468, no. 4, pp. 596-613, 2004, doi: 10.1002/cne.10977.

[131] H. Augustin, Y. Grosjean, K. Chen, Q. Sheng, and D. E. Featherstone, "Nonvesicular release of glutamate by glial xCT transporters suppresses glutamate receptor clustering in vivo," *Journal of Neuroscience,* vol. 27, no. 1, pp. 111-123, 2007, doi: 10.1523/JNEUROSCI.4770-06.2007.

[132] K. S. Kerr *et al.*, "Glial wingless/wnt regulates glutamate receptor clustering and synaptic physiology at the Drosophila neuromuscular junction," *Journal of Neuroscience,* vol. 34, no. 8, pp. 2910-2920, 2014, doi: 10.1523/JNEUROSCI.3714-13.2014.

[133] Y. Fuentes-Medel, J. Ashley, R. Barria, R. Maloney, M. Freeman, and V. Budnik, "Integration of a retrograde signal during synapse formation by glia-secreted TGF-β ligand," *Current Biology,* 2012, doi: 10.1016/j.cub.2012.07.063.

[134] Y. Fuentes-Medel, M. A. Logan, J. Ashley, B. Ataman, V. Budnik, and M. R. Freeman, "Glia and muscle sculpt neuromuscular arbors by engulfing destabilized synaptic boutons and shed presynaptic debris," *PLoS Biology,* vol. 7, no. 8, 2009, doi: 10.1371/journal.pbio.1000184.

[135] Z. Liu, Y. Chen, D. Wang, S. Wang, and Y. Q. Zhang, "Distinct presynaptic and postsynaptic dismantling processes of Drosophila neuromuscular junctions during metamorphosis," *Journal of Neuroscience,* vol. 30, no. 35, pp. 11624-11634, 2010, doi: 10.1523/JNEUROSCI.0410-10.2010.

[136] R. Danjo, F. Kawasaki, and R. W. Ordway, "A tripartite synapse model in Drosophila," *PLoS ONE,* vol. 6, no. 2, pp. 2-7, 2011, doi: 10.1371/journal.pone.0017131.

[137] A. L. Strauss, F. Kawasaki, and R. W. Ordway, "A distinct perisynaptic glial cell type forms tripartite neuromuscular synapses in the Drosophila adult," *PLoS ONE,* vol. 10, no. 6, pp. 1-13, 2015, doi: 10.1371/journal.pone.0129957.

[138] C. F. Rose, A. Verkhratsky, and V. Parpura, "Astrocyte glutamine synthetase: Pivotal in health and disease," *Biochemical Society Transactions,* vol. 41, no. 6, pp. 1518-1524, 2013, doi: 10.1042/BST20130237.

[139] Y. W. Tsai *et al.*, "Glia-derived exosomal miR-274 targets Sprouty in trachea and synaptic boutons to modulate growth and responses to hypoxia," *Proceedings of the National Academy of Sciences of the United States of America,* vol. 116, no. 49, pp. 24651-24661, 2019, doi: 10.1073/pnas.1902537116.

[140] P. Y. Chen, Y. W. Tsai, Y. J. Cheng, A. Giangrande, and C. T. Chien, "Glial response to hypoxia in mutants of NPAS1/3 homolog Trachealess through Wg signaling to modulate synaptic bouton organization," *PLoS Genetics,* vol. 15, no. 8, pp. 1-25, 2019, doi: 10.1371/journal.pgen.1007980.

[141] F. Kawasaki *et al.*, "Small heat shock proteins mediate cell-autonomous and -nonautonomous protection in a Drosophila model for environmental-stress-induced degeneration," *DMM Disease Models and Mechanisms,* vol. 9, no. 9, pp. 953-964, 2016, doi: 10.1242/dmm.026385.

[142] F. Seidel, "Untersuchungen über das Bildungsprinzip der Keimanlage im Ei der Libelle Platycnemis pennipes.," (in ger), *Wilhelm Roux Arch Entwickl Mech Org,* vol. 119, no. 1, pp. 322-440, Jun 1929, doi: 10.1007/BF02111187.

[143] E. Hafen, A. Kuroiwa, and W. J. Gehring, "Spatial distribution of transcripts from the segmentation gene fushi tarazu during Drosophila embryonic development," *Cell,* vol. 37, no. 3, pp. 833-841, 1984, doi: 10.1016/0092-8674(84)90418-5.

[144] P. W. Ingham, K. R. Howard, and D. Ish-Horowicz, "Transcription pattern of the Drosophila segmentation gene hairy," *Nature,* vol. 318, no. 6045, pp. 439-445, 1985, doi: 10.1038/318439a0.

[145] G. Frigerio, M. Burri, D. Bopp, S. Baumgartner, and M. Noll, "Structure of the segmentation gene paired and the Drosophila PRD gene set as part of a gene network," *Cell,* vol. 47, no. 5, pp. 735-746, 1986, doi: 10.1016/0092-8674(86)90516-7.

[146] H. G. Frohnhofer, R. Lehmann, and C. Nusslein-Volhard, "Manipulating the anteroposterior pattern of the Drosophila embryo," *Journal of Embryology and Experimental Morphology,* vol. 97, no. SUPPL., pp. 169-179, 1986.

[147] D. R. Micklem, "mRNA localisation during development," *Developmental Biology,* vol. 172, no. 2, pp. 377-395, 1995, doi: 10.1006/dbio.1995.8048.

[148] T. L. Williamson *et al.*, "Neurofilaments, radial growth of axons, and mechanisms of motor neuron disease," (in eng), *Cold Spring Harb Symp Quant Biol,* vol. 61, pp. 709-23, 1996.

[149] M. A. Sutton and E. M. Schuman, "Dendritic Protein Synthesis, Synaptic Plasticity, and Memory," *Cell,* vol. 127, no. 1, pp. 49-58, 2006, doi: 10.1016/j.cell.2006.09.014.

[150] D. O. Wang, K. C. Martin, and R. S. Zukin, "Spatially restricting gene expression by local translation at synapses," *Trends in Neurosciences,* vol. 33, no. 4, pp. 173-182, 2010, doi: 10.1016/j.tins.2010.01.005.

[151] V. Rangaraju, S. tom Dieck, and E. M. Schuman, "Local translation in neuronal compartments: how local is local?," *EMBO reports,* vol. 18, no. 5, pp. 693-711, 2017, doi: 10.15252/embr.201744045.

[152] M. Terenzio, G. Schiavo, and M. Fainzilber, "Compartmentalized Signaling in Neurons: From Cell Biology to Neuroscience," *Neuron,* vol. 96, no. 3, pp. 667-679, 2017, doi: 10.1016/j.neuron.2017.10.015.

[153] A. Biever, P. G. Donlin-Asp, and E. M. Schuman, "Local translation in neuronal processes," *Current Opinion in Neurobiology,* vol. 57, pp. 141-148, 2019, doi: 10.1016/j.conb.2019.02.008.

[154] C. E. Holt, K. C. Martin, and E. M. Schuman, "Local translation in neurons: visualization and function," (in eng), *Nat Struct Mol Biol,* vol. 26, no. 7, pp. 557-566, 07 2019, doi: 10.1038/s41594-019-0263-5.

[155] W. C. Xiong, H. Okano, N. H. Patel, J. A. Blendy, and C. Montell, "repo encodes a glial-specific homeo domain protein required in the Drosophila nervous system," *Genes and Development,* vol. 8, no. 8, pp. 981-994, 1994, doi: 10.1101/gad.8.8.981.

[156] L. Sancho, M. Contreras, and N. J. Allen, "Glia as sculptors of synaptic plasticity," *Neuroscience Research,* vol. 167, pp. 17-29, 2021, doi: 10.1016/j.neures.2020.11.005.

[157] A. Butt and A. Verkhratsky, "Neuroglia: Realising their true potential," *Brain and Neuroscience Advances,* vol. 2, pp. 239821281881749-239821281881749, 2018, doi: 10.1177/2398212818817495.

[158] O. Steward and G. A. Banker, "Getting the message from the gene to the synapse: sorting and intracellular transport of RNA in neurons," *Trends in Neurosciences,* vol. 15, no. 5, pp. 180-186, 1992, doi: 10.1016/0166-2236(92)90170-D.

[159] M. E. Martone, J. A. Pollock, and M. H. Ellisman, "Subcellular localization of mRNA in neuronal cells: Contributions of high-resolution in situ hybridization techniques," *Molecular Neurobiology,* vol. 18, no. 3, pp. 227-246, 1998, doi: 10.1007/BF02741301.

[160] D. R. Colman, G. Kreibich, A. B. Frey, and D. D. Sabatini, "Synthesis and incorporation of myelin polypeptides into CNS myelin," *Journal of Cell Biology,* vol. 95, no. 2, pp. 598-608, 1982, doi: 10.1083/jcb.95.2.598.

[161] R. M. Gould and G. Mattingly, "Regional localization of RNA and protein metabolism in Schwann cells in vivo," *Journal of Neurocytology,* vol. 19, no. 3, pp. 285-301, 1990, doi: 10.1007/BF01188399.

[162] B. D. Trapp, T. Moench, M. Pulley, E. Barbosa, G. Tennekoon, and J. Griffin, "Spatial segregation of mRNA encoding myelin-specific proteins," *Proceedings of the National Academy of Sciences of the United States of America,* vol. 84, no. 21, pp. 7773-7777, 1987, doi: 10.1073/pnas.84.21.7773.

[163] C. F. Landry, J. B. Watson, T. Kashima, and A. T. Campagnoni, "Cellular influences on RNA sorting in neurons and glia: an in situ hybridization histochemical study," *Molecular Brain Research,* vol. 27, no. 1, pp. 1-11, 1994, doi: 10.1016/0169-328X(94)90178-3.

[164] K. Ainger *et al.*, "Transport and localization of exogenous myelin basic protein mRNA microinjected into oligodendrocytes," *Journal of Cell Biology,* vol. 123, no. 2, pp. 431-441, 1993, doi: 10.1083/jcb.123.2.431.

[165] K. Ainger, D. Avossa, A. S. Diana, C. Barry, E. Barbarese, and J. H. Carson, "Transport and localization elements in myelin basic protein mRNA," *Journal of Cell Biology,* vol. 138, no. 5, pp. 1077-1087, 1997, doi: 10.1083/jcb.138.5.1077.

[166] T. P. Munro *et al.*, "Mutational analysis of a heterogeneous nuclear ribonucleoprotein A2 response element for RNA trafficking," (in eng), *J Biol Chem,* vol. 274, no. 48, pp. 34389-95, Nov 26 1999, doi: 10.1074/jbc.274.48.34389.

[167] R. M. Gould, C. M. Freund, and E. Barbarese, "Myelin-Associated Oligodendrocytic Basic Protein mRNAs Reside at Different Subcellular Locations," *Journal of Neurochemistry,* vol. 73, no. 5, pp. 1913-1924, 2002, doi: 10.1046/j.1471-4159.1999.01913.x.

[168] J. H. Carson, K. Worboys, K. Ainger, and E. Barbarese, "Translocation of myelin basic protein mRNA in oligodendrocytes requires microtubules and kinesin," *Cell Motility and the Cytoskeleton,* vol. 38, no. 4, pp. 318-328, 1997, doi: 10.1002/(sici)1097-0169(1997)38:4<318::aid-cm2>3.0.co;2-%23.

[169] J. H. Carson, H. Cui, W. Krueger, B. Schlepchenko, C. Brumwell, and E. Barbarese, "RNA trafficking in oligodendrocytes," *Results and problems in cell differentiation,* vol. 34, no. May 2014, pp. 69-81, 2001, doi: 10.1007/978-3-540-40025-7_5.

[170] E. Barbarese, C. Brumwell, S. Kwon, H. Cui, and J. H. Carson, "RNA on the road to myelin," *Journal of Neurocytology,* 1999, doi: 10.1023/A:1007097226688.

[171] K. C. Martin and A. Ephrussi, "mRNA Localization: Gene Expression in the Spatial Dimension," *Cell,* vol. 136, no. 4, pp. 719-730, 2009, doi: 10.1016/j.cell.2009.01.044.

[172] P. Percipalle, "New insights into co-transcriptional sorting of mRNA for cytoplasmic transport during development," *Seminars in Cell and Developmental Biology,* vol. 32, pp. 55-62, 2014, doi: 10.1016/j.semcdb.2014.03.009.

[173] N. Neriec and P. Percipalle, "Sorting mRNA Molecules for Cytoplasmic Transport and Localization," *Frontiers in Genetics,* vol. 9, no. November, pp. 1-9, 2018, doi: 10.3389/fgene.2018.00510.

[174] I. Casci and U. B. Pandey, "A fruitful endeavor: Modeling ALS in the fruit fly," *Brain Research,* vol. 1607, pp. 47-74, 2015, doi: 10.1016/j.brainres.2014.09.064.

[175] H. Bolus, K. Crocker, G. Boekhoff-Falk, and S. Chtarbanova, "Modeling neurodegenerative disorders in drosophila melanogaster," *International Journal of Molecular Sciences,* vol. 21, no. 9, 2020, doi: 10.3390/ijms21093055.

[176] R. Islam, E. L. Kumimoto, H. Bao, and B. Zhang, "ALS-linked SOD1 in glial cells enhances ß-N-Methylamino L-Alanine (BMAA)-induced toxicity in Drosophila," *F1000Research,* vol. 1, pp. 1-13, 2012, doi: 10.12688/f1000research.1-47.v1.

[177] J. Gal *et al.*, "ALS mutant SOD1 interacts with G3BP1 and affects stress granule dynamics," (in eng), *Acta Neuropathol,* vol. 132, no. 4, pp. 563-76, 10 2016, doi: 10.1007/s00401-016-1601-x.

[178] M. Da Ros, H. K. Deol, A. Savard, H. Guo, E. M. Meiering, and D. Gibbings, "Wild-type and mutant SOD1 localizes to RNA-rich structures in cells and mice but does not bind RNA," (in eng), *J Neurochem,* vol. 156, no. 4, pp. 524-538, 02 2021, doi: 10.1111/jnc.15126.

[179] D. C. Diaper *et al.*, "Drosophila TDP-43 dysfunction in glia and muscle cells cause cytological and behavioural phenotypes that characterize ALS and FTLD," *Human Molecular Genetics,* vol. 22, no. 19, pp. 3883-3893, 2013, doi: 10.1093/hmg/ddt243.

[180] P. S. Estes *et al.*, "Motor neurons and glia exhibit specific individualized responses to TDP-43 expression in a Drosophila model of amyotrophic lateral sclerosis," *DMM Disease Models and Mechanisms,* vol. 6, no. 3, pp. 721-733, 2013, doi: 10.1242/dmm.010710.

[181] J. S. Titlow *et al.*, "Systematic analysis of YFP traps reveals common mRNA/protein discordance in neural tissues," (in eng), *J Cell Biol,* vol. 222, no. 6, Jun 05 2023, doi: 10.1083/jcb.202205129.

[182] N. Lowe *et al.*, "Analysis of the expression patterns, Subcellular localisations and interaction partners of drosophila proteins using a pigp protein trap library," *Development (Cambridge),* 2014, doi: 10.1242/dev.111054.

[183] J. R. Brent, K. M. Werner, and B. D. McCabe, "Drosophila larval NMJ dissection," *Journal of Visualized Experiments,* 2009, doi: 10.3791/1107.

[184] J. Brent, K. Werner, and B. D. McCabe, "Drosophila larval NMJ immunohistochemistry," *Journal of Visualized Experiments,* 2009, doi: 10.3791/1108.

[185] J. S. Titlow, L. Yang, R. M. Parton, A. Palanca, and I. Davis, "Super-Resolution Single Molecule FISH at the Drosophila Neuromuscular Junction," (in eng), *Methods Mol Biol,* vol. 1649, pp. 163-175, 2018, doi: 10.1007/978-1-4939-7213-5_10.

[186] F. J. Martin *et al.*, "Ensembl 2023," (in eng), *Nucleic Acids Res,* vol. 51, no. D1, pp. D933-D941, Jan 06 2023, doi: 10.1093/nar/gkac958.

[187] X. Xie and V. J. Auld, "Integrins are necessary for the development and maintenance of the glial layers in the Drosophila peripheral nerve," (in eng), *Development,* vol. 138, no. 17, pp. 3813-22, Sep 2011, doi: 10.1242/dev.064816.

[188] M. Buszczak *et al.*, "The carnegie protein trap library: a versatile tool for Drosophila developmental studies," (in eng), *Genetics,* vol. 175, no. 3, pp. 1505-31, Mar 2007, doi: 10.1534/genetics.106.065961.

[189] L. S. Gramates *et al.*, "FlyBase: a guided tour of highlighted features," (in eng), *Genetics,* vol. 220, no. 4, Apr 04 2022, doi: 10.1093/genetics/iyac035.

[190] J. P. Roche, M. C. Packard, S. Moeckel-Cole, and V. Budnik, "Regulation of synaptic plasticity and synaptic vesicle dynamics by the PDZ protein scribble," *Journal of Neuroscience,* 2002, doi: 10.1523/jneurosci.22-15-06471.2002.

[191] B. Ataman *et al.*, "Rapid Activity-Dependent Modifications in Synaptic Structure and Function Require Bidirectional Wnt Signaling," *Neuron,* 2008, doi: 10.1016/j.neuron.2008.01.026.

[192] I. Gaspar, F. Wippich, and A. Ephrussi, "Enzymatic production of single-molecule FISH and RNA capture probes," *RNA,* 2017, doi: 10.1261/rna.061184.117.

[193] L. Y. Jan and Y. N. Jan, "Antibodies to horseradish peroxidase as specific neuronal markers in Drosophila and in grasshopper embryos," (in eng), *Proc Natl Acad Sci U S A,* vol. 79, no. 8, pp. 2700-4, Apr 1982, doi: 10.1073/pnas.79.8.2700.

[194] C. A. Schneider, W. S. Rasband, and K. W. Eliceiri, "NIH Image to ImageJ: 25 years of image analysis," (in eng), *Nat Methods,* vol. 9, no. 7, pp. 671-5, Jul 2012, doi: 10.1038/nmeth.2089.

[195] M. D. Abràmoff, P. J. Magalhães, and S. J. Ram, "Image processing with ImageJ," *Biophotonics international,* vol. 11, no. 7, pp. 36-42, 2004.

[196] A. Imbert *et al.*, "FISH-quant v2: a scalable and modular analysis tool for smFISH image analysis," *bioRxiv,* p. 2021.07.20.453024, 2021, doi: 10.1101/2021.07.20.453024.

[197] Z. D. Piccioli and J. T. Littleton, "Retrograde BMP signaling modulates rapid activity-dependent synaptic growth via presynaptic LIM kinase regulation of cofilin," (in eng), *J Neurosci,* vol. 34, no. 12, pp. 4371-81, Mar 19 2014, doi: 10.1523/JNEUROSCI.4943-13.2014.

[198] M. Balakrishnan, W. J. Sisso, and M. K. Baylies, "Analyzing muscle structure and function throughout the larval instars in live," (in eng), *STAR Protoc,* vol. 2, no. 1, p. 100291, Mar 19 2021, doi: 10.1016/j.xpro.2020.100291.

[199] A. Torres-Méndez *et al.*, "Parallel evolution of a splicing program controlling neuronal excitability in flies and mammals," (in eng), *Sci Adv,* vol. 8, no. 4, p. eabk0445, Jan 28 2022, doi: 10.1126/sciadv.abk0445.

[200] D. J. McLean and M. A. Skowron Volponi, "trajr: An R package for characterisation of animal trajectories," *Ethology,* vol. 124, no. 6, pp. 440-448, 2018, doi: https://doi.org/10.1111/eth.12739.

[201] J. Schulte, U. Tepass, and V. J. Auld, "Gliotactin, a novel marker of tricellular junctions, is necessary for septate junction development in Drosophila," (in eng), *J Cell Biol,* vol. 161, no. 5, pp. 991-1000, Jun 09 2003, doi: 10.1083/jcb.200303192.

[202] J. L. Genova and R. G. Fehon, "Neuroglian, Gliotactin, and the Na+/K+ ATPase are essential for septate junction function in Drosophila," (in eng), *J Cell Biol,* vol. 161, no. 5, pp. 979-89, Jun 09 2003, doi: 10.1083/jcb.200212054.

[203] S. M. Paul, M. Ternet, P. M. Salvaterra, and G. J. Beitel, "The Na+/K+ ATPase is required for septate junction function and epithelial tube-size control in the Drosophila tracheal system," *Development,* 2003, doi: 10.1242/dev.00691.

[204] M. Llimargas, M. Strigini, M. Katidou, D. Karagogeos, and J. Casanova, "Lachesin is a component of a septate junction-based mechanism that controls tube size and epithelial integrity in the Drosophila tracheal system," *Development,* 2004, doi: 10.1242/dev.00917.

[205] M. Strigini, R. Cantera, X. Morin, M. J. Bastiani, M. Bate, and D. Karagogeos, "The IgLON protein Lachesin is required for the blood-brain barrier in Drosophila," (in eng), *Mol Cell Neurosci,* vol. 32, no. 1-2, pp. 91-101, 2006, doi: 10.1016/j.mcn.2006.03.001.

[206] A. Nilton *et al.*, "Crooked, coiled and crimpled are three Ly6-like proteins required for proper localization of septate junction components," (in eng), *Development,* vol. 137, no. 14, pp. 2427-37, Jul 2010, doi: 10.1242/dev.052605.

[207] E. Rouka *et al.*, "The Drosophila septate junctions beyond barrier function: Review of the literature, prediction of human orthologs of the SJ-related proteins and identification of protein

domain families," (in eng), *Acta Physiol (Oxf),* vol. 231, no. 1, p. e13527, Jan 2021, doi: 10.1111/apha.13527.

[208] A. Hijazi, M. Haenlin, L. Waltzer, and F. Roch, "The Ly6 protein coiled is required for septate junction and blood brain barrier organisation in Drosophila," *PLoS ONE,* 2011, doi: 10.1371/journal.pone.0017763.

[209] G. Blanco and R. W. Mercer, "Isozymes of the Na-K-ATPase: heterogeneity in structure, diversity in function," (in eng), *Am J Physiol,* vol. 275, no. 5, pp. F633-50, Nov 1998, doi: 10.1152/ajprenal.1998.275.5.F633.

[210] S. Limmer, A. Weiler, A. Volkenhoff, F. Babatz, and C. Klämbt, "The Drosophila blood-brain barrier: development and function of a glial endothelium," (in eng), *Front Neurosci,* vol. 8, p. 365, 2014, doi: 10.3389/fnins.2014.00365.

[211] F. Galbiati *et al.*, "Identification, sequence and developmental expression of invertebrate flotillins from Drosophila melanogaster," (in eng), *Gene,* vol. 210, no. 2, pp. 229-37, Apr 14 1998, doi: 10.1016/s0378-1119(98)00064-x.

[212] S. Gerdøe-Kristensen, V. K. Lund, H. H. Wandall, and O. Kjaerulff, "Mactosylceramide prevents glial cell overgrowth by inhibiting insulin and fibroblast growth factor receptor signaling," (in eng), *J Cell Physiol,* vol. 232, no. 11, pp. 3112-3127, Nov 2017, doi: 10.1002/jcp.25762.

[213] M. Hoehne, H. G. de Couet, C. A. Stuermer, and K. F. Fischbach, "Loss- and gain-of-function analysis of the lipid raft proteins Reggie/Flotillin in Drosophila: they are posttranslationally regulated, and misexpression interferes with wing and eye development," (in eng), *Mol Cell Neurosci,* vol. 30, no. 3, pp. 326-38, Nov 2005, doi: 10.1016/j.mcn.2005.07.007.

[214] M. J. Palladino, J. E. Bower, R. Kreber, and B. Ganetzky, "Neural dysfunction and neurodegeneration in Drosophila Na+/K+ ATPase alpha subunit mutants," (in eng), *J Neurosci,* vol. 23, no. 4, pp. 1276-86, Feb 15 2003, doi: 10.1523/JNEUROSCI.23-04-01276.2003.

[215] L. A. McGraw, A. G. Clark, and M. F. Wolfner, "Post-mating gene expression profiles of female Drosophila melanogaster in response to time and to four male accessory gland proteins," (in eng), *Genetics,* vol. 179, no. 3, pp. 1395-408, Jul 2008, doi: 10.1534/genetics.108.086934.

[216] N. E. Wolins, J. R. Skinner, M. J. Schoenfish, A. Tzekov, K. G. Bensch, and P. E. Bickel, "Adipocyte protein S3-12 coats nascent lipid droplets," (in eng), *J Biol Chem,* vol. 278, no. 39, pp. 37713-21, Sep 26 2003, doi: 10.1074/jbc.M304025200.

[217] Y. Hu *et al.*, "An integrative approach to ortholog prediction for disease-focused and other functional studies," (in eng), *BMC Bioinformatics,* vol. 12, p. 357, Aug 31 2011, doi: 10.1186/1471-2105-12-357.

[218] H. Härönen *et al.*, "Collagen XIII secures pre- and postsynaptic integrity of the neuromuscular synapse," (in eng), *Hum Mol Genet,* vol. 26, no. 11, pp. 2076-2090, Jun 01 2017, doi: 10.1093/hmg/ddx101.

[219] K. S. Sinsimer, R. A. Jain, S. Chatterjee, and E. R. Gavis, "A late phase of germ plasm accumulation during Drosophila oogenesis requires lost and rumpelstiltskin," (in eng), *Development,* vol. 138, no. 16, pp. 3431-40, Aug 2011, doi: 10.1242/dev.065029.

[220] S. A. Davies *et al.*, "Analysis and inactivation of vha55, the gene encoding the vacuolar ATPase B-subunit in Drosophila melanogaster reveals a larval lethal phenotype," (in eng), *J Biol Chem,* vol. 271, no. 48, pp. 30677-84, Nov 29 1996, doi: 10.1074/jbc.271.48.30677.

[221] T. Hermle, D. Saltukoglu, J. Grünewald, G. Walz, and M. Simons, "Regulation of Frizzled-dependent planar polarity signaling by a V-ATPase subunit," (in eng), *Curr Biol,* vol. 20, no. 14, pp. 1269-76, Jul 27 2010, doi: 10.1016/j.cub.2010.05.057.

[222] T. Schwabe, R. J. Bainton, R. D. Fetter, U. Heberlein, and U. Gaul, "GPCR signaling is required for blood-brain barrier formation in Drosophila," *Cell,* vol. 123, no. 1, pp. 133-144, 2005, doi: 10.1016/j.cell.2005.08.037.

[223] F. Mayer, N. Mayer, L. Chinn, R. L. Pinsonneault, D. Kroetz, and R. J. Bainton, "Evolutionary conservation of vertebrate blood-brain barrier chemoprotective mechanisms in Drosophila," (in eng), *J Neurosci,* vol. 29, no. 11, pp. 3538-50, Mar 18 2009, doi: 10.1523/JNEUROSCI.5564-08.2009.

[224] R. Desai, R. Sarpal, N. Ishiyama, M. Pellikka, M. Ikura, and U. Tepass, "Monomeric α-catenin links cadherin to the actin cytoskeleton," (in eng), *Nat Cell Biol,* vol. 15, no. 3, pp. 261-73, Mar 2013, doi: 10.1038/ncb2685.

[225] J. Jurado, J. de Navascués, and N. Gorfinkiel, "α-Catenin stabilises Cadherin-Catenin complexes and modulates actomyosin dynamics to allow pulsatile apical contraction," (in eng), *J Cell Sci,* vol. 129, no. 24, pp. 4496-4508, Dec 15 2016, doi: 10.1242/jcs.193268.

[226] R. Sarpal, M. Pellikka, R. R. Patel, F. Y. Hui, D. Godt, and U. Tepass, "Mutational analysis supports a core role for Drosophila α-catenin in adherens junction function," (in eng), *J Cell Sci,* vol. 125, no. Pt 1, pp. 233-45, Jan 01 2012, doi: 10.1242/jcs.096644.

[227] L. Hjelmqvist, M. Tuson, G. Marfany, E. Herrero, S. Balcells, and R. Gonzàlez-Duarte, "ORMDL proteins are a conserved new family of endoplasmic reticulum membrane proteins," (in eng), *Genome Biol,* vol. 3, no. 6, p. RESEARCH0027, 2002, doi: 10.1186/gb-2002-3-6-research0027.

[228] K. Kallsen *et al.*, "ORMDL deregulation increases stress responses and modulates repair pathways in Drosophila airways," (in eng), *J Allergy Clin Immunol,* vol. 136, no. 4, pp. 1105-8, Oct 2015, doi: 10.1016/j.jaci.2015.04.009.

[229] J. Malin, C. Rosa Birriel, S. Astigarraga, J. E. Treisman, and V. Hatini, "Sidekick dynamically rebalances contractile and protrusive forces to control tissue morphogenesis," (in eng), *J Cell Biol,* vol. 221, no. 5, May 02 2022, doi: 10.1083/jcb.202107035.

[230] S. Astigarraga *et al.*, "Sidekick is required in developing photoreceptors to enable visual motion detection," (in eng), *Development,* vol. 145, no. 3, Feb 05 2018, doi: 10.1242/dev.158246.

[231] D. N. Nguyen, Y. Liu, M. L. Litsky, and R. Reinke, "The sidekick gene, a member of the immunoglobulin superfamily, is required for pattern formation in the Drosophila eye," (in eng), *Development,* vol. 124, no. 17, pp. 3303-12, Sep 1997, doi: 10.1242/dev.124.17.3303.

[232] H. Uechi and E. Kuranaga, "The Tricellular Junction Protein Sidekick Regulates Vertex Dynamics to Promote Bicellular Junction Extension," (in eng), *Dev Cell,* vol. 50, no. 3, pp. 327-338.e5, Aug 05 2019, doi: 10.1016/j.devcel.2019.06.017.

[233] M. D. Phillips and C. M. Thomas, "Brush border spectrin is required for early endosome recycling in Drosophila," (in eng), *J Cell Sci,* vol. 119, no. Pt 7, pp. 1361-70, Apr 01 2006, doi: 10.1242/jcs.02839.

[234] N. Pogodalla, H. Kranenburg, S. Rey, S. Rodrigues, A. Cardona, and C. Klämbt, "Drosophila ß," (in eng), *Nat Commun,* vol. 12, no. 1, p. 6357, Nov 04 2021, doi: 10.1038/s41467-021-26462-x.

[235] D. Ricolo and S. J. Araujo, "Coordinated crosstalk between microtubules and actin by a spectraplakin regulates lumen formation and branching," (in eng), *Elife,* vol. 9, Oct 28 2020, doi: 10.7554/eLife.61111.

[236] A. Subramanian *et al.*, "Shortstop recruits EB1/APC1 and promotes microtubule assembly at the muscle-tendon junction," (in eng), *Curr Biol,* vol. 13, no. 13, pp. 1086-95, Jul 01 2003, doi: 10.1016/s0960-9822(03)00416-0.

[237] N. Sanchez-Soriano, M. Travis, F. Dajas-Bailador, C. Gonçalves-Pimentel, A. J. Whitmarsh, and A. Prokop, "Mouse ACF7 and drosophila short stop modulate filopodia formation and microtubule organisation during neuronal growth," (in eng), *J Cell Sci,* vol. 122, no. Pt 14, pp. 2534-42, Jul 15 2009, doi: 10.1242/jcs.046268.

[238] S. Ahmed, W. Bu, R. T. Lee, S. Maurer-Stroh, and W. I. Goh, "F-BAR domain proteins: Families and function," (in eng), *Commun Integr Biol,* vol. 3, no. 2, pp. 116-21, Mar 2010, doi: 10.4161/cib.3.2.10808.

[239] S. Yan *et al.*, "The F-BAR protein Cip4/Toca-1 antagonizes the formin Diaphanous in membrane stabilization and compartmentalization," (in eng), *J Cell Sci,* vol. 126, no. Pt 8, pp. 1796-805, Apr 15 2013, doi: 10.1242/jcs.118422.

[240] M. Nahm *et al.*, "dCIP4 (Drosophila Cdc42-interacting protein 4) restrains synaptic growth by inhibiting the secretion of the retrograde Glass bottom boat signal," (in eng), *J Neurosci,* vol. 30, no. 24, pp. 8138-50, Jun 16 2010, doi: 10.1523/JNEUROSCI.0256-10.2010.

[241] M. H. Syed, A. Krudewig, D. Engelen, T. Stork, and C. Klämbt, "The CD59 family member Leaky/Coiled is required for the establishment of the blood-brain barrier in Drosophila," (in eng), *J Neurosci,* vol. 31, no. 21, pp. 7876-85, May 25 2011, doi: 10.1523/JNEUROSCI.0766-11.2011.

[242] A. C. Wilmes, N. Klinke, B. Rotstein, H. Meyer, and A. Paululat, "Biosynthesis and assembly of the Collagen IV-like protein Pericardin in," (in eng), *Biol Open,* vol. 7, no. 4, Apr 23 2018, doi: 10.1242/bio.030361.

[243] R. R. McKay, L. Zhu, and R. D. Shortridge, "A Drosophila gene that encodes a member of the protein disulfide isomerase/phospholipase C-alpha family," (in eng), *Insect Biochem Mol Biol,* vol. 25, no. 5, pp. 647-54, May 1995, doi: 10.1016/0965-1748(95)00001-c.

[244] E. M. Enneking *et al.*, "Transsynaptic coordination of synaptic growth, function, and stability by the L1-type CAM Neuroglian," (in eng), *PLoS Biol,* vol. 11, no. 4, p. e1001537, 2013, doi: 10.1371/journal.pbio.1001537.

[245] T. Goossens *et al.*, "The Drosophila L1CAM homolog Neuroglian signals through distinct pathways to control different aspects of mushroom body axon development," (in eng), *Development,* vol. 138, no. 8, pp. 1595-605, Apr 2011, doi: 10.1242/dev.052787.

[246] T. A. Godenschwege, L. V. Kristiansen, S. B. Uthaman, M. Hortsch, and R. K. Murphey, "A conserved role for Drosophila Neuroglian and human L1-CAM in central-synapse formation," (in eng), *Curr Biol,* vol. 16, no. 1, pp. 12-23, Jan 10 2006, doi: 10.1016/j.cub.2005.11.062.

[247] R. Caizzi, M. P. Bozzetti, C. Caggese, and F. Ritossa, "Homologous nuclear genes encode cytoplasmic and mitochondrial glutamine synthetase in Drosophila melanogaster," *Journal of Molecular Biology,* 1990, doi: 10.1016/0022-2836(90)90301-2.

[248] D. S. Gala, J. Y. Lee, M. Kiourlappou, J. S. Titlow, R. O. Teodoro, and I. Davis, "Mammalian glial protrusion transcriptomes predict localization of Drosophila glial transcripts required for synaptic plasticity," *bioRxiv,* p. 2022.11.30.518536, 2023, doi: 10.1101/2022.11.30.518536.

[249] A. Ghosh *et al.*, "A Global In Vivo Drosophila RNAi Screen Identifies a Key Role of Ceramide Phosphoethanolamine for Glial Ensheathment of Axons," *PLoS Genetics,* 2013, doi: 10.1371/journal.pgen.1003980.

[250] H. Darabid, A. St-Pierre-See, and R. Robitaille, "Purinergic-Dependent Glial Regulation of Synaptic Plasticity of Competing Terminals and Synapse Elimination at the Neuromuscular Junction," *Cell Reports,* 2018, doi: 10.1016/j.celrep.2018.10.075.

[251] B. A. Clarke *et al.*, "The Ormdl genes regulate the sphingolipid synthesis pathway to ensure proper myelination and neurologic function in mice," *eLife,* 2019, doi: 10.7554/eLife.51067.

[252] S. Negro *et al.*, "Hydrogen peroxide is a neuronal alarmin that triggers specific RNAs, local translation of Annexin A2, and cytoskeletal remodeling in Schwann cells," *Rna,* vol. 24, no. 7, pp. 915-925, 2018, doi: 10.1261/rna.064816.117.

[253] P. J. Armati and E. K. Mathey, "An update on Schwann cell biology--immunomodulation, neural regulation and other surprises," (in eng), *J Neurol Sci,* vol. 333, no. 1-2, pp. 68-72, Oct 15 2013, doi: 10.1016/j.jns.2013.01.018.

[254] R. Thomsen, T. F. Daugaard, I. E. Holm, and A. L. Nielsen, "Alternative mRNA Splicing from the Glial Fibrillary Acidic Protein (GFAP) Gene Generates Isoforms with Distinct Subcellular mRNA Localization Patterns in Astrocytes," *PLoS ONE,* vol. 8, no. 8, 2013, doi: 10.1371/journal.pone.0072110.

[255] H. J. Bellen, C. Tong, and H. Tsuda, "100 years of Drosophila research and its impact on vertebrate neuroscience: a history lesson for the future," (in eng), *Nat Rev Neurosci,* vol. 11, no. 7, pp. 514-22, Jul 2010, doi: 10.1038/nrn2839.

[256] D. F. Poulson, "Histogenesis, organogenesis, and differentiation in the embryo of Drosophila melanogaster," *Biology of Drosophila,* pp. 168-274, 1950 1950.

[257] G. Jurgens, E. Wieschaus, C. Nusslein-Volhard, and H. Kluding, "Mutations affecting the pattern of the larval cuticle in Drosophila melanogaster. II: Zygotic loci on the third chromosome," *Wilhelm Roux's archives of developmental biology,* vol. 193, no. 5, pp. 283-295, 1984.

[258] E. Wieschaus, C. Nüsslein-Volhard, and G. Jürgens, "Mutations affecting the pattern of the larval cuticle in Drosophila melanogaster: III. Zygotic loci on the X-chromosome and fourth chromosome," *Wilhelm Roux's archives of developmental biology,* vol. 193, pp. 296-307, 1984.

[259] C. Nüsslein-Volhard and E. Wieschaus, "Mutations affecting segment number and polarity in Drosophila," (in eng), *Nature,* vol. 287, no. 5785, pp. 795-801, Oct 30 1980, doi: 10.1038/287795a0.

[260] K. S. Ho and M. P. Scott, "Sonic hedgehog in the nervous system: functions, modifications and mechanisms," *Current opinion in neurobiology,* vol. 12, no. 1, pp. 57-63, 2002.

[261] N. Gaiano, "Strange bedfellows: Reelin and Notch signaling interact to regulate cell migration in the developing neocortex," *Neuron,* vol. 60, no. 2, pp. 189-191, 2008.

[262] F. Charron and M. Tessier-Lavigne, "The Hedgehog, TGF-β/BMP and Wnt families of morphogens in axon guidance," *Axon growth and guidance,* pp. 116-133, 2007.

[263] C. D. Pozniak and S. J. Pleasure, "A tale of two signals: Wnt and Hedgehog in dentate neurogenesis," *Science's STKE,* vol. 2006, no. 319, pp. pe5-pe5, 2006.

[264] R. Mollá-Albaladejo and J. A. Sánchez-Alcañiz, "Behavior Individuality: A Focus on," (in eng), *Front Physiol,* vol. 12, p. 719038, 2021, doi: 10.3389/fphys.2021.719038.

[265] W. S. Neckameyer and P. Bhatt, "Protocols to Study Behavior in Drosophila," (in eng), *Methods Mol Biol,* vol. 1478, pp. 303-320, 2016, doi: 10.1007/978-1-4939-6371-3_19.

[266] C. E. McKellar and R. A. Wyttenbach, "A Protocol Demonstrating 60 Different," (in eng), *J Undergrad Neurosci Educ,* vol. 15, no. 2, pp. A110-A116, 2017.

[267] K. P. Menon, R. A. Carrillo, and K. Zinn, "Development and plasticity of the Drosophila larval neuromuscular junction," *Wiley Interdisciplinary Reviews: Developmental Biology,* vol. 2, no. 5, pp. 647-670, 2013.

[268] C. A. Collins and A. DiAntonio, "Synaptic development: insights from Drosophila," (in eng), *Curr Opin Neurobiol,* vol. 17, no. 1, pp. 35-42, Feb 2007, doi: 10.1016/j.conb.2007.01.001.

[269] A. DiAntonio, "Glutamate receptors at the Drosophila neuromuscular junction," *International review of neurobiology,* vol. 75, pp. 165-179, 2006.

[270] G. Marqués, "Morphogens and synaptogenesis in Drosophila," *Journal of neurobiology,* vol. 64, no. 4, pp. 417-434, 2005.

[271] D. Fernandes and A. L. Carvalho, "Mechanisms of homeostatic plasticity in the excitatory synapse," (in eng), *J Neurochem,* vol. 139, no. 6, pp. 973-996, Dec 2016, doi: 10.1111/jnc.13687.

[272] G. W. Davis and C. S. Goodman, "Genetic analysis of synaptic development and plasticity: homeostatic regulation of synaptic efficacy," (in eng), *Curr Opin Neurobiol,* vol. 8, no. 1, pp. 149-56, Feb 1998, doi: 10.1016/s0959-4388(98)80018-4.

[273] A. Vasin, L. Zueva, C. Torrez, D. Volfson, J. T. Littleton, and M. Bykhovskaia, "Synapsin regulates activity-dependent outgrowth of synaptic boutons at the Drosophila neuromuscular junction," (in eng), *J Neurosci,* vol. 34, no. 32, pp. 10554-63, Aug 06 2014, doi: 10.1523/JNEUROSCI.5074-13.2014.

[274] A. R. Fernandes, J. P. Martins, E. R. Gomes, C. S. Mendes, and R. O. Teodoro, "Drosophila motor neuron boutons remodel through membrane blebbing coupled with muscle contraction," (in eng), *Nat Commun,* vol. 14, no. 1, p. 3352, Jun 08 2023, doi: 10.1038/s41467-023-38421-9.

[275] C. Maldonado-Díaz, M. Vazquez, and B. Marie, "A comparison of three different methods of eliciting rapid activity-dependent synaptic plasticity at the Drosophila NMJ," (in eng), *PLoS One,* vol. 16, no. 11, p. e0260553, 2021, doi: 10.1371/journal.pone.0260553.

[276] Y. Hu, C. Roesel, I. Flockhart, L. Perkins, N. Perrimon, and S. E. Mohr, "UP-TORR: online tool for accurate and Up-to-Date annotation of RNAi Reagents," (in eng), *Genetics,* vol. 195, no. 1, pp. 37-45, Sep 2013, doi: 10.1534/genetics.113.151340.

[277] Y. R. Lin, B. V. Reddy, and K. D. Irvine, "Requirement for a core 1 galactosyltransferase in the Drosophila nervous system," (in eng), *Dev Dyn,* vol. 237, no. 12, pp. 3703-14, Dec 2008, doi: 10.1002/dvdy.21775.

[278] R. Pandey, J. Blanco, and G. Udolph, "The glucuronyltransferase GlcAT-P is required for stretch growth of peripheral nerves in Drosophila," (in eng), *PLoS One,* vol. 6, no. 11, p. e28106, 2011, doi: 10.1371/journal.pone.0028106.

[279] S. Meyer, I. Schmidt, and C. Klämbt, "Glia ECM interactions are required to shape the Drosophila nervous system," (in eng), *Mech Dev,* vol. 133, pp. 105-16, Aug 2014, doi: 10.1016/j.mod.2014.05.003.

[280] M. Agrawal and K. Welshhans, "Local Translation Across Neural Development: A Focus on Radial Glial Cells, Axons, and Synaptogenesis," (in eng), *Front Mol Neurosci,* vol. 14, p. 717170, 2021, doi: 10.3389/fnmol.2021.717170.

[281] B. Olofsson and D. T. Page, "Condensation of the central nervous system in embryonic Drosophila is inhibited by blocking hemocyte migration or neural activity," (in eng), *Dev Biol,* vol. 279, no. 1, pp. 233-43, Mar 01 2005, doi: 10.1016/j.ydbio.2004.12.020.

[282] S. Moe and E. McNeill, "Highlighting the role of glial-specific miR-92 on synaptogenesis of developing Drosophila melanogaster," *Physiology,* vol. 38, no. S1, p. 5730467, 2023.

[283] M. Formica *et al.*, "V-ATPase controls tumor growth and autophagy in a Drosophila model of gliomagenesis," *Autophagy,* vol. 17, no. 12, pp. 4442-4452, 2021/12/02 2021, doi: 10.1080/15548627.2021.1918915.

[284] A. Voelzmann *et al.*, "Drosophila Short stop as a paradigm for the role and regulation of spectraplakins," in *Seminars in cell & developmental biology*, 2017, vol. 69: Elsevier, pp. 40-57.

[285] S. Huelsmann and N. H. Brown, "Spectraplakins," *Current Biology,* vol. 24, no. 8, pp. R307-R308, 2014.

[286] K. C. Suozzi, X. Wu, and E. Fuchs, "Spectraplakins: master orchestrators of cytoskeletal dynamics," *Journal of Cell Biology,* vol. 197, no. 4, pp. 465-475, 2012.

[287] T. Sun *et al.*, "Spectraplakin Shot Maintains Perinuclear Microtubule Organization in Drosophila Polyploid Cells," (in eng), *Dev Cell,* vol. 49, no. 5, pp. 731-747.e7, Jun 03 2019, doi: 10.1016/j.devcel.2019.03.027.

[288] K. Singh *et al.*, "Neural cell adhesion molecule Negr1 deficiency in mouse results in structural brain endophenotypes and behavioral deviations related to psychiatric disorders," *Scientific Reports,* vol. 9, no. 1, p. 5457, 2019/04/01 2019, doi: 10.1038/s41598-019-41991-8.

[289] S. Ateaque, S. Merkouris, and Y. A. Barde, "Neurotrophin signalling in the human nervous system," (in eng), *Front Mol Neurosci,* vol. 16, p. 1225373, 2023, doi: 10.3389/fnmol.2023.1225373.

[290] L. R. Lizarraga-Valderrama and G. K. Sheridan, "Extracellular vesicles and intercellular communication in the central nervous system," (in eng), *FEBS Lett,* vol. 595, no. 10, pp. 1391-1410, May 2021, doi: 10.1002/1873-3468.14074.

[291] P. Doherty, M. S. Fazeli, and F. S. Walsh, "The neural cell adhesion molecule and synaptic plasticity," (in eng), *J Neurobiol,* vol. 26, no. 3, pp. 437-46, Mar 1995, doi: 10.1002/neu.480260315.

[292] C. Kasper *et al.*, "Structural basis of cell-cell adhesion by NCAM," (in eng), *Nat Struct Biol,* vol. 7, no. 5, pp. 389-93, May 2000, doi: 10.1038/75165.

[293] H. Togashi, T. Sakisaka, and Y. Takai, "Cell adhesion molecules in the central nervous system," (in eng), *Cell Adh Migr,* vol. 3, no. 1, pp. 29-35, 2009, doi: 10.4161/cam.3.1.6773.

[294] A. M. Craig and Y. Kang, "Neurexin-neuroligin signaling in synapse development," (in eng), *Curr Opin Neurobiol,* vol. 17, no. 1, pp. 43-52, Feb 2007, doi: 10.1016/j.conb.2007.01.011.

[295] C. Reissner, F. Runkel, and M. Missler, "Neurexins," (in eng), *Genome Biol,* vol. 14, no. 9, p. 213, 2013, doi: 10.1186/gb-2013-14-9-213.

[296] T. C. Südhof, "Synaptic Neurexin Complexes: A Molecular Code for the Logic of Neural Circuits," (in eng), *Cell,* vol. 171, no. 4, pp. 745-769, Nov 2017, doi: 10.1016/j.cell.2017.10.024.

[297] K. Suzuki and M. Yuzaki, "La Dolce Vita of Neurexin: Synaptic Partnerships through Glycosaminoglycans," (in eng), *Cell,* vol. 174, no. 6, pp. 1337-1338, Sep 2018, doi: 10.1016/j.cell.2018.08.052.

[298] K. Tabuchi and T. C. Südhof, "Structure and evolution of neurexin genes: insight into the mechanism of alternative splicing," (in eng), *Genomics,* vol. 79, no. 6, pp. 849-59, Jun 2002, doi: 10.1006/geno.2002.6780.

[299] S. Cheng *et al.*, "Family of neural wiring receptors in bilaterians defined by phylogenetic, biochemical, and structural evidence," (in eng), *Proc Natl Acad Sci U S A,* vol. 116, no. 20, pp. 9837-9842, May 14 2019, doi: 10.1073/pnas.1818631116.

[300] C. Vogel, S. A. Teichmann, and C. Chothia, "The immunoglobulin superfamily in Drosophila melanogaster and Caenorhabditis elegans and the evolution of complexity," (in eng), *Development,* vol. 130, no. 25, pp. 6317-28, Dec 2003, doi: 10.1242/dev.00848.

[301] A. F. Pimenta *et al.*, "The limbic system-associated membrane protein is an Ig superfamily member that mediates selective neuronal growth and axon targeting," (in eng), *Neuron,* vol. 15, no. 2, pp. 287-97, Aug 1995, doi: 10.1016/0896-6273(95)90034-9.

[302] H. Venkannagari *et al.*, "Highly Conserved Molecular Features in IgLONs Contrast Their Distinct Structural and Biological Outcomes," (in eng), *J Mol Biol,* vol. 432, no. 19, pp. 5287-5303, Sep 04 2020, doi: 10.1016/j.jmb.2020.07.014.

[303] N. Kubick, D. Brösamle, and M. E. Mickael, "Molecular Evolution and Functional Divergence of the IgLON Family," (in eng), *Evol Bioinform Online,* vol. 14, p. 1176934318775081, 2018, doi: 10.1177/1176934318775081.

[304] N. Funatsu *et al.*, "Characterization of a novel rat brain glycosylphosphatidylinositol-anchored protein (Kilon), a member of the IgLON cell adhesion molecule family," (in eng), *J Biol Chem,* vol. 274, no. 12, pp. 8224-30, Mar 19 1999, doi: 10.1074/jbc.274.12.8224.

[305] R. O. Karlstrom, L. P. Wilder, and M. J. Bastiani, "Lachesin: an immunoglobulin superfamily protein whose expression correlates with neurogenesis in grasshopper embryos," (in eng), *Development,* vol. 118, no. 2, pp. 509-22, Jun 1993, doi: 10.1242/dev.118.2.509.

[306] R. P. A. Tan *et al.*, "Neuronal growth regulator 1 (NEGR1) promotes synaptic targeting of glutamic acid decarboxylase 65 (GAD65)," *bioRxiv,* p. 2022.02.08.479601, 2022, doi: 10.1101/2022.02.08.479601.

[307] J. Szczurkowska *et al.*, "NEGR1 and FGFR2 cooperatively regulate cortical development and core behaviours related to autism disorders in mice," *Brain,* vol. 141, no. 9, pp. 2772-2794, 2018.

[308] E. Tassano, A. Gamucci, M. E. Celle, P. Ronchetto, C. Cuoco, and G. Gimelli, "Clinical and molecular cytogenetic characterization of a de novo interstitial 1p31. 1p31. 3 deletion in a boy

with moderate intellectual disability and severe language impairment," *Cytogenetic and Genome Research,* vol. 146, no. 1, pp. 39-43, 2015.

[309] A. M. Veerappa, M. Saldanha, P. Padakannaya, and N. B. Ramachandra, "Genome-wide copy number scan identifies disruption of PCDH11X in developmental dyslexia," *American Journal of Medical Genetics Part B: Neuropsychiatric Genetics,* vol. 162, no. 8, pp. 889-897, 2013.

[310] A. Genovese, D. M. Cox, and M. G. Butler, "Partial deletion of chromosome 1p31. 1 including only the neuronal growth regulator 1 gene in two siblings," *Journal of pediatric genetics,* vol. 4, no. 01, pp. 023-028, 2015.

[311] K. Zinn and E. Özkan, "Neural immunoglobulin superfamily interaction networks," (in eng), *Curr Opin Neurobiol,* vol. 45, pp. 99-105, Aug 2017, doi: 10.1016/j.conb.2017.05.010.

[312] R. P. A. Tan, I. Leshchyns'ka, and V. Sytnyk, "Glycosylphosphatidylinositol-Anchored Immunoglobulin Superfamily Cell Adhesion Molecules and Their Role in Neuronal Development and Synapse Regulation," (in eng), *Front Mol Neurosci,* vol. 10, p. 378, 2017, doi: 10.3389/fnmol.2017.00378.

[313] E. Cortés, J. S. Pak, and E. Özkan, "Structure and evolution of neuronal wiring receptors and ligands," (in eng), *Dev Dyn,* vol. 252, no. 1, pp. 27-60, Jan 2023, doi: 10.1002/dvdy.512.

[314] J. Ashley *et al.*, "Transsynaptic interactions between IgSF proteins DIP-α and Dpr10 are required for motor neuron targeting specificity," (in eng), *Elife,* vol. 8, Feb 04 2019, doi: 10.7554/eLife.42690.

[315] S. Cheng *et al.*, "Molecular basis of synaptic specificity by immunoglobulin superfamily receptors in," (in eng), *Elife,* vol. 8, Jan 28 2019, doi: 10.7554/eLife.41028.

[316] R. A. Carrillo *et al.*, "Control of Synaptic Connectivity by a Network of Drosophila IgSF Cell Surface Proteins," (in eng), *Cell,* vol. 163, no. 7, pp. 1770-1782, Dec 17 2015, doi: 10.1016/j.cell.2015.11.022.

[317] A. P. Sergeeva *et al.*, "DIP/Dpr interactions and the evolutionary design of specificity in protein families," (in eng), *Nat Commun,* vol. 11, no. 1, p. 2125, May 01 2020, doi: 10.1038/s41467-020-15981-8.

[318] E. Özkan *et al.*, "An extracellular interactome of immunoglobulin and LRR proteins reveals receptor-ligand networks," (in eng), *Cell,* vol. 154, no. 1, pp. 228-39, Jul 03 2013, doi: 10.1016/j.cell.2013.06.006.

[319] S. Barish *et al.*, "Combinations of DIPs and Dprs control organization of olfactory receptor neuron terminals in Drosophila," (in eng), *PLoS Genet,* vol. 14, no. 8, p. e1007560, Aug 2018, doi: 10.1371/journal.pgen.1007560.

[320] T. M. Finegan and D. T. Bergstralh, "Neuronal immunoglobulin superfamily cell adhesion molecules in epithelial morphogenesis: insights from," (in eng), *Philos Trans R Soc Lond B Biol Sci,* vol. 375, no. 1809, p. 20190553, Oct 12 2020, doi: 10.1098/rstb.2019.0553.

[321] M. Furuse and S. Tsukita, "Claudins in occluding junctions of humans and flies," (in eng), *Trends Cell Biol,* vol. 16, no. 4, pp. 181-8, Apr 2006, doi: 10.1016/j.tcb.2006.02.006.

[322] N. J. Abbott, "Dynamics of CNS Barriers: Evolution, Differentiation, and Modulation," *Cellular and Molecular Neurobiology,* vol. 25, no. 1, pp. 5-23, 2005/02/01 2005, doi: 10.1007/s10571-004-1374-y.

[323] B. Obermeier, A. Verma, and R. M. Ransohoff, "Chapter 3 - The blood–brain barrier," in *Handbook of Clinical Neurology*, vol. 133, S. J. Pittock and A. Vincent Eds.: Elsevier, 2016, pp. 39-59.

[324] T. Kitamura and M. Imafuku, "Behavioural mimicry in flight path of Batesian intraspecific polymorphic butterfly Papilio polytes," (in eng), *Proc Biol Sci,* vol. 282, no. 1809, p. 20150483, Jun 22 2015, doi: 10.1098/rspb.2015.0483.

[325] S. Baumgartner *et al.*, "A Drosophila neurexin is required for septate junction and blood-nerve barrier formation and function," (in eng), *Cell,* vol. 87, no. 6, pp. 1059-68, Dec 13 1996, doi: 10.1016/s0092-8674(00)81800-0.

[326] J. Vijayakumar, C. Perrois, M. Heim, L. Bousset, S. Alberti, and F. Besse, "The prion-like domain of Drosophila Imp promotes axonal transport of RNP granules in vivo," (in eng), *Nat Commun,* vol. 10, no. 1, p. 2593, Jun 13 2019, doi: 10.1038/s41467-019-10554-w.

[327] K. L. Boylan *et al.*, "Motility screen identifies Drosophila IGF-II mRNA-binding protein--zipcode-binding protein acting in oogenesis and synaptogenesis," (in eng), *PLoS Genet,* vol. 4, no. 2, p. e36, Feb 2008, doi: 10.1371/journal.pgen.0040036.

[328] C. Medioni, M. Ramialison, A. Ephrussi, and F. Besse, "Imp promotes axonal remodeling by regulating profilin mRNA during brain development," (in eng), *Curr Biol,* vol. 24, no. 7, pp. 793-800, Mar 31 2014, doi: 10.1016/j.cub.2014.02.038.

[329] K. J. Sepp, J. Schulte, and V. J. Auld, "Peripheral glia direct axon guidance across the CNS/PNS transition zone," *Developmental Biology,* vol. 238, no. 1, pp. 47-63, 2001, doi: 10.1006/dbio.2001.0411.

[330] K. J. Sepp and V. J. Auld, "Reciprocal Interactions between Neurons and Glia Are Required for," *Cell,* vol. 23, no. 23, pp. 8221-8230, 2003.

[331] H. Hertenstein, E. McMullen, A. Weiler, A. Volkenhoff, H. M. Becker, and S. Schirmeier, "Starvation-induced regulation of carbohydrate transport at the blood-brain barrier is TGF-β-signaling dependent," (in eng), *Elife,* vol. 10, May 25 2021, doi: 10.7554/eLife.62503.

[332] G. Guangming, G. Junhua, Z. Chenchen, M. Yang, and X. Wei, "Neurexin and Neuroligins Maintain the Balance of Ghost and Satellite Boutons at the," (in eng), *Front Neuroanat,* vol. 14, p. 19, 2020, doi: 10.3389/fnana.2020.00019.

[333] B. Ataman *et al.*, "Nuclear trafficking of Drosophila Frizzled-2 during synapse development requires the PDZ protein dGRIP," (in eng), *Proc Natl Acad Sci U S A,* vol. 103, no. 20, pp. 7841-6, May 16 2006, doi: 10.1073/pnas.0600387103.

[334] B. Sutcliffe, M. G. Forero, B. Zhu, I. M. Robinson, and A. Hidalgo, "Neuron-type specific functions of DNT1, DNT2 and Spz at the Drosophila neuromuscular junction," (in eng), *PLoS One,* vol. 8, no. 10, p. e75902, 2013, doi: 10.1371/journal.pone.0075902.

[335] L.-J. Pilaz *et al.*, "Subcellular mRNA localization and local translation of Arhgap11a in radial glial cells regulates cortical development," *bioRxiv,* p. 2020.07.30.229724, 2020, doi: 10.1101/2020.07.30.229724.

[336] N. von Kügelgen and M. Chekulaeva, "Conservation of a core neurite transcriptome across neuronal types and species," ed, 2020.

[337] J. M. Halstead *et al.*, "An RNA biosensor for imaging the first round of translation from single cells to living animals," *Science,* vol. 347, no. 6228, pp. 1367-1671, 2015/03/20 2015, doi: 10.1126/science.aaa3380.

[338] B. Wu, C. Eliscovich, Y. J. Yoon, and R. H. Singer, "Translation dynamics of single mRNAs in live cells and neurons," (in eng), *Science,* vol. 352, no. 6292, pp. 1430-5, Jun 17 2016, doi: 10.1126/science.aaf1084.

[339] K. S. Burke, K. A. Antilla, and D. A. Tirrell, "A Fluorescence in Situ Hybridization Method To Quantify mRNA Translation by Visualizing Ribosome-mRNA Interactions in Single Cells," (in eng), *ACS Cent Sci,* vol. 3, no. 5, pp. 425-433, May 24 2017, doi: 10.1021/acscentsci.7b00048.

[340] S. Sanyal, "Genomic mapping and expression patterns of C380, OK6 and D42 enhancer trap lines in the larval nervous system of Drosophila," (in eng), *Gene Expr Patterns,* vol. 9, no. 5, pp. 371-80, Jun 2009, doi: 10.1016/j.gep.2009.01.002.

[341] M. Q. Clark, A. A. Zarin, A. Carreira-Rosario, and C. Q. Doe, "Neural circuits driving larval locomotion in Drosophila," (in eng), *Neural Dev,* vol. 13, no. 1, p. 6, Apr 19 2018, doi: 10.1186/s13064-018-0103-z.

[342] S. L. Lai and T. Lee, "Genetic mosaic with dual binary transcriptional systems in Drosophila," (in eng), *Nat Neurosci,* vol. 9, no. 5, pp. 703-9, May 2006, doi: 10.1038/nn1681.

[343] A. del Valle Rodríguez, D. Didiano, and C. Desplan, "Power tools for gene expression and clonal analysis in Drosophila," (in eng), *Nat Methods,* vol. 9, no. 1, pp. 47-55, Dec 28 2011, doi: 10.1038/nmeth.1800.

[344] B. V. Zlokovic, "The blood-brain barrier in health and chronic neurodegenerative disorders," (in eng), *Neuron,* vol. 57, no. 2, pp. 178-201, Jan 24 2008, doi: 10.1016/j.neuron.2008.01.003.

[345] M. Segarra, M. R. Aburto, and A. Acker-Palmer, "Blood-Brain Barrier Dynamics to Maintain Brain Homeostasis," (in eng), *Trends Neurosci,* vol. 44, no. 5, pp. 393-405, May 2021, doi: 10.1016/j.tins.2020.12.002.

[346] E. G. Knox, M. R. Aburto, G. Clarke, J. F. Cryan, and C. M. O'Driscoll, "The blood-brain barrier in aging and neurodegeneration," *Molecular Psychiatry,* vol. 27, no. 6, pp. 2659-2673, 2022/06/01 2022, doi: 10.1038/s41380-022-01511-z.

[347] E. Swissa, Y. Serlin, U. Vazana, O. Prager, and A. Friedman, "Blood-brain barrier dysfunction in status epileptics: Mechanisms and role in epileptogenesis," (in eng), *Epilepsy Behav,* vol. 101, no. Pt B, p. 106285, Dec 2019, doi: 10.1016/j.yebeh.2019.04.038.

[348] C. P. Profaci, R. N. Munji, R. S. Pulido, and R. Daneman, "The blood–brain barrier in health and disease: Important unanswered questions," *Journal of Experimental Medicine,* vol. 217, no. 4, 2020, doi: 10.1084/jem.20190062.

[349] I. Galea, "The blood–brain barrier in systemic infection and inflammation," *Cellular & Molecular Immunology,* vol. 18, no. 11, pp. 2489-2501, 2021/11/01 2021, doi: 10.1038/s41423-021-00757-x.

[350] E. G. Contreras and C. Klämbt, "The Drosophila blood-brain barrier emerges as a model for understanding human brain diseases," (in eng), *Neurobiol Dis,* vol. 180, p. 106071, May 2023, doi: 10.1016/j.nbd.2023.106071.

[351] W. Pereanu, D. Shy, and V. Hartenstein, "Morphogenesis and proliferation of the larval brain glia in Drosophila," (in eng), *Dev Biol,* vol. 283, no. 1, pp. 191-203, Jul 01 2005, doi: 10.1016/j.ydbio.2005.04.024.

[352] S. D. Carlson, J. L. Juang, S. L. Hilgers, and M. B. Garment, "Blood barriers of the insect," (in eng), *Annu Rev Entomol,* vol. 45, pp. 151-74, 2000, doi: 10.1146/annurev.ento.45.1.151.

[353] N. Trotta, C. K. Rodesch, T. Fergestad, and K. Broadie, "Cellular bases of activity-dependent paralysis in Drosophila stress-sensitive mutants," (in eng), *J Neurobiol,* vol. 60, no. 3, pp. 328-47, Sep 05 2004, doi: 10.1002/neu.20017.

[354] B. R. Ransom and C. B. Ransom, *Astrocytes: Multitalented stars of the central nervous system*. 2012, pp. 3-7.

[355] S. Das, M. Vera, V. Gandin, R. H. Singer, and E. Tutucci, "Intracellular mRNA transport and localized translation," *Nature Reviews Molecular Cell Biology,* vol. 22, no. 7, pp. 483-504, 2021/07/01 2021, doi: 10.1038/s41580-021-00356-8.

[356] P. G. Donlin-Asp, C. Polisseni, R. Klimek, A. Heckel, and E. M. Schuman, "Differential regulation of local mRNA dynamics and translation following long-term potentiation and depression," (in eng), *Proc Natl Acad Sci U S A,* vol. 118, no. 13, 03 30 2021, doi: 10.1073/pnas.2017578118.

[357] J. D. Perez, C. M. Fusco, and E. M. Schuman, "A Functional Dissection of the mRNA and Locally Synthesized Protein Population in Neuronal Dendrites and Axons," (in eng), *Annu Rev Genet,* vol. 55, pp. 183-207, 11 23 2021, doi: 10.1146/annurev-genet-030321-054851.

[358] O. Steward and E. M. Schuman, "Compartmentalized Synthesis and Degradation of Proteins in Neurons," *Neuron,* vol. 40, no. 2, pp. 347-359, 2003/10/09/ 2003, doi: https://doi.org/10.1016/S0896-6273(03)00635-4.

[359] M. Corkrum *et al.*, "Dopamine-Evoked Synaptic Regulation in the Nucleus Accumbens Requires Astrocyte Activity," (in eng), *Neuron,* vol. 105, no. 6, pp. 1036-1047.e5, Mar 18 2020, doi: 10.1016/j.neuron.2019.12.026.

[360] S. Banerjee, A. M. Pillai, R. Paik, J. Li, and M. A. Bhat, "Axonal ensheathment and septate junction formation in the peripheral nervous system of Drosophila," *Journal of Neuroscience,* vol. 26, no. 12, pp. 3319-3329, 2006, doi: 10.1523/JNEUROSCI.5383-05.2006.

[361] C. M. Lye, H. W. Naylor, and B. Sanson, "Subcellular localisations of the CPTI collection of YFP-tagged proteins in Drosophila embryos," (in eng), *Development,* vol. 141, no. 20, pp. 4006-17, Oct 2014, doi: 10.1242/dev.111310.

[362] C. Hoppe and H. L. Ashe, "Live imaging and quantitation of nascent transcription using the MS2/MCP system in the," (in eng), *STAR Protoc,* vol. 2, no. 1, p. 100379, Mar 19 2021, doi: 10.1016/j.xpro.2021.100379.

[363] M. A. Seeger, L. Haffley, and T. C. Kaufman, "Characterization of amalgam: a member of the immunoglobulin superfamily from Drosophila," *Cell,* vol. 55, no. 4, pp. 589-600, 1988.

[364] E. C. Liebl *et al.*, "Interactions between the secreted protein Amalgam, its transmembrane receptor Neurotactin and the Abelson tyrosine kinase affect axon pathfinding," 2003.

[365] F. Fremion, I. Darboux, M. Diano, R. Hipeau-Jacquotte, M. Seeger, and M. Piovant, "Amalgam is a ligand for the transmembrane receptor neurotactin and is required for neurotactin-mediated cell adhesion and axon fasciculation in Drosophila," *The EMBO Journal,* vol. 19, no. 17, pp. 4463-4472, 2000.

[366] I. Rousse and R. Robitaille, "Calcium signaling in Schwann cells at synaptic and extra-synaptic sites: active glial modulation of neuronal activity," (in eng), *Glia,* vol. 54, no. 7, pp. 691-9, Nov 15 2006, doi: 10.1002/glia.20388.

Appendix

A

Table A-1 The sequences of primers used in the ORMDL::YFP RT-PCR experiment

Venus YFP Forward Primer	ACGTAAACGGCCACAAGTTC
Venus YFP Reverse Primer	GTCCATGCCGAGAGTGATCC
ORMDL Forward Primer	CGCGGTCACATTGAGCGTAA
ORMDL Reverse Primer	GGCCCATGGAATGCTAACGA

B

Table B-1 smFISH probe sequences

YFP exon	*ORMDL* exon	*Lac* exon	*Lac* intron
cggtgaacagctcctcgc	ctcaatgtgaccgcgcat	gatactcggccgccacat	gtgagtcacggtcactca
cagctcgaccaggatggg	gttaacctttggttccga	ggtgctccacacgcaatt	agcatttgcacttgtccg
ctgaacttgtggccgttt	tggacgtcatgtggctga	gcacaaaaatggccagga	ccgggaattaagctggct
ttgccgtaggtggcatcg	ggagctgtttggattcgc	ttcgctgtgctagcgttt	gccgaagctgatagctga
gtggtgcagatcagcttc	caaaatccccgggcactc	cctgcgtgatgtaggata	gcacgcctggtttttatt
agggtggtcacgagggtg	gcccaggaggtatgctag	cgccgatatccttgatct	cgtggagcgtatccaact
aagcactgcaggccgtag	agaagagcaggtgcaccg	cggagcaatcgaactcca	tgtgctgtttgcctaagc
atgtggtcggggtagcgg	ggcccatggaatgctaac	tgtactctttggcatact	tttgactcggctcgttgg
ttgaagaagtcgtgctgc	gaagcaggttggtagccg	ccgtcttcaggaacagca	gtacacctctatgtcctc
acgtagccttcgggcatg	tacaggtgggctgcattg	agaggaagacgggatcgc	gcacaaaggctgtgcagt
aagaagatggtgcgctcc	cccttgatgacgtgcaga	gatgaccagcgtggagcc	tgcggaagcaattgcgcg
tcttgtagttgccgtcgt	atcgttctccgtgctcag	cagcgagaagcgcgaatc	ggtccgtggaacgttttc
tcgaacttcacctcggcg	ttcccagtgcgtccaacg	ggacgagttgggatcgta	cgtttttgcacgggttgt
atgcggttcaccagggtg	tgtaccccgtcatcgatc	cttgatctgcagcttgta	aaaagcccagaccgtgtc
gaagtcgatgcccttcag	cttgcgcgttgtggtcat	cgcgtccgtctcctgaat	ttccacctctgagtttca
caggatgttgccgtcctc	tgggaacagctgtgagga	accacctggcaggtgtag	ctcaggatccctttgttt
gttgtactccagcttgtg	tcgggtgtacagacaggt	gctcactttgtgaacggt	tgggcatagaagggctcg
atagacgttgtggctgtt	gggataaagtgttccgtg	caccgatagcttcacttc	gatgggatcaggggttgt
cgttcttctgcttgtcgg	tgacgaccaccagggata	cgagatgacgggggggacg	tgggcgggacgaaatgcg
tcttgaagttggccttga	tggaactgcggcagcttg	caccgactgcgtggagtt	taggggttcctcaatggg
cgtcctcgatgttgtggc	atgttgaacagccgcacg	tccatctggacctcgctg	tcaacaccccgaatacca
tgttctgctggtagtggt	acaggagctagtacttgt	ggatagccgctggcgtag	cagctatgagccatctct
ttgtcgggcagcagcacg	ataaatgcggcccgttct	ctccaggtgatggtgggt	cgttgctttctttgcagc
ggactggtagctcaggta	ttgagcaagagctgtgcc	ggcagaatggcattgttc	cggaacaacaatgcccca
gttggggtctttgctcag	ctcaatgtgaccgcgcat	ccacataggtggcactat	ttcagacaccccgaagtg
gaccatgtgatcgcgctt	gttaacctttggttccga	ctgacttgatgcgcaggg	cctgtggcatctgaggaa
ggcggtcacgaactccag	tggacgtcatgtggctga	agtagtaggtgccgcgat	ttctcgttttgccttcga
tccatgccgagagtgatc	ggagctgtttggattcgc	cttgctcactccattgtc	ctacgtcatcgccgttta
	caaaatccccgggcactc	cacgttgatattgcgcct	cccagcaaccaacattca
	gcccaggaggtatgctag	atcactggtgcgaactcc	cccatgaaatggccatgt
	agaagagcaggtgcaccg	tgtcccaaacgaggacgc	ggaatggcctcatggaca
	ggcccatggaatgctaac	ccaagtccatgtcgtact	ttgtgagccgagtaccta
	gaagcaggttggtagccg	gataggcctcaatgtggc	cccttctcgagtagtaca
	tacaggtgggctgcattg	ccttggtccacacaatgg	agacaaggccacagacgc
	cccttgatgacgtgcaga	ttgttggccagctggatg	caagccacccacaattca
	atcgttctccgtgctcag	tgcgagatgctgtagtgc	tgtggagcggggaaaggg
	ttcccagtgcgtccaacg	gtatactcgtcggcggtg	atttgtctcctcttcctg
	tgtaccccgtcatcgatc	atcacacggagcgtcgag	atccagtttggtttggca
		tactggcgcttctcaacg	gcgggtgcgcttttaatg
		gccttgcacacataatct	caaccacccaaaagggct
		gcctctccaaagcgattg	gtgcaggtagataggtcc
		aagagattgacgcgcgcc	ctaacgcaacacccccttg
		gtgggcacacgggaatga	tgatgatgctgcgtccat
		atgtacgcctgtccacag	atgccaaccatcatccat
		gaagtggcggacacatcc	ttccctaacgtgctgttt
		caggatgcccacaagagc	tctcattctccgcttgta
		tctggcgaagagcaacgc	gagcgaatacagctgcca

C

Figure C-1 Violin and dot-plots containing raw data of glial protrusion and neurite areas upon knockdown of glial protrusion-localised transcripts when compared to unstimulated control

Next page: violin plots with accompanying raw data presenting the NMJ results quantification for RNAi knockdown of candidate transcripts in glia. See genotype above each plot and legend for details. Raw data is plotted as black dots. Point range (orange) indicates the mean ± SEM. Significance levels are denoted as follows: *p < 0.05; **p < 0.01; ***p < 0.001; ****p < 0.0001.

Comparison of glial and neuronal areas in unstimulated candidate gene knockdown NMJs

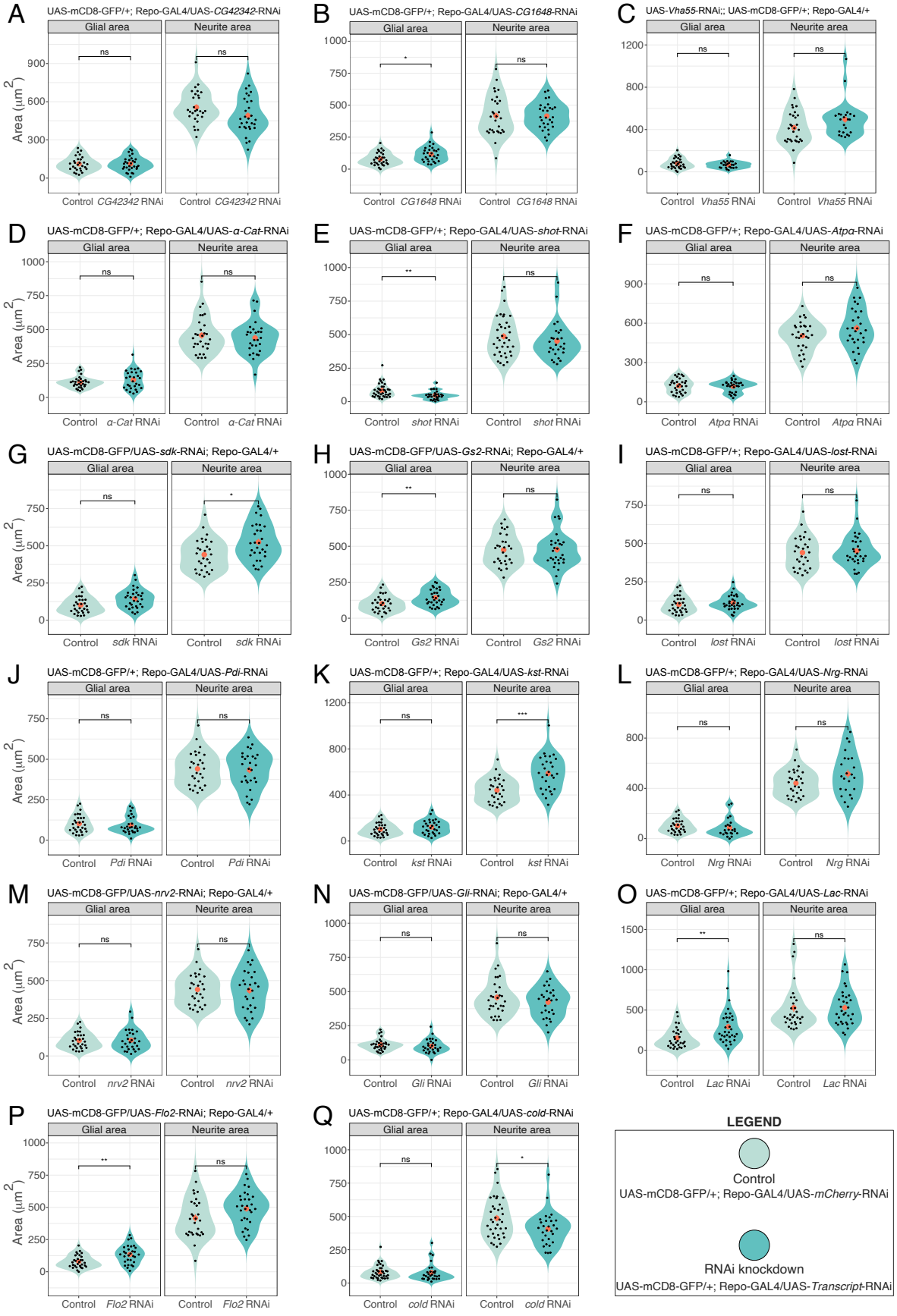

Figure C-2 Violin and dot-plots containing raw data of glial protrusion and neurite protrusion area ratios upon knockdown of glial protrusion-localised transcripts when compared to unstimulated control

Next page: violin plots with accompanying raw data presenting the NMJ results quantification for RNAi knockdown of candidate transcripts in glia. See genotype above each plot and legend for details. Raw data is plotted as black dots. Point range (cyan) indicates the mean ± SEM. Significance levels are denoted as follows: *p < 0.05; **p < 0.01; ***p < 0.001; ****p < 0.0001.

Comparison of glial and neuronal area ratios in unstimulated candidate gene knockdown NMJs

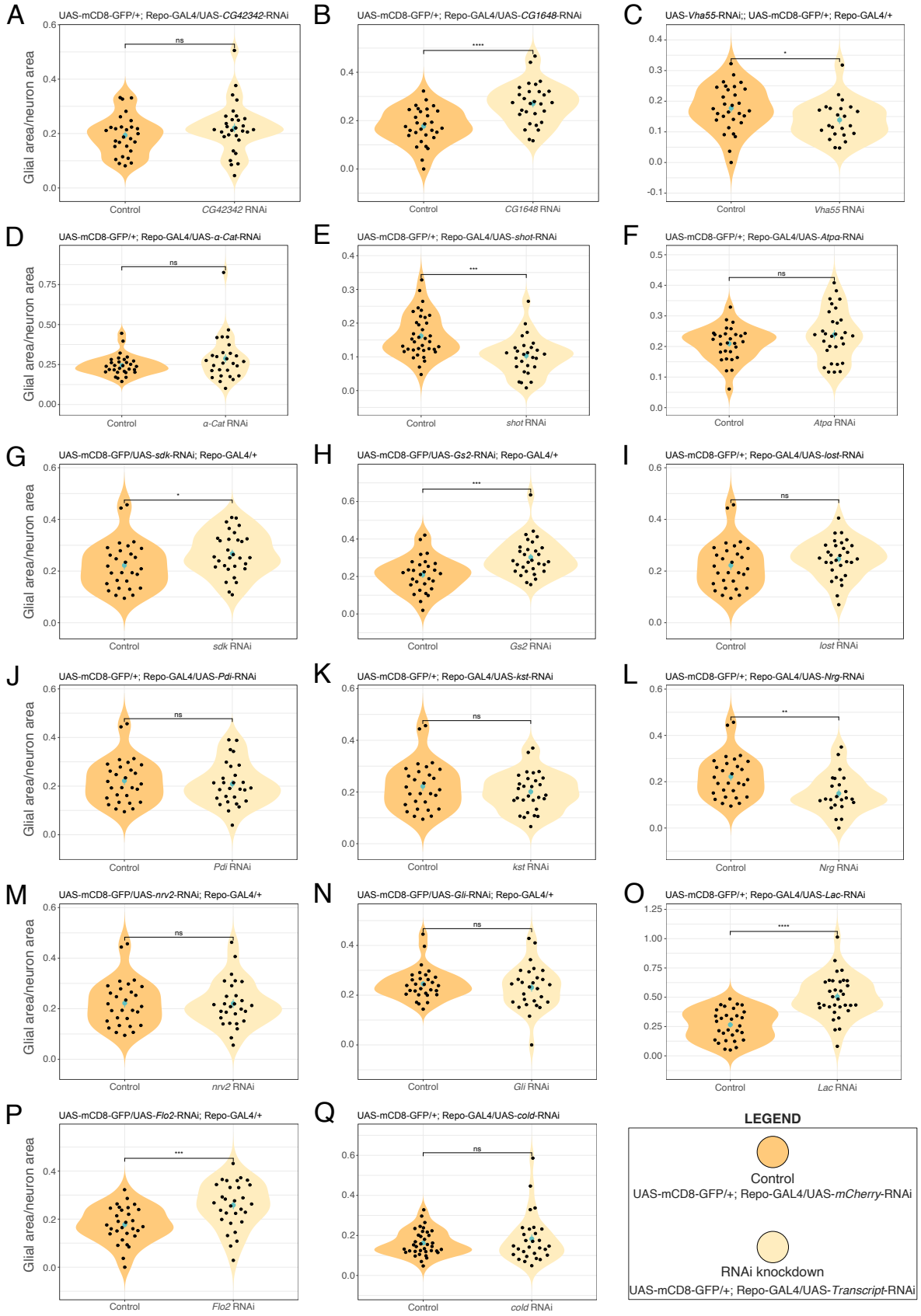

Table C-1 Summary statistics for glial and neurite area and their ratios

Measurement	RNAi target	p	control n	RNAi n	RNAi mean	control mean	Foldchange
Glial area	*Atpα*	N.S.	29	30	122.780567	118.748207	1.03395723
Neurite area	*Atpα*	N.S.	29	30	503.811133	562.277862	0.89601809
Ratio Glial/Neurite	*Atpα*	N.S.	29	30	0.2386353	0.20926125	1.14037023
Glial area	*CG1648*	* < 0.05	30	29	117.141483	79.4147333	1.47505983
Neurite area	*CG1648*	N.S.	30	29	415.068172	417.509933	0.99415161
Ratio Glial/Neurite	*CG1648*	*** < 0.001	30	29	0.2703896	0.17721365	1.52578314
Glial area	*CG42342*	N.S.	28	30	111.323133	112.205464	0.99213647
Neurite area	*CG42342*	N.S.	28	30	490.693533	556.423821	0.8818701
Ratio Glial/Neurite	*CG42342*	N.S.	28	30	0.22066552	0.19364235	1.13955194
Glial area	*cold*	N.S.	37	29	79.2400345	82.7811351	0.95722334
Neurite area	*cold*	* < 0.05	37	29	406.218345	487.031	0.83407082
Ratio Glial/Neurite	*cold*	N.S.	37	29	0.18298526	0.16198966	1.12961078
Glial area	*Flo2*	** < 0.01	30	30	134.0072	79.4147333	1.68743499
Neurite area	*Flo2*	N.S.	30	30	490.3435	417.509933	1.17444751
Ratio Glial/Neurite	*Flo2*	** < 0.01	30	30	0.25835289	0.17721365	1.45786113
Glial area	*Gli*	N.S.	30	28	100.388821	112.231667	0.89447858
Neurite area	*Gli*	N.S.	30	28	421.878071	457.349233	0.92244185
Ratio Glial/Neurite	*Gli*	N.S.	30	28	0.2309974	0.24538726	0.94135855
Glial area	*Gs2*	** < 0.01	29	30	143.748667	101.753724	1.4127116
Neurite area	*Gs2*	N.S.	29	30	477.0776	474.741448	1.00492089
Ratio Glial/Neurite	*Gs2*	*** < 0.001	29	30	0.30249693	0.20935829	1.44487678
Glial area	*kst*	N.S.	29	29	121.328931	102.007379	1.18941327
Neurite area	*kst*	*** < 0.001	29	29	587.651103	440.957414	1.33267088
Ratio Glial/Neurite	*kst*	N.S.	29	29	0.20108743	0.22202905	0.90568069
Glial area	*Lac*	** < 0.01	30	33	293.135152	152.709667	1.91955858
Neurite area	*Lac*	N.S.	30	33	528.816394	527.990133	1.00156492
Ratio Glial/Neurite	*Lac*	**** < 0.0001	30	33	0.50495065	0.26516741	1.90427115
Glial area	*lost*	N.S.	29	30	113.5727	102.007379	1.11337729
Neurite area	*lost*	N.S.	29	30	451.3791	440.957414	1.02363422
Ratio Glial/Neurite	*lost*	N.S.	29	30	0.24684059	0.22202905	1.11174903
Glial area	*Nrg*	N.S.	29	23	86.8262174	102.007379	0.85117585
Neurite area	*Nrg*	N.S.	29	23	515.694391	440.957414	1.16948797
Ratio Glial/Neurite	*Nrg*	* < 0.05	29	23	0.14926781	0.22202905	0.67228954
Glial area	*nrv2*	N.S.	29	28	104.778643	102.007379	1.02716729
Neurite area	*nrv2*	N.S.	29	28	435.200179	440.957414	0.98694378
Ratio Glial/Neurite	*nrv2*	N.S.	29	28	0.22049061	0.22202905	0.993071
Glial area	*α-Cat*	N.S.	30	28	129.531286	112.231667	1.15414205
Neurite area	*α-Cat*	N.S.	30	28	438.190536	457.349233	0.95810926
Ratio Glial/Neurite	*α-Cat*	N.S.	30	28	0.28802281	0.24538726	1.17374799
Glial area	*Pdi*	N.S.	29	28	92.4456071	102.007379	0.90626392
Neurite area	*Pdi*	N.S.	29	28	434.129714	440.957414	0.98451619
Ratio Glial/Neurite	*Pdi*	N.S.	29	28	0.20904506	0.22202905	0.94152119
Glial area	*sdk*	N.S.	29	30	144.020633	102.007379	1.41186485
Neurite area	*sdk*	* < 0.05	29	30	525.337633	440.957414	1.19135685
Ratio Glial/Neurite	*sdk*	N.S.	29	30	0.26754263	0.22202905	1.20498929
Glial area	*shot*	** < 0.01	37	27	47.9187778	82.7811351	0.57886109
Neurite area	*shot*	N.S.	37	27	452.000741	487.031	0.92807386
Ratio Glial/Neurite	*shot*	*** < 0.001	37	27	0.10310839	0.16198966	0.63651219
Glial area	*Vha55*	N.S.	30	23	67.1933478	79.4147333	0.84610682
Neurite area	*Vha55*	N.S.	30	23	496.064087	417.509933	1.18814918
Ratio Glial/Neurite	*Vha55*	N.S.	30	23	0.13876663	0.17721365	0.7830471

D

Figure D-1 Violin and dot-plots containing raw data of glial protrusion and neurite areas upon knockdown of glial protrusion-localised transcripts after stimulation

Next page: Violin plots with accompanying raw data presenting the NMJ results quantification for RNAi knockdown of candidate transcripts in glia after spaced potassium stimulation. See genotype above each plot and legend for details. Raw data is plotted as black dots. Point range (orange) indicates the mean ± SEM. Significance levels are denoted as follows: *p < 0.05; **p < 0.01; ***p < 0.001; ****p < 0.0001.

Comparison of glial and neuronal areas in stimulated candidate gene knockdown NMJs

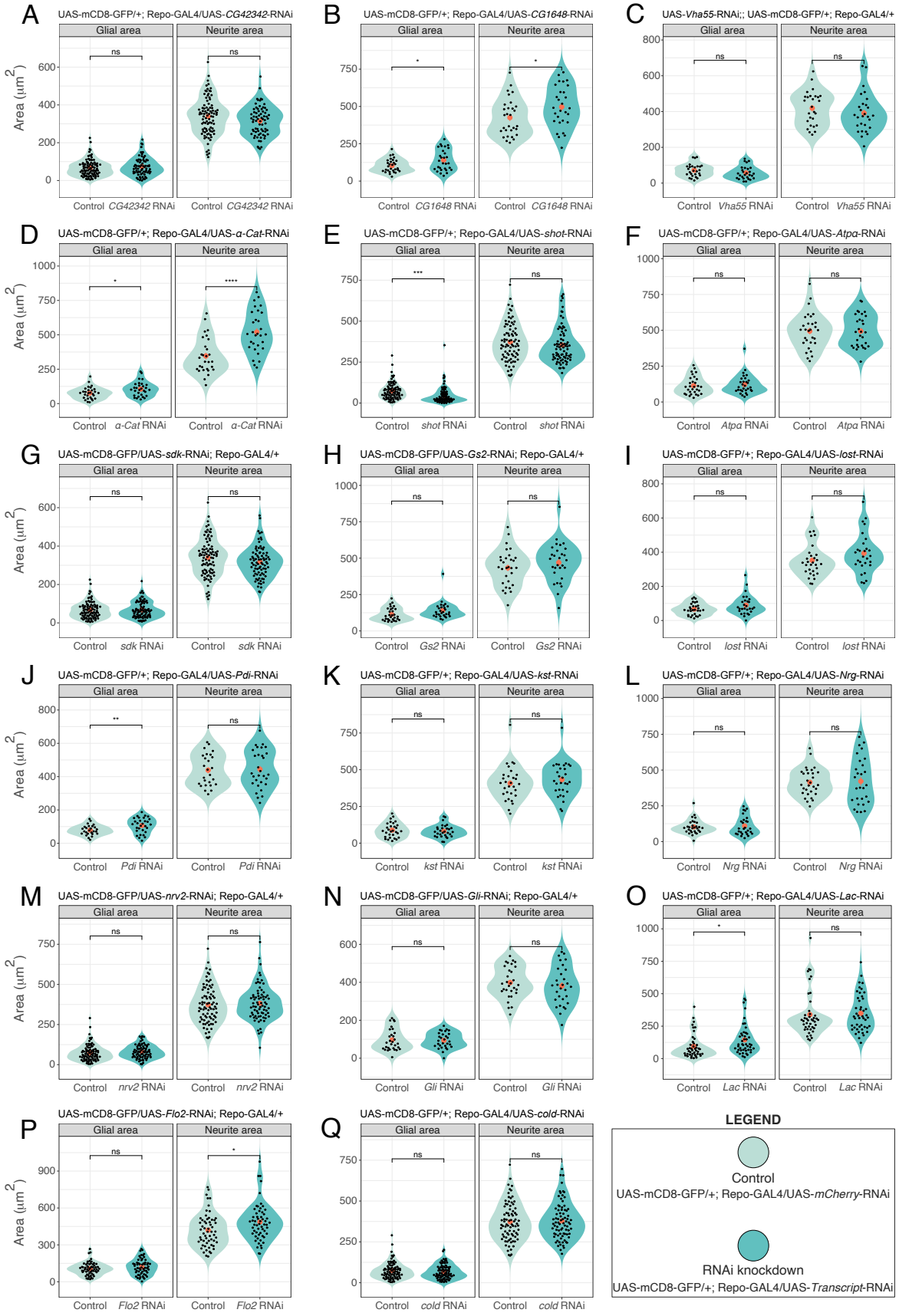

Figure D-2 Violin and dot-plots containing raw data of glial protrusion and neurite protrusion area ratios upon knockdown of glial protrusion-localised transcripts after stimulation

Next page: Violin plots with accompanying raw data presenting the NMJ results quantification for RNAi knockdown of candidate transcripts in glia after spaced potassium stimulation. See genotype above each plot and legend for details. Raw data is plotted as black dots. Point range (cyan) indicates the mean ± SEM. Significance levels are denoted as follows: *p < 0.05; **p < 0.01; ***p < 0.001; ****p < 0.0001.

Comparison of glial and neuronal area ratios for stimulated candidate gene knockdown NMJs

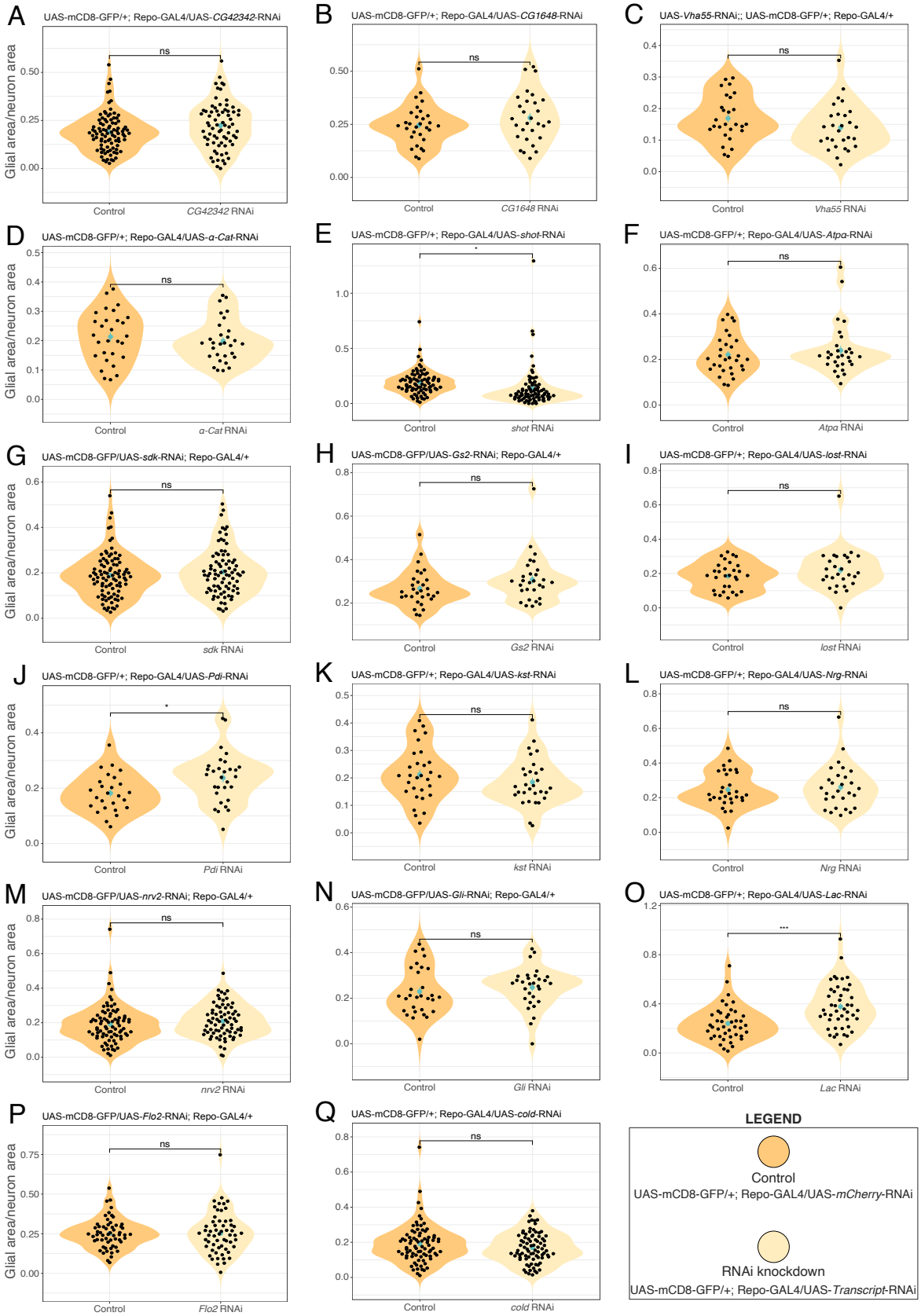

Table D-1 Summary statistics for glial and neurite area and their ratios after stimulation

Measurement	RNAi target	p	control n	RNAi n	RNAi mean	control mean	Foldchange
Glial area	*α-Cat*	* < 0.05	29	30	105.5822	76.3654138	1.38259187
Neurite area	*α-Cat*	**** < 0.0001	29	30	520.169333	345.854379	1.50401257
Ratio Glial/Neurite	*α-Cat*	N.S.	29	30	0.19858018	0.21319387	0.9314535
Glial area	*Atpα*	N.S.	30	30	121.338567	113.8816	1.06548
Neurite area	*Atpα*	N.S.	30	30	494.632133	494.5497	1.00016668
Ratio Glial/Neurite	*Atpα*	N.S.	30	30	0.23990171	0.22095308	1.08575859
Glial area	*CG1648*	* < 0.05	30	29	140.288207	102.669367	1.36640764
Neurite area	*CG1648*	* < 0.05	30	29	496.750345	425.282433	1.16804812
Ratio Glial/Neurite	*CG1648*	N.S.	30	29	0.28111762	0.246236	1.14165931
Glial area	*CG42342*	N.S.	92	71	73.6225775	67.60375	1.08903097
Neurite area	*CG42342*	N.S.	92	71	314.865028	339.48325	0.92748325
Ratio Glial/Neurite	*CG42342*	N.S.	92	71	0.22294116	0.18912138	1.17882577
Glial area	*cold*	N.S.	82	81	67.3065062	74.0356951	0.90910886
Neurite area	*cold*	N.S.	82	81	378.289284	372.99	1.01420758
Ratio Glial/Neurite	*cold*	N.S.	82	81	0.16859239	0.19065006	0.88430288
Glial area	*Flo2*	N.S.	58	58	121.559121	107.031155	1.13573586
Neurite area	*Flo2*	* < 0.05	58	58	485.50531	420.053414	1.15581803
Ratio Glial/Neurite	*Flo2*	N.S.	58	58	0.25387414	0.25170565	1.00861521
Glial area	*Gli*	N.S.	30	30	93.8198	96.2835	0.97441202
Neurite area	*Gli*	N.S.	30	30	381.144067	398.7545	0.9558364
Ratio Glial/Neurite	*Gli*	N.S.	30	30	0.24716696	0.22931514	1.07784843
Glial area	*Gs2*	N.S.	30	29	140.104862	113.8259	1.23086979
Neurite area	*Gs2*	N.S.	30	29	469.846862	433.254233	1.08445995
Ratio Glial/Neurite	*Gs2*	N.S.	30	29	0.30854951	0.26708577	1.15524503
Glial area	*kst*	N.S.	30	30	81.5034333	88.4618667	0.92133974
Neurite area	*kst*	N.S.	30	30	432.572733	407.270233	1.06212705
Ratio Glial/Neurite	*kst*	N.S.	30	30	0.18445957	0.21203757	0.86993813
Glial area	*Lac*	* < 0.05	43	46	144.341065	95.1815349	1.5164818
Neurite area	*Lac*	N.S.	43	46	349.304913	338.956535	1.0305301
Ratio Glial/Neurite	*Lac*	*** < 0.001	43	46	0.37743706	0.23969659	1.57464508
Glial area	*lost*	N.S.	30	28	90.1303214	66.4762667	1.35582706
Neurite area	*lost*	N.S.	30	28	393.512786	352.200133	1.1172988
Ratio Glial/Neurite	*lost*	N.S.	30	28	0.22089379	0.18502038	1.19388897
Glial area	*Nrg*	N.S.	30	28	109.610071	102.706433	1.06721719
Neurite area	*Nrg*	N.S.	30	28	421.478571	414.340033	1.0172287
Ratio Glial/Neurite	*Nrg*	N.S.	30	28	0.26119771	0.24609554	1.06136707
Glial area	*nrv2*	N.S.	82	73	80.3282466	74.0356951	1.08499348
Neurite area	*nrv2*	N.S.	82	73	382.141753	372.99	1.02453619
Ratio Glial/Neurite	*nrv2*	N.S.	82	73	0.20899176	0.19065006	1.0962061
Glial area	*Pdi*	** < 0.01	26	30	106.6677	78.8305	1.35312728
Neurite area	*Pdi*	N.S.	26	30	444.043933	438.648	1.01230128
Ratio Glial/Neurite	*Pdi*	* < 0.05	26	30	0.23706184	0.18220216	1.30109239
Glial area	*sdk*	N.S.	92	82	67.9094024	67.60375	1.00452123
Neurite area	*sdk*	N.S.	92	82	317.450951	339.48325	0.93510048
Ratio Glial/Neurite	*sdk*	N.S.	92	82	0.20434589	0.18912138	1.08050122
Glial area	*shot*	*** < 0.001	82	79	46.4964051	74.0356951	0.62802686
Neurite area	*shot*	N.S.	82	79	354.366633	372.99	0.95007006
Ratio Glial/Neurite	*shot*	* < 0.05	82	79	0.13401183	0.19065006	0.70292049
Glial area	*Vha55*	N.S.	27	28	57.1433929	71.9879259	0.79379135
Neurite area	*Vha55*	N.S.	27	28	391.39175	418.79437	0.93456784
Ratio Glial/Neurite	*Vha55*	N.S.	27	28	0.14005804	0.16907098	0.82839785

Figure D-3 Violin and dot-plots containing raw data of the numbers of “ghost boutons” counts after potassium stimulation relative to RNAi controls

Next page: Violin plots with accompanying raw data presenting the NMJ results quantification of the numbers of “ghost boutons” counts after potassium stimulation relative to RNAi controls. See genotype above each plot and legend for details. Raw data is plotted as black dots. Point range (orange) indicates the mean ± SEM. Significance levels are denoted as follows: *p < 0.05; **p < 0.01; ***p < 0.001; ****p < 0.0001.

Numbers of "ghost bouton" counts after potassium stimulation relative to RNAi Controls

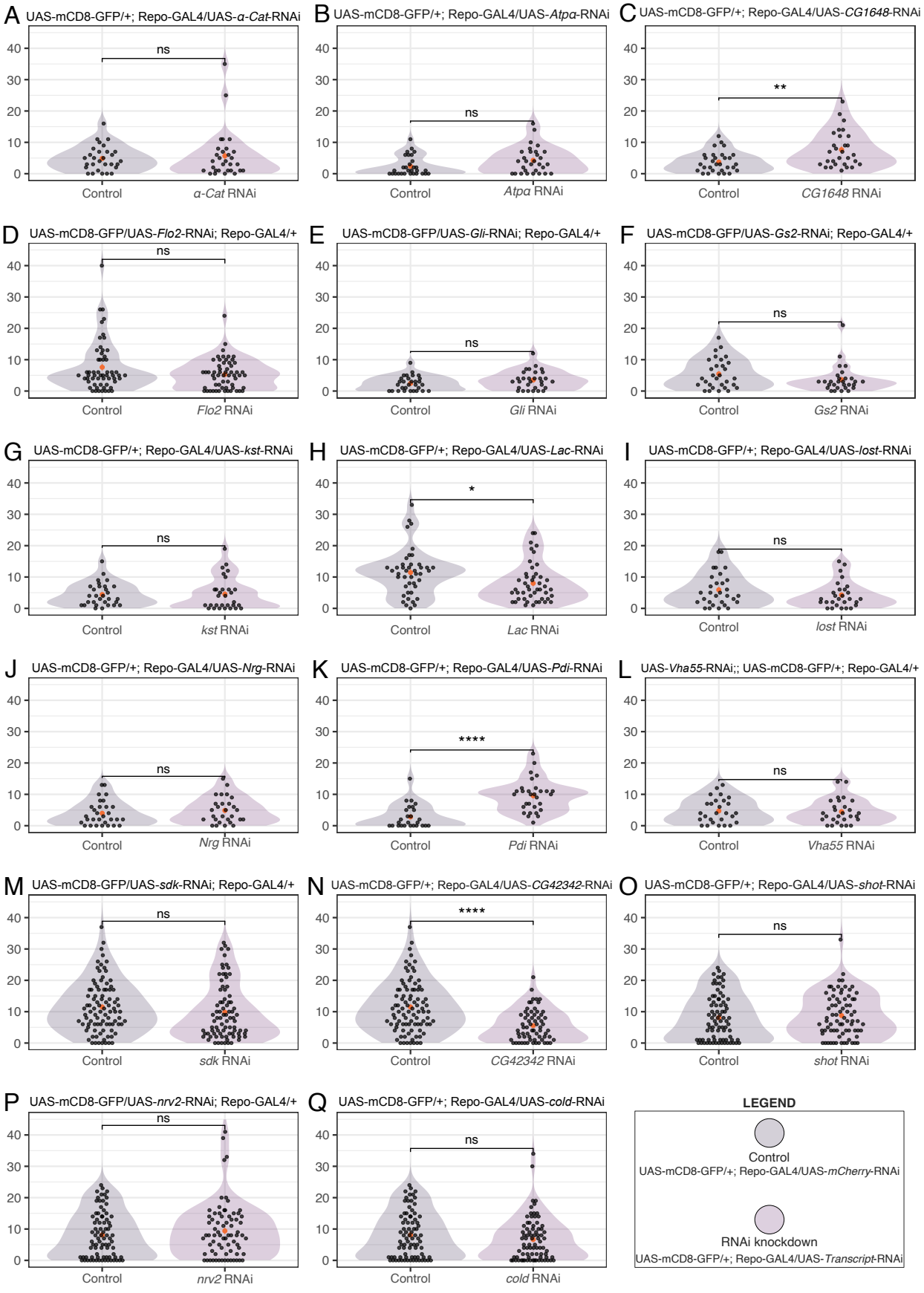

Table D-2 Summary statistics for bouton numbers after stimulation

RNAi target	p	control n	RNAi n	RNAi mean bouton number	control mean bouton number	Foldchange	P significance	log2foldchange
α-Cat	0.766	29	30	5.7	4.86206897	1.17234043	N.S.	0.22939156
Atpα	0.0666	30	30	4.26666667	2.36666667	1.8028169	N.S.	0.85025288
CG1648	0.00381	30	29	7.65517241	3.73333333	2.05049261	** < 0.01	1.03597054
Flo2	0.257	28	28	5.46428571	4.5	1.21428571	N.S.	0.28010792
Gli	0.155	30	30	3.5	2.43333333	1.43835616	N.S.	0.52442096
Gs2	0.131	30	29	3.65517241	5.46666667	0.6686291	N.S.	-0.5807219
kst	0.421	30	30	4.53333333	4.4	1.03030303	N.S.	0.04306872
Lac	0.01	43	46	8	11.4418605	0.69918699	* < 0.05	-0.516249751
lost	0.25	30	28	4.28571429	5.9	0.72639225	N.S.	-0.4611793
Nrg	0.363	30	28	4.85714286	3.96666667	1.2244898	N.S.	0.29218075
Pdi	1.30E-06	26	30	9.56666667	2.80769231	3.40730594	**** < 0.0001	1.76863149
CG42342	1.74E-06	92	65	5.55384615	11.4891304	0.48340004	**** < 0.0001	-1.0487105
sdk	0.079	92	82	9.82926829	11.4891304	0.85552761	N.S.	-0.2251137
cold	0.19	82	81	6.65432099	8.09756098	0.82176856	N.S.	-0.283196
nrv2	0.532	82	73	9.39726027	8.09756098	1.16050503	N.S.	0.21475278
shot	0.526	82	76	8.77631579	8.09756098	1.08382213	N.S.	0.11612801
Vha55	0.839	27	28	4.46428571	4.7037037	0.94910011	N.S.	-0.0753678